COMMONWEALTH OF PENNSYLVANIA
DEPARTMENT OF TRANSPORTATION

PennDOT/MAUTC PARTNERSHIP

FIELD MONITORING OF INTEGRAL ABUTMENT BRIDGES

PennDOT/MAUTC PARTNERSHIP - Contract No. 510401, Work Order No. 1

FINAL REPORT

July 12, 2006

By J. A. Laman, K. Pugasap, and W. Kim

PENNSTATE

Pennsylvania Transportation Institute

The Pennsylvania State University
Transportation Research Building
University Park, PA 16802-4710
(814) 865-1891 www.pti.psu.edu

FIELD MONITORING OF INTEGRAL ABUTMENT BRIDGES

FINAL REPORT

PennDOT/MAUTC PARTNERSHIP
Contract No. 510401, Work Order No. 1

Prepared for

Commonwealth of Pennsylvania
Department of Transportation

By
Jeffrey A. Laman
Kongsak Pugasap
and
WooSeok Kim

Pennsylvania Transportation Institute
The Pennsylvania State University
Transportation Research Building
University Park, PA 16802-4710

July 12, 2006

PTI 2006-21

This work was sponsored by the Pennsylvania Department of Transportation and the U.S. Department of Transportation. The contents of this report reflect the views of the authors, who are responsible for the facts and the accuracy of the data presented herein. The contents do not necessarily reflect the official views or policies of either the U.S. Department of Transportation or the Commonwealth of Pennsylvania at the time of publication. This report does not constitute a standard, specification, or regulation.

Technical Report Documentation Page

1. Report No.	2. Government Accession No.	3. Recipient's Catalog No.
FHWA-PA-2006-006-510401-01		

4. Title and Subtitle	5. Report Date
Field Monitoring of Integral Abutment Bridges	July 12, 2006
	6. Performing Organization Code
7. Author(s)	**8. Performing Organization Report No.**
Jeffrey A. Laman, Kongsak Pugasap, and WooSeok Kim	PTI 2006-21
9. Performing Organization Name and Address	**10. Work Unit No. (TRAIS)**
The Pennsylvania Transportation Institute The Pennsylvania State University 201 Transportation Research Building University Park, PA 16802	**11. Contract or Grant No.** 510401, Work Order No. 1
12. Sponsoring Agency Name and Address	**13. Type of Report and Period Covered**
The Pennsylvania Department of Transportation Bureau of Planning and Research Commonwealth Keystone Building 400 North Street, 6th Floor Harrisburg, PA 17120-0064	Final Report 6/13/2005 – 7/12/2006
	14. Sponsoring Agency Code

15. Supplementary Notes
COTR: Beverly Miller, 717-783-4338

16. Abstract

The project described in this report involved the instrumentation of bridge 109 on the new I-99 extension in central Pennsylvania and continued monitoring and collection of engineering bridge response data at the three previously instrumented bridges and a weather station. The development of a bridge 109 numerical model and evaluation of the PennDOT IA Design Spreadsheet was completed. Detailed instrument descriptions and installation of each bridge 109 instrument are provided in this report. Bridge response data are presented for bridges 203, 211, and 222, composed of longitudinal abutment displacements, abutment earth pressures, abutment and girder rotations, H-pile bending moments about the weak axis and axial forces, girder strains, and approach slab strains. Four 3-dimensional numerical models were developed to predict IA bridge response for bridges 203, 211, 222, and 109. Comparison between observed bridge response and predicted bridge response is presented and discussed. Finally, evaluation of the PennDOT IA Design Spreadsheet was performed to provide suggested program improvements for all four instrumented bridges. Comparison of predicted bridge response based on the PennDOT IA program and the original design to observed bridge response is also presented and discussed.

17. Key Words	18. Distribution Statement
Integral, abutment, bridge, monitoring, field, data, behavior	No restrictions. This document is available from the National Technical Information Service, Springfield, VA 22161

19. Security Classif. (of this report)	20. Security Classif. (of this page)	21. No. of Pages	22. Price
Unclassified	Unclassified	293	

Form DOT F 1700.7 (8-72) Reproduction of completed page authorized

TABLE OF CONTENTS

TABLE OF CONTENTS (Continued)

LIST OF FIGURES

LIST OF TABLES

CHAPTER 1

INTRODUCTION

1.1 INTRODUCTION AND PROBLEM STATEMENT

The early success realized in initially constructed integral abutment (IA) bridges has led to the application of this bridge type to increasingly longer spans. However, many engineering uncertainties exist in the prediction of long- and short-term behavior of all spans of integral abutment bridges. A majority of design principles continue to be empirically based and anecdotal. Performance problems have arisen due to the many differences in integral abutment detailing philosophy and other parameters of bridge construction. This research project instrumented a longer span IA bridge on the I-99 corridor to obtain field-based bridge response data that will provide information regarding the actual response of this bridge type to thermal loads through a comprehensive field monitoring program on the I-99 corridor. In addition, data were collected from acquisition systems at three previously instrumented bridges and a weather station throughout the duration of the project.

1.2 SCOPE OF RESEARCH

The scope of the research project is detailed below. The project encompassed instrumentation installation, continuous monitoring, numerical model comparisons, and software evaluation of the four selected I-99 bridges. All results of the research project were to be formally reported to PennDOT, which is the purpose of this project report.

1. Installation of instrumentation and data acquisition equipment on bridge 109. Details and descriptions for the instrumentation are included in this final project report.
2. Continuous monitoring of bridges 109, 203, 211, 222 and the weather station. A summary of the collected data is provided in this final project report. In addition, electronic files containing all raw data are provided.
3. Evaluation of the PennDOT IA Design Spreadsheet. Predicted behavior using results from the PennDOT Integral Abutment design spreadsheet were compared to observed bridge 203, 211, and 222 behaviors. A summary of the comparison is included in this final project report.
4. Comparison of field observations of bridges 202, 211, 222, and 109 to numerical predictions. These comparisons are included in this final project report.
5. Draft Final Report. All activities falling under the scope and objectives for the present research project have been summarized in this draft final project report for review.
6. Final Report. This draft final project report will be revised and submitted as a final report after receipt of PennDOT final review comments and archived for future reference.

1.3 OBJECTIVES

The objectives of this project were to: (1) install several electronic monitoring instruments on bridge 109 of section C10 on I-99 south of Port Matilda, Pennsylvania; (2) install a data acquisition system on bridge 109 to power and read these instruments;

(3) continuously monitor and collect data from bridges 203, 211, 222, 109, and the weather station; (4) archive electronically and summarize the collected data from each of the four bridges and the weather station; (5) compare field observations to numerical models; and (6) evaluate observed structure behaviors and results from numerical models with the integral abutment design methodology as presented in PennDOT's Integral Abutment Spreadsheet. These objectives have been met and exceeded for the project. This project scope and objectives supports the research partnership objective as identified in Exhibit A of the Agreement.

1.4 REPORT ORGANIZATION

This report consists of eight chapters. Chapter 2 describes instrumentation installation of bridge 109. Chapter 3 discusses collected data from long-term monitoring of all four instrumented bridges. Chapter 4 covers methodologies to incorporate time-dependent effects, soil-structure interaction behavior, and abutment-backwall connection behavior into numerical models. Chapter 5 presents modeling techniques and applied loads for all four numerical bridge models. Chapter 6 discusses comparisons between measured response from monitoring data and predicted response from numerical models. Chapter 7 presents an evaluation of the PennDOT IA program as compared to the original design and measured response. Finally, Chapter 8 provides a summary and conclusions of this report.

CHAPTER 2

BRIDGE INSTRUMENTATION

2.1 INSTRUMENTATION DESCRIPTION

The present research includes instrumentation installation at bridge 109 and monitoring of the four integral abutment bridges of the present study: bridges 109, 203, 211 and 222 on the US 220 section of I-99 at Port Matilda. Detailed descriptions and locations of the four bridges are presented in the PennDOT research report by Laman et al. (2003). Bridges 203, 211 and 222 were previously instrumented and data acquisition systems installed as shown in Figures 2.6 through 2.18, with data download as an ongoing activity. This chapter describes in detail the bridge instrumentation program for bridge 109. Bridge 109 has been designed and constructed with both abutments as integral. An overview of critical parameters for the brief description of bridge 109 is presented in Table 2.1 and a plan view of the structure is presented in Figure 2.1.

Table 2.1. Bridge 109 Critical Parameters

Bridge No.	Girder Type	Skew	No. of Spans	Spans (ft)	Total Length (ft)	RSR 6220 Over:	Design Section
109	P/S I	0	4	88-122-122-88	420	Blue Spring Hollow Stream	A10

Sixty-four vibrating wire based instruments were installed on Structure 109 between November 2005 and May 2006. These instruments consist of 5 pressure cells (VW-4820), 5 extensometers (VW-4450), 8 tiltmeters (VW-6350), 6 reinforcing bar strain gages (VK-4911) and 40 strain gages (VSM-4000). Detailed descriptions, specifications, and explanations of each instrument are presented in Laman et al. (2003). Two pressure cells and two extensometers were installed on the south abutment (abutment 1) and three pressure cells and three extensometers were installed on the north abutment (abutment 2). Refer to Figures 2.1 through 2.5 for detailed drawings of bridge 109 and the placement of each of the 64 instruments. Pressure cells were placed to face the backfill. Four pressure cells were installed along the centerline of the abutment, each at a different elevation. A pressure cell was located on abutment 1 at the same elevation as the upper pressure cell at abutment 2 and located at the middle of the exterior and interior girder on abutment 2.

Twenty-four strain gages were installed on four HP12x74 piles. Two piles with 12 attached strain gages (6 each) were driven under abutment 1 and two piles with 12 attached strain gages were driven under abutment 2 (see Figures 2.3 and 2.5). Six strain gages were mounted on each of the four piles with three gages placed at each of two different elevations. These elevations are approximately 1 ft and 9 ft below the bottom of the abutment. The arrangement of three strain gages at two different elevations permits the measurement of both axial load and moment variation.

Sixteen strain gages were installed on four precast concrete girders at both the top and bottom flanges (see Figures 2.3 and 2.5). Each girder has a total of four strain gages. Each set of two strain gages was mounted on each girder end, one on the side surface of the top flanges, and the other on the centerline of the bottom surface of the bottom flanges. Each strain gage was 1 ft apart from the abutments.

Four tilt meters were mounted on the pre-cast concrete girders with the remaining four tilt-meters mounted on abutments 1 and 2. A tilt meter was located at each abutment end of the west interior girder and attached to the web, and a tilt meter was located similarly on each end of the east exterior girder. These tilt meters were placed 3 inches away from the abutment. Each tilt meter placed on the abutment was placed 1 ft below the girders, which also were instrumented with tilt meters. In addition, six reinforcing bar strain gages were placed in the approach slab to monitor stresses at this location.

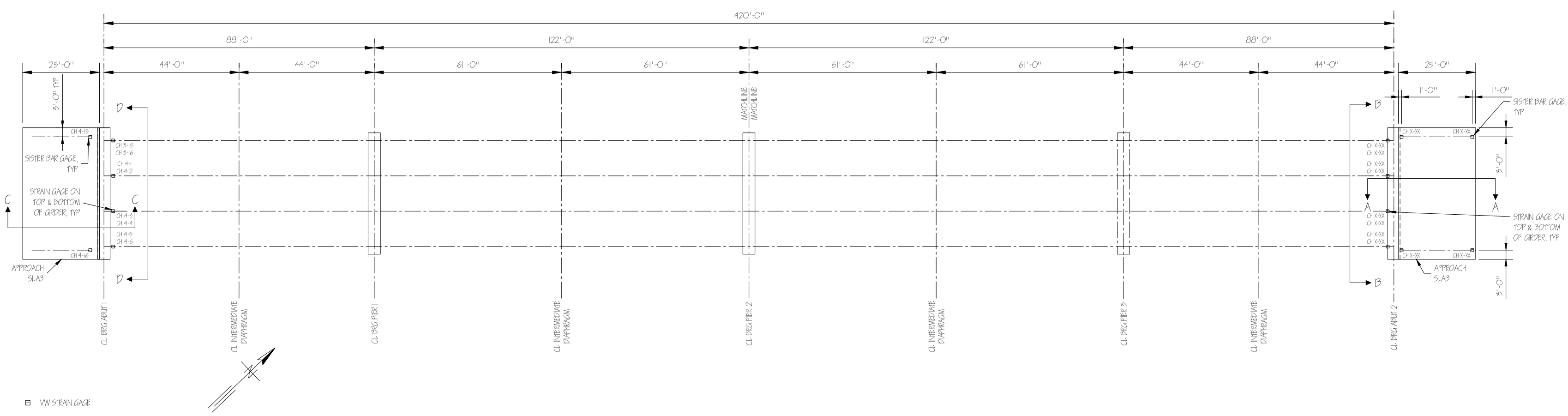

Figure 2.1: Bridge 109 Instrumentation Plan

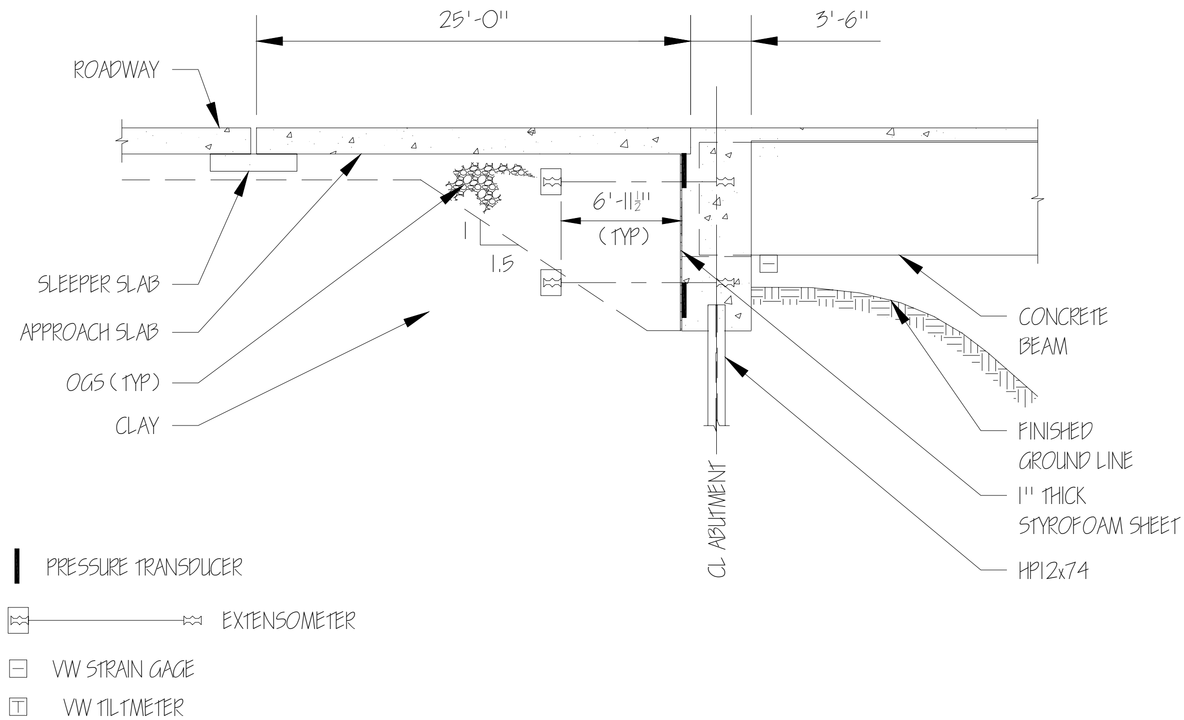

Figure 2.2: Bridge 109 cross-section through north abutment (section A-A)

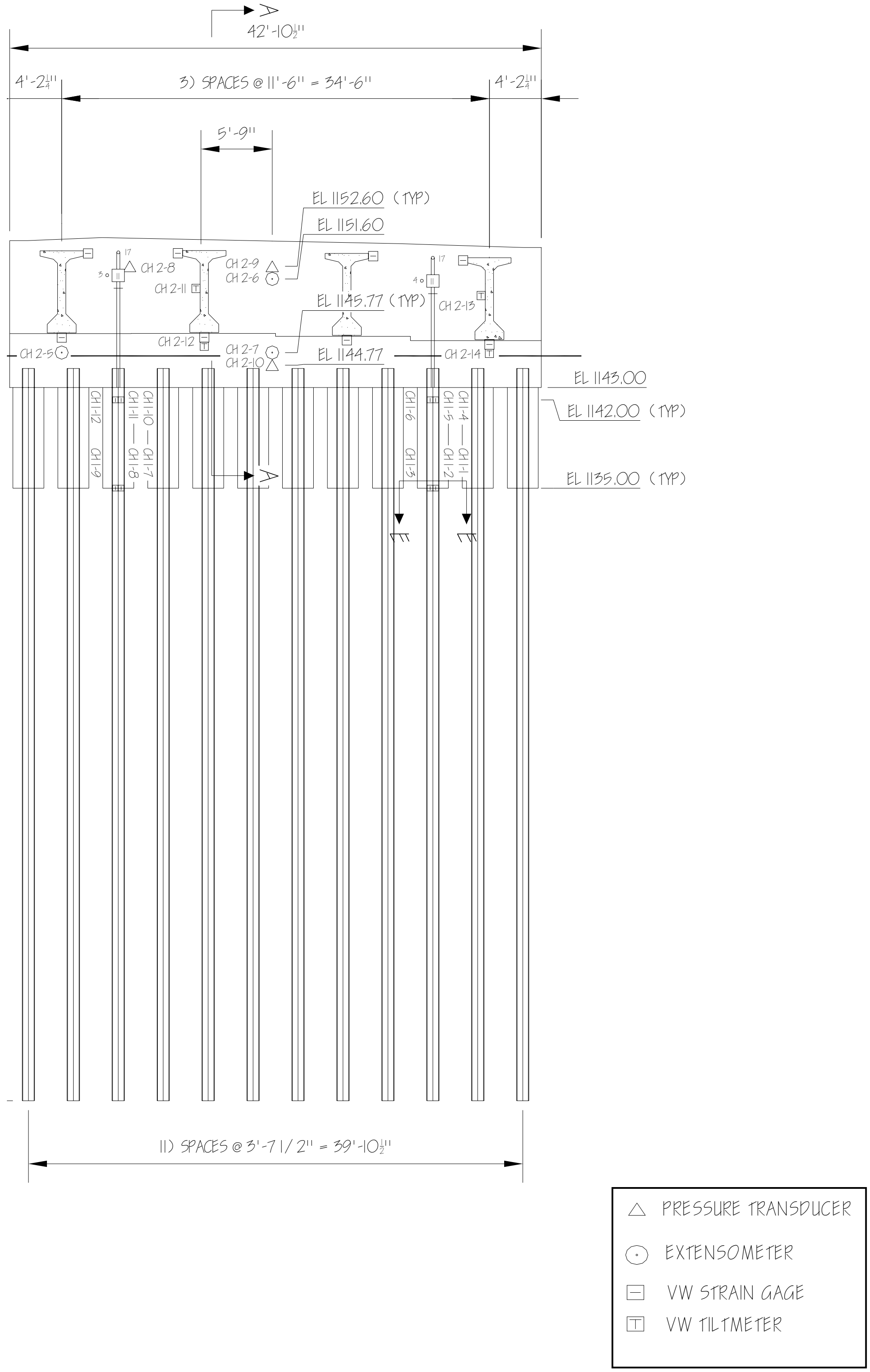

Figure 2.3: Bridge 109 Abutment 2 Elevation (Section B-B)

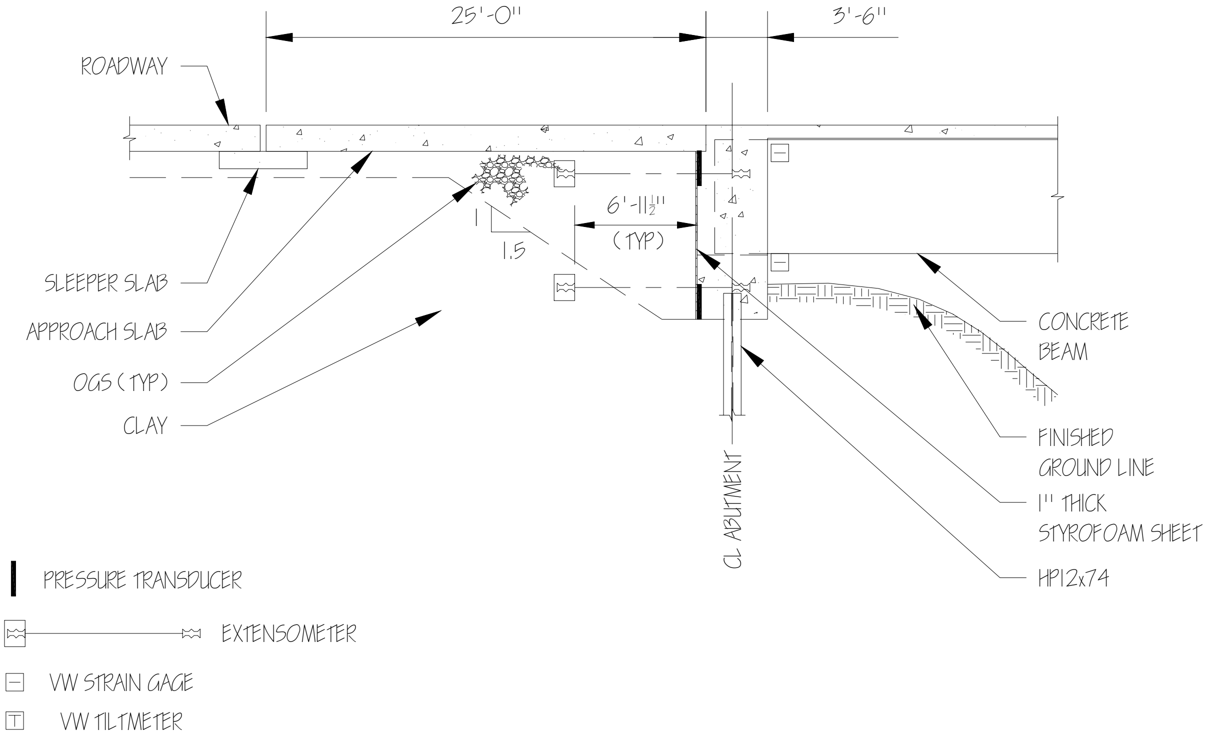

Figure 2.4: Structure 109 Cross-Section through south abutment (Section C-C)

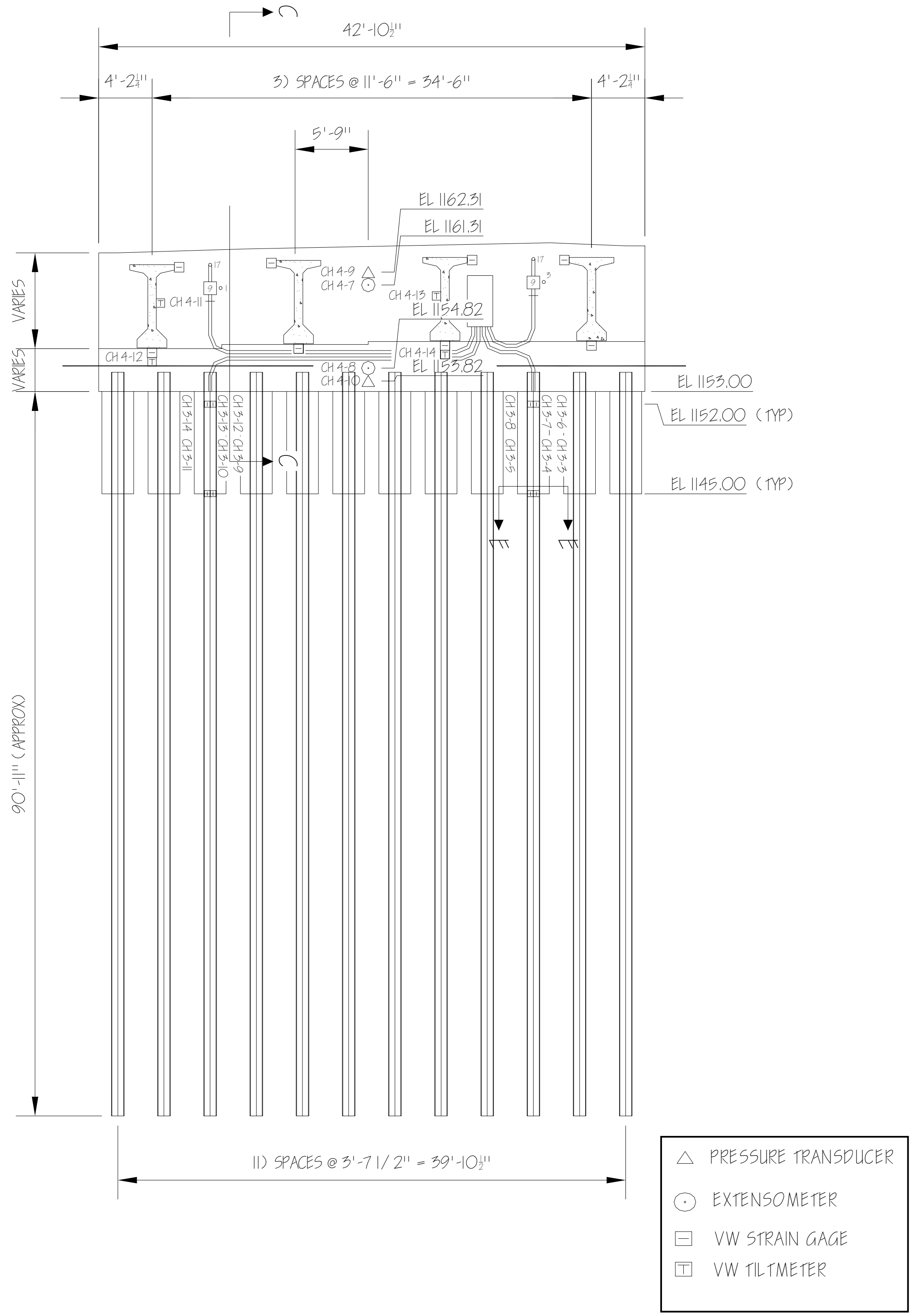

Figure 2.5: Structure 109 Abutment 1 Elevation (Section D-D)

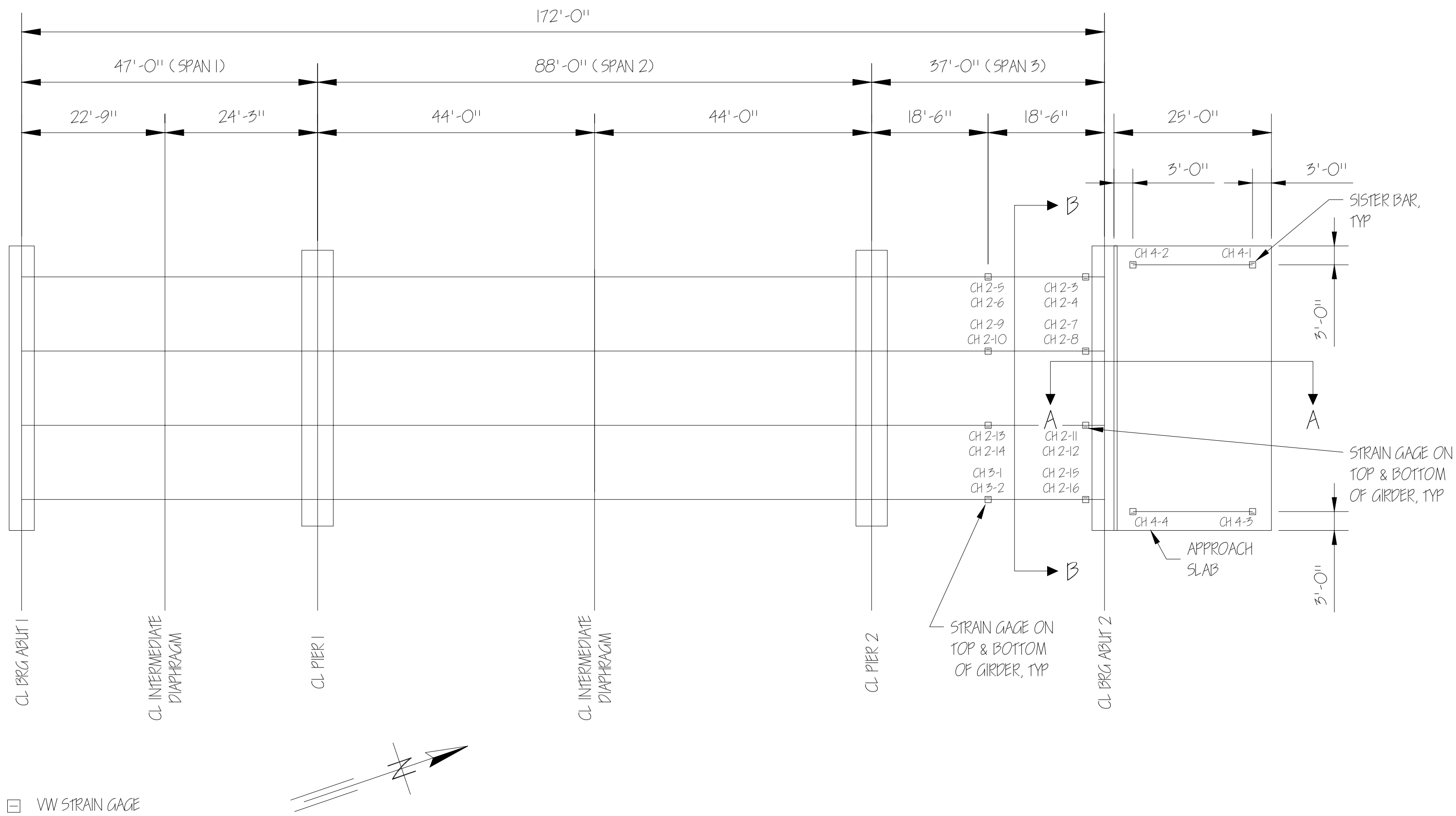

Figure 2.6: Structure 203 Instrumentation Plan

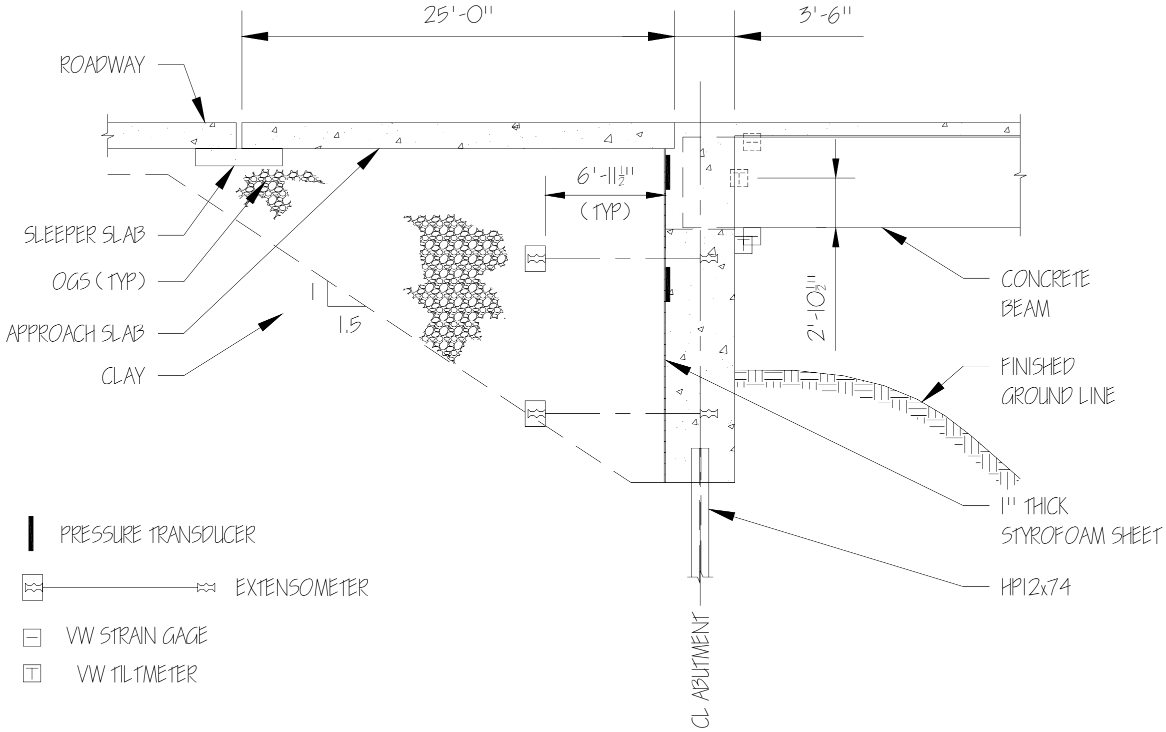

Figure 2.7: Structure 203 Cross-Section Through Abutment 2 (Section A-A)

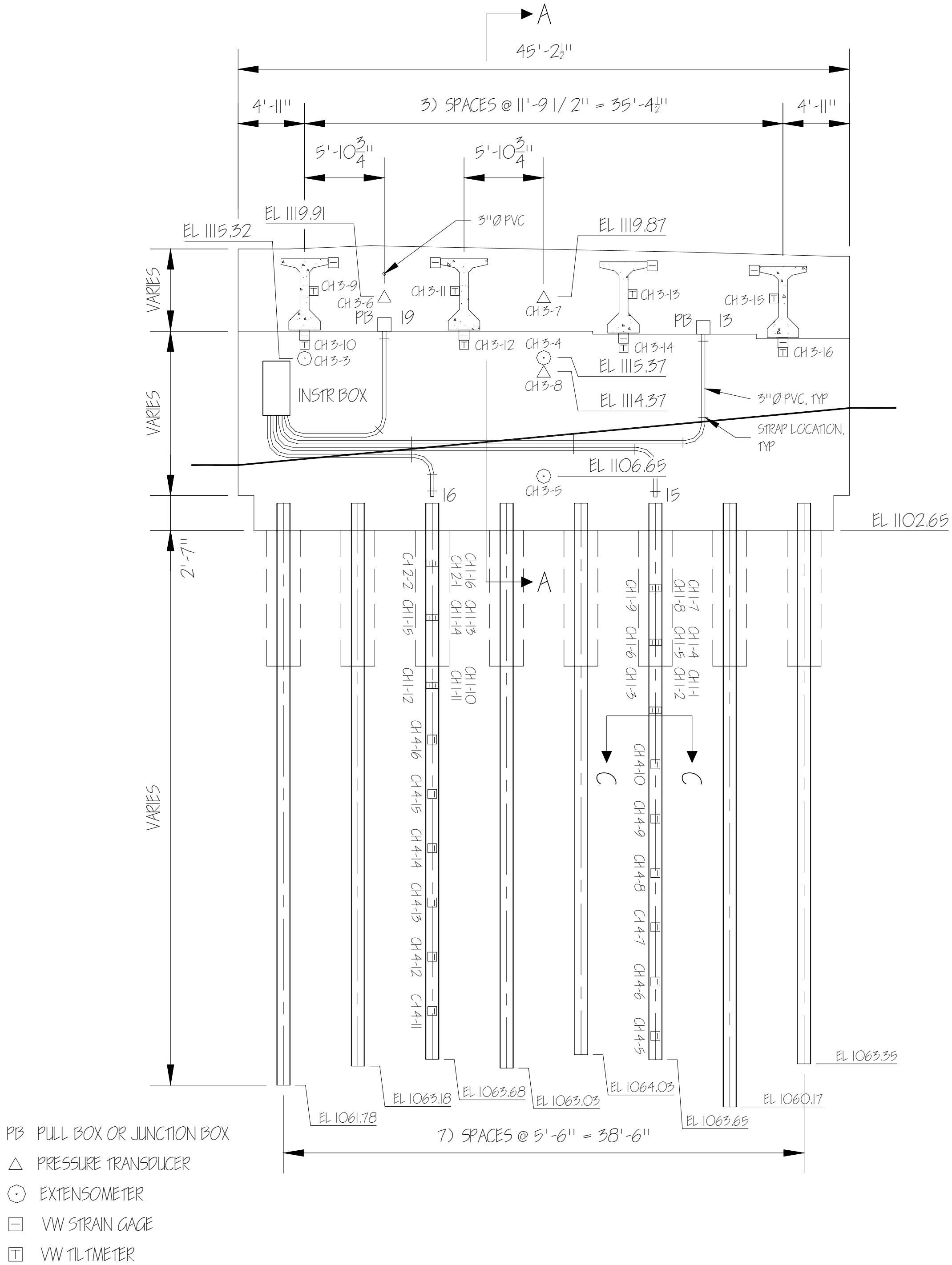

Figure 2.8: Structure 203 Abutment 2 Elevation (Section B-B)

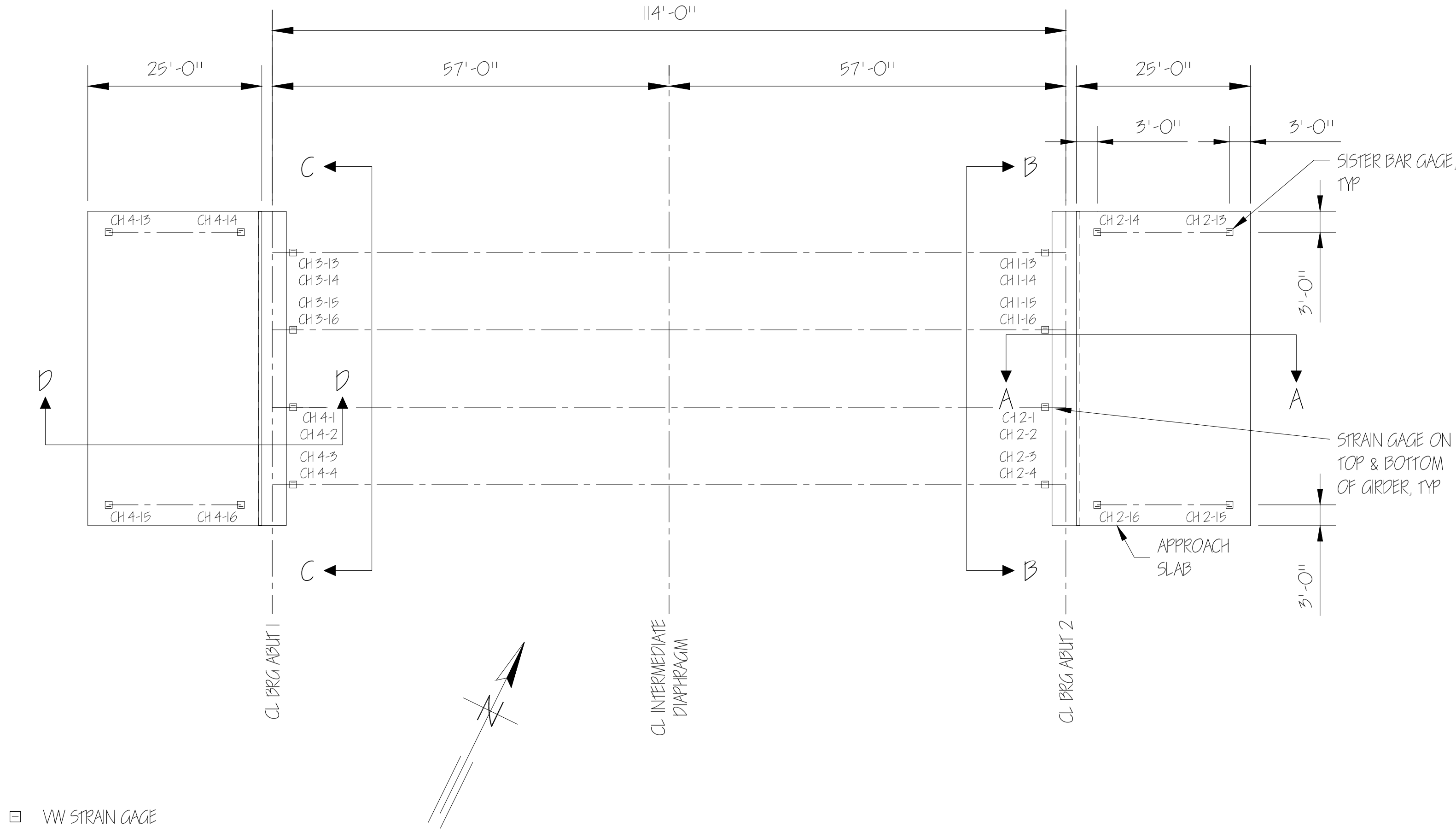

Figure 2.9:Structure 211 Instrumentation Plan

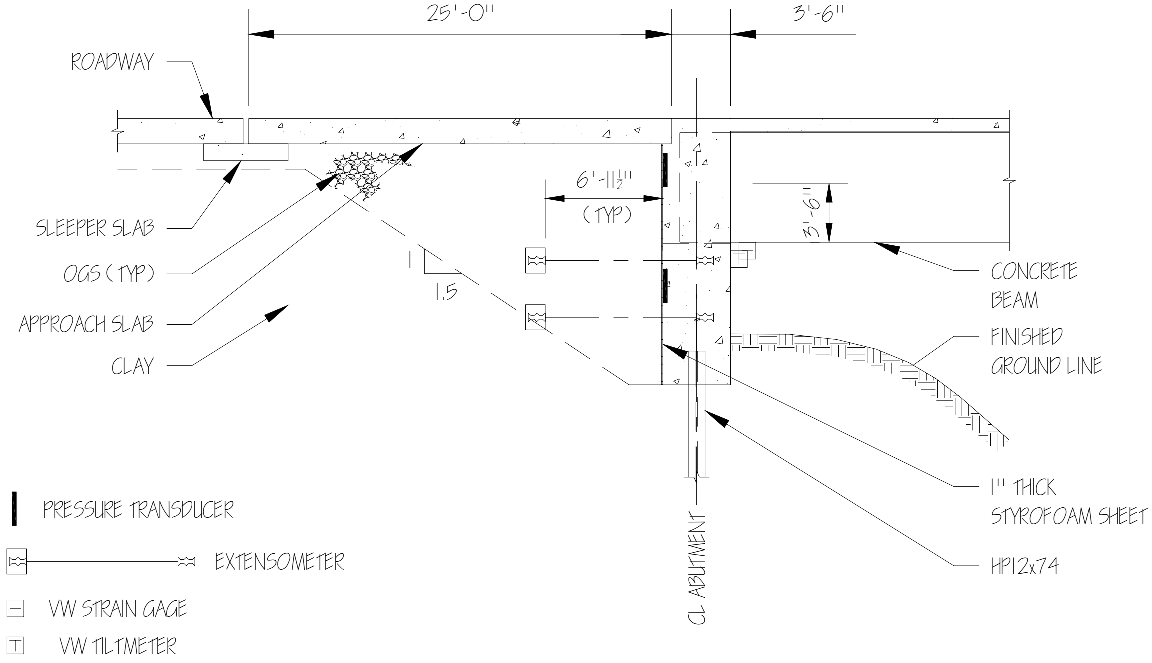

Figure 2.10: Structure 211 Cross-Section Through Abutment 2 (Section A-A)

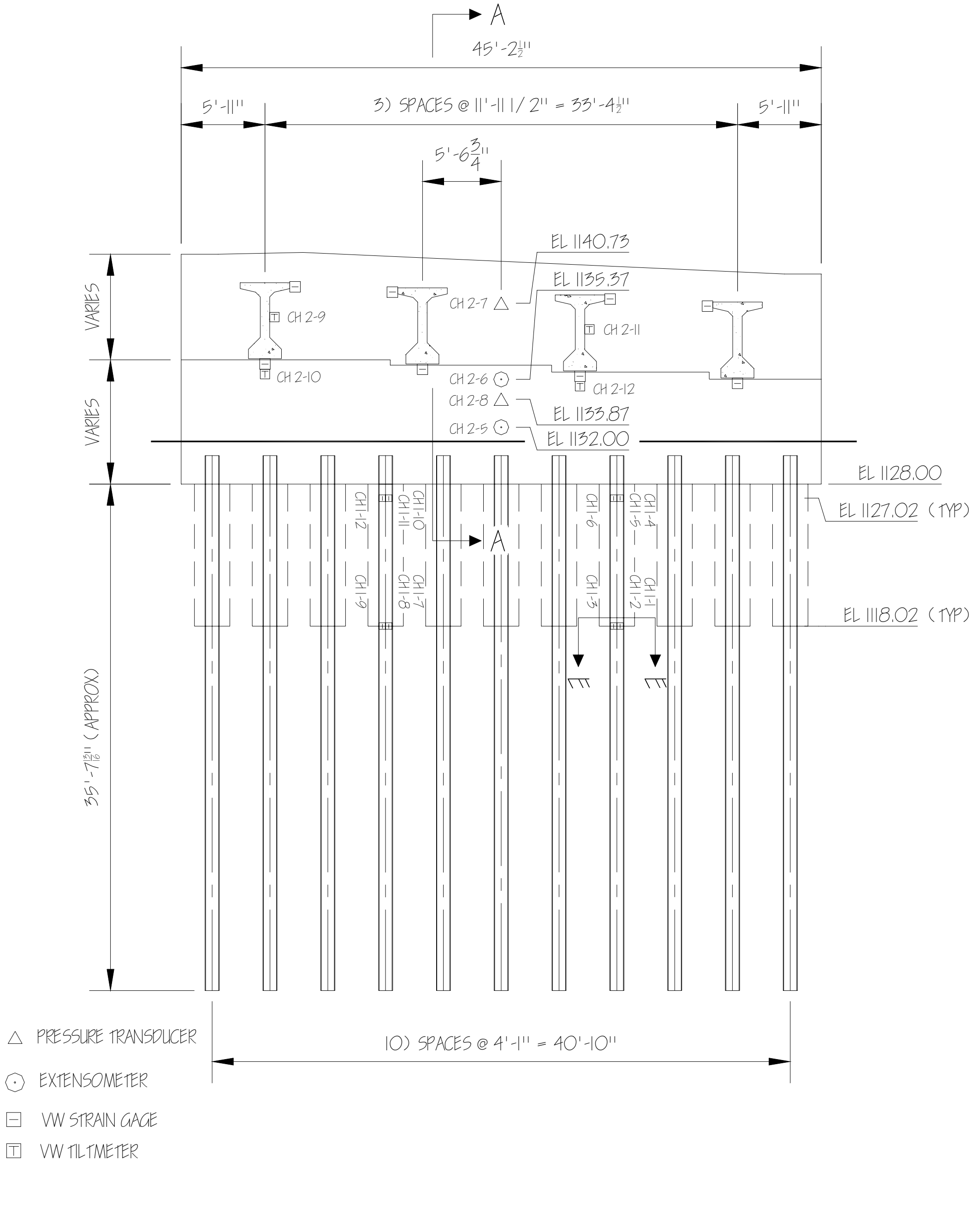

Figure 2.11: Structure 211 Abutment 2 Elevation (Section B-B)

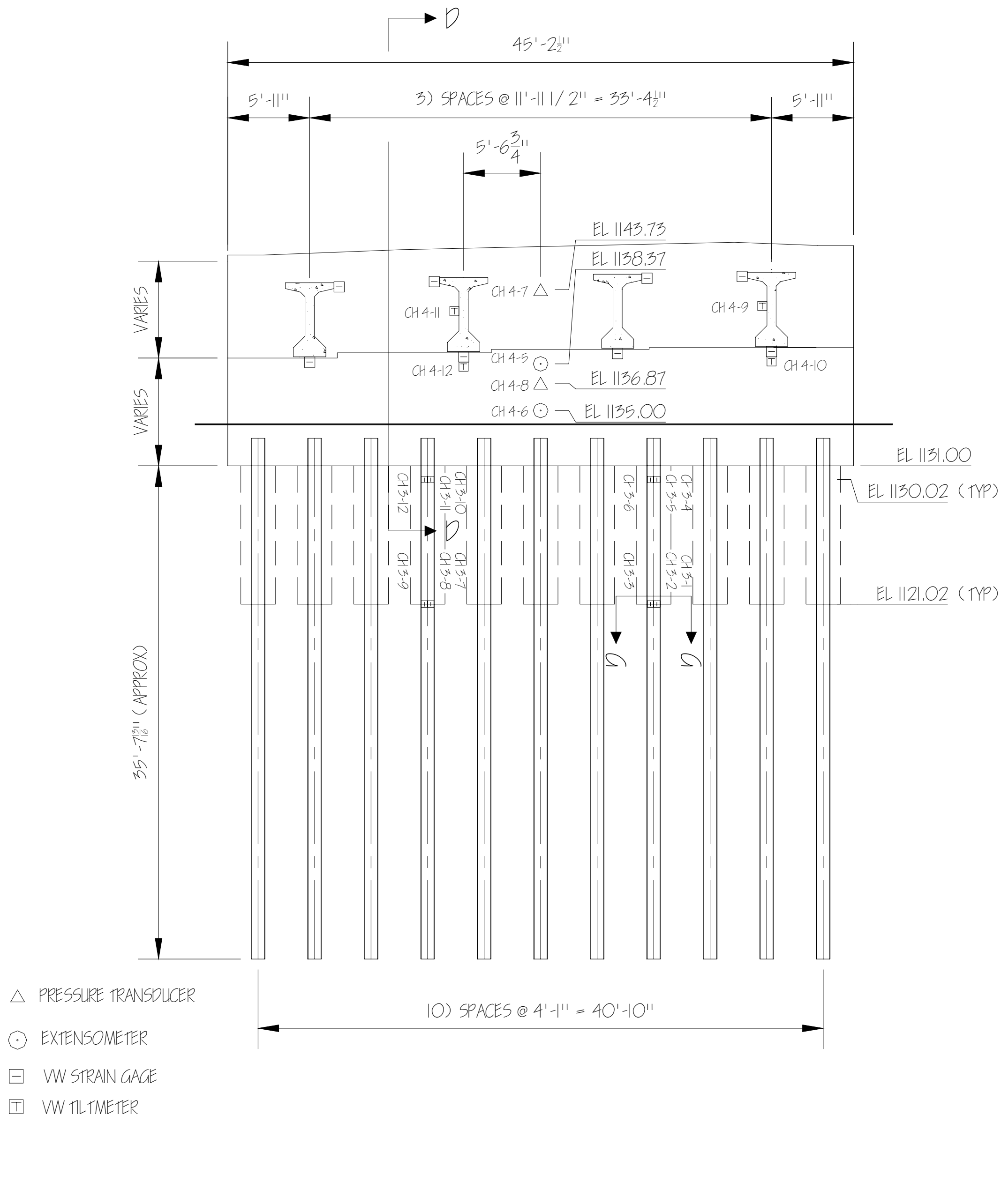

Figure 2.12: Structure 211 Abutment 1 Elevation (Section C-C)

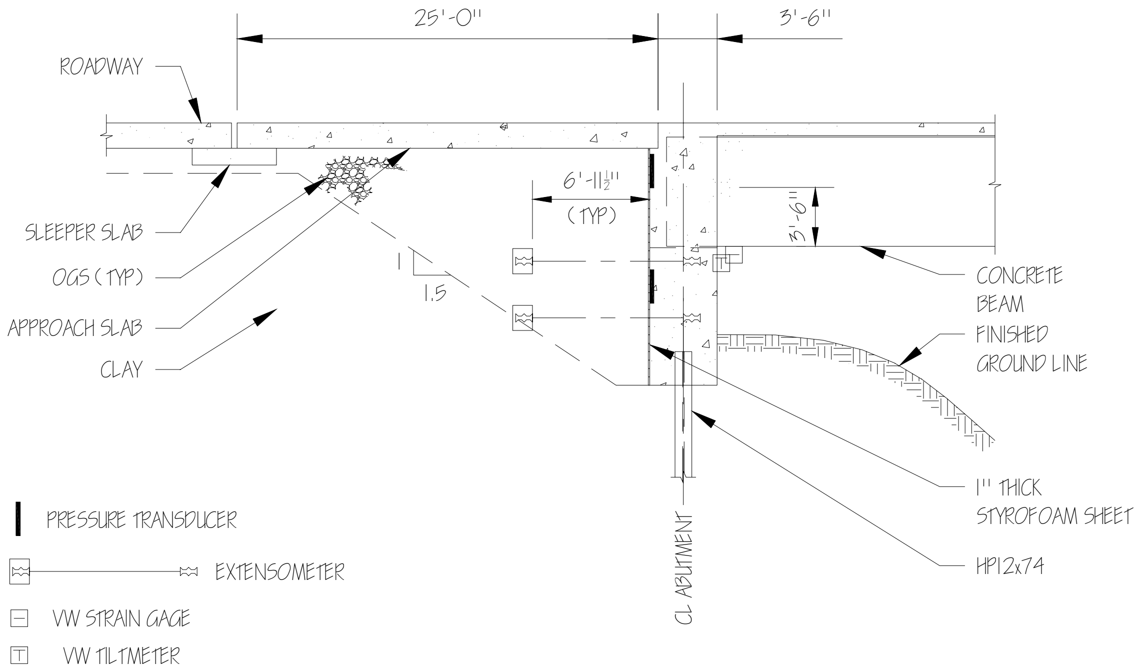

Figure 2.13: Structure 211 Cross-Section Through Abutment 1 (Section D-D)

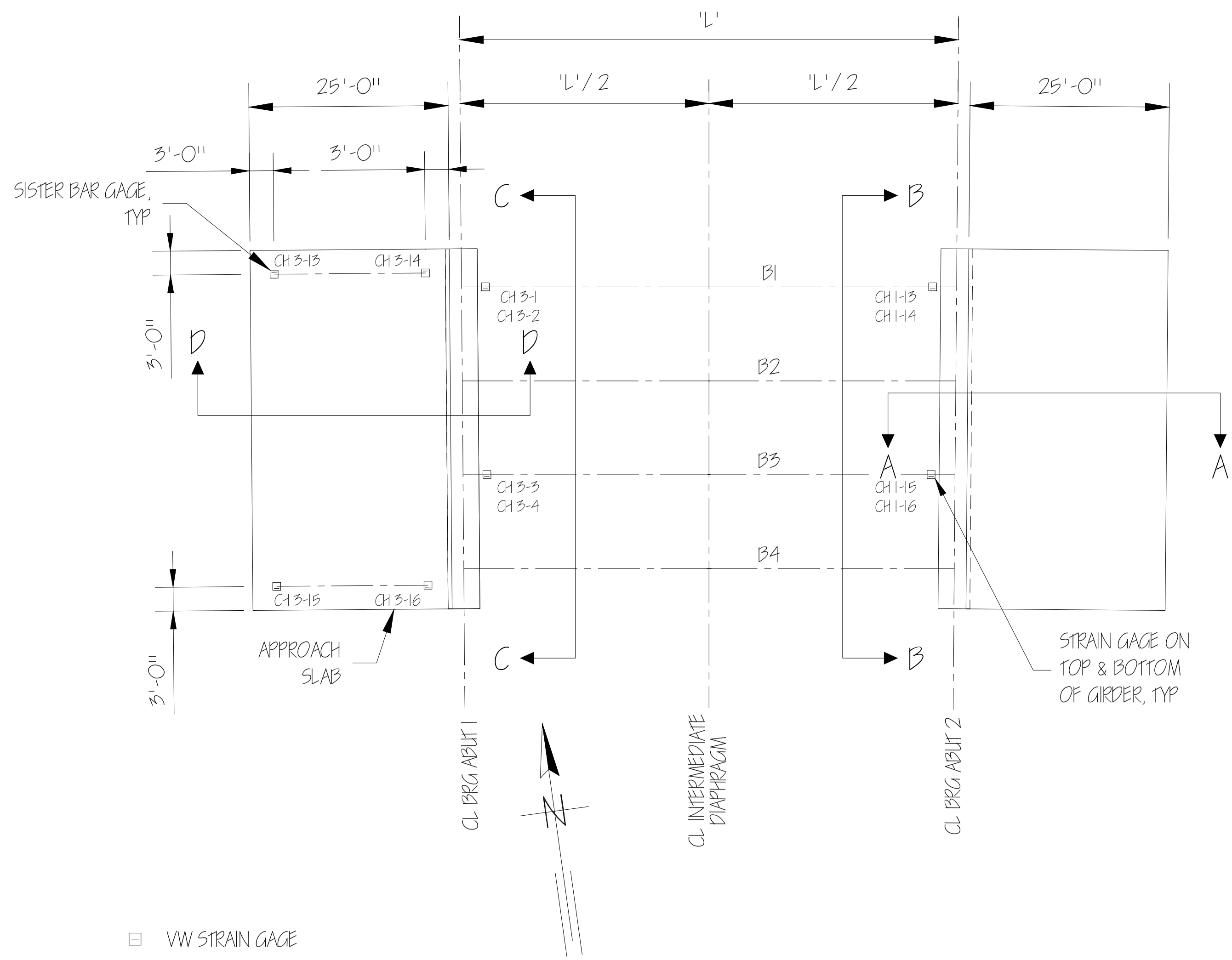

Figure 2.14:Structure 222 Instrumentation Plan

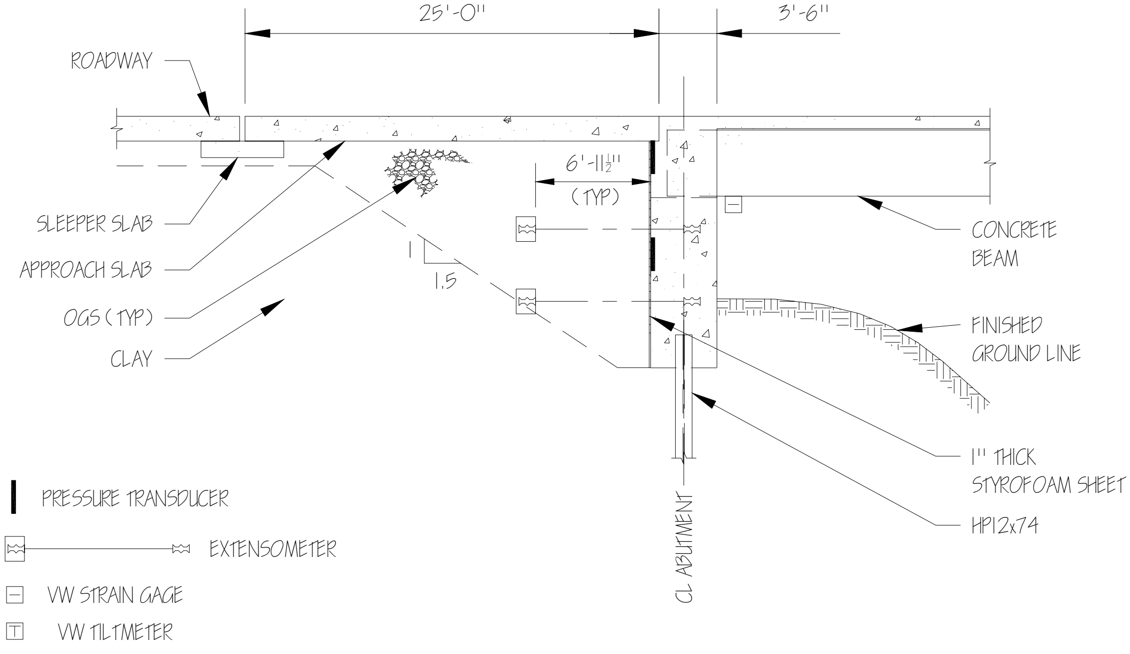

Figure 2.15: Structure 222 Cross-Section Through Abutment 2 (Section A-A)

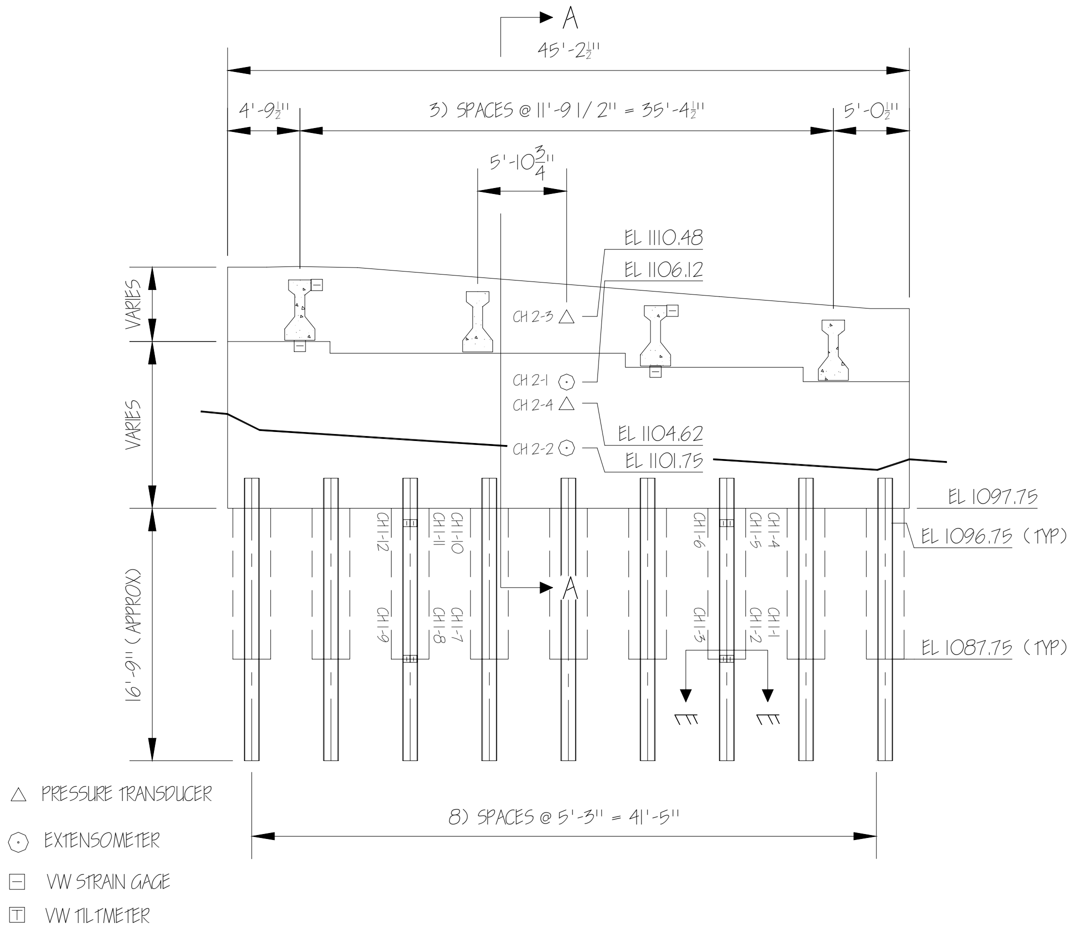

Figure 2.16: Structure 222 Abutment 2 Elevation (Section B-B)

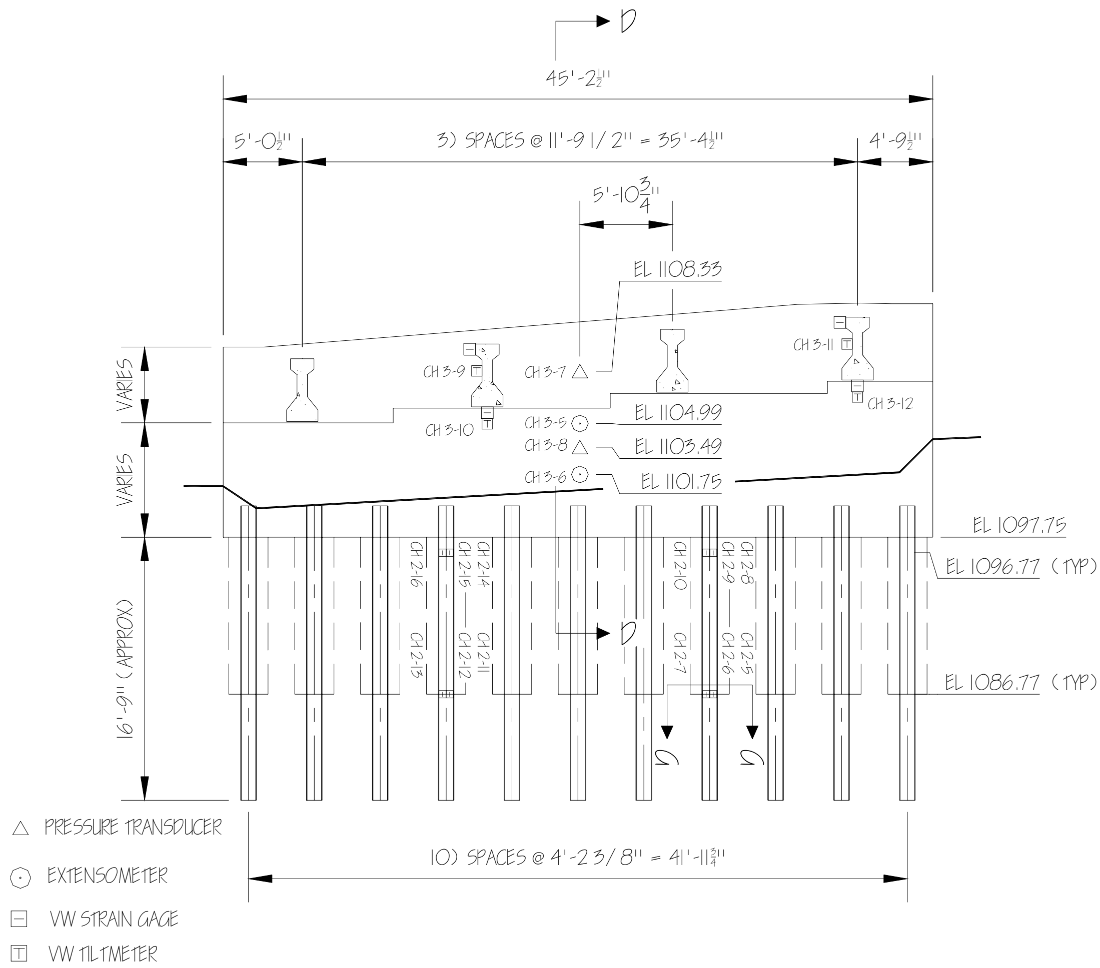

Figure 2.17: Structure 222 Abutment 1 Elevation (Section C-C)

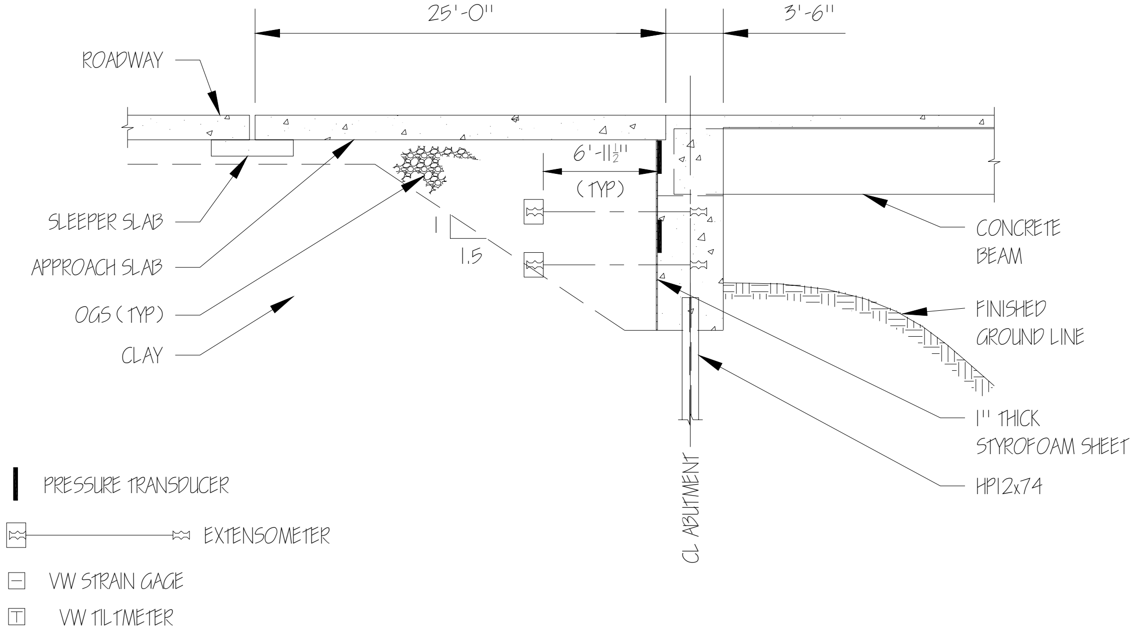

Figure 2.18: Structure 222 Cross-Section Through Abutment 1 (Section D-D)

2.2 INSTUMENTATION INSTALLATION

Installation of instrumentation completed for bridge 109 is described in this section. The 64 vibrating wire instruments consisted of 40 strain gages (VSM-4000), 5 pressure cells (VW-4820), 5 extensometers (VW-4450), 8 tilt-meters (VW-6350) and 6 reinforcing bar strain gages (VK-4911).

Pile Strain Gages

Pile strain gages were mounted on the inner face flanges of selected HP12x74 piles as shown in the previous figures. Installed elevations of the gages are also provided in the previous figures. The gages were attached prior to driving, therefore the precise, final locations were difficult to pinpoint; however, the general locations are 1'-0" and 9'-6" below the abutment bottom. Strain gages were centered 1 inch from the HP flange tip. Each gage clamp was fixed by welding, then the gage was placed in the clamps. The entire assembly of gages and cables was then protected with L2x2x$^{1}/_{8}$ cover angle. A cross-section and elevation view of installed strain gages and cover angles is presented in Figure 2.19 and a photograph of a welded strain gage on an HP pile is shown in Figure 2.20. After mounting all protective cover angles by welding, the upper, open end of the cover angle was filled with expanding foam to prevent invasion of soil and water (see Figure 2.21).

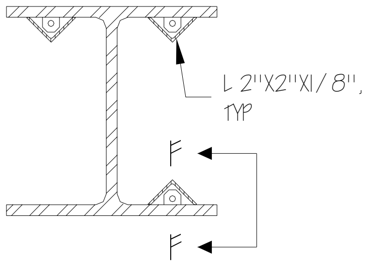

(a) Cross-Section of Pile (Section E-E)

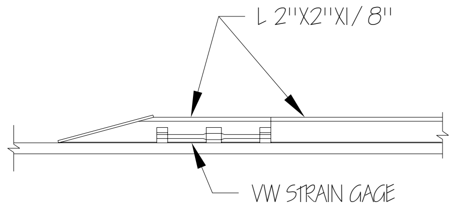

(b) End Cover Angle Detail (Section F-F)

Figure 2.19: Bridge 109 Pile Instrumentation Details and Cover Angle

Figure 2.20: Photograph of Strain Gage on H-Pile After Welding

Figure 2.21: Photograph of Strain Gage on H-Pile After Driving

Abutment/Backwall Pressure Cells

Five pressure cells were installed within the abutments. Each pressure cell was placed in the abutment concrete and oriented toward the backfill to measure backfill earth pressure. A photograph of an installed pressure cell is shown in Figure 2.22. Two pressure cells were mounted on the south abutment and located at the centerline of the abutment. Three pressure cells were mounted on the north abutment: two at the middle of the abutment and the third at the middle between the west exterior and interior girder. Detailed locations are presented in Figures 2.3 and 2.5.

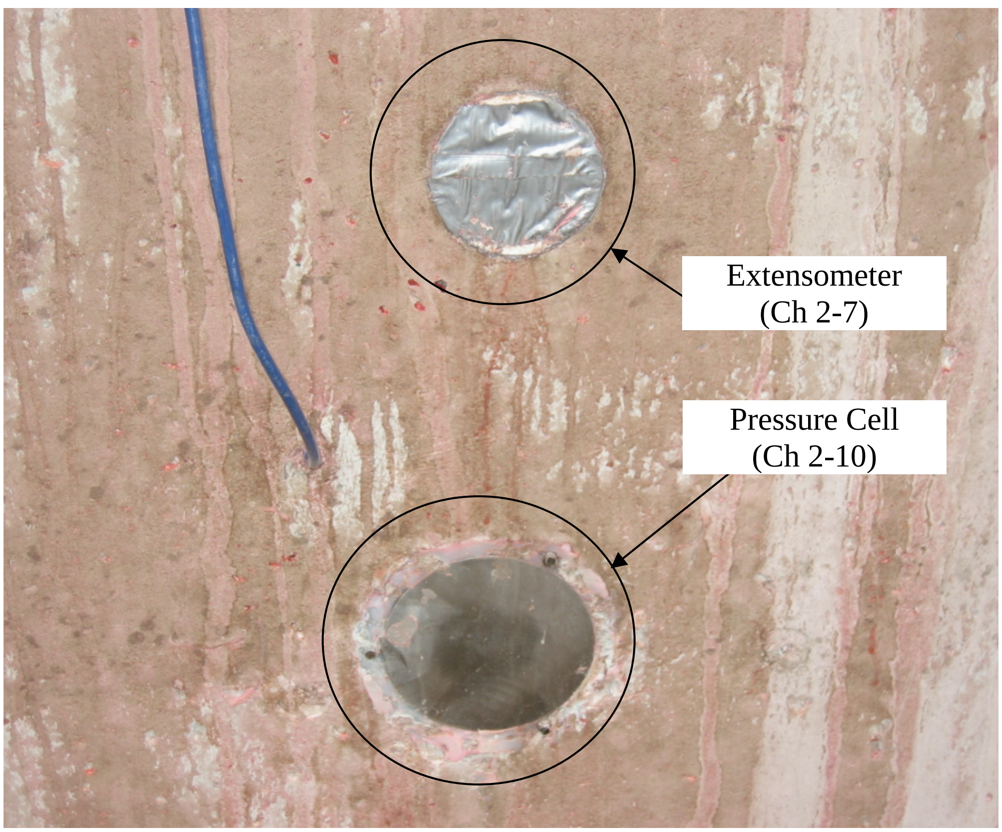

Figure 2.22: Photograph of Installed Pressure Cell on North Abutment

Abutment/Backwall Displacement Transducers

Four borehole extensometers were installed for both abutments as shown in Figures 2.2 and 2.4. Two extensometers were positioned in the north abutment and two were positioned in the south abutment. The extensometers measured horizontal displacement directly and indirectly measured rotation of the abutment. A detailed cross-section of the typical extensometer installation is presented in Figure 2.23. One-ft-6-inch cube concrete blocks (see Figure 2.24) were constructed at the fixed end of the borehole extensometer using an embedded, groutable anchor in the backfill and a long, steel rod. The extensometer displacement transducer was connected at the abutment to the long, steel rod forming the free end. The extensometer transducers are protected with PVC tubing inside the abutments (see Figure 2.25). Extensometer cabling is shown in Figure 2.26, viewed from the bridge side of the abutment.

Abutment/Girder Tilt Meters

A total of eight tilt meters were mounted on bridge 109 girders. One tilt meter each was mounted on the west interior girder of span 1 and span 4, respectively. One tilt meter each was mounted on the east exterior girder of span 1 and span 4, respectively. Each of these four tilt meters was placed at the vertical center of the girder web to monitor girder rotation at each end. Two tilt meters each were mounted on the north and south abutments directly adjacent to the instrumented girders. Biaxial brackets were used to fix the location of the tilt meters and arrange the rotation as designed (see Figure 2.27). The rotations from abutment and girder tilt meters were positioned to allow comparison between girder and abutment rotation.

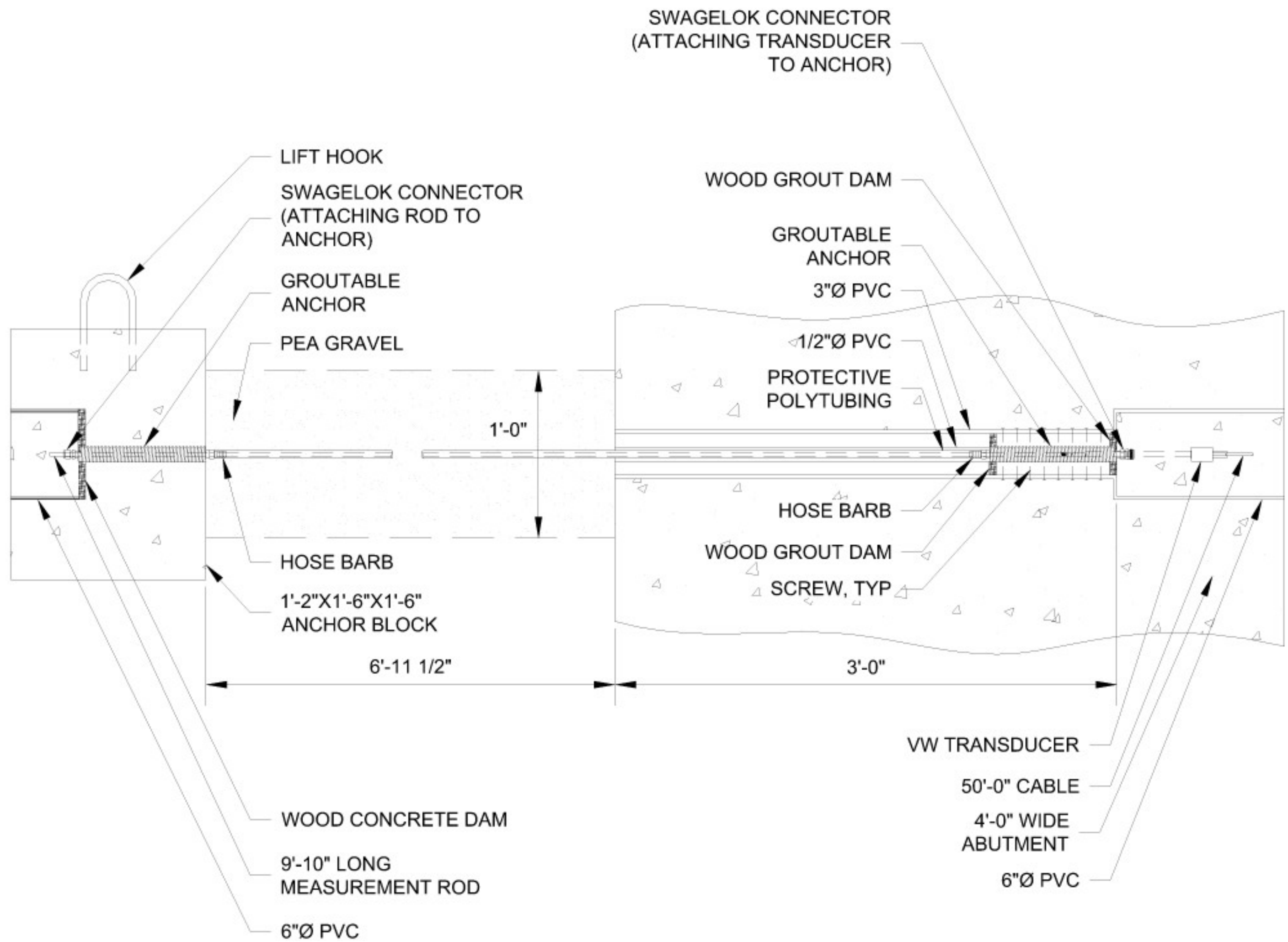

Figure 2.23: Cross-Section of Extensometer Instrumentation

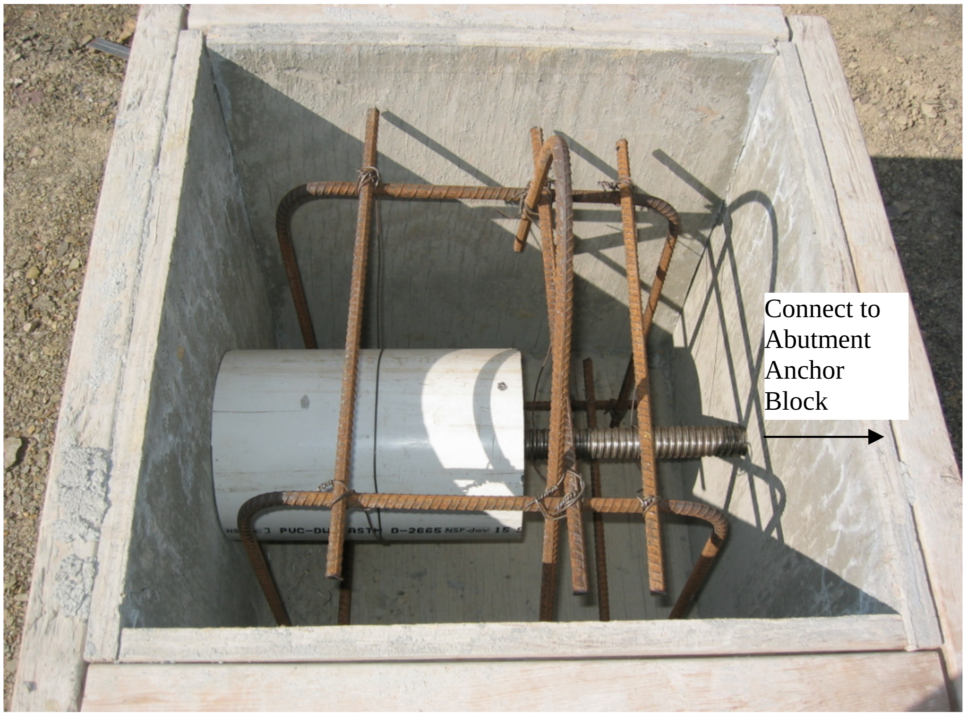

Figure 2.24: Photograph of Form Work of Concrete Block for Extensometer

Figure 2.25: Photograph of Plan View of Installed Plastic Tube for Extensometer

Figure 2.26: Photograph of Extensometer on Front Face of Abutment

Figure 2.27: Photograph of Installed Tilt Meter and Bracket on Abutment

Girder Strain Gages

A total of sixteen strain gages were mounted to prestressed concrete girders on bridge 109. Eight strain gages were attached in span 1 and eight gages were attached in span 4. The gages were all located 1 ft from the front face of the respective abutments for span 1 and span 4. In each span, two strain gages were mounted on each of the four girders, one gage at the bottom flange and one gage on the side of the top flange. The strain gage at the bottom flange was placed at the centerline of the bottom flange and the strain gage on the top flange was located 1½ inches from the bottom edge of top flange. Strain measurements consist of major axis bending moments and axial forces at the respective locations. A photo of a mounted girder strain gage on the bottom flange is shown in Figure 2.28.

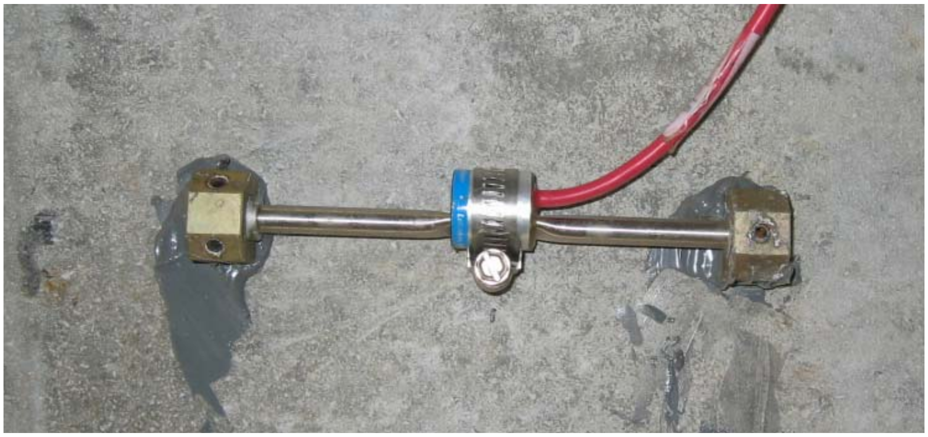

Figure 2.28: Photograph of Mounted Strain Gage on Bottom Flange of Girder

Approach Slab Reinforcing Bar Strain Gages

Six reinforcing bar strain gages (sister bar gages) were installed in the approach slabs: two strain gages in the south abutment approach slab and four strain gages in the north abutment approach slab (see Figure 2.1). Each gage was located at mid-thickness of the approach slab to minimize strains due to flexure. These sister bar gages are installed to measure the strains developed due to drag of the approach slabs. The actual strain gage installed in reinforcing bar cage is shown in Figure 2.29.

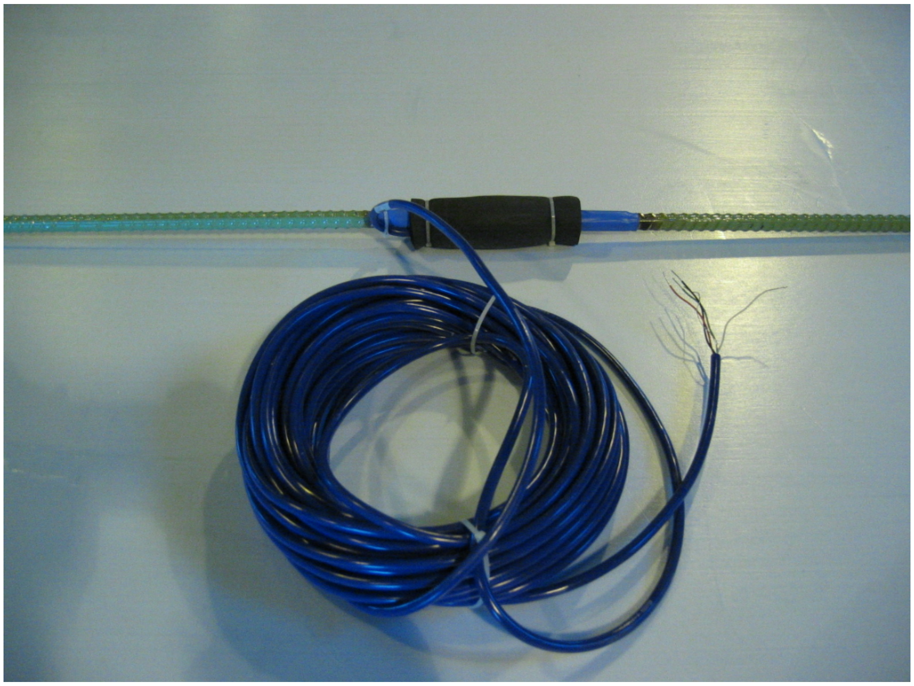

Figure 2.29: Photograph of Sister Bar Strain Gage

CHAPTER 3

COLLECTED DATA

This chapter presents collected data from the weather station and the four instrumented bridges. Weather station data collection was initiated in August 2002. Data collection at bridges 203, 211, 203, and 109 was initiated in November 2002, September 2004, November 2003, and September 2005 respectively. The data sampling rate at all locations for all instruments was set to a period of 15 minutes. All data were collected manually on a monthly basis; however, the data acquisition systems were capable of remote download via cell phones. Data obtained from each weather station instrument and each bridge instrument were plotted, including 7-day averages and data envelope in order to present the overall tendency and daily variations of the actual field data.

3.1 WEATHER STATION

Data obtained from the weather station consisted of ambient temperature, relative humidity, air pressure, solar radiation, wind speed, wind direction, and rainfall. Presented here are ambient temperature, relative humidity, air pressure, and solar radiation.

Ambient temperature is presented in Figure 3.1. The temperature ranged from 0 °F in January to 90 °F in July with the corresponding 7-day average varying from 14 °F to 70 °F. Daily temperature ranges from 25 °F to 40 °F, indicating a fluctuation of daily temperatures. Ambient temperature serves as an important analysis parameter in FE models to determine longitudinal abutment displacements induced by thermal bridge expansion and contraction.

Relative humidity data are presented in Figure 3.2. Relative humidity varied over the time period from 15 to 100 percent with the 7-day average ranging from 45 to 95 percent. The average relative humidity over the 43-month collection period was 77 percent, 7 percent greater than the design value of 70 percent specified in AASHTO LRFD (2004) for a central area of Pennsylvania.

Barometric pressure data are presented in Figure 3.3. The barometric pressure varied from 28.8 to 30.4 inches Hg (975 to 1029 mbar) over the 43-month collection period. The average pressure over the period was 29.7 inches Hg (1006 mbar). Air pressure serves as an input parameter used in conjunction with pressure cell data to determine earth pressures behind abutments and backwalls.

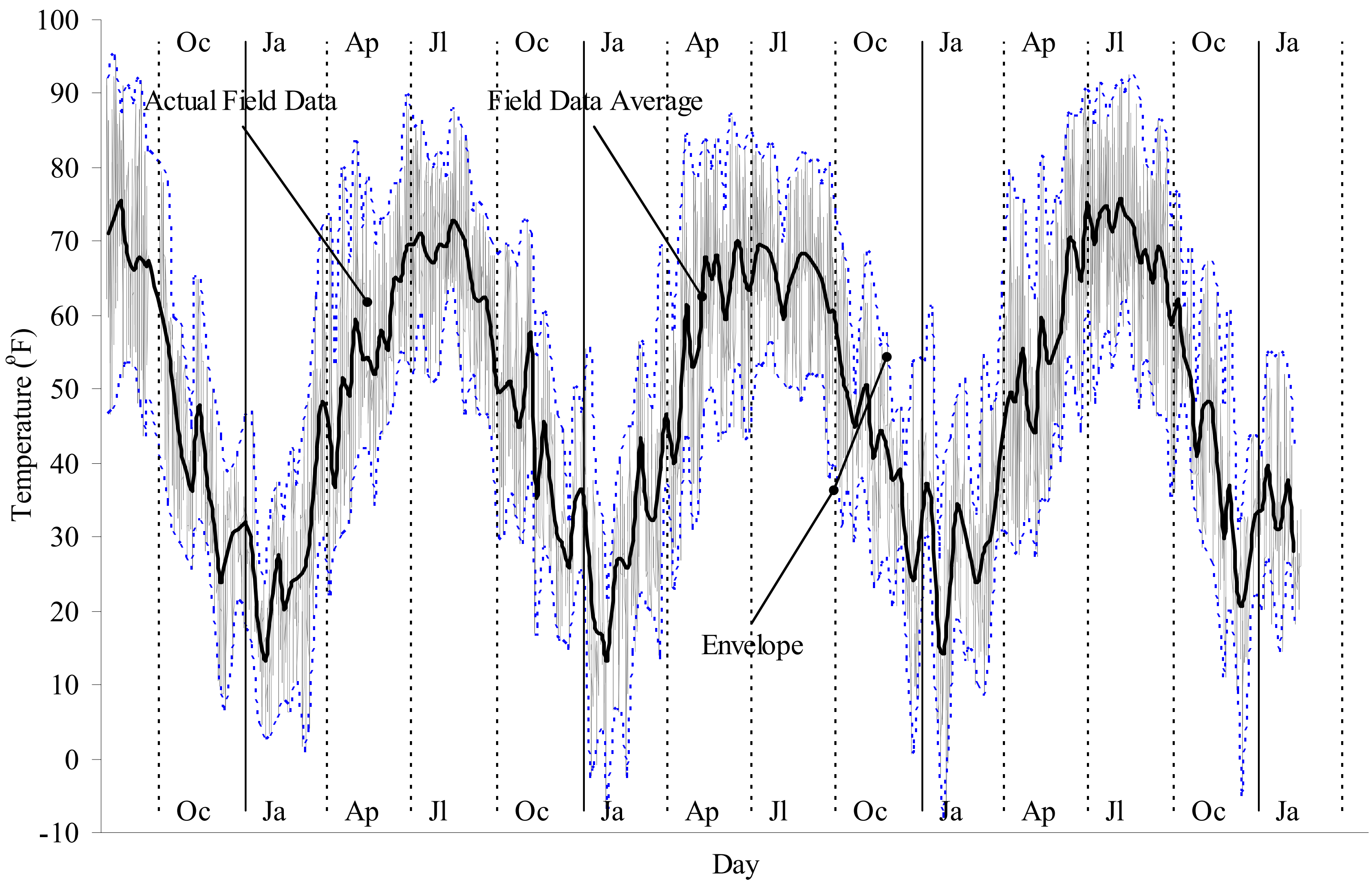

Figure 3.1. Ambient Air Temperature

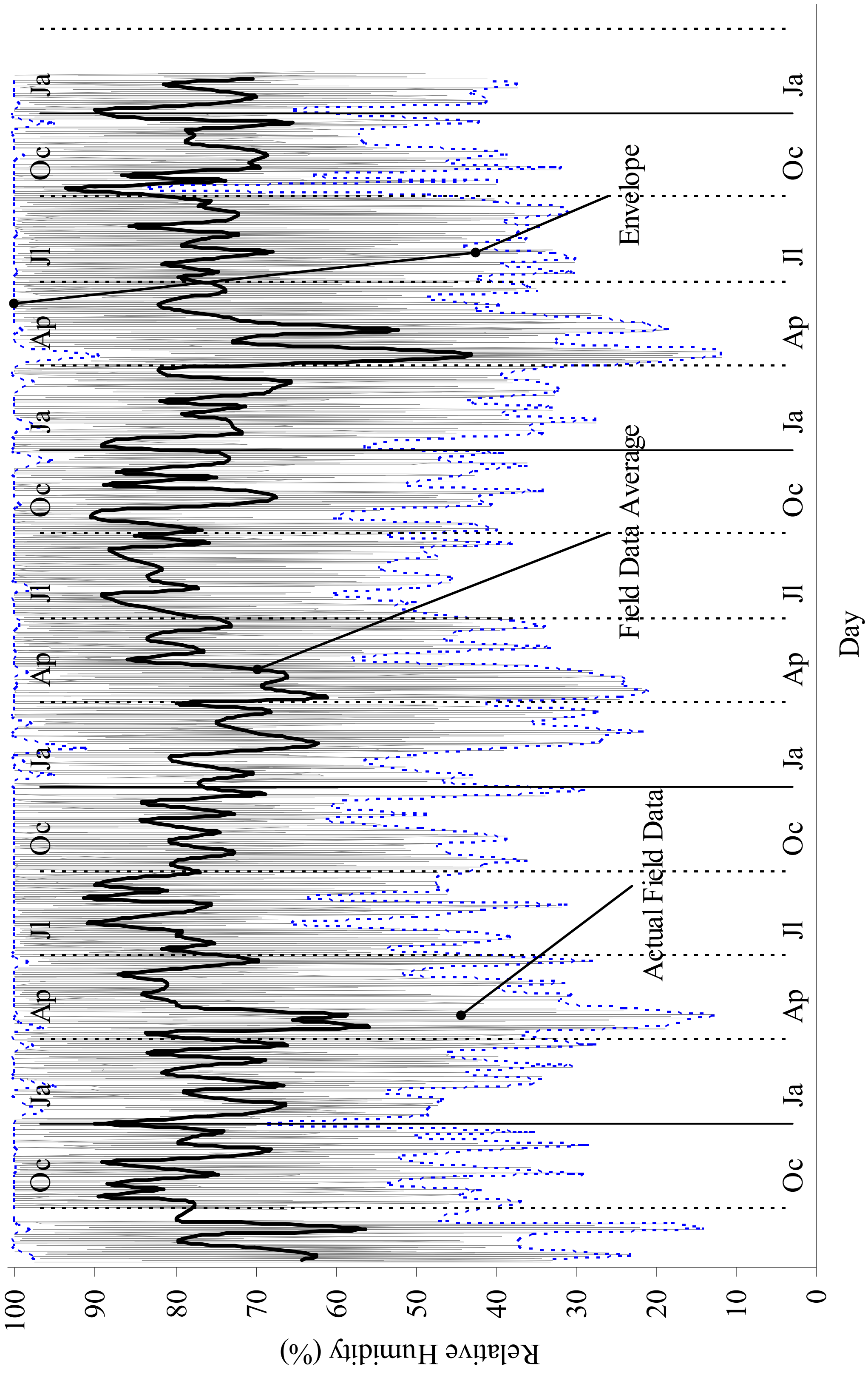

Figure 3.2. Relative Humidity

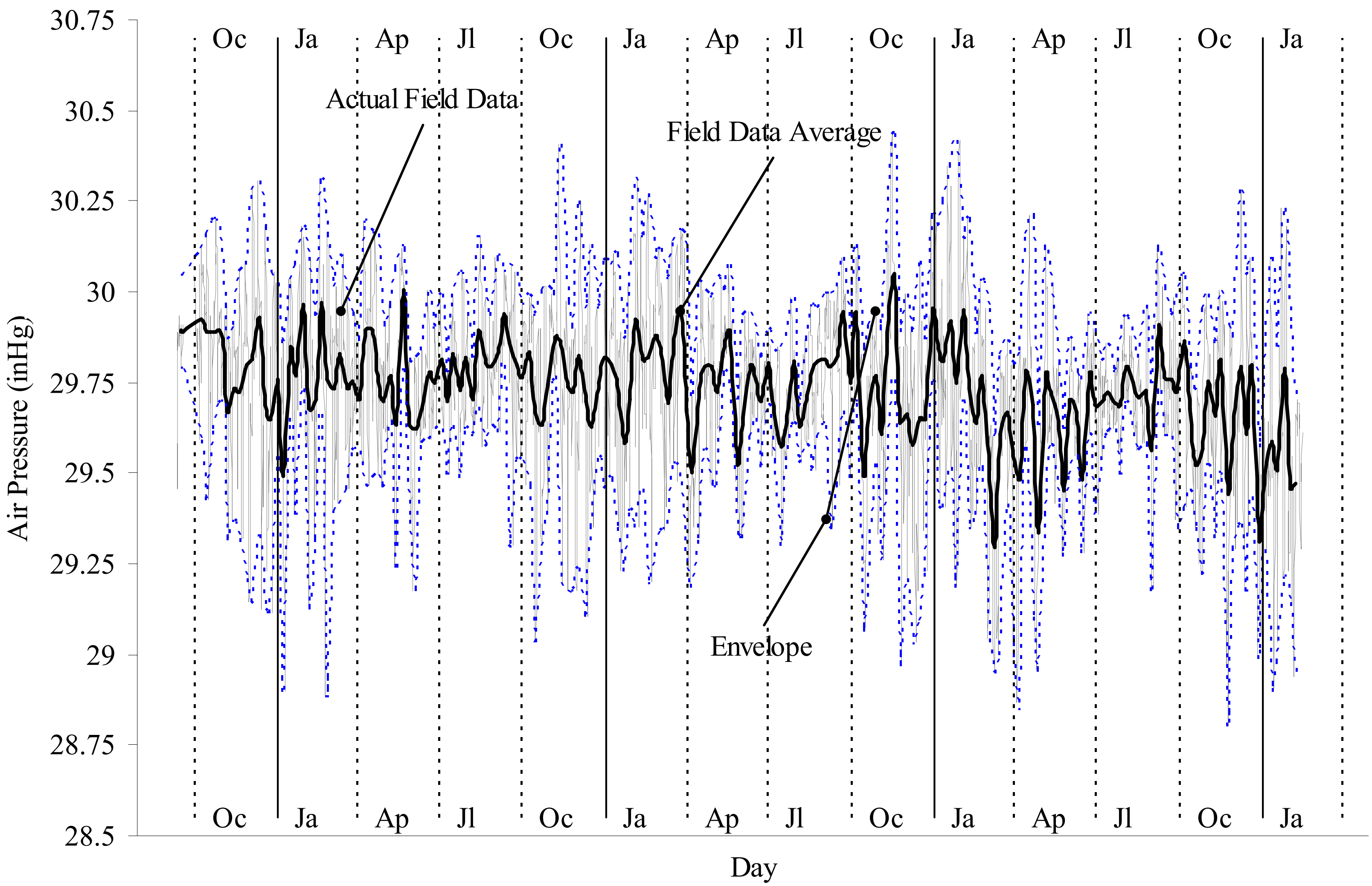

Figure 3.3. Air Pressure

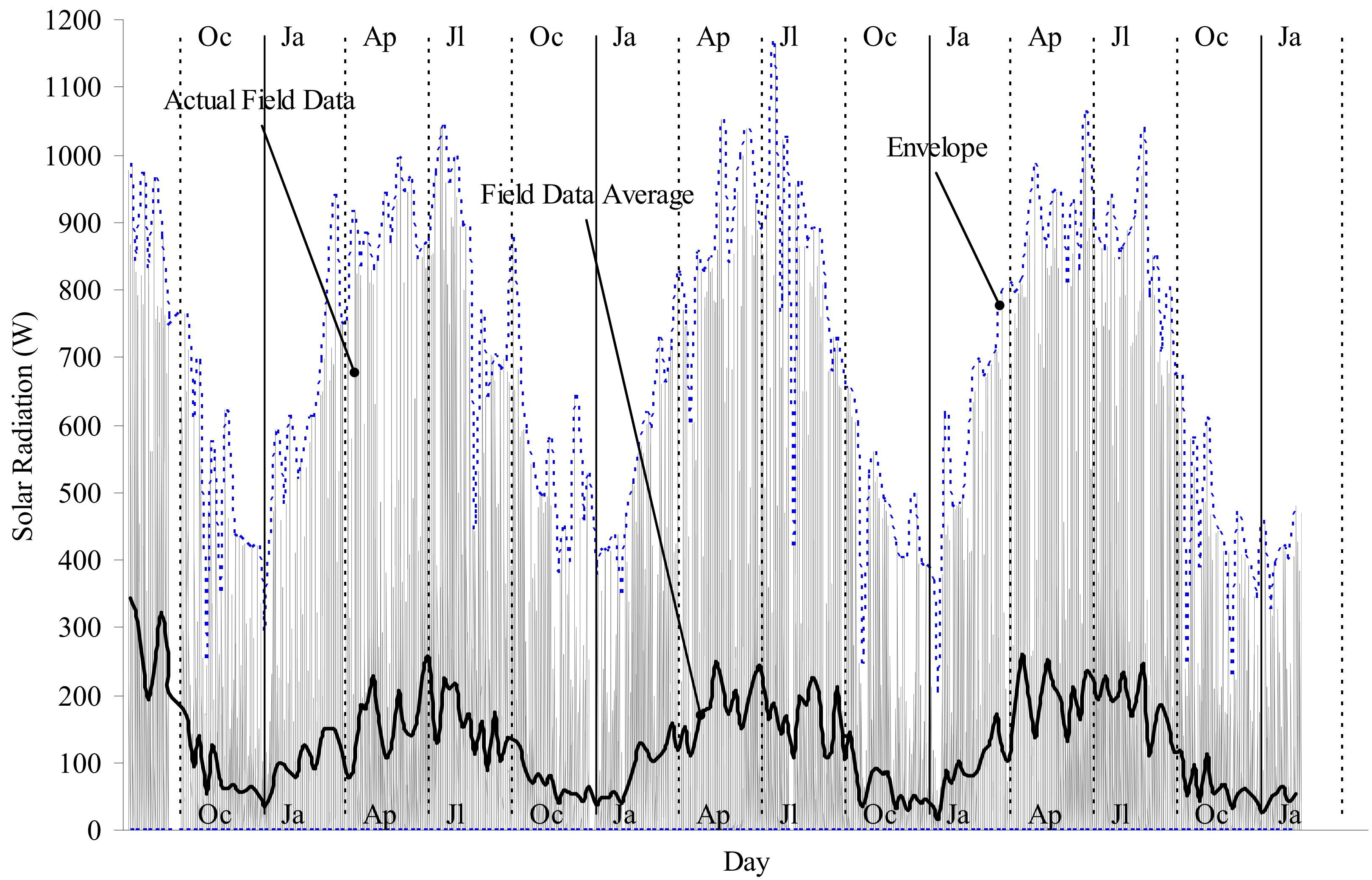

Figure 3.4. Solar Radiation

Solar radiation data are presented in Figure 3.4. The solar radiation over the collection period varied from 0 to 1100 watts and the corresponding 7-day average varied from 40 watts in January to 250 watts in July.

3.2 BRIDGE 203 MONITORING RESULTS

This section presents field data obtained from bridge 203 instruments consisting of 3 extensometers, 3 pressure cells, 8 tilt meters, 30 strain gages on 2 piles, 16 strain gages on 4 prestressed concrete girders, and 4 sister bar gages. Of the 64 instruments total installed on bridge 203, there were initially 3 damaged strain gages on the east pile (Channels 1-4, 1-7, and 4-9) and 1 damaged strain gage on the west pile (Channel 4-16). There were two additional damaged strain gages on the east pile (Channels 1-2 and 4-8) since September 2004 and October 2004, respectively, and one additional damaged strain gage on the west pile (Channel 1-10) since October 2005. However, the thermostats of all 7 damaged strain gages continue to function.

Extensometer data are presented in Figure 3.5. These three extensometers measure longitudinal abutment displacements. As can be observed from Figure 3.5, both top extensometers measured a similar trend during the first 10 months of data collection, then diverged. The top corner extensometer reveals the overall contraction trend with greater displacement amplitude while the overall expansion trend is observed from the data of the top center extensometer. Over the collection period of 40 months, the top corner extensometer measured the maximum contraction displacement of 0.42 inches during winter 2005/2006 and the maximum expansion displacement of 0.1 inches during summer 2003. The top center extensometer measured the maximum contraction displacement of 0.2 inches during winter 2003/2004 and the maximum expansion displacement of 0.2 inches during summer 2005. The bottom extensometer data indicate continuous movement of the lower abutment toward the bridge with the maximum current displacement of 0.2 inches.

Pressure cell data are presented in Figure 3.6. The three pressure cells measure earth pressures behind the abutment and backwall. As can be observed from Figure 3.6, both center pressure cells measured similar earth pressure magnitudes because they are both located near the girder elevation. Earth pressures obtained from the bottom center pressure cell are greater by approximately 2 psi, as expected due to the deeper elevation. Over the 40-month collection period, the top center pressure cell measured a maximum earth pressure of 17 psi during summer 2005 and the bottom center extensometer measured a maximum earth pressure of 19 psi during summer 2005. The top corner cell measured the smallest pressure amplitude and daily variations, measuring a maximum earth pressure of 8.5 psi during summer 2005.

Abutment tilt meter data are presented in Figure 3.7. All four tilt meters measured a similar trend of abutment rotations. There were abrupt changes in data during June 2003 for the tilt meter at the centerline of girder 1 and during July 2003 for the tilt meter at the centerline of girder 4 of approximately 0.06 and 0.03 degrees, respectively. These data anomalies are attributed to construction personnel as the instruments are within reach from grade. Tilt meter data are intended to measure changes in rotation rather than absolute angles; therefore any anomalies can be corrected. Corrected data at the four tilt meters located at girder 1, 2, 3 and 4 centerlines are maximum changes in rotation of 0.07, 0.16, 0.12, and 0.09 degrees, respectively. These abutment rotations derived from tilt meters are consistent with rotations derived from extensometers data with the abutment base continuously displacing toward the bridge. In addition, the center section of the abutment supporting the two interior girders rotates farther than the end sections of the abutment.

Girder tilt meter data are presented in Figure 3.8. These four tilt meters were placed directly on girders 1 through 4, respectively. The tilt meter on girder 1 measured a rotation trend marginally different from the other three girder tilt meters. It can be observed that the rotation amplitudes of the interior girders are greater than the rotation amplitudes of the exterior girders and that the angle between the abutment and the girder continues to close, consistent with all other measurements.

H-pile bending moments about the weak axis on the west pile are presented in Figure 3.9. The bending moment was calculated using the three strain gage data set installed at the same elevation. There are three sets of three gages installed on the west pile: one at depth = 2′-5″; a second at depth = 6′-5″; and the third at depth = 11′-5″ from the abutment base. As can be observed from Figure 3.9, the moments at all depths indicate that pile bending is continuously increasing, with the pile head moving toward the bridge. This observation is consistent with data obtained from extensometers and tilt meters on the abutment. Initial moment magnitudes of +25, +3, and -7 ft-kips at the depths 2′-5″, 6′-5″, and 11′-5″ are primarily due to pile driving and initial crookedness. Over the 40-month collection period, the moments at the three depths reached maximum values of +55, +18, and -9 ft-kips. The H-pile plastic moment capacity = 194 ft-kips (F_y = 50 ksi).

H-pile bending moments about the weak axis on the east pile are presented in Figure 3.10. Due to the strain gage damage discussed previously, limited reporting of moments was possible. The initial moment magnitude was -10 ft-kips and remained nearly constant over the 23-month collection period. The very small variation in the moment over time is due to the location of the gages at a depth of 13′-3″ below the abutment, near the point of fixity.

H-pile axial force in the west and east piles is presented in Figure 3.11 and Figure 3.12. Pile axial force was calculated at each strain gage installed at the pile cross section neutral axis, intended for measuring pile down-drag forces. There are five strain gages on each pile at five depths. Pile axial forces varied from 67 to 107 kips for the west pile and from 40 to 100 kips for the east pile. The strain gages on both piles indicate downdrag forces of approximately 5 to 15 kips during the period from November 2002 to August 2003.

Girder strain data are presented in Figure 3.13 through Figure 3.16. At the two instrumented locations on each girder; abutment end and end-span mid-span, two strain gages were placed on the top and bottom flanges, as described previously. End strains suggest a small and consistent girder tension, indicating contraction resulting from concrete creep and shrinkage. Strains at girder mid-span were not consistent between girders 3 and 4. Over the 40-month collection period, girder 3 strains indicate expansion of approximately 450 $\mu\varepsilon$, while girder 4 strains indicate contraction of approximately 150 $\mu\varepsilon$.

Sister-bar strain data at the approach slab are presented in Figure 3.17. Sister bar gages measured steep changes in compressive strain ranging from 100 to 200 $\mu\varepsilon$ during the early life of the approach slab, indicating shrinkage effects. Thereafter, a more gradual effect was observed in the four instruments, primarily attributed to seasonal temperature changes.

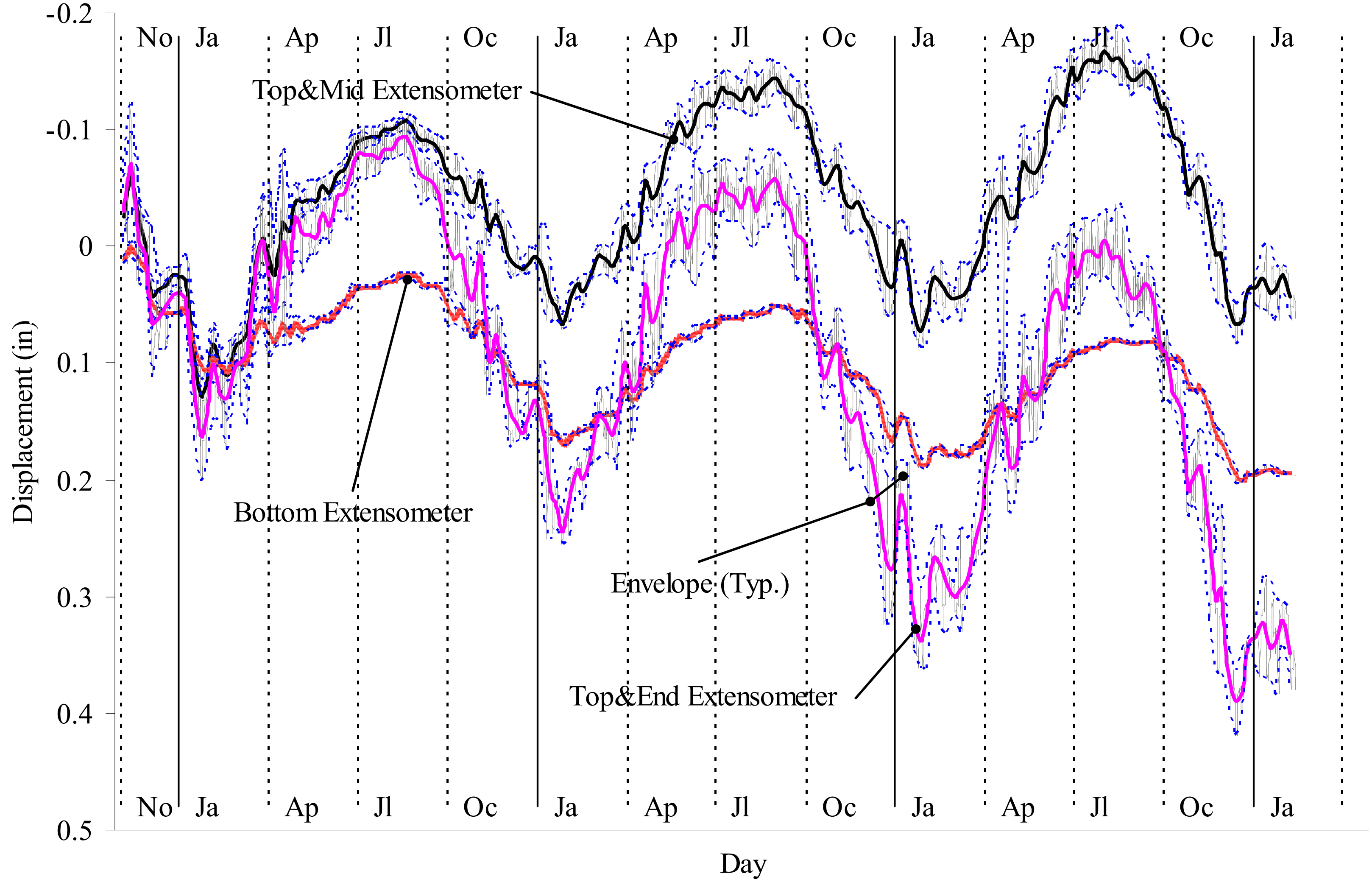

Figure 3.5. Bridge 203: Extensometers

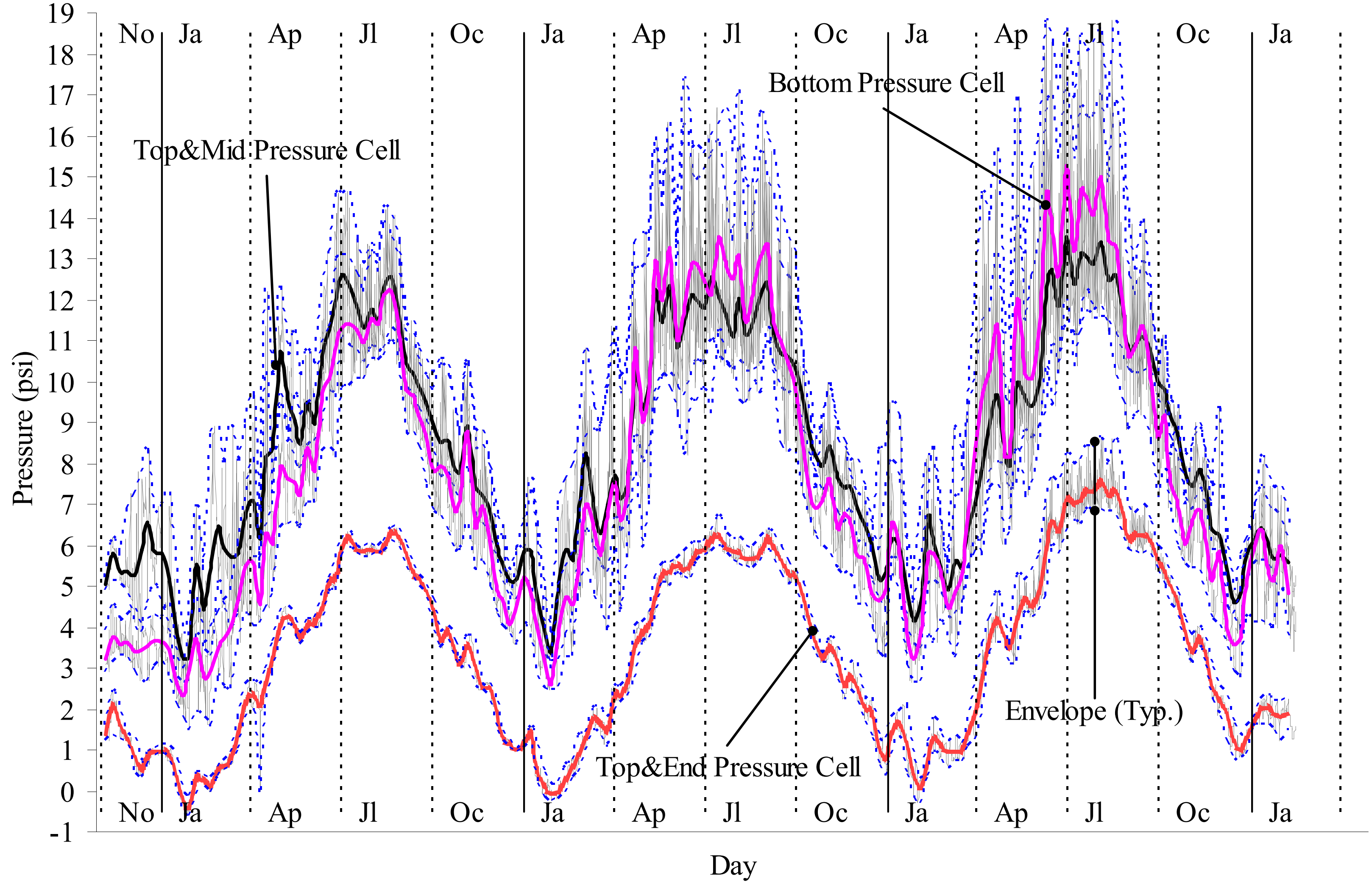

Figure 3.6. Bridge 203: Pressure Cells

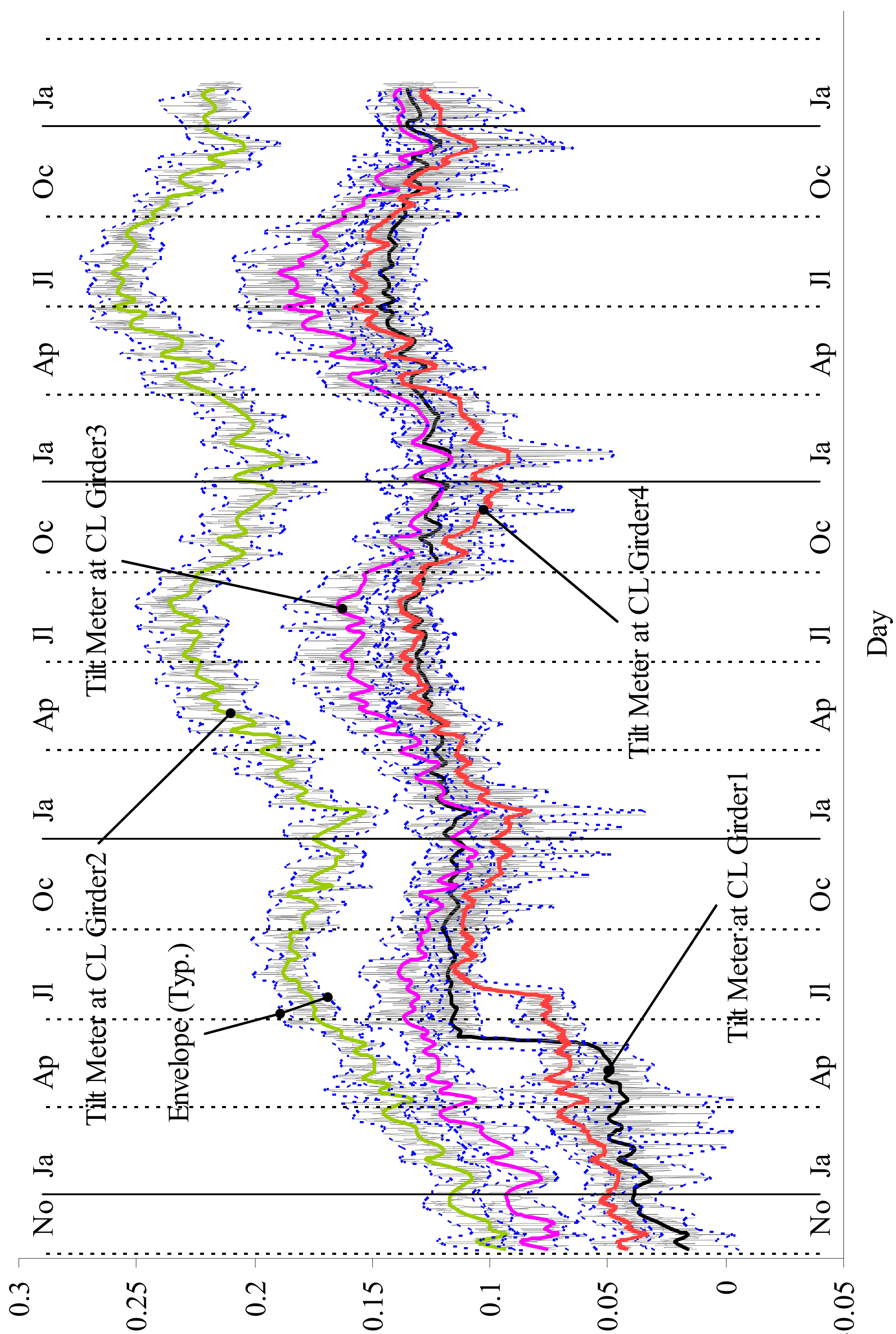

Figure 3.7. Bridge 203: Tilt Meter (On Abutment)

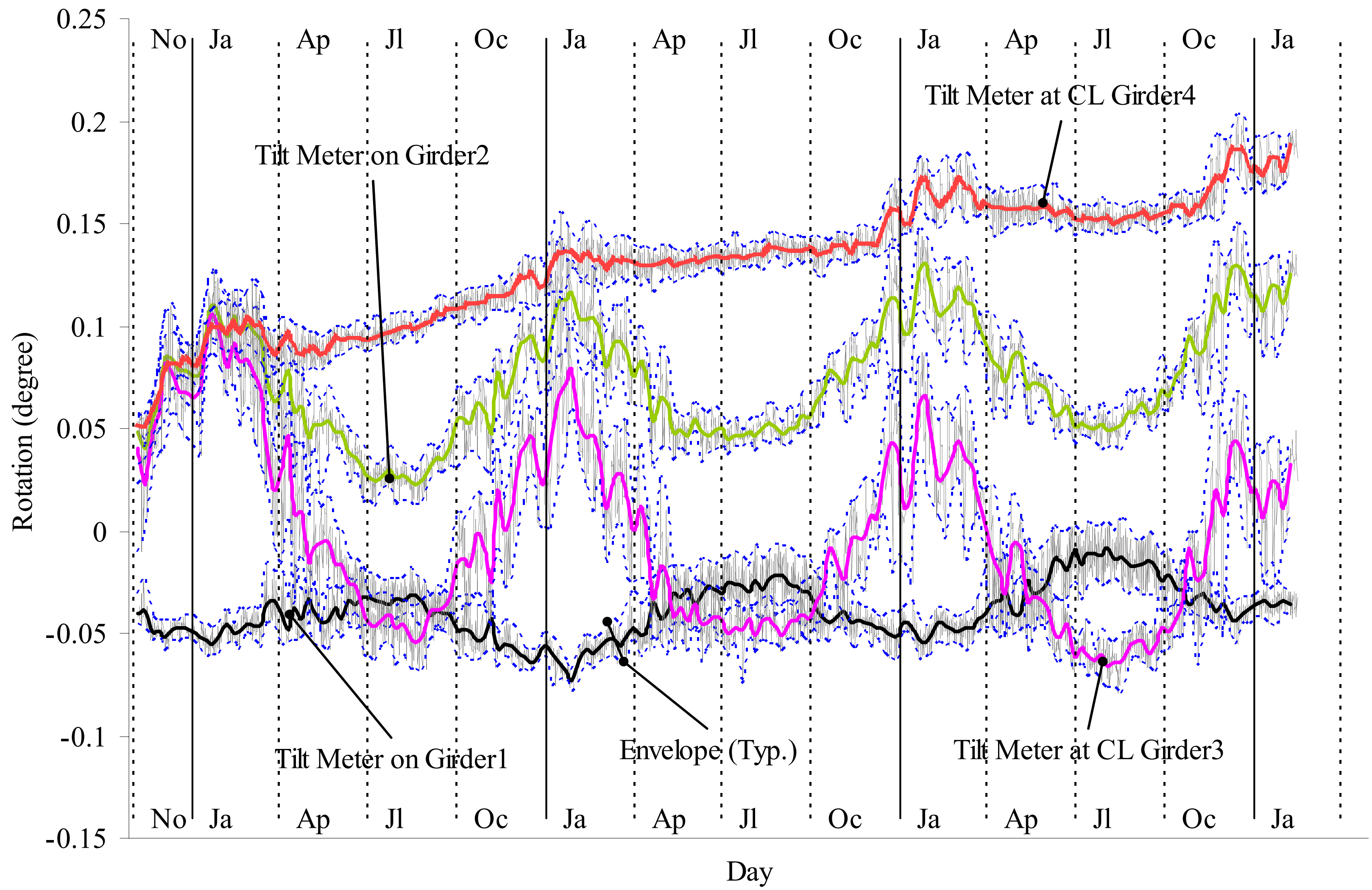

Figure 3.8. Bridge 203: Tilt Meter (On Girders)

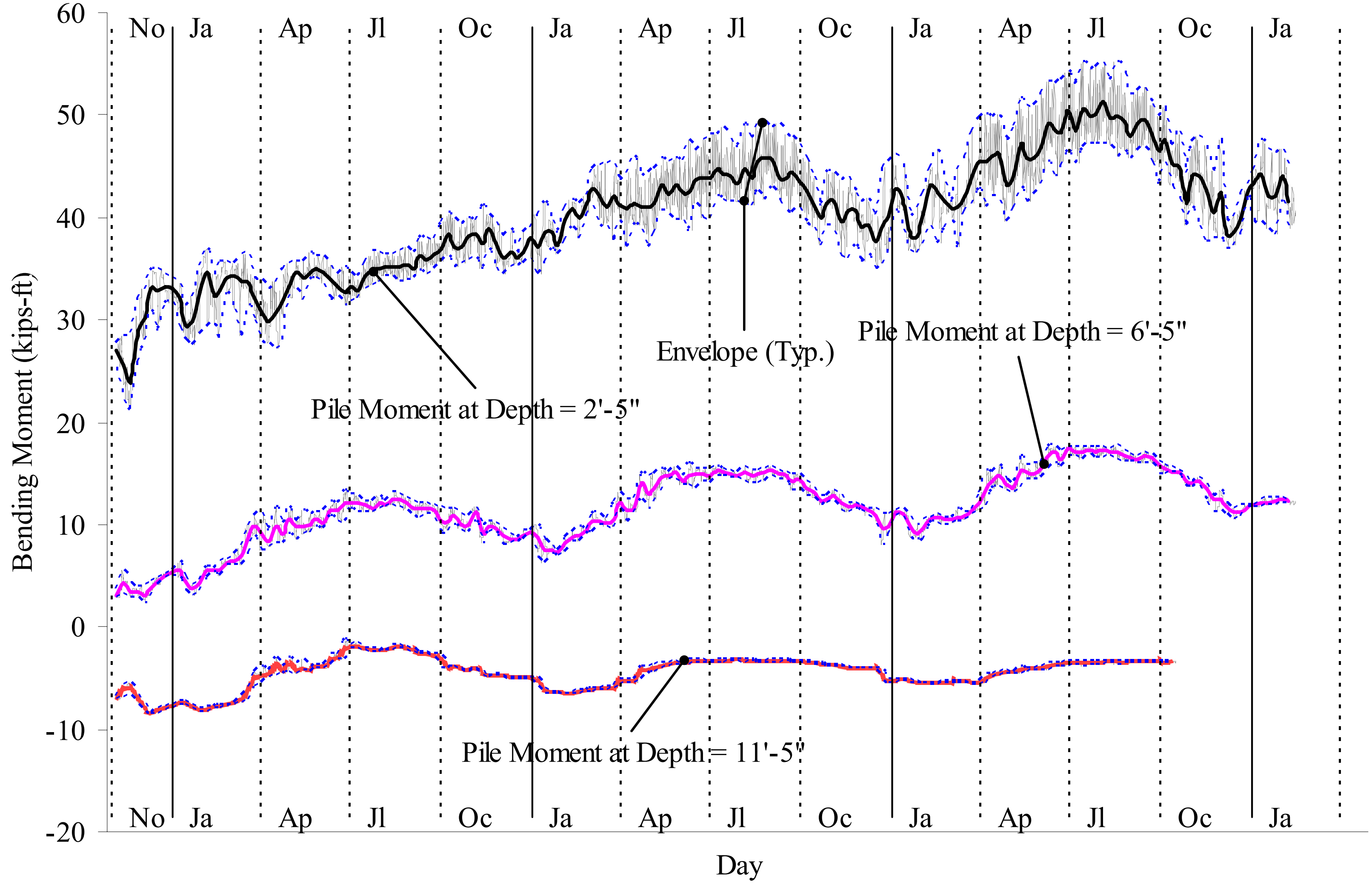

Figure 3.9. Bridge 203: Moments on West Pile

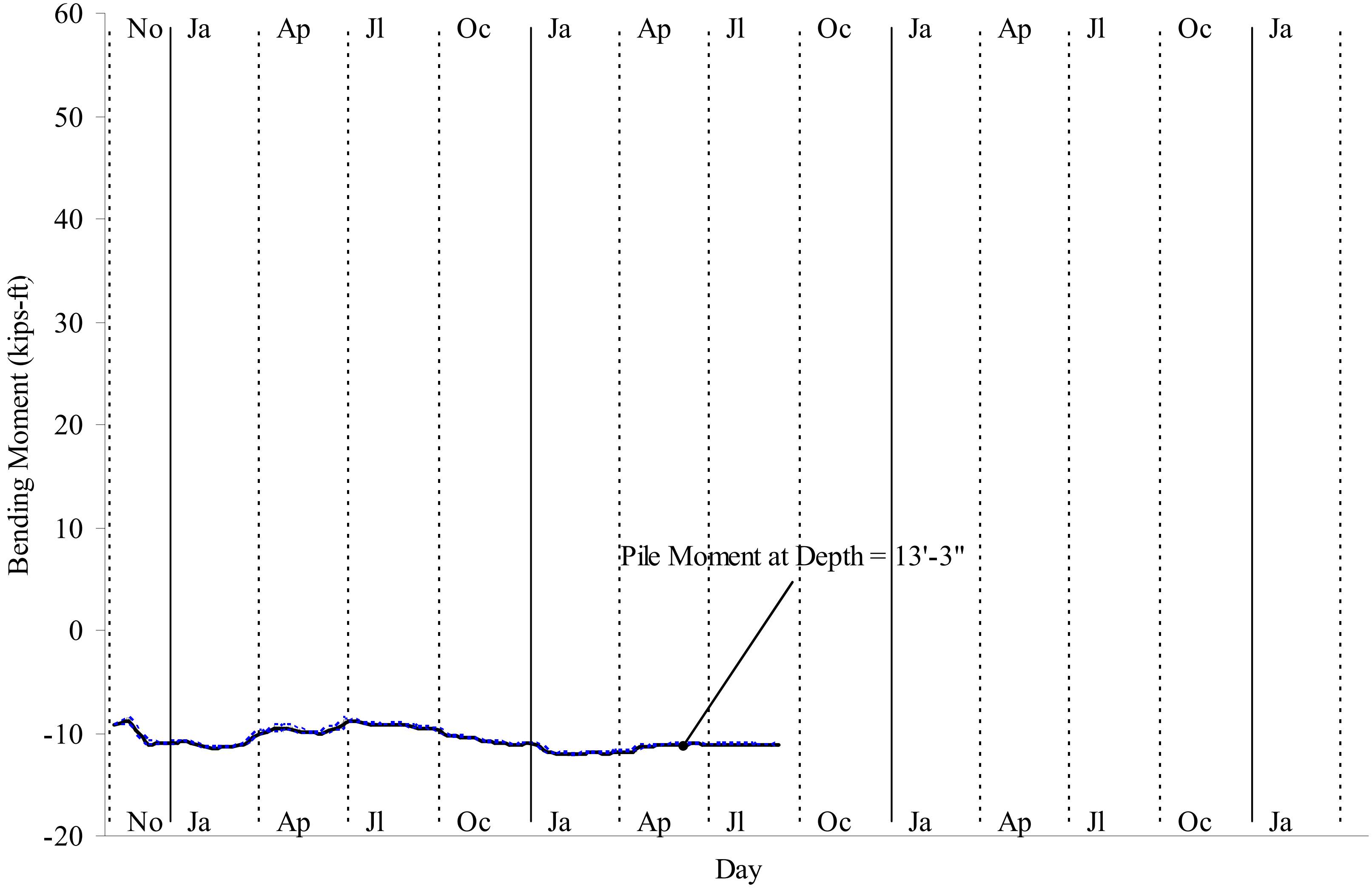

Figure 3.10. Bridge 203: Moments on East Pile

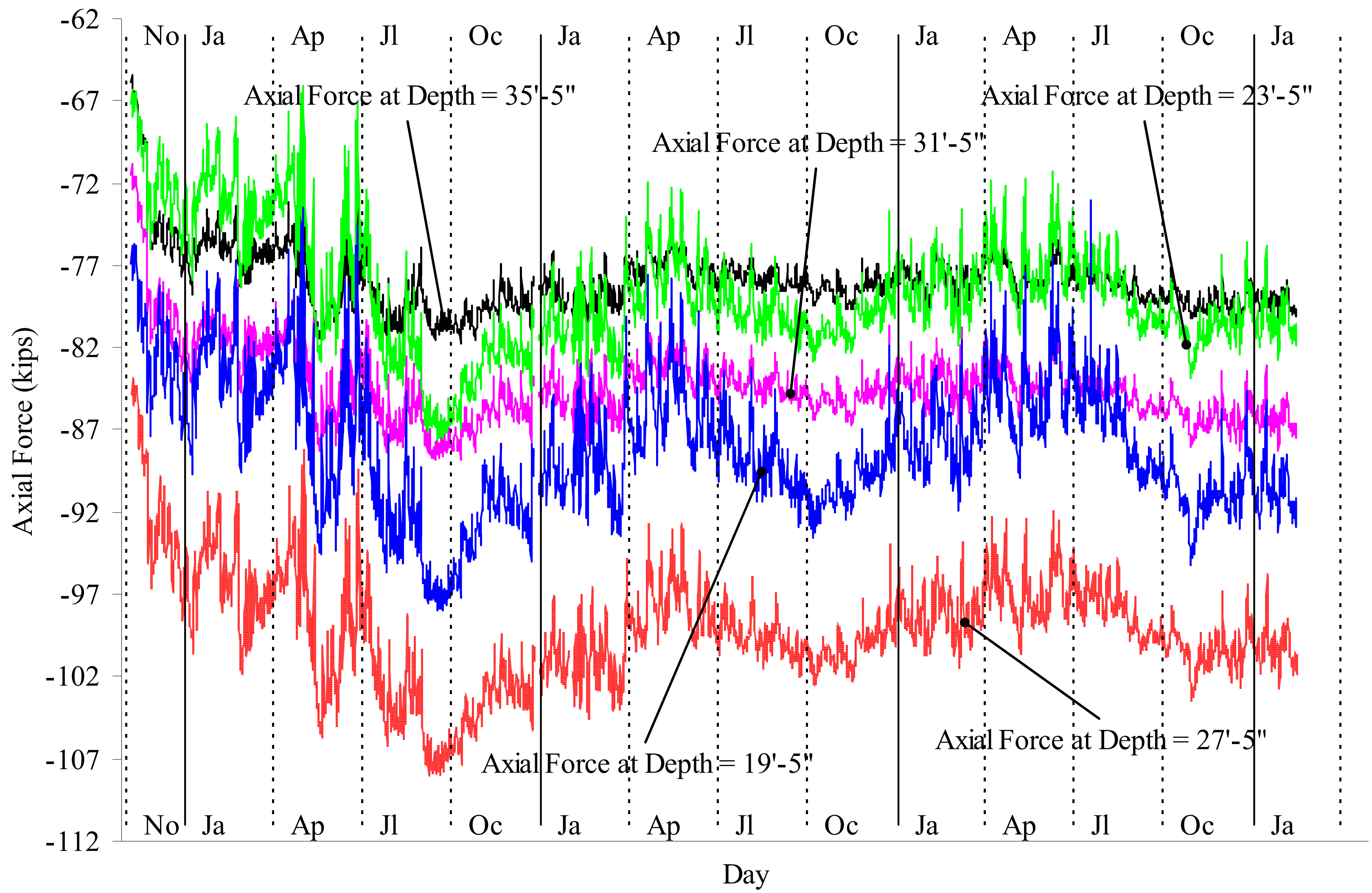

Figure 3.11. Bridge 203: Axial Forces on West Pile

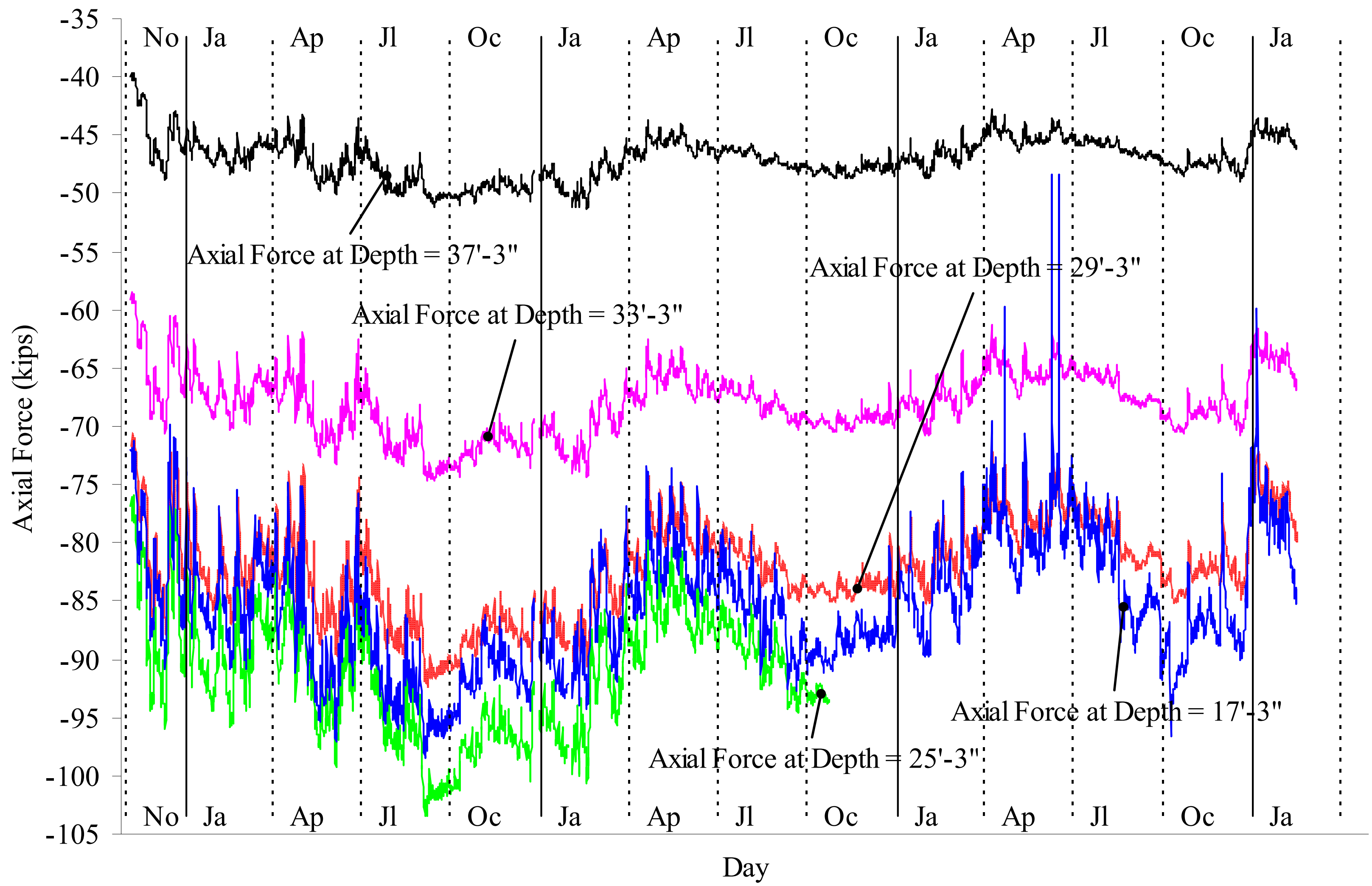

Figure 3.12. Bridge 203: Axial Forces on East Pile

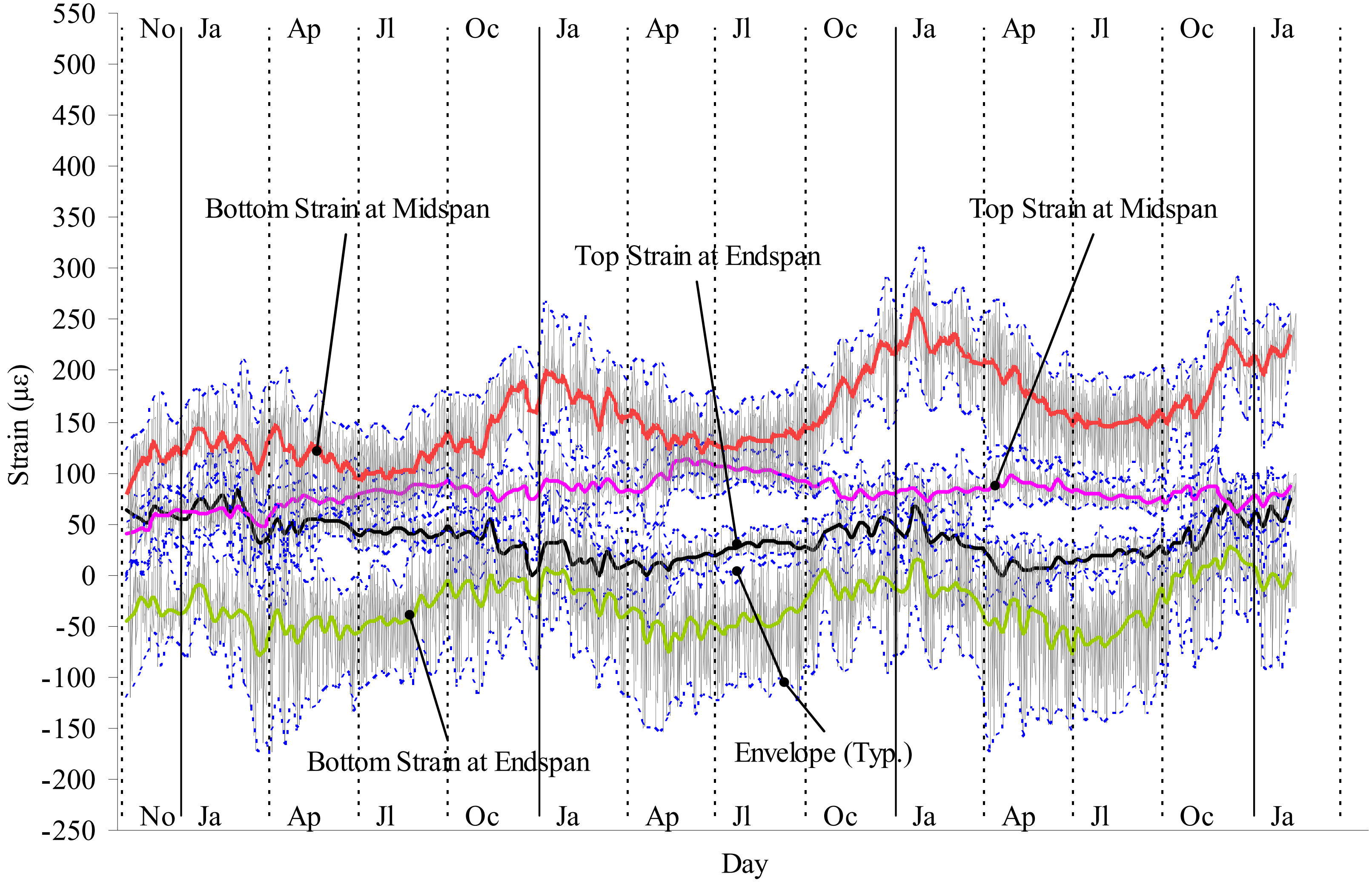

Figure 3.13. Bridge 203: Strain Gages on Girder 1

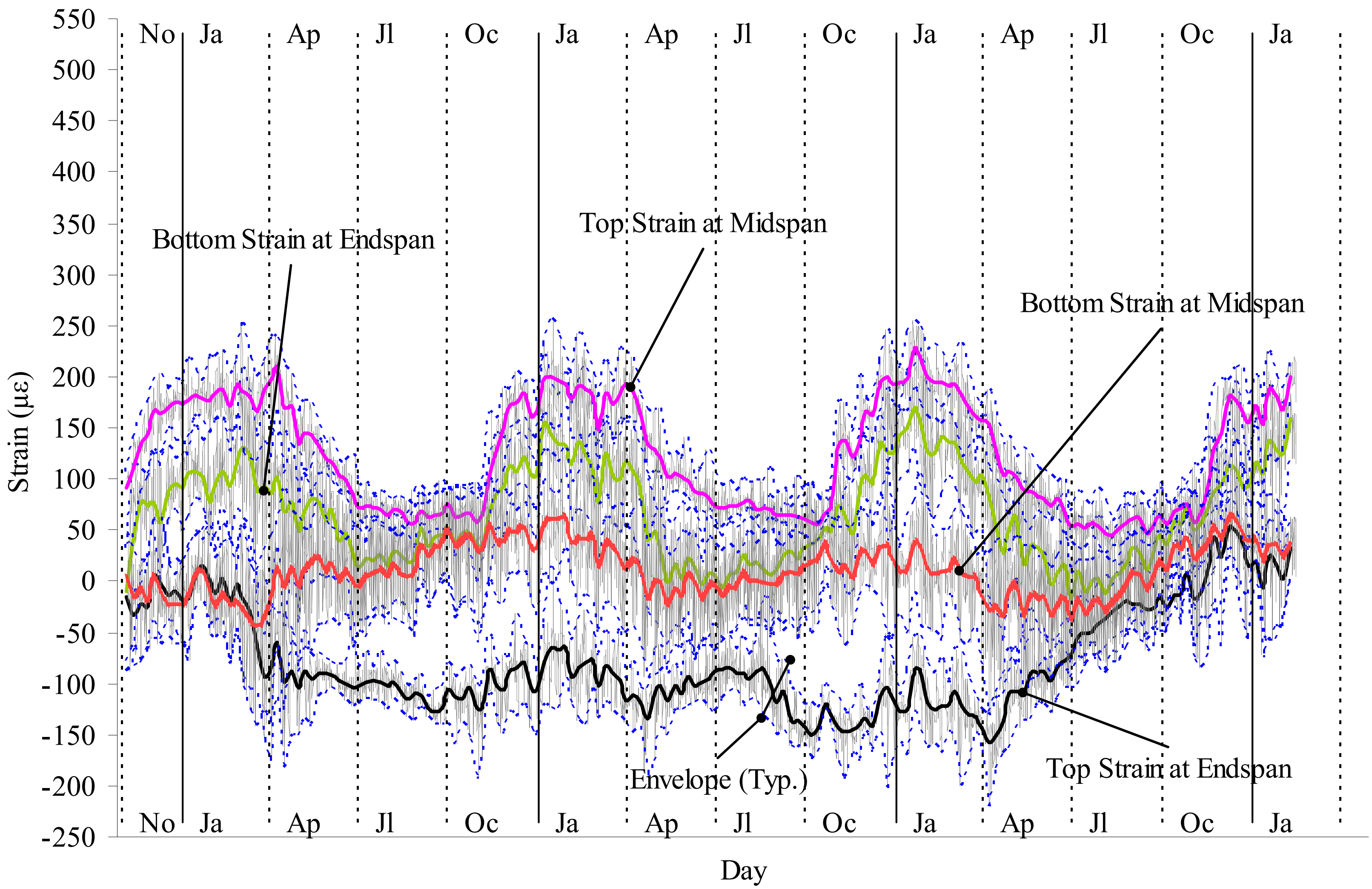

Figure 3.14. Bridge 203: Strain Gages on Girder 2

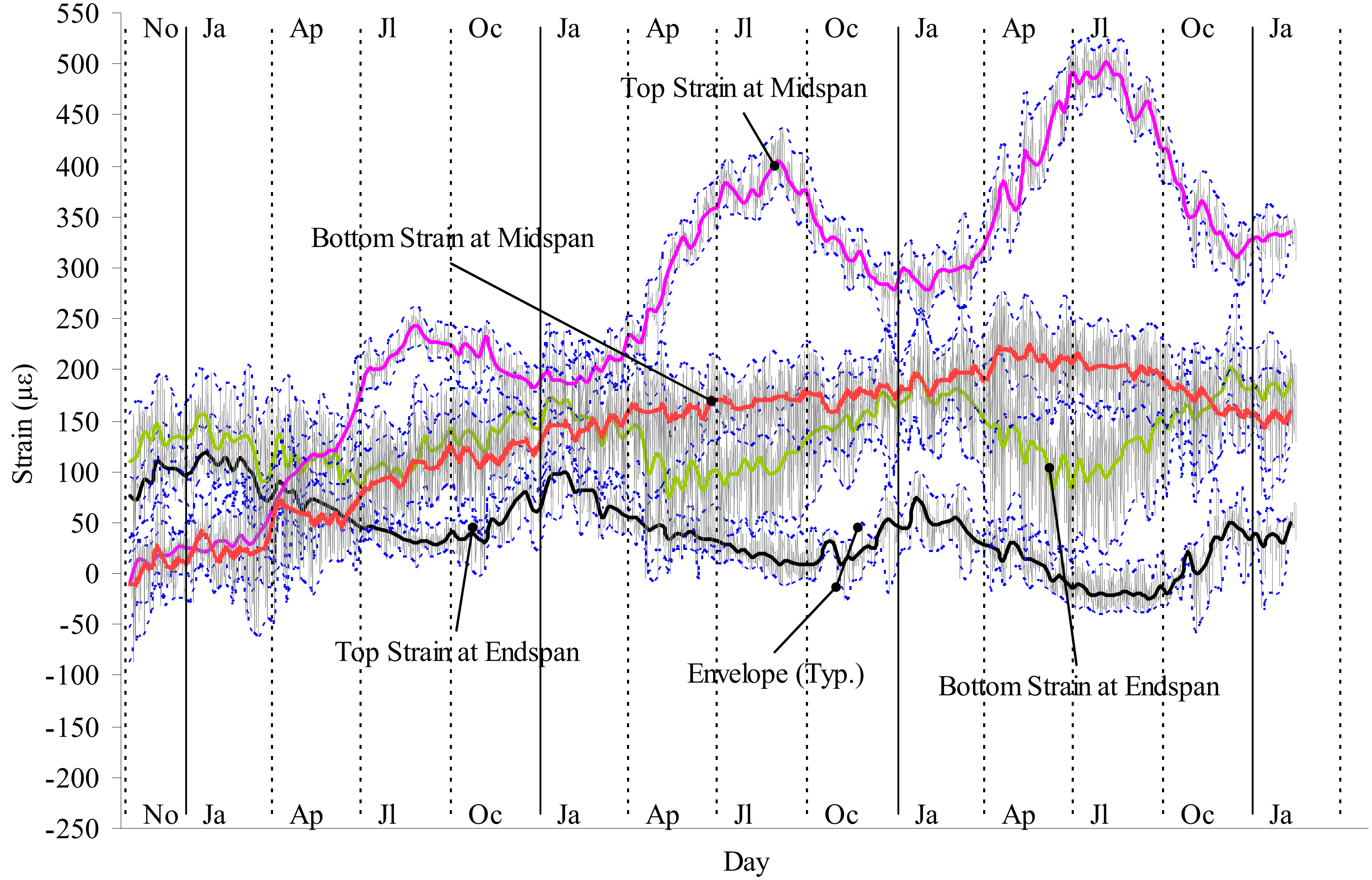

Figure 3.15. Bridge 203: Strain Gages on Girder 3

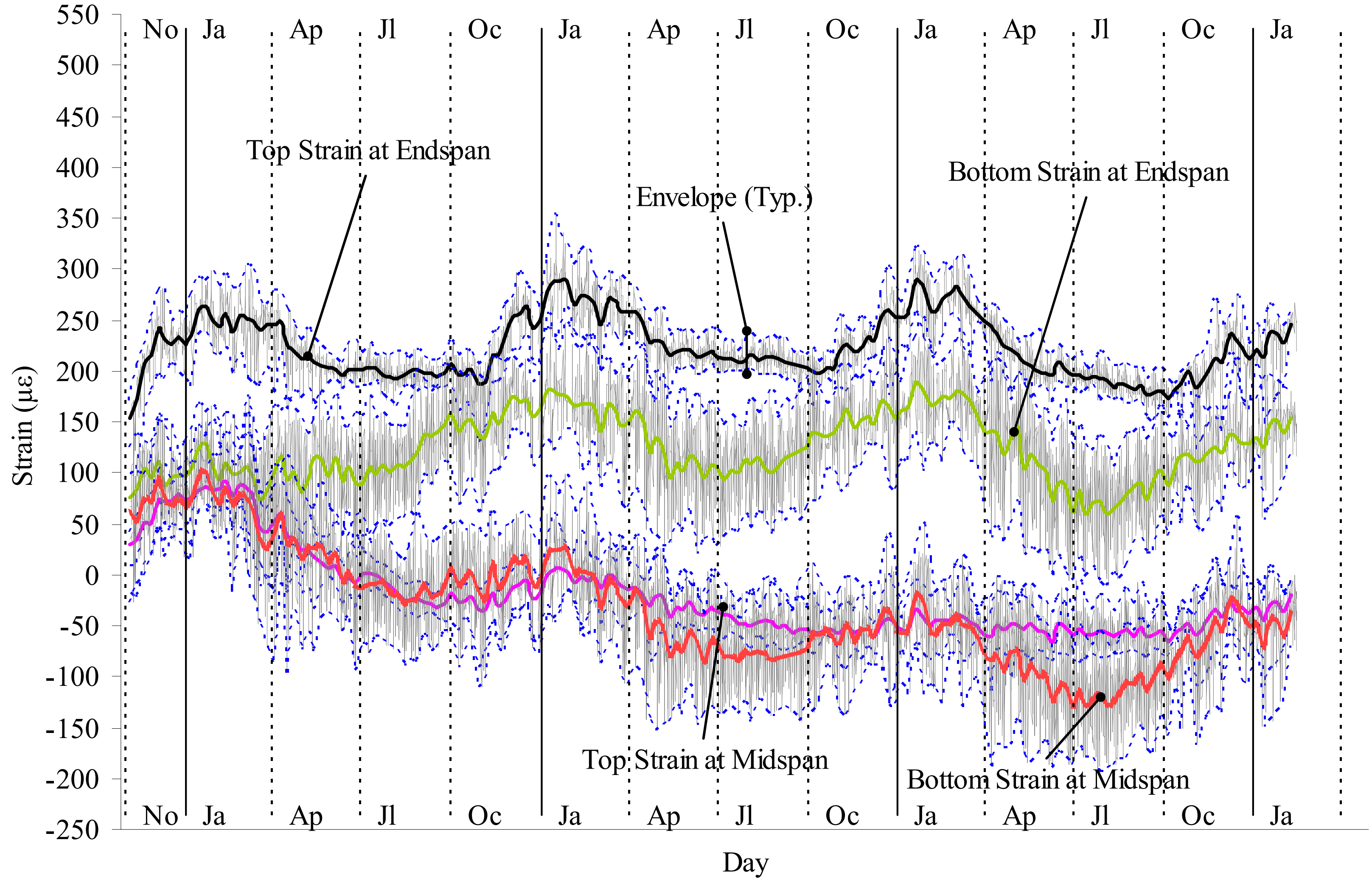

Figure 3.16. Bridge 203: Strain Gages on Girder 4

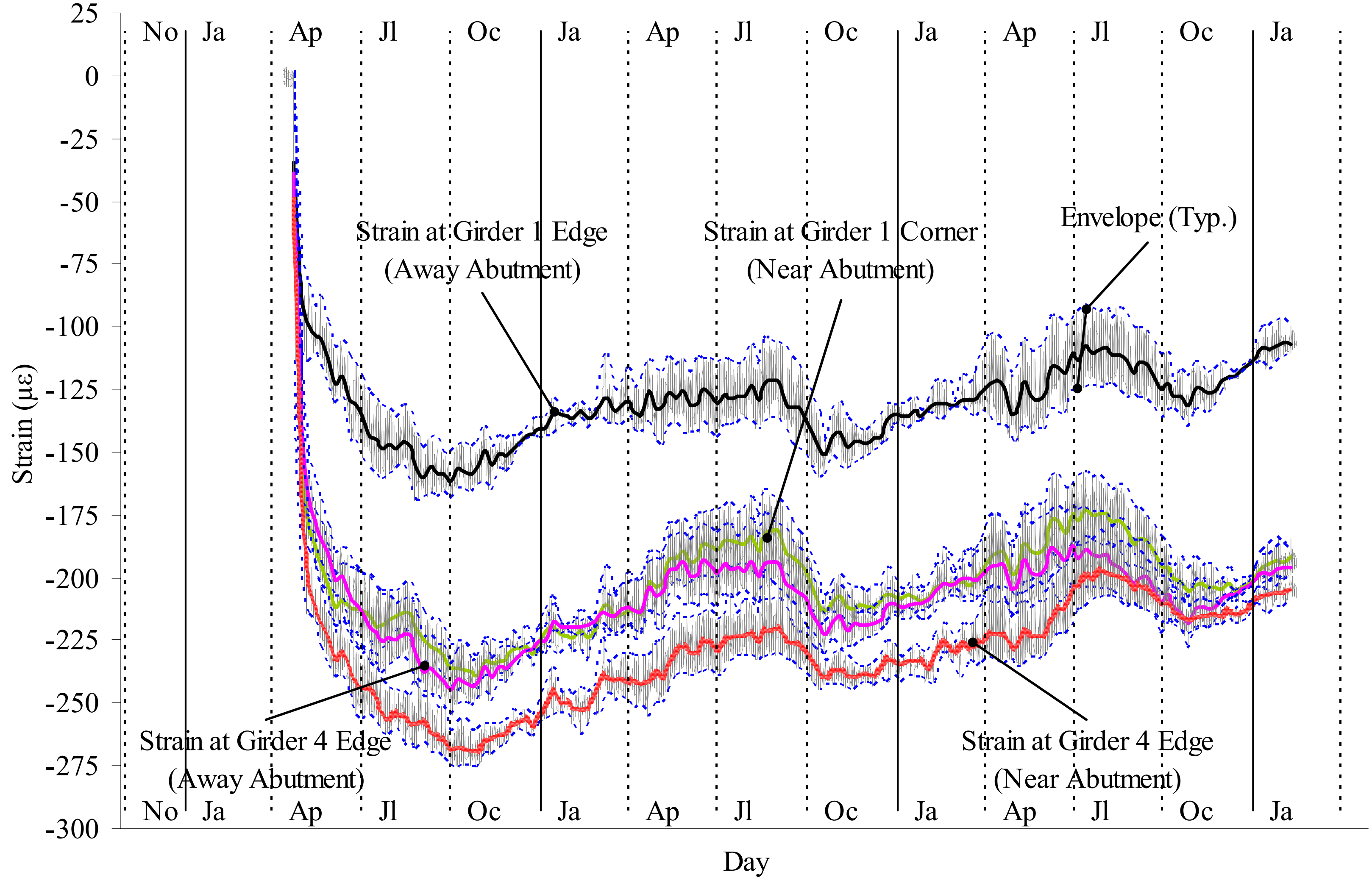

Figure 3.17. Bridge 203: Sister Bar Gages

3.3 BRIDGE 211 MONITORING RESULTS

This section presents field data obtained from bridge 211 instruments consisting of 4 extensometers, 4 pressure cells, 8 tilt meters, 24 strain gages on 4 piles, 16 strain gages on 4 prestressed concrete girders, and 8 sister bar gages. Of the 64 instruments installed on bridge 211, no gages were damaged until February 2006.

Collected data from top and bottom extensometers at abutments 1 and 2 are presented in Figure 3.18 and Figure 3.19, respectively. The top extensometers at abutment 1 measured the expansion trend; the bottom extensometer at abutment 1 measured the contraction trend; the top extensometer at abutment 2 measured the contraction trend; and the bottom extensometer at abutment 2 measured the expansion trend. Over the collection period of 17 months, the top extensometer at abutment 1 measured the maximum contraction displacement of 0.09 inches during winter 2005/2006 and the maximum expansion displacement of 0.03 inches during summer 2005. The top extensometer at abutment 2 measured the maximum contraction displacement of 0.07 inches during winter 2004/2005 and the maximum expansion displacement of 0.03 inches during summer 2005. The bottom extensometer at abutment 1 measured the maximum contraction displacement of 0.19 inches during winter 2005/2006 and no expansion displacement was observed. The bottom extensometer at abutment 2 measured the maximum contraction displacement of 0.11 inches during winter 2004/2005 and no expansion displacement was observed. The bottom extensometer data at abutment 1 indicate continuous movement of the lower abutment toward the bridge with the maximum current displacement of 0.19 inches.

Pressure cell data are presented in Figures 3.20 and 3.21. The two pressure cells measure earth pressures behind abutment 1 and the other two pressure cells measure earth pressures behind abutment 2. All of the pressure cells produced very similar earth pressure variation trends to each other. Earth pressures obtained from the bottom pressure cell in abutment 1 were greater by approximately 2 psi as expected, due to the approximately 7 ft deeper elevation. Earth pressures from the bottom pressure cell in abutment 2 were very similar to those of abutment 1 while the top pressure cell in abutment 2 produced approximately 8 psi lower pressures. In abutment 1, the top and bottom pressure cell measured maximum earth pressures of 13.7 and 13 psi during summer 2005, respectively. In abutment 2 the top and bottom pressure cell measured maximum earth pressures of 4.7 and 13.6 psi during summer 2005. The top and bottom cell in abutment 2 measured relatively small pressure amplitude and daily variations, measuring an approximate amplitude of 2 psi.

Abutment tilt meter data are presented in Figures 3.22 through 3.23. Of four tilt meters on both abutments, three—the exception being the tilt meter at the centerline of girder 3 on abutment 1—measured a similar trend of abutment rotations. There were abrupt changes in data during September 2004 for the tilt meter at the centerline of the girder of approximately 0.47 degrees. These data anomalies might be attributed to construction personnel or birds. Tilt meter data are intended to measure changes in rotation rather than absolute angles; therefore any anomalies can be corrected. Data from the two tilt meters located on abutment 1 at the centerline of girders 1 and 3 were maximum changes in rotation of 0.09 and 0.19 degrees, respectively, and data from the two tilt meters on abutment 2 were 0.13 and 0.16, respectively.

Girder tilt meter data are presented in Figures 3.24 and 3.25. Two tilt meters were placed directly on girders 1 and 3, respectively. Two tilt meters on both ends of girder 1 measured a similar trend but did not exhibit obvious seasonal variation. Two tilt meters on both ends of girder 3 measured a similar trend and did exhibit clear seasonal variation. Both tilt meters on girder 1 near abutments 1 and 2 measured the maximum changes in rotation of approximately 0.07 and 0.09 degree, respectively. Both tilt meters on girder 3 near abutments 1 and 2 measured the maximum changes in rotation of approximately 0.16 and 0.08, respectively.

H-pile bending moments about the weak axis on four piles are presented in Figure 3.26 through Figure 3.29, respectively. There are two sets of three gages installed on pile 1 (north pile supporting abutment 1): (1) at depth = 2′-7″ and (2) at depth = 9′-7″from the abutment base. There are two sets of three gages installed on pile 2 (south pile supporting abutment 1): (1) at depth = 1′-1″ and (2) at depth = 8′-1″ from the abutment base. Similarly, there are two sets for pile 3 (north pile supporting abutment 2): (1) at depth = 0′-6″ and (2) at depth = 7′-6″ from the abutment base, and two sets for pile 4 (south pile supporting abutment 2): (1) at depth = (-) 0′-6″ (6″ embedded into abutment 2) and (2) at depth = 6′-6″. As can be observed from Figure 3.26 through Figure 3.29, the moments at all depths from all piles indicate that pile bending is continuously increasing with the pile head moving toward the bridge. This observation is consistent with data obtained from extensometers and tilt meters on the abutments. Over the collection period of 17 months, the moments at the depths near the abutment base have reached maximum values of +23, +13, +21, and +7 ft-kips for piles 1 to 4, respectively. The H-pile plastic moment capacity = 194 ft-kips (F_y = 50 ksi). H-pile bending moments from the strain gage sets at a greater depth are generally smaller due to the location of the gages near the point of fixity.

H-pile axial force in piles 1 and 2 (at abutment 1) is presented in Figure 3.30, and H-pile axial force in piles 3 and 4 (at abutment 2) is presented in Figure 3.31. Pile axial force for piles 1 and 2 varied from 80 to 115 kips. For piles 3 and 4, pile axial force was from 70 to 110 kips except anomalies of bottom gage sets of the north pile. All pile axial forces exhibited approximately 20 kips of seasonal variations.

Collected data from strain gages on girders 1, 2, 3 and 4 are presented in Figure 3.32 and Figure 3.35, respectively. At the two instrumented locations on each of girders, both girder ends, two strain gages were placed on the top and bottom flanges. All the bottom strain gages experienced compressive strain while all the top strain gages exhibited only tensile strain. The bottom strain gages of all girders exhibited larger seasonal strain variations (approximately 160 με) than did the top strain gages. The seasonal variation ranges of the top strain gages were approximately 100 με.

Sister-bar strain data at the approach slab on abutments 1 and 2 are presented in Figures 3.36 and 3.37. Sister bar gages measured changes in compressive strain ranging from 60 to 70 με during the early life of the approach slab. Another significant compressive strain change was observed during spring 2005. Daily temperature variations for all sister-bar strain gages were significant during summer (approximately 20 με), while daily strain changes during winter were less than 10 με.

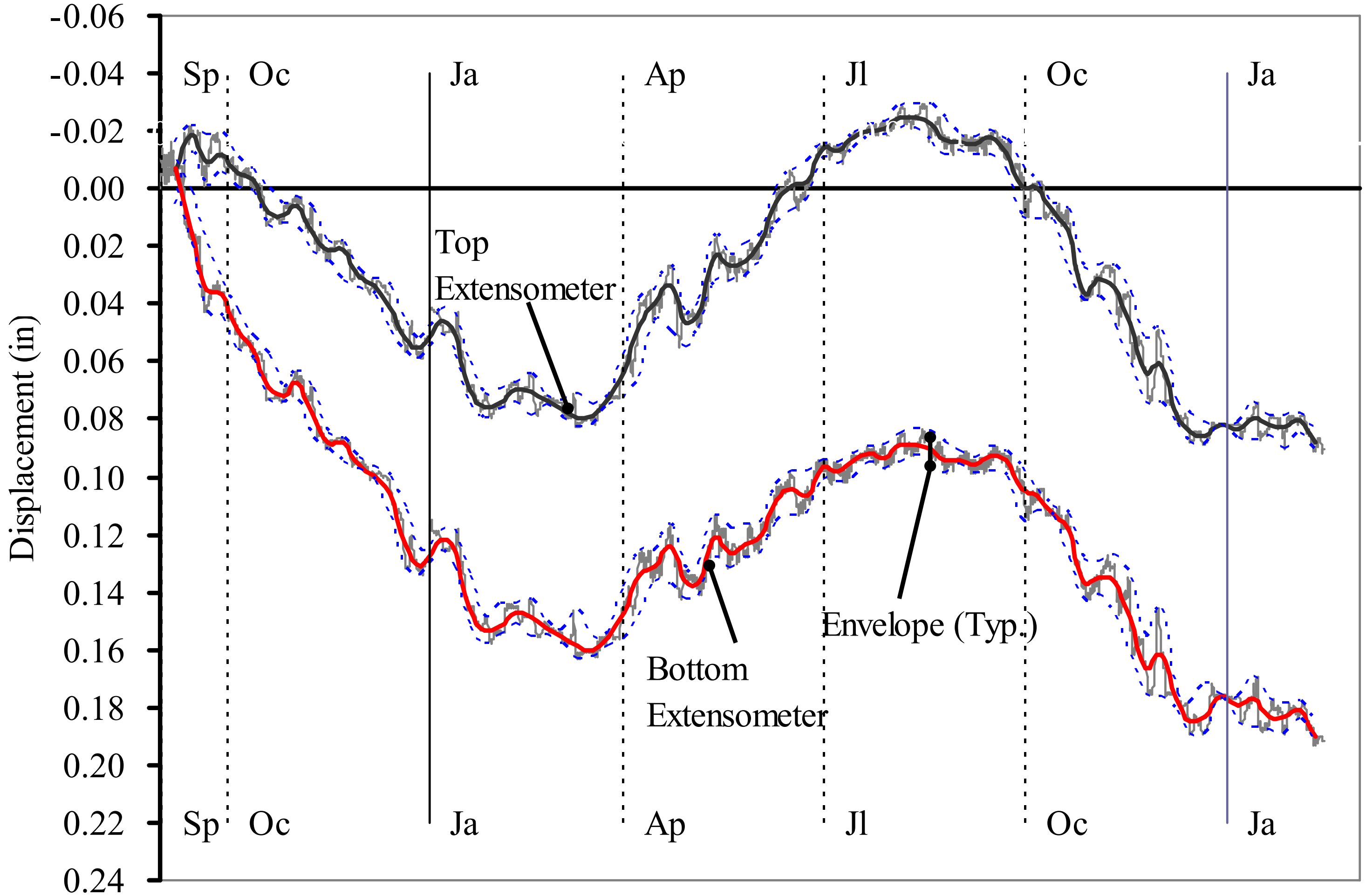

Figure 3.18. Bridge 211: Extensometers on Abutment 1

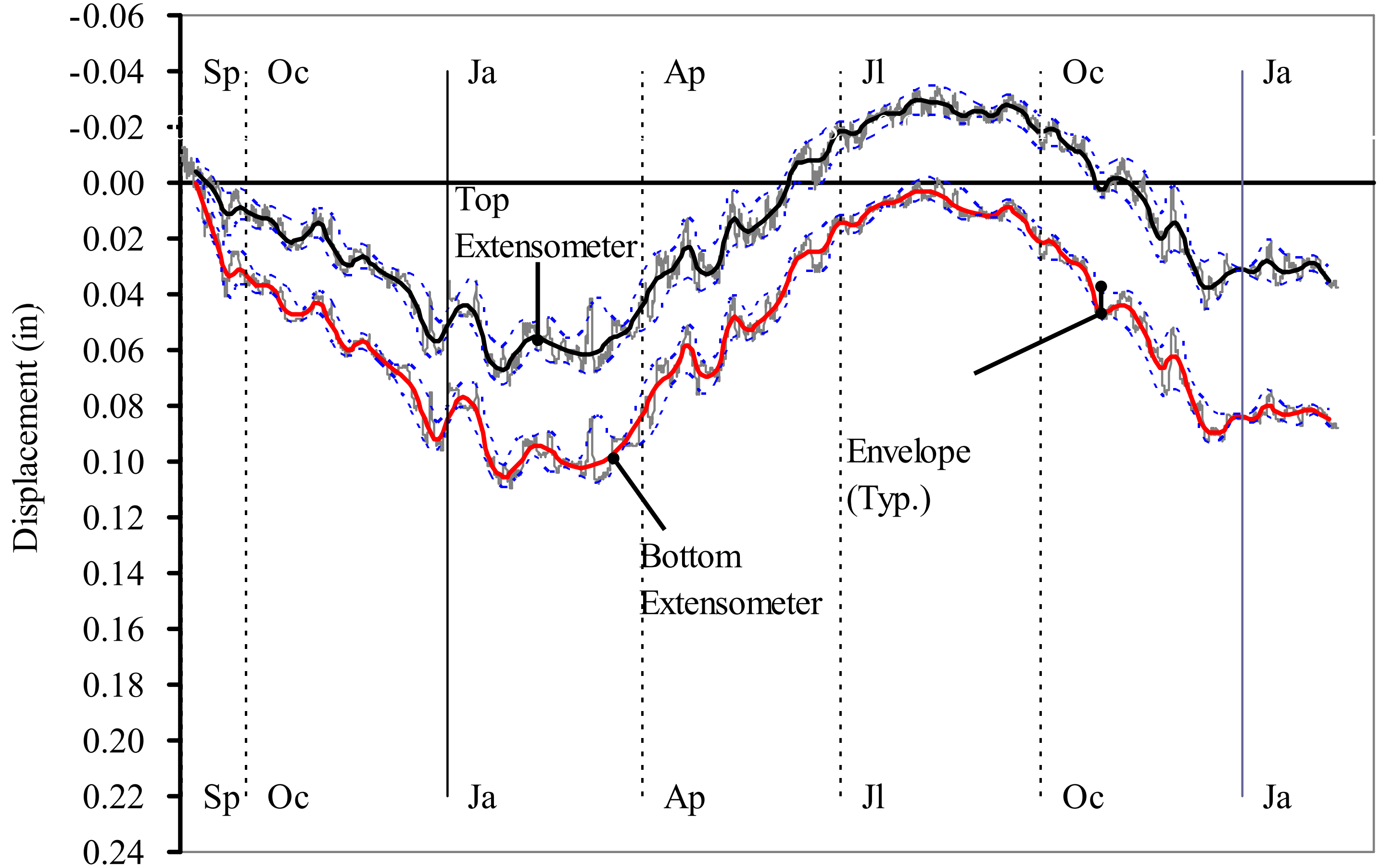

Figure 3.19. Bridge 211: Extensometers on Abutment 2

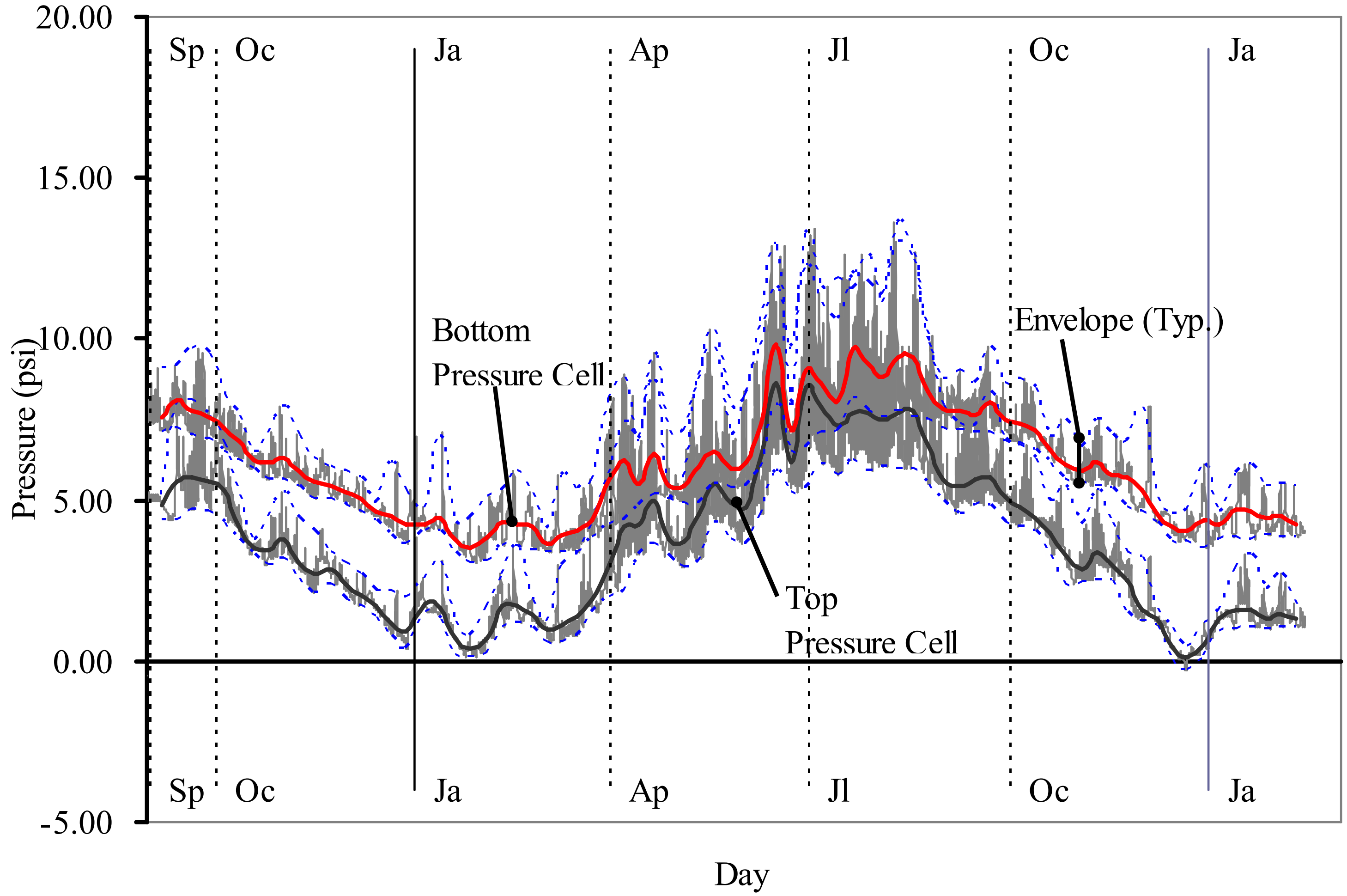

Figure 3.20. Bridge 211: Pressure Cells on Abutment 1

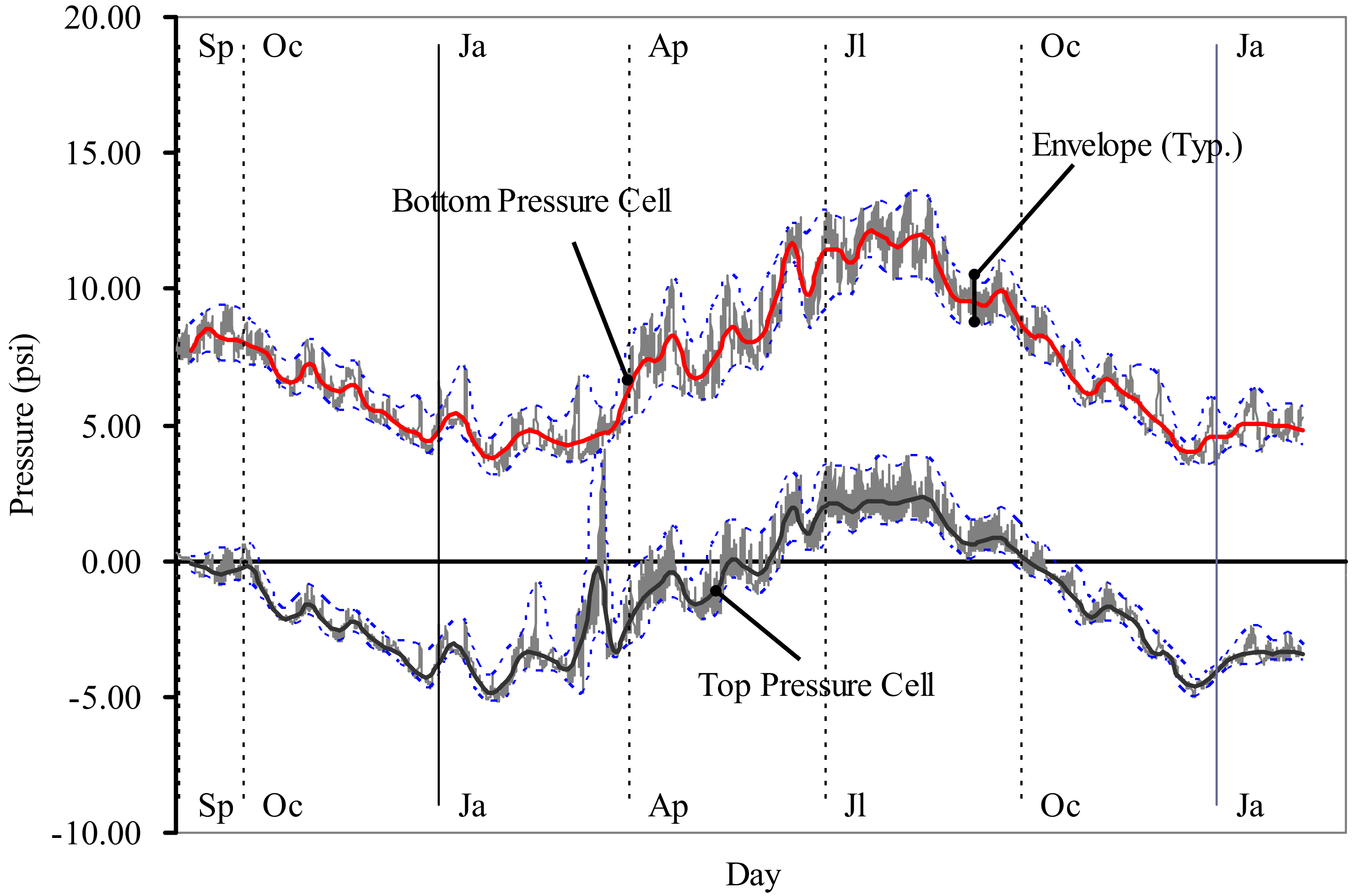

Figure 3.21. Bridge 211: Pressure Cells on Abutment 2

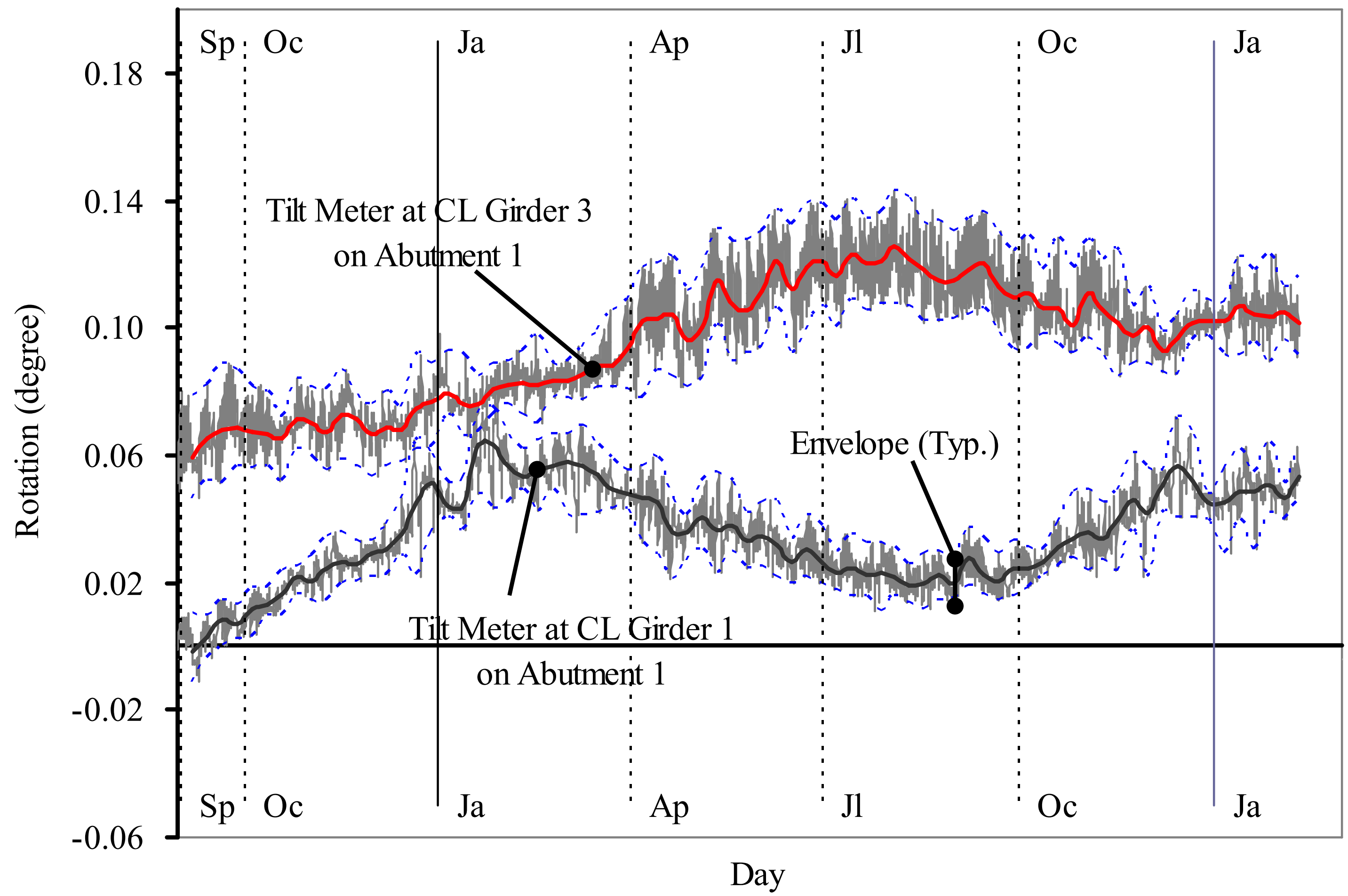

Figure 3.22. Bridge 211: Tilt Meters on Abutment 1

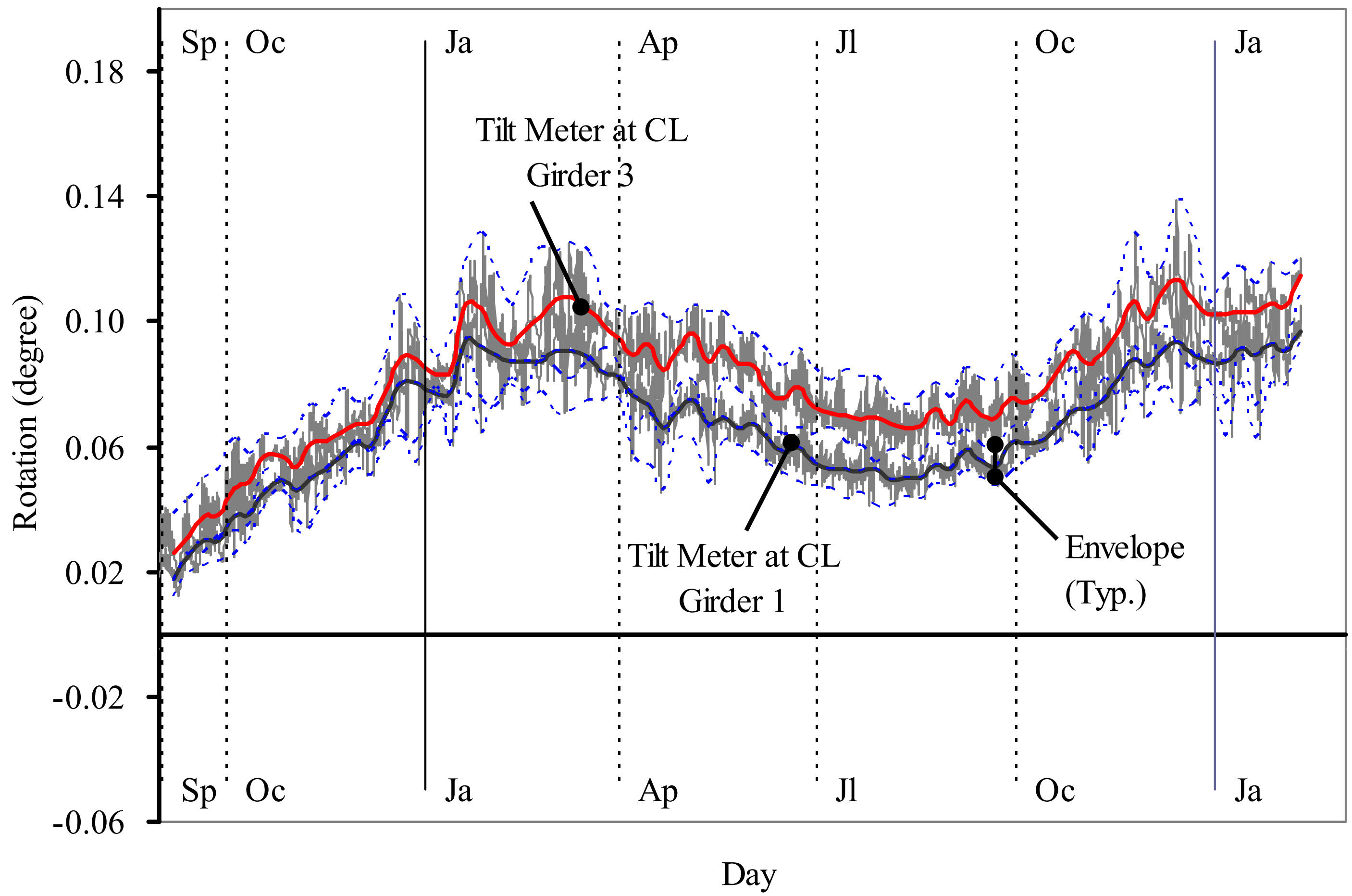

Figure 3.23. Bridge 211: Tilt Meters on Abutment 2

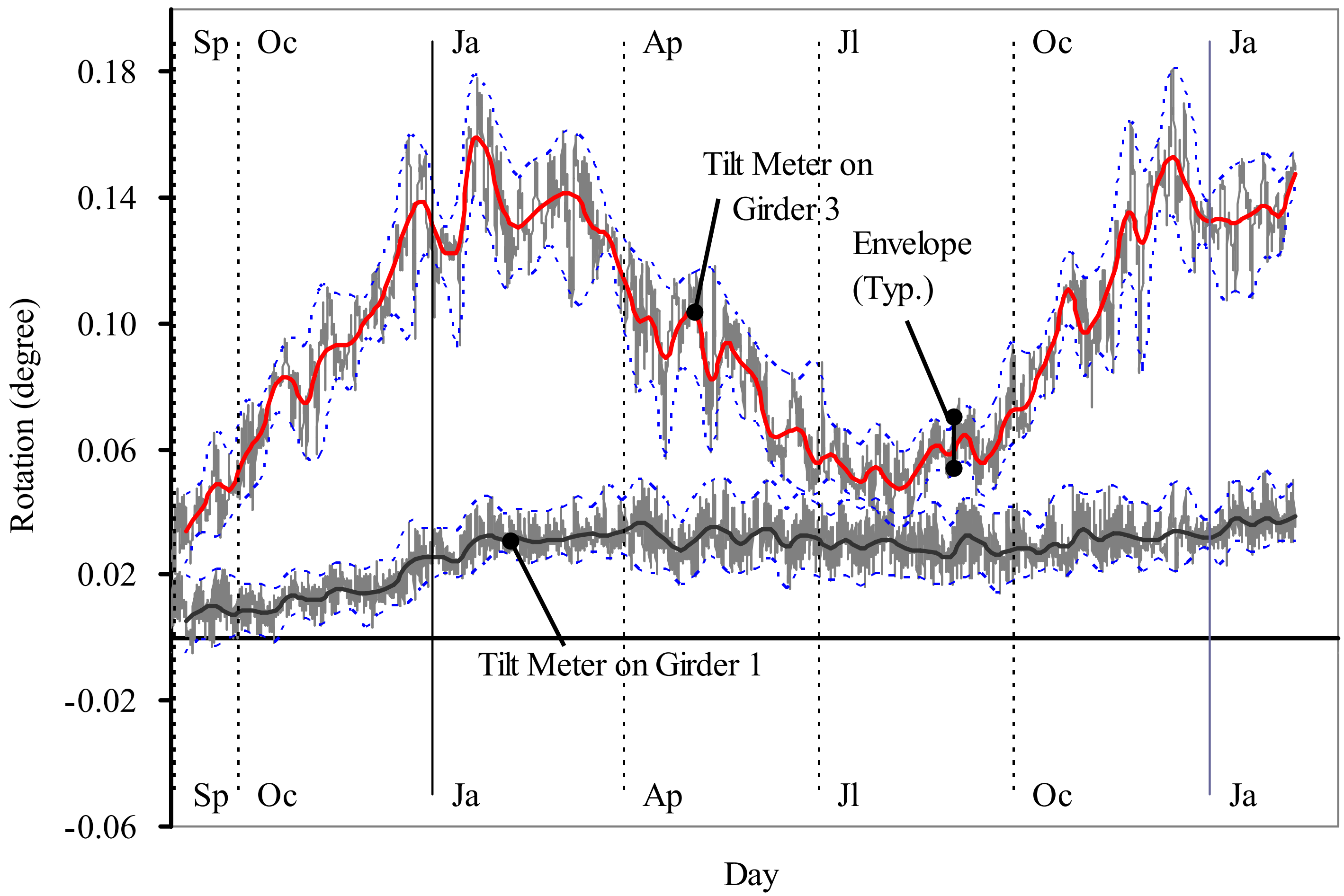

Figure 3.24. Bridge 211: Tilt Meters on Girders near Abutment 1

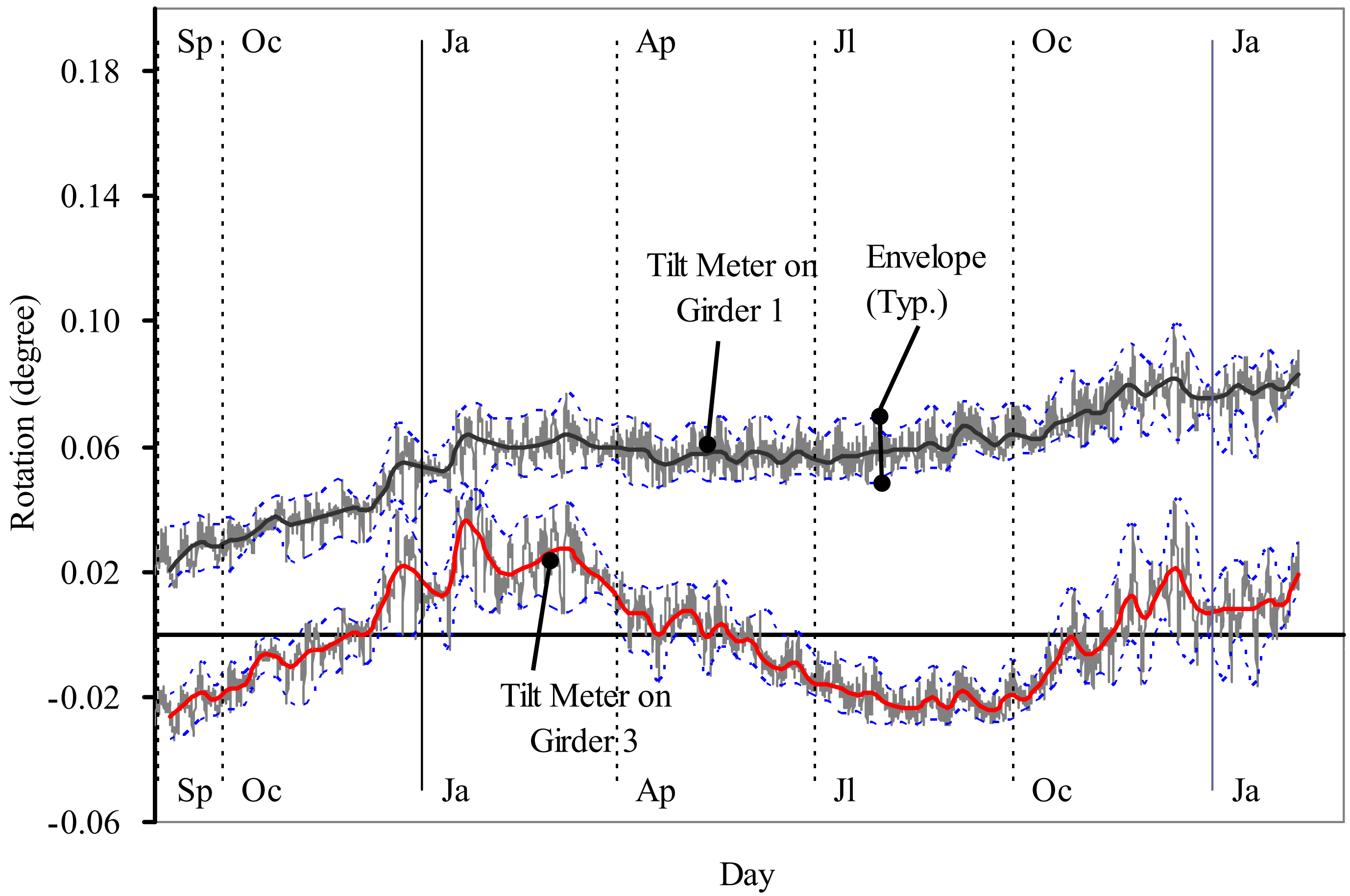

Figure 3.25. Bridge 211: Tilt Meters on Girders near Abutment 2

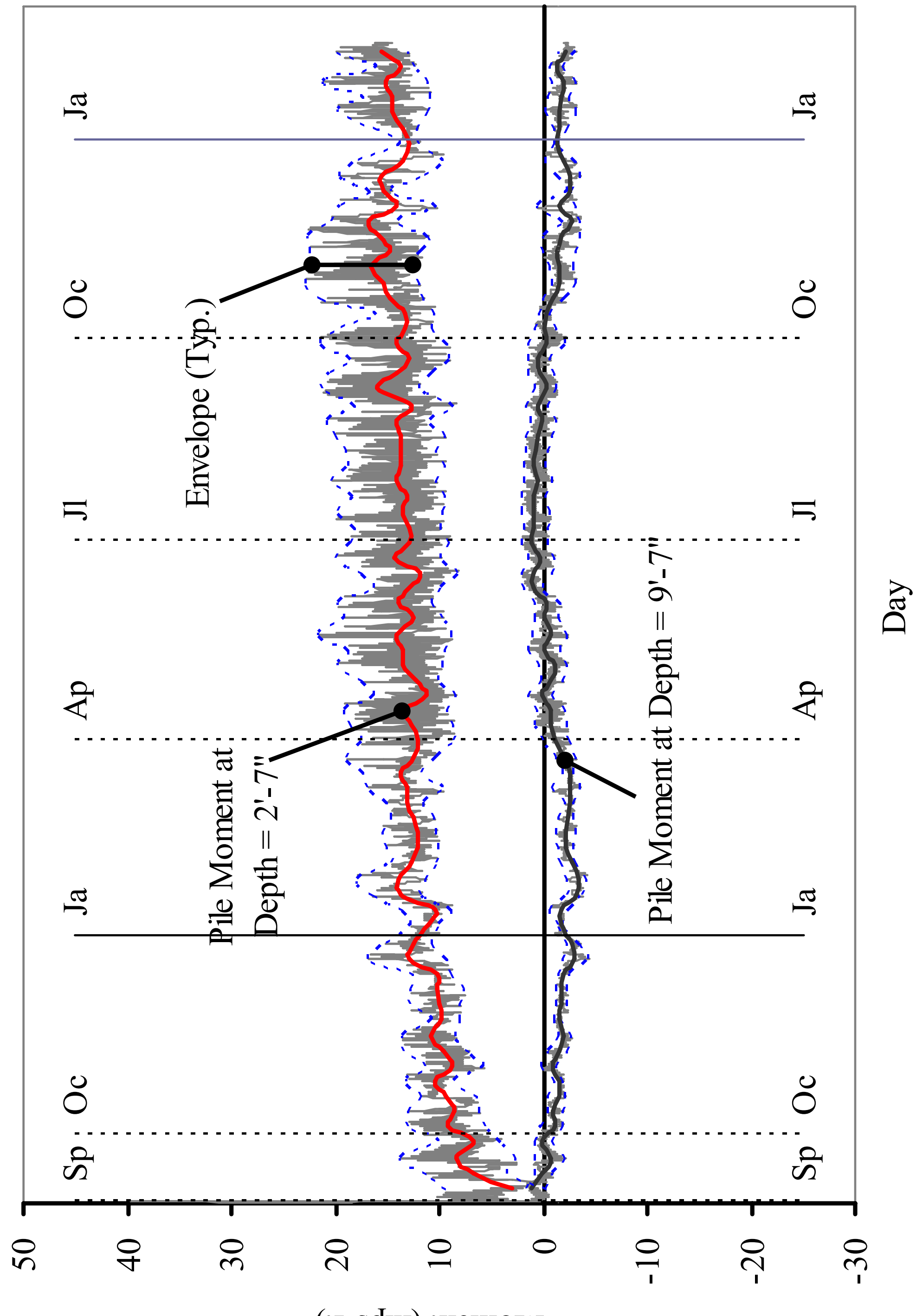

Figure 3.26. Bridge 211: Moments on North Pile (Abutment 1)

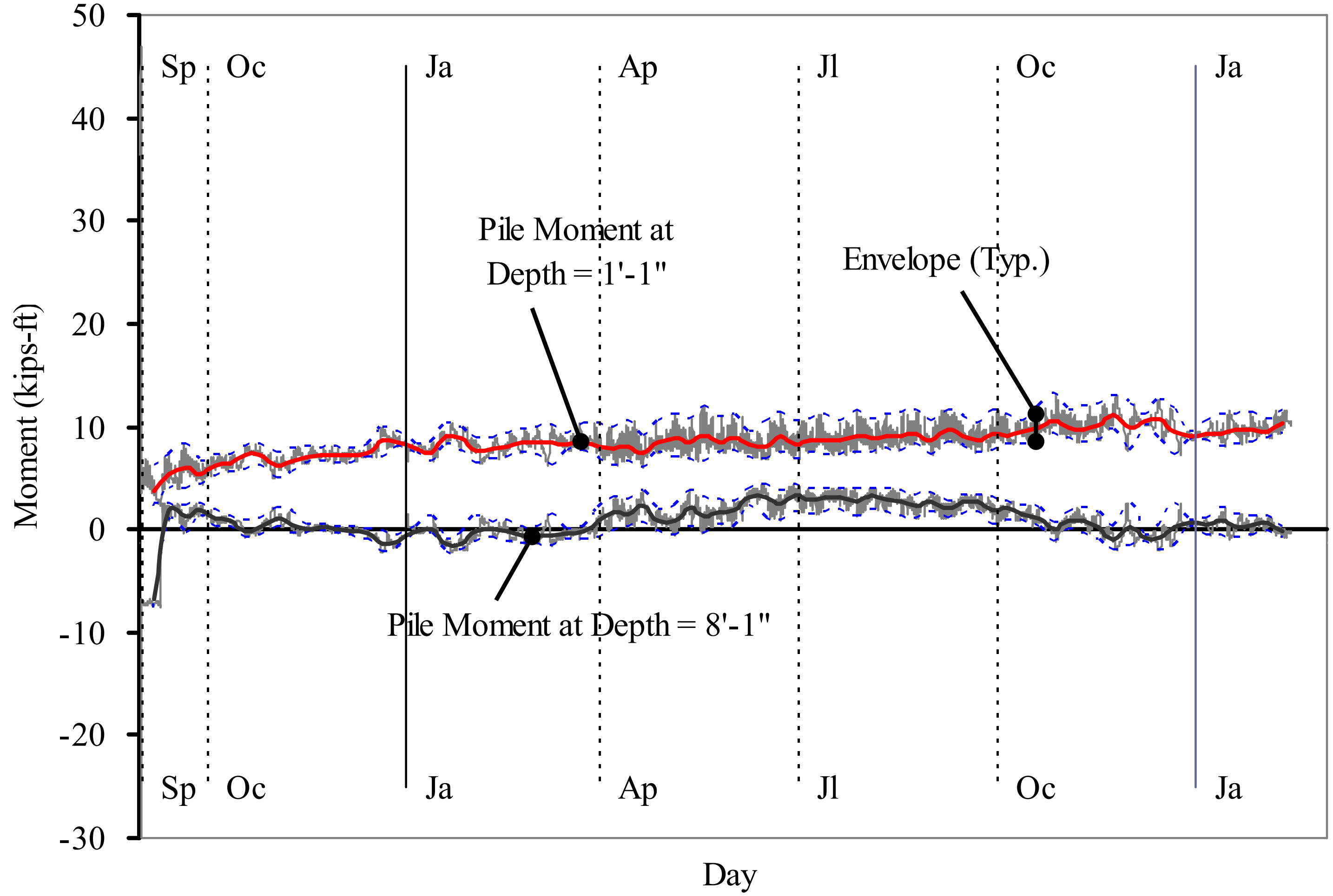

Figure 3.27. Bridge 211: Moments on South Pile (Abutment 1)

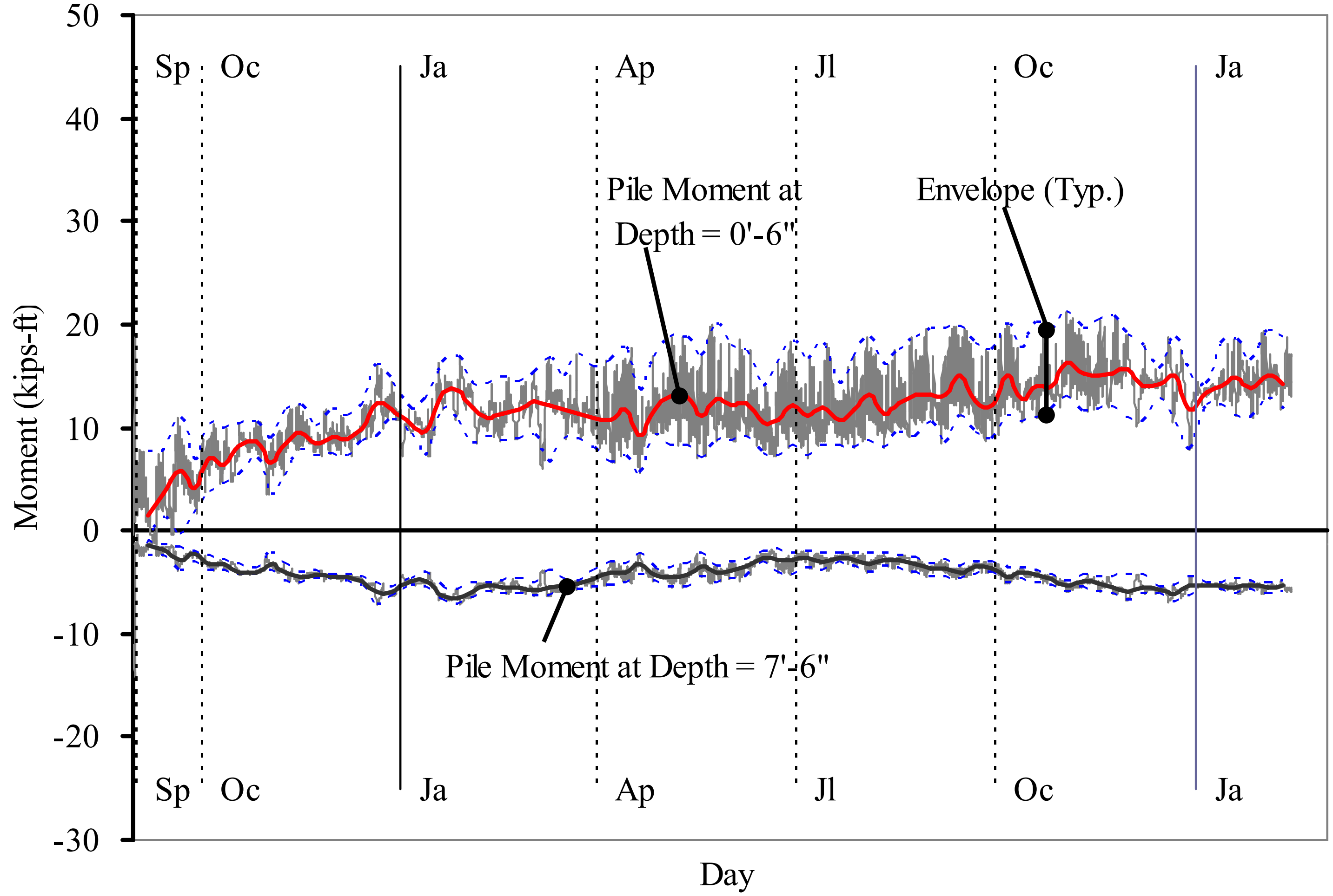

Figure 3.28. Bridge 211: Moments on North Pile (Abutment 2)

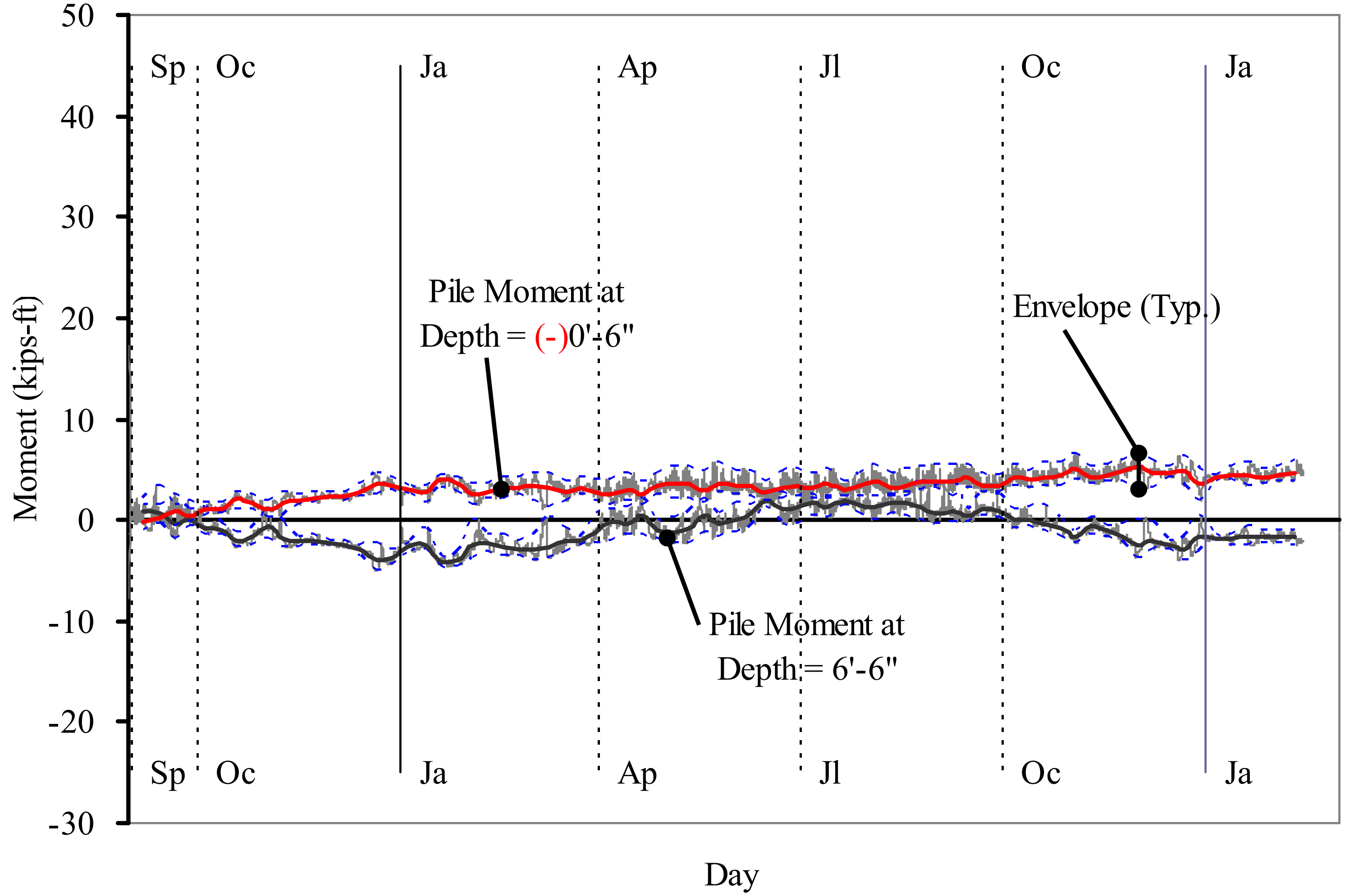

Figure 3.29. Bridge 211: Moments on South Pile (Abutment 2)

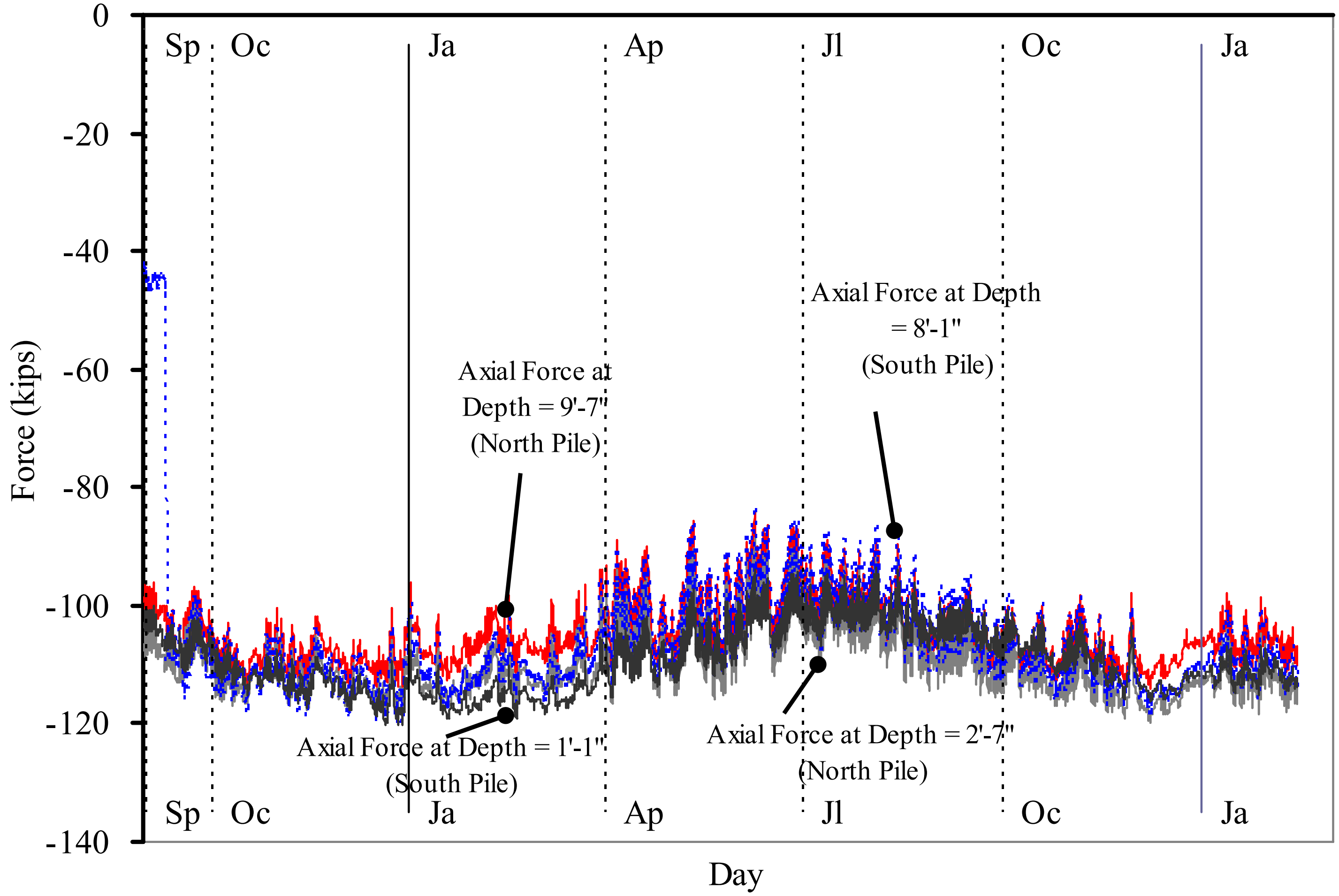

Figure 3.30. Bridge 211: Axial Force on Piles (Abutment 1)

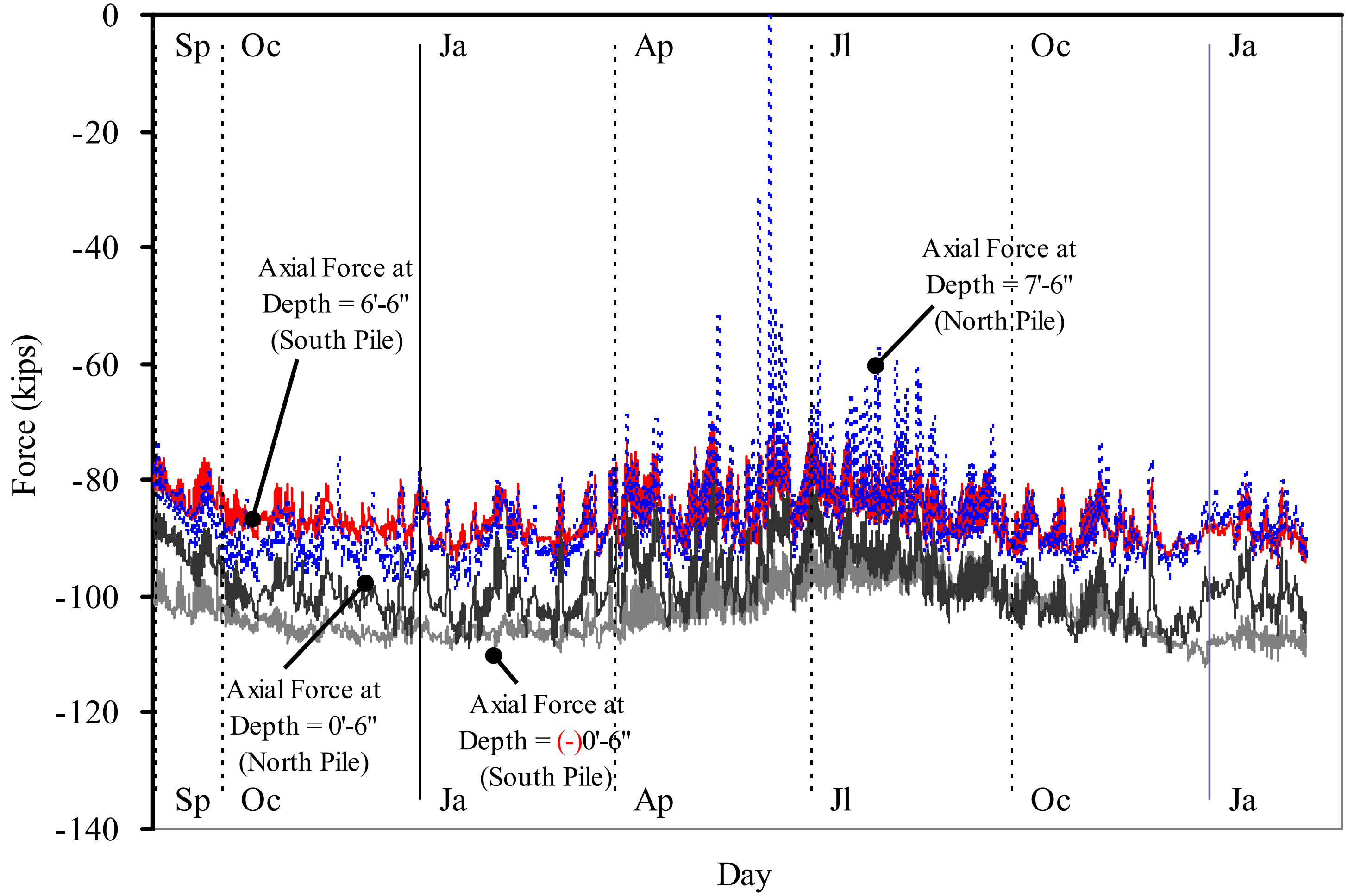

Figure 3.31. Bridge 211: Axial Force on Piles (Abutment 2)

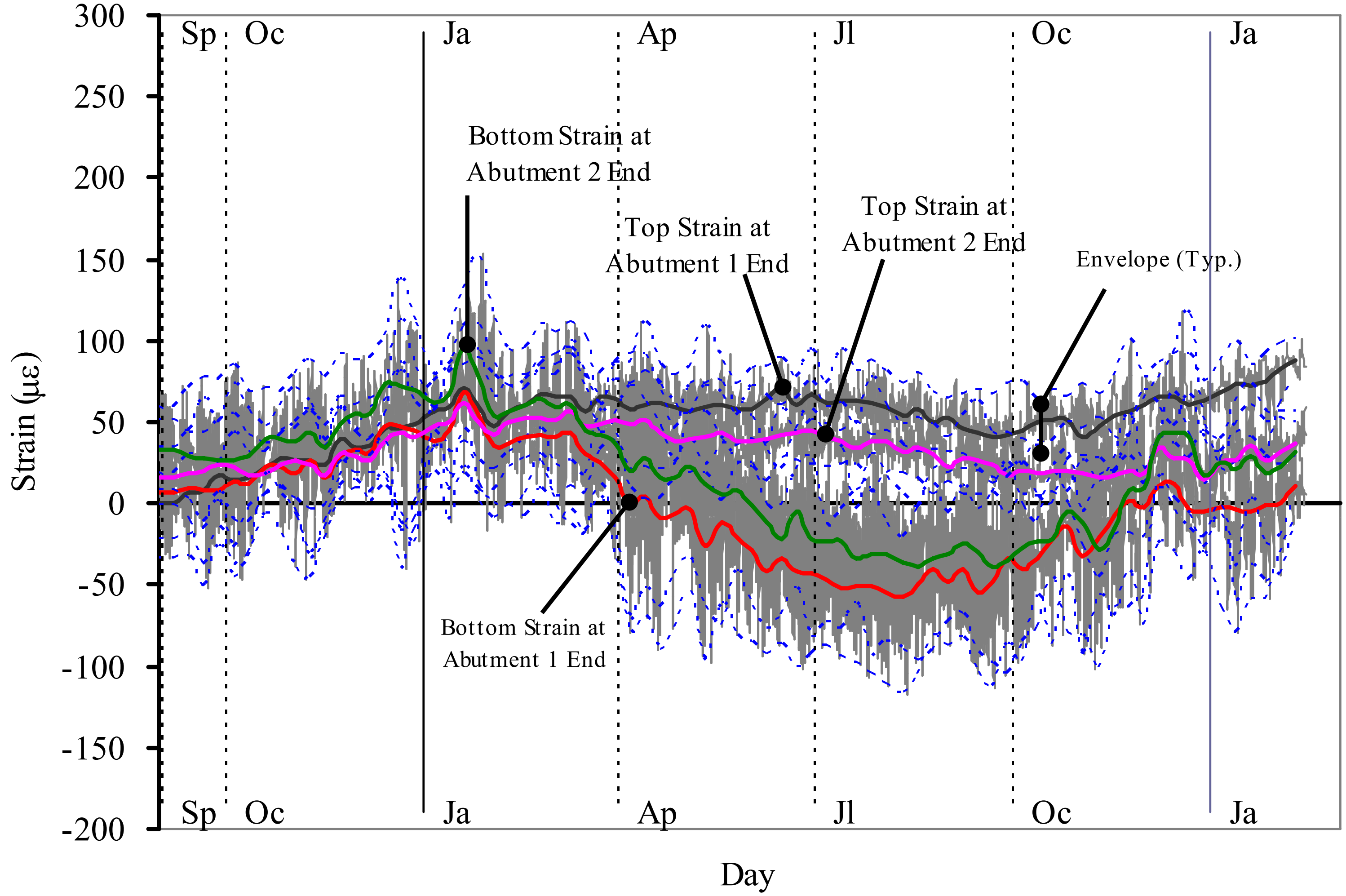

Figure 3.32. Bridge 211: Strain Gages on Girder 1

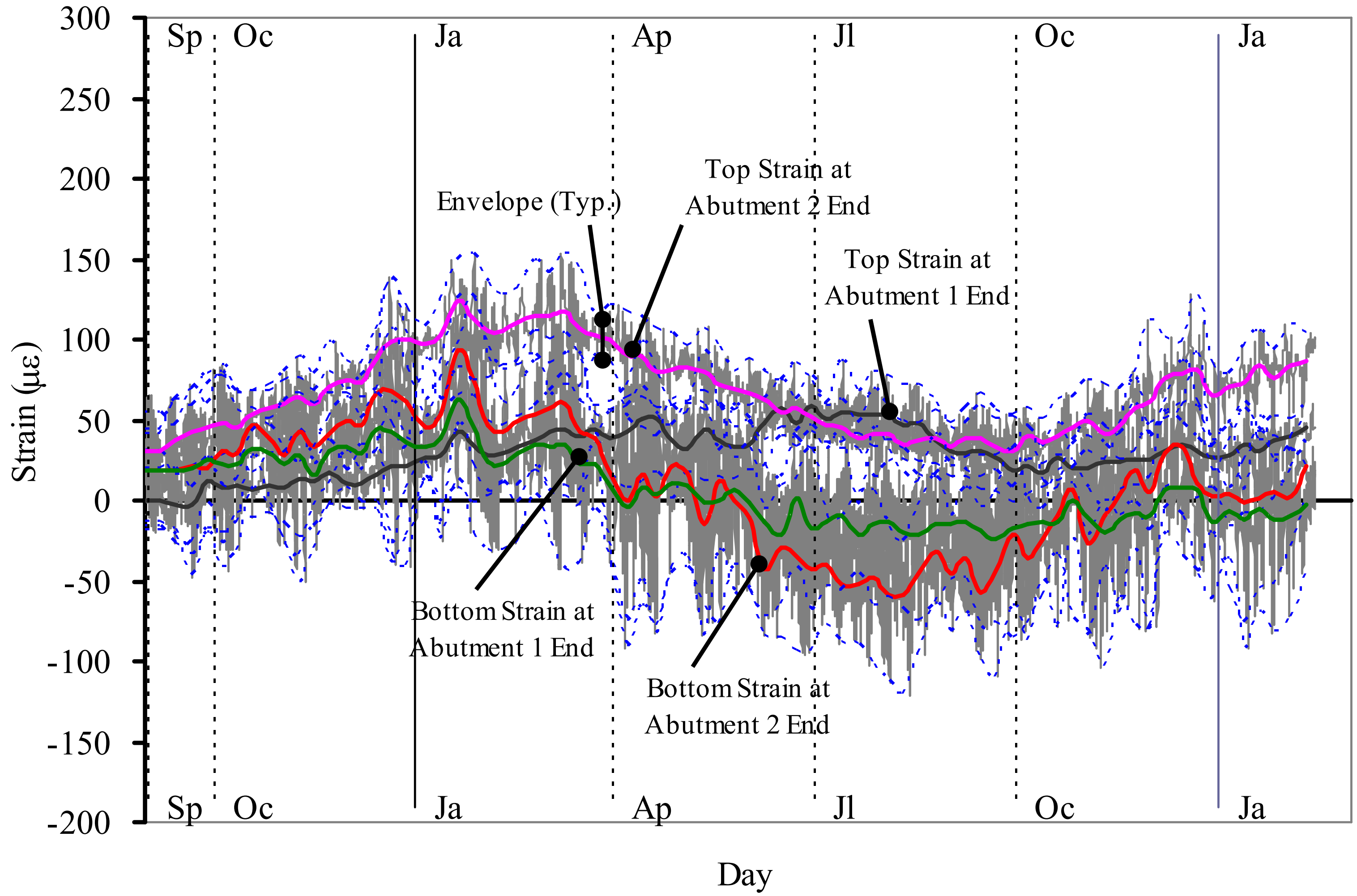

Figure 3.33. Bridge 211: Strain Gages on Girder 2

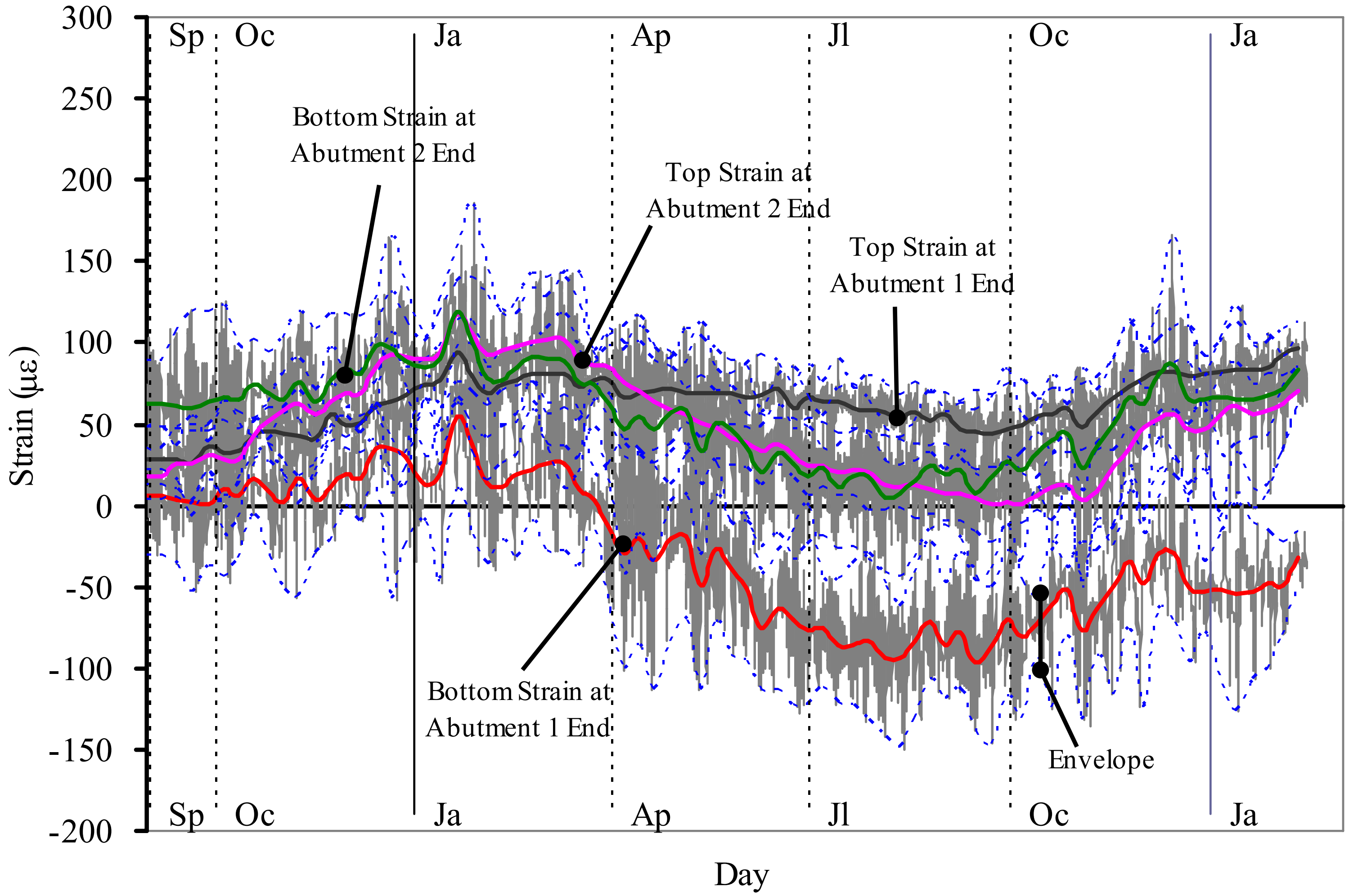

Figure 3.34. Bridge 211: Strain Gages on Girder 3

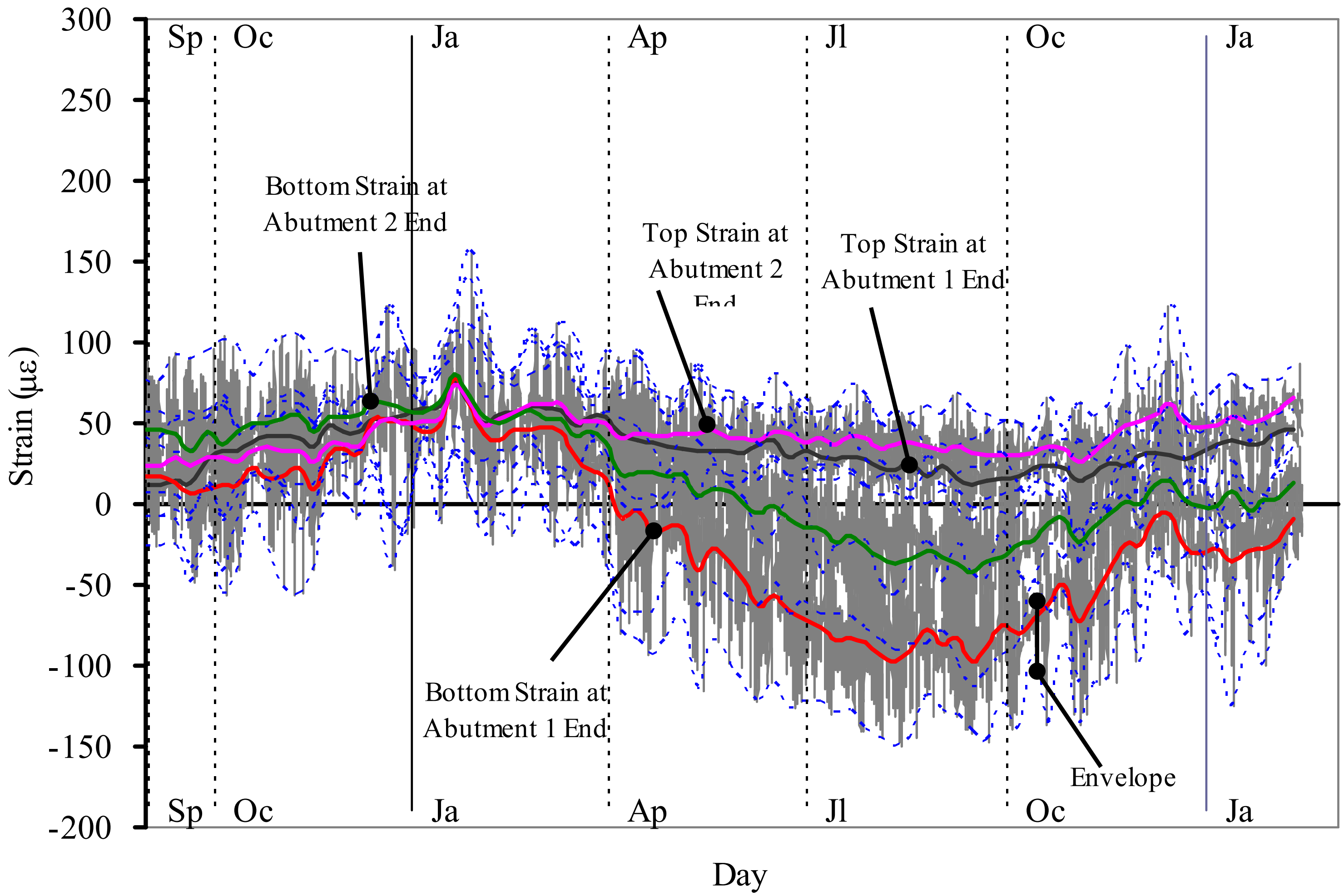

Figure 3.35. Bridge 211: Strain Gages on Girder 4

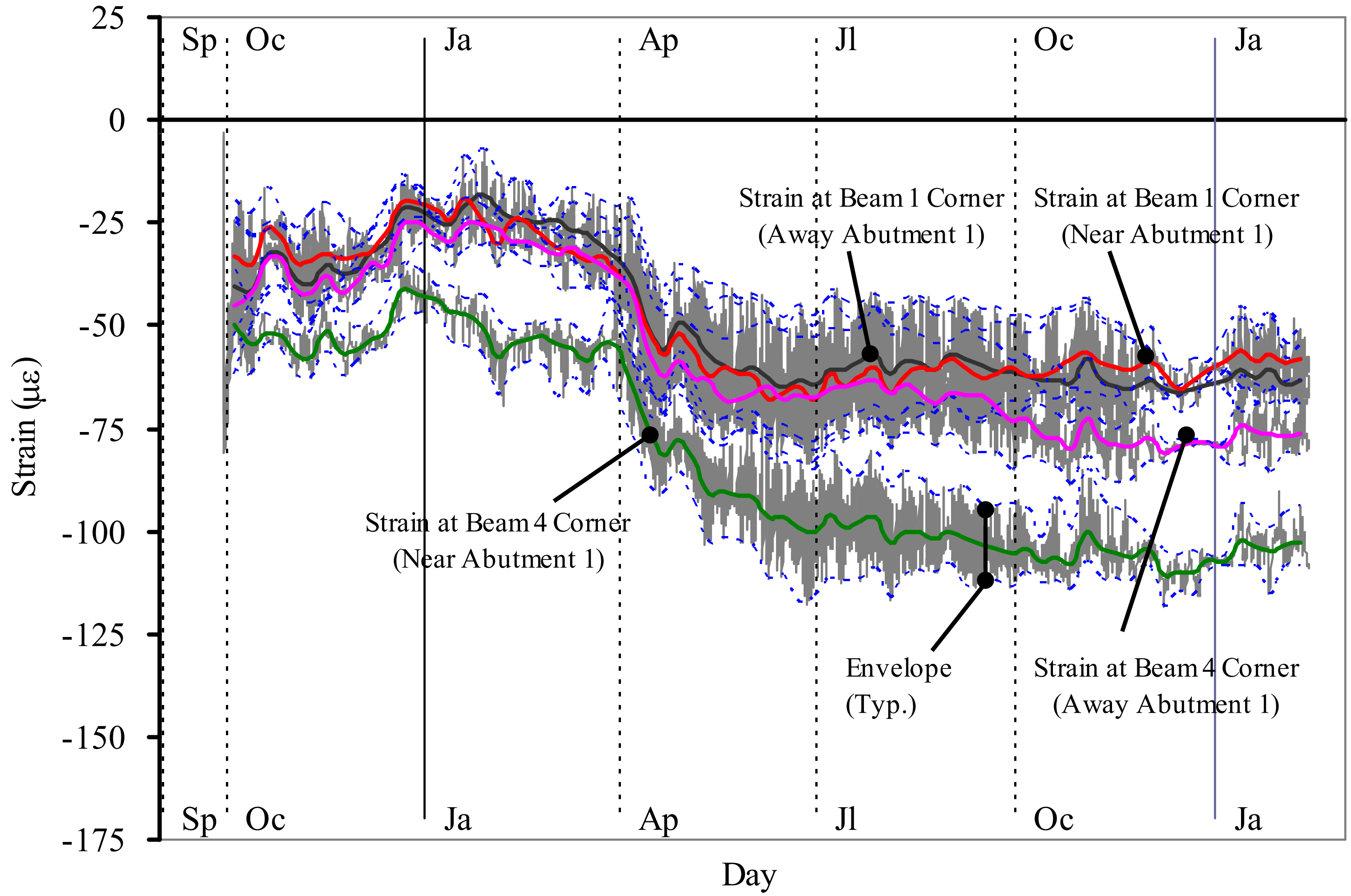

Figure 3.36. Bridge 211: Sister Bar Gages (Abutment 1)

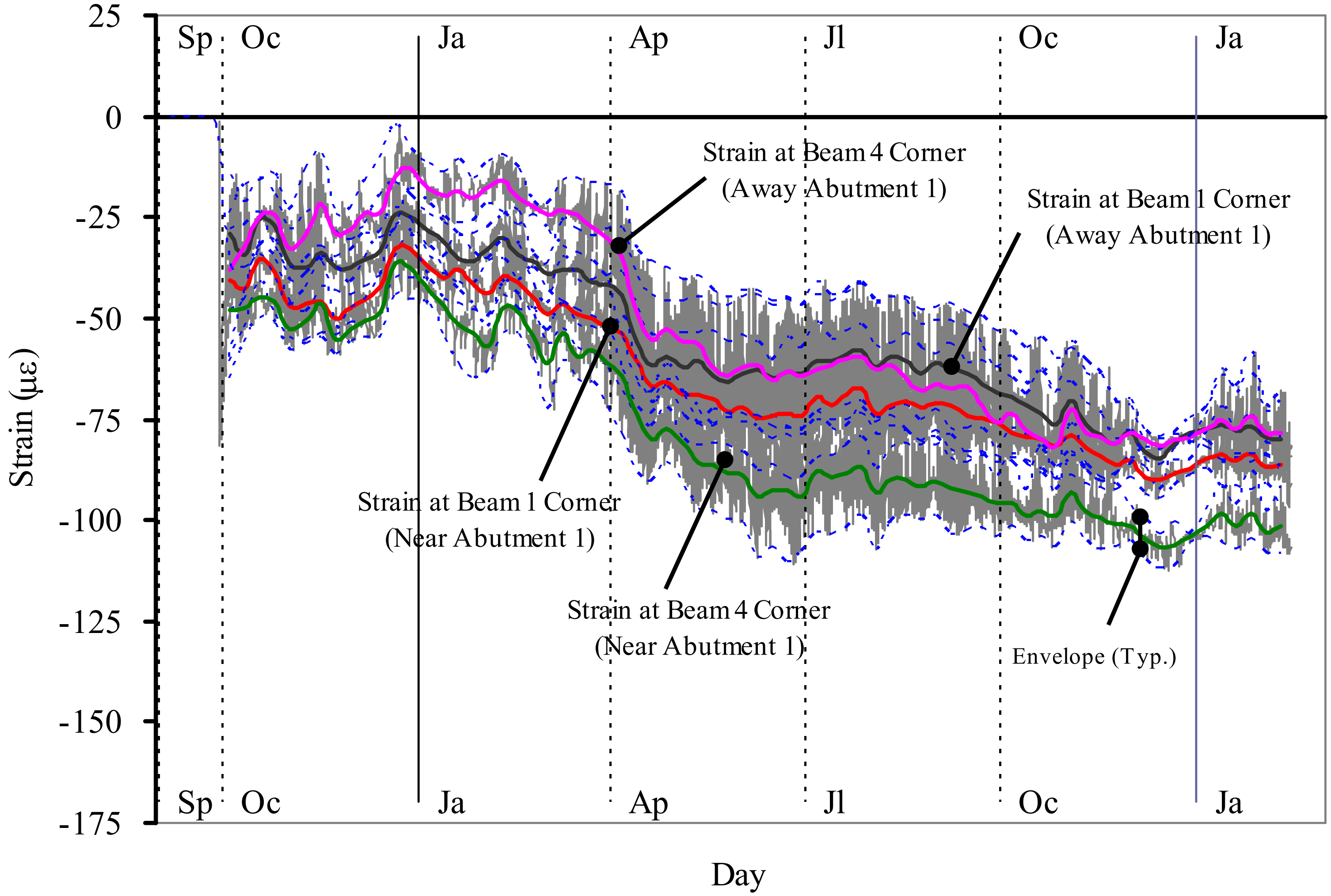

Figure 3.37. Bridge 211: Sister Bar Gages (Abutment 2)

3.4 BRIDGE 222 MONITORING RESULTS

This section presents field data obtained from bridge 222 instruments consisting of 4 extensometers, 4 pressure cells, 4 tilt meters, 24 strain gages on 4 piles, 8 strain gages on 2 prestressed concrete girders, and 4 sister bar gages. Of the 48 instruments installed on bridge 222, there was 1 damaged strain gage on the south pile of abutment 2 (Channels 1-2) since September 2005. However, the thermostat of this damaged strain gage continues to function.

Collected data from the top and bottom extensometers at abutments 1 and 2 are presented in Figure 3.38 and Figure 3.39, respectively. The top extensometers at both abutments measured the overall expansion trend, the bottom extensometer at abutment 1 measured the significant contraction trend, and the bottom extensometer at abutment 2 measured the insignificant expansion trend. Over the collection period of 28 months, the top extensometer at abutment 1 measured the maximum contraction displacement of 0.05 inches during winter 2004/2005 and the maximum expansion displacement of 0.11 inches during summer 2005. The top extensometer at abutment 2 measured the maximum contraction displacement of 0.04 inches during winter 2004/2005 and the maximum expansion displacement of 0.04 inches during summer 2005. The bottom extensometer at abutment 1 measured the maximum contraction displacement of 0.13 inches during winter 2005/2006 and no expansion displacement was observed. The bottom extensometer at abutment 2 measured the maximum contraction displacement of 0.05 inches during winter 2004/2005 and no expansion displacement was observed. The bottom extensometer data at abutment 1 indicate continuous movement of the lower abutment toward the bridge with a maximum current displacement of 0.13 inches.

Collected data from top and bottom pressure cells at abutments 1 and 2 are presented in Figure 3.40 and Figure 3.41, respectively. Both top pressure cells measured similar earth pressure magnitudes of 8 psi during summers and similar earth pressure amplitudes of 7 psi. Both bottom pressure cells measured earth pressure magnitudes of 8 psi; however, higher earth pressure amplitudes of 10 psi were observed. It can be observed that daily variations measured from the top pressure cell at abutment 2 were relatively higher than those measured from the other pressure cells.

Abutment tilt meter data are presented in Figure 3.42. The tilt meter on abutment 1 at the centerline of girder 4 measured higher abutment rotations than the tilt meter on abutment 1 at the centerline of girder 2. The tilt meters at the centerlines of girders 2 and 4 measured a similar trend, indicating continuous movement of the lower abutment toward the bridge with maximum changes in rotation of 0.07 and 0.11 degrees, respectively.

Girder tilt meter data are presented in Figure 3.43. Two tilt meters were placed directly on girders 2 and 4, respectively. Both tilt meters measured similar girder rotations with maximum changes in rotation of approximately 0.08 degree.

H-pile bending moments about the weak axis on 4 piles are presented in Figure 3.44 through Figure 3.47, respectively. Two sets of three gages were installed on pile 1 (south pile supporting abutment 1): (1) at depth = 1′-7″ and (2) at depth = 7′-7″ from the abutment base. Two sets of three gages were installed on pile 2 (north pile supporting abutment 1): (1) at depth = 1′-3″ and (2) at depth = 7′-3″ from the abutment base. Similarly, there were two sets for pile 3 (south pile supporting abutment 2): (1) at depth = 0′-3″ and (2) at depth = 6′-3″, and two sets for pile 4 (north pile supporting abutment 2):

(1) at depth = 0′-5″ and (2) at depth = 6′-5″ from the abutment base. As can be observed from Figure 3.44 through Figure 3.47, the moments at all depths from all piles indicate that pile bending is continuously increasing, with the pile head moving toward the bridge. This observation is consistent with data obtained from extensometers and tilt meters on the abutments. Over the collection period of 28 months, the moments at the depths near the abutment base have reached maximum values of +22, +23, +21, and +25 ft-kips for piles 1 to 4, respectively. The H-pile plastic moment capacity = 140 ft-kips (F_y = 36 ksi). H-pile bending moments from the strain gage sets at a greater depth are generally smaller due to the location of the gages near the point of fixity.

H-pile axial force in piles 1 and 2 (at abutment 1) is presented in Figure 3.48, and H-pile axial force in piles 3 and 4 (at abutment 2) is presented in Figure 3.49. Pile axial forces vary from 10 to 90 kips for piles 1 and 2 and from 10 to 120 kips for piles 3 and 4. The strain gage sets at a greater depth measured higher axial force magnitudes than the strain gage sets near the abutment bases.

Collected data from strain gages on girders 2 and 4 are presented in Figure 3.50 and Figure 3.51, respectively. At the two instrumented locations on each of girders 2 and 4, both girder ends, two strain gages were placed on the top and bottom flanges. As can be observed from Figure 3.50 and Figure 3.51, most strain gages indicate contraction ranging from 25 to 50με for girder 2 and ranging from 40 to 80 με for girder 4. However, one strain gage on girder 2 and one strain gage on girder 4 measured an inconsistent trend of expansion ranging from 100 to 150 με.

Sister-bar strain data at the approach slab on abutment 1 are presented in Figure 3.52. Sister bar gages measured changes in compressive strain ranging from 80 to 130 με during the early life of the approach slab, indicating shrinkage effects. Thereafter, a more gradual effect was observed in the four instruments, primarily attributed to seasonal temperature changes.

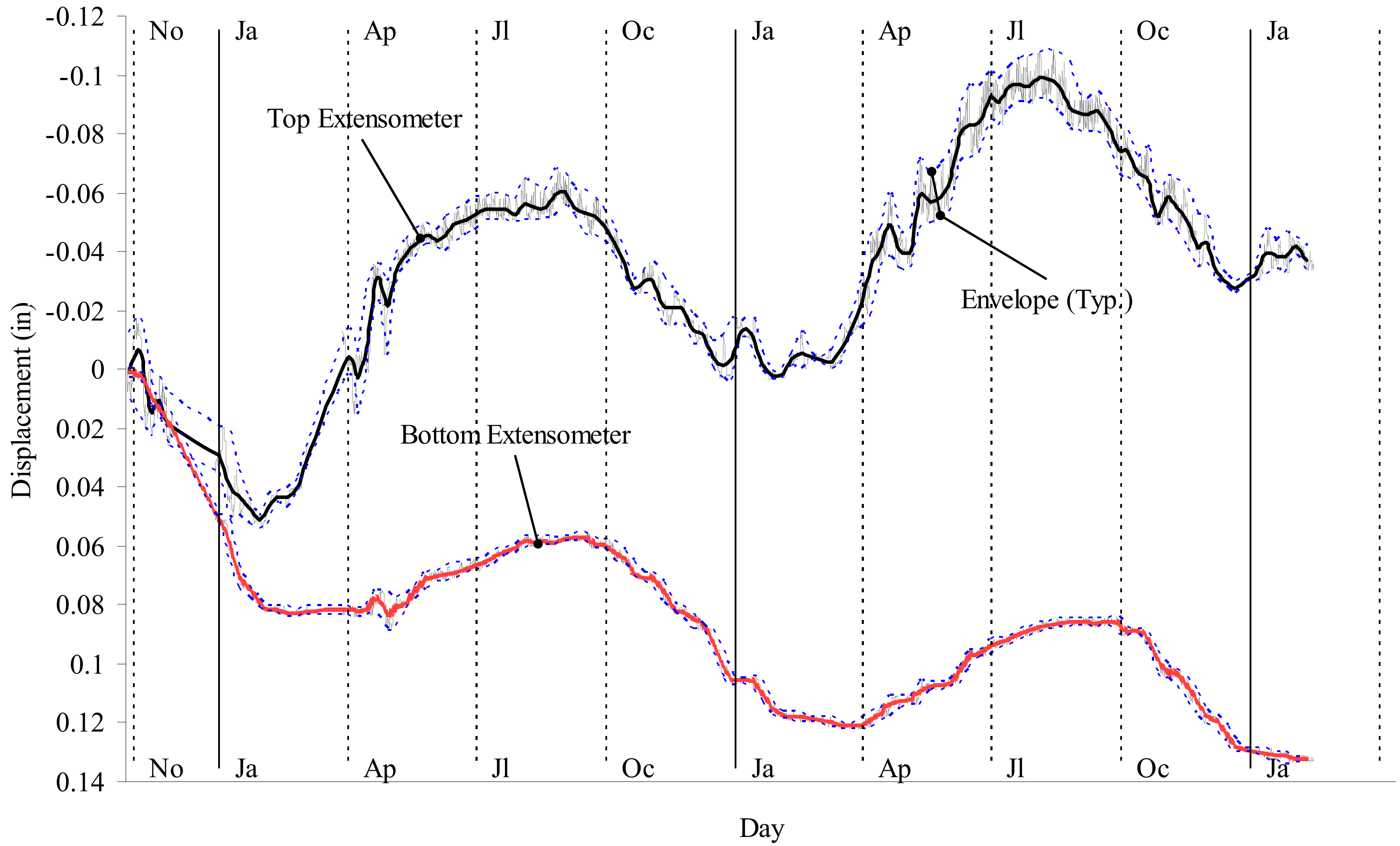

Figure 3.38. Bridge 222: Extensometers (On Abutment 1)

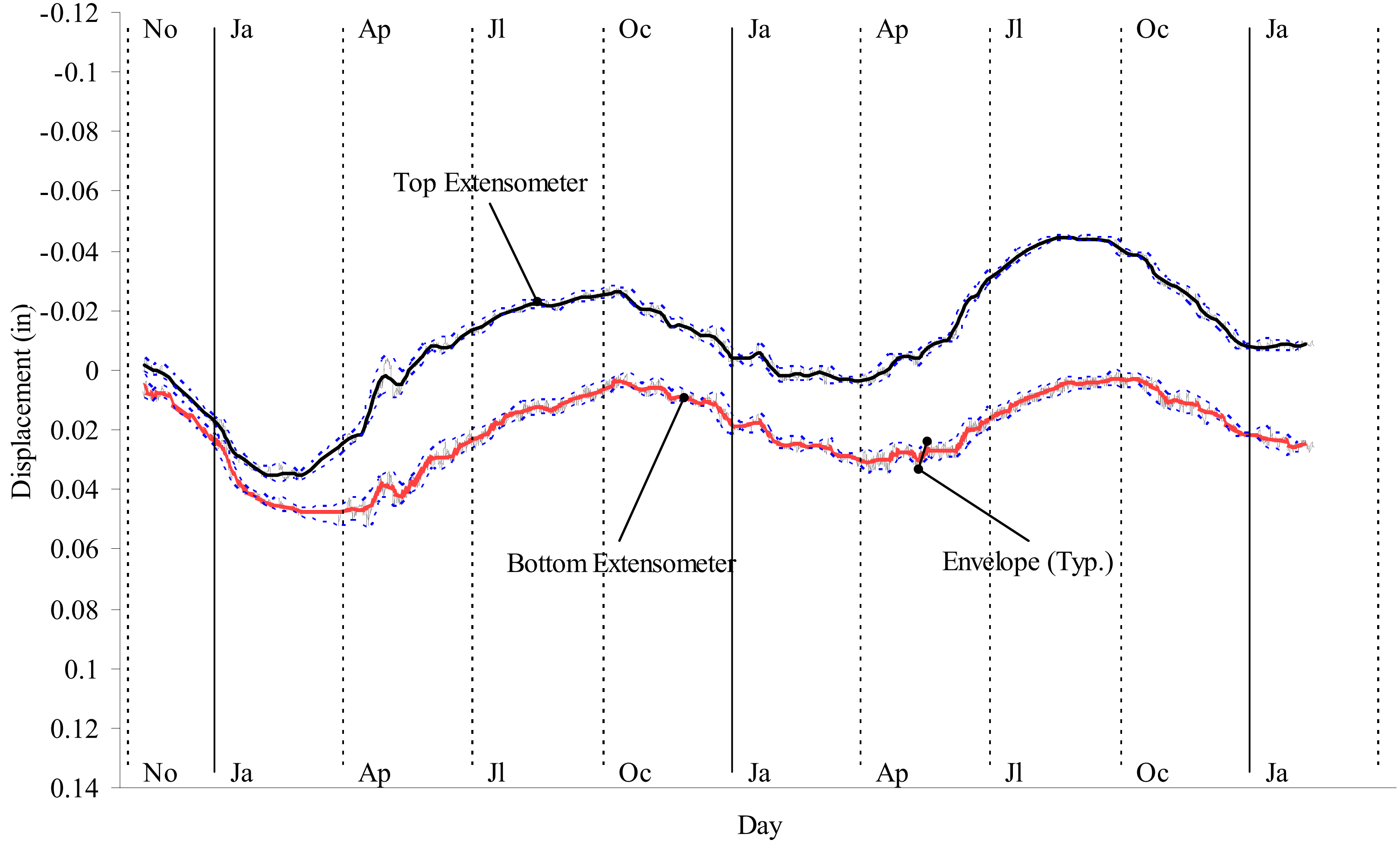

Figure 3.39. Bridge 222: Extensometers (On Abutment 2)

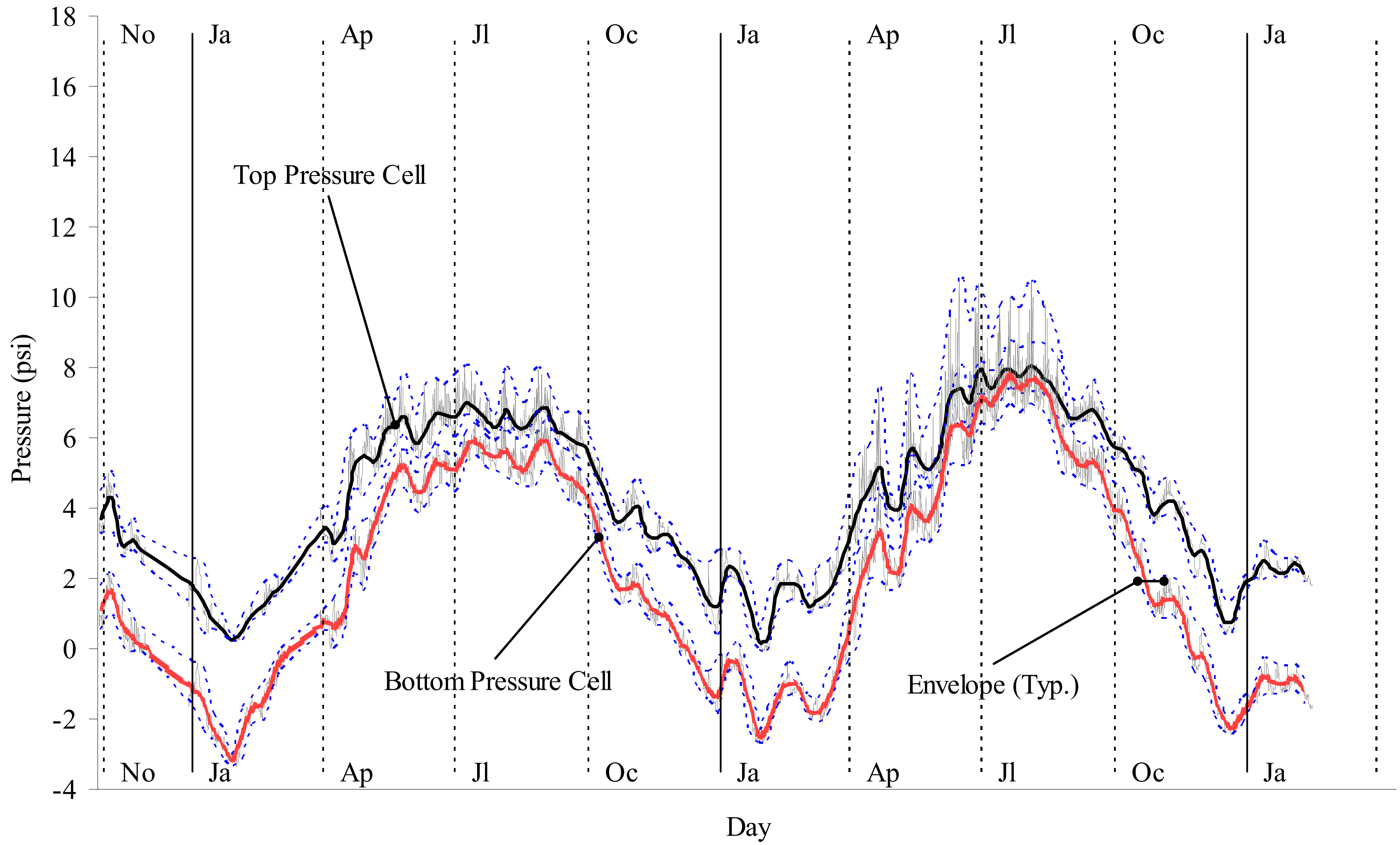

Figure 3.40. Bridge 222: Pressure Cells (On Abutment 1)

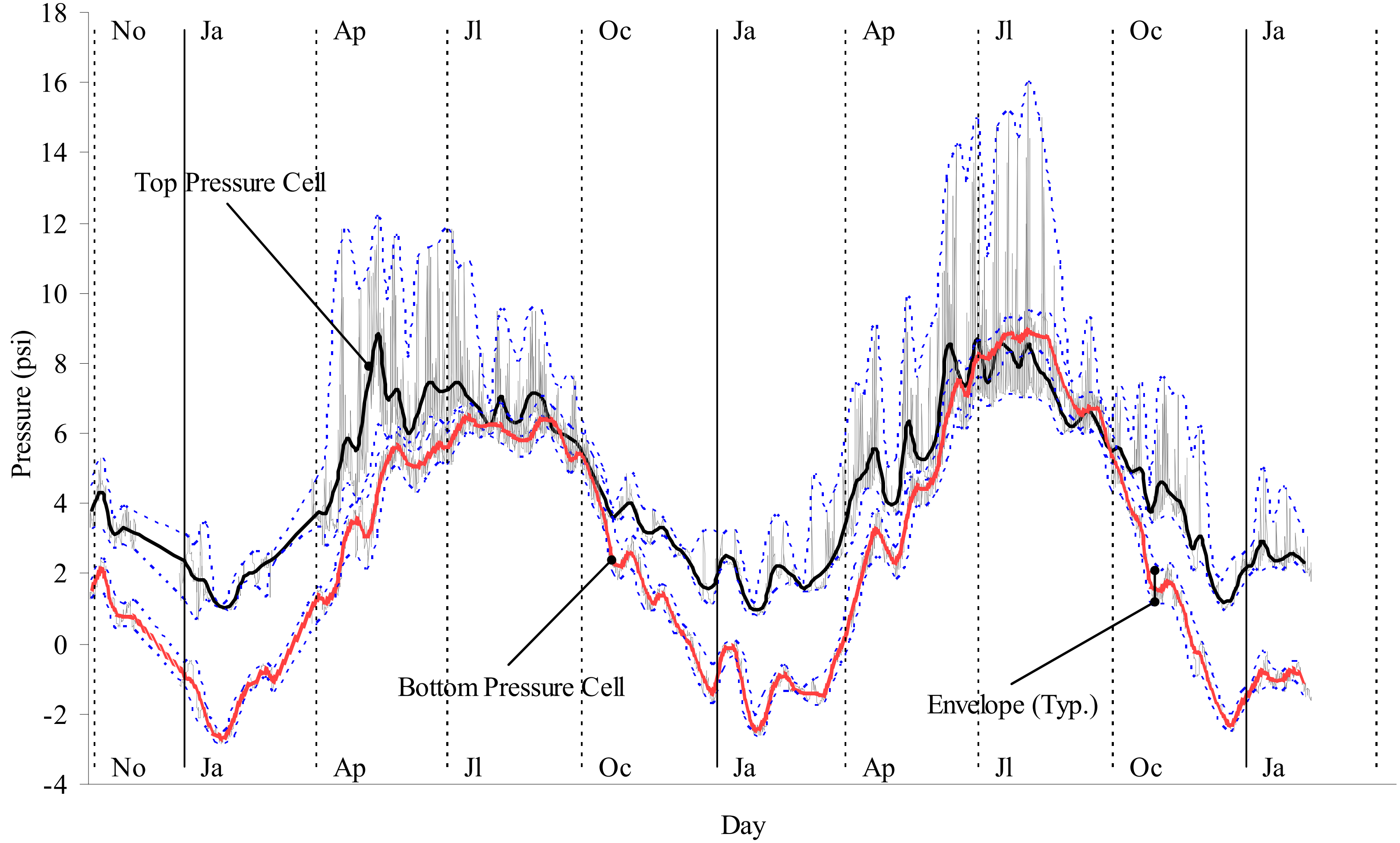

Figure 3.41. Bridge 222: Pressure Cells (On Abutment 2)

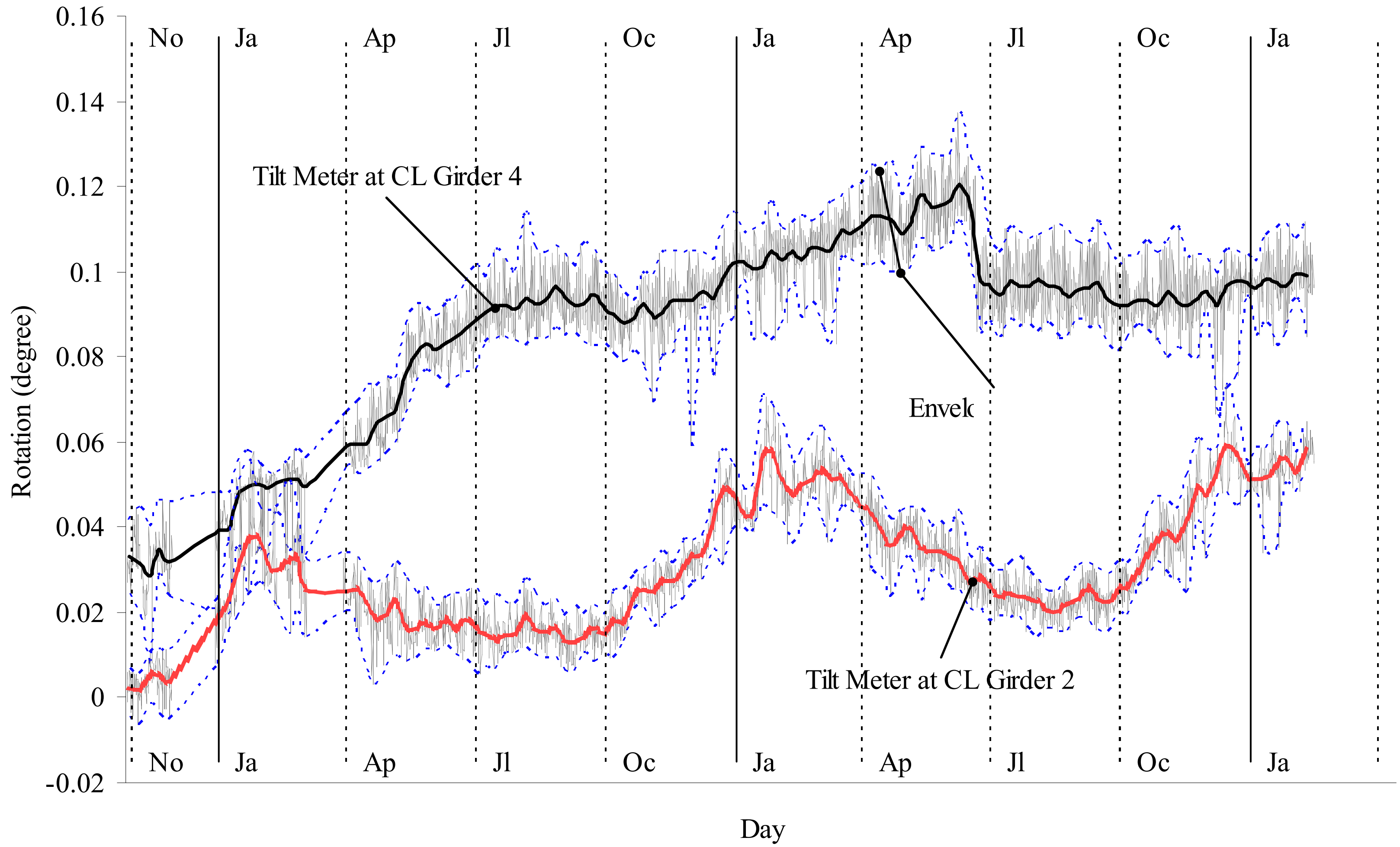

Figure 3.42. Bridge 222: Tilt Meter (On Abutment)

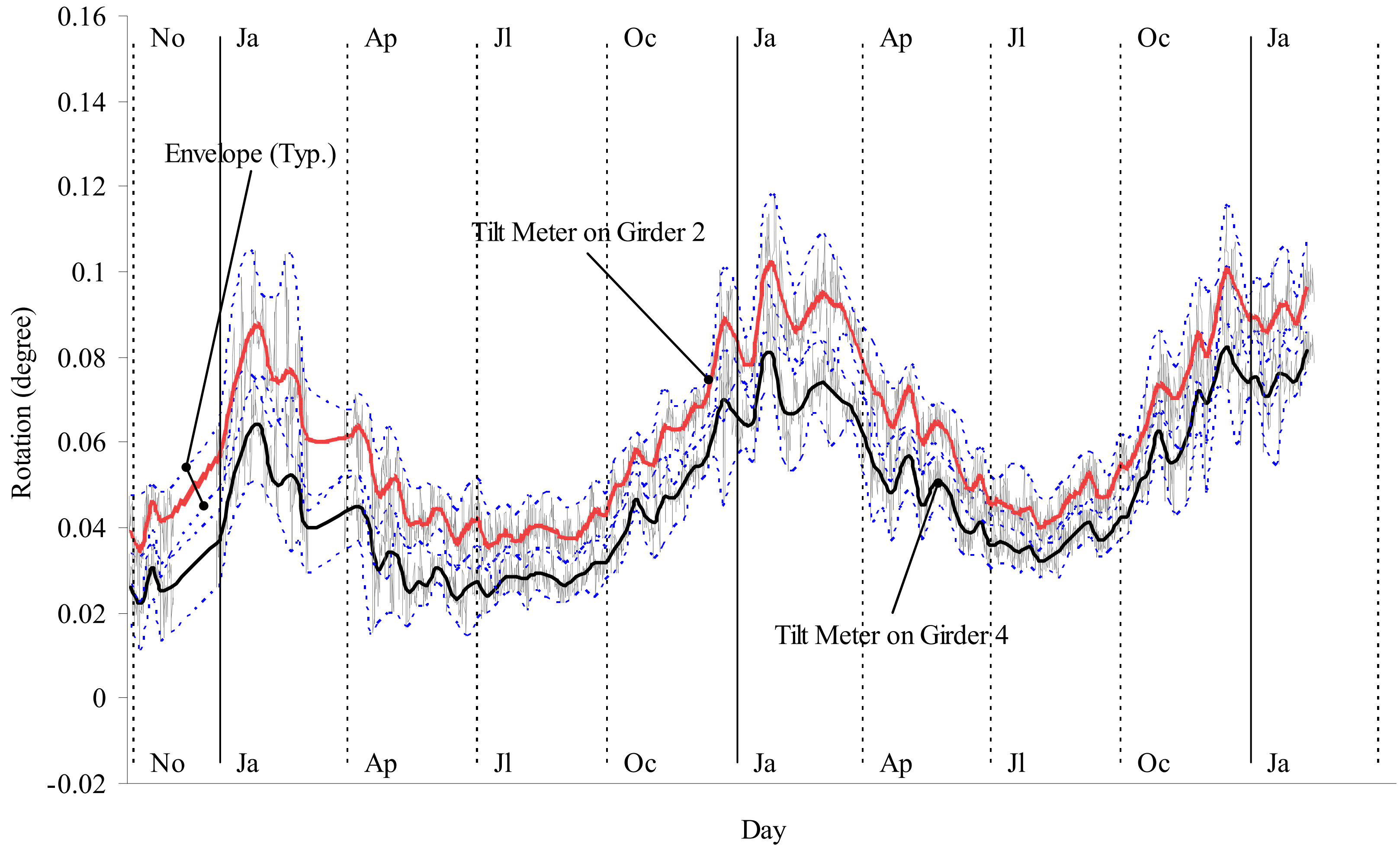

Figure 3.43. Bridge 222: Tilt Meter (On Girders)

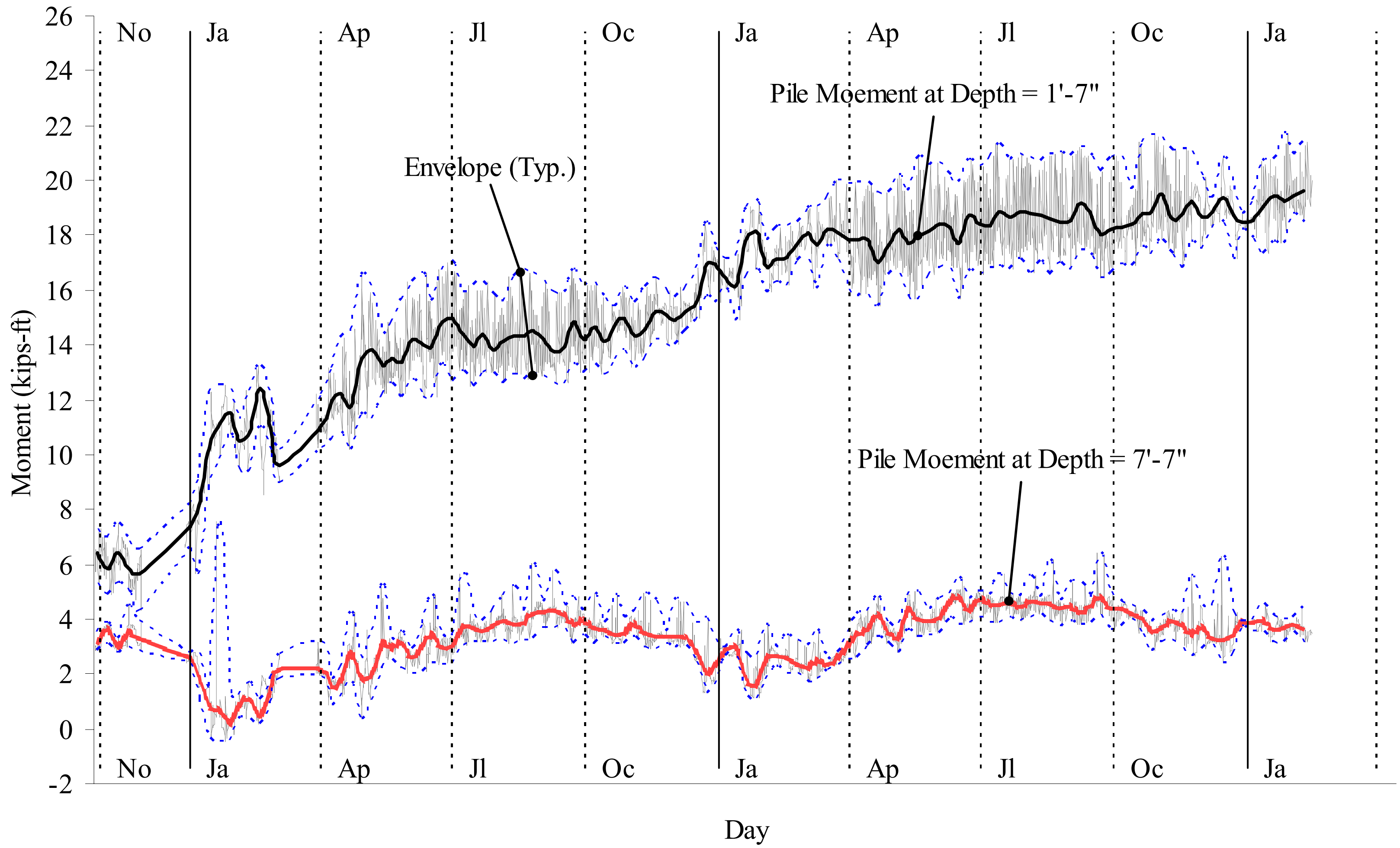

Figure 3.44. Bridge 222: Moments on South Pile (Abutment 1)

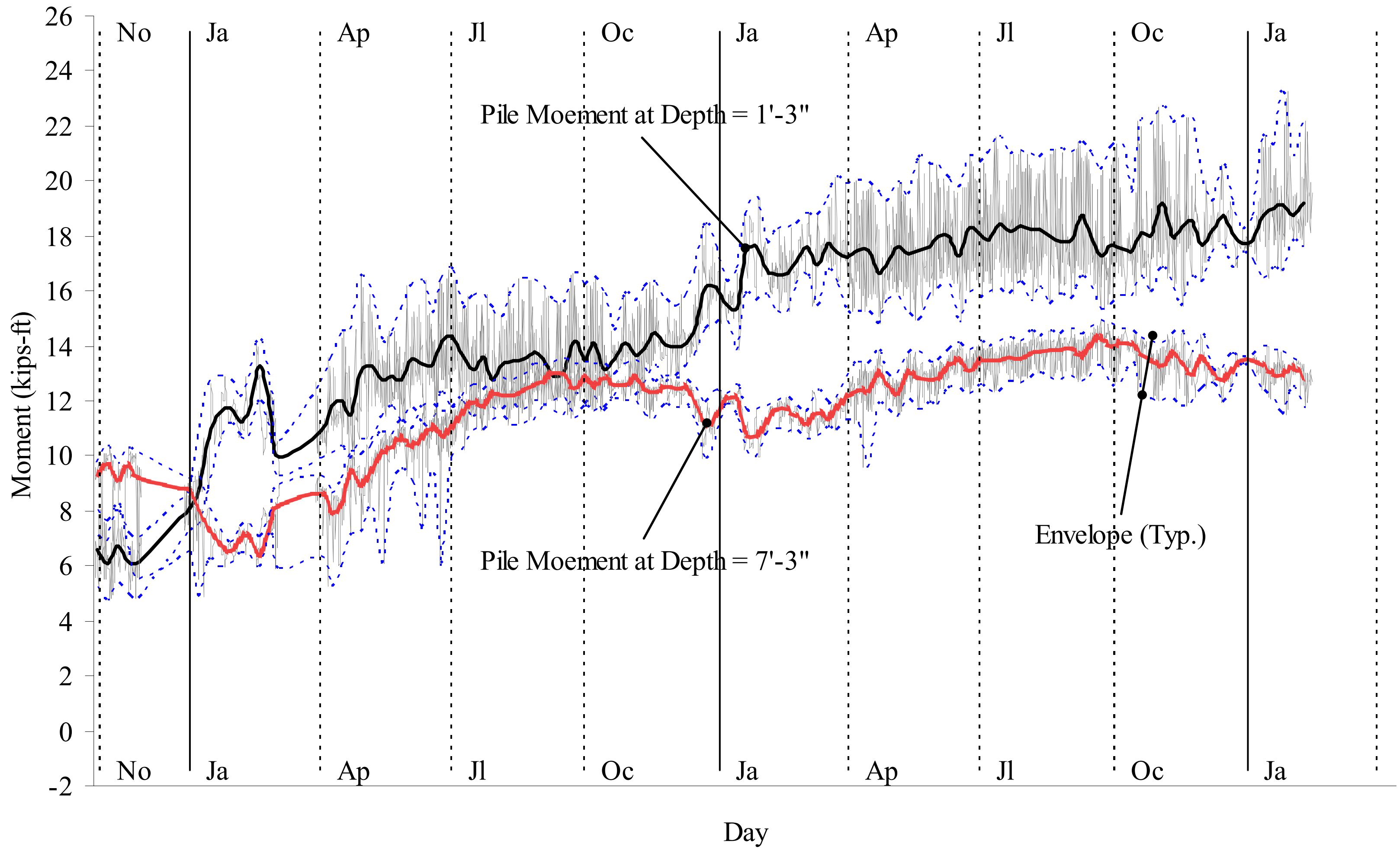

Figure 3.45. Bridge 222: Moments on North Pile (Abutment 1)

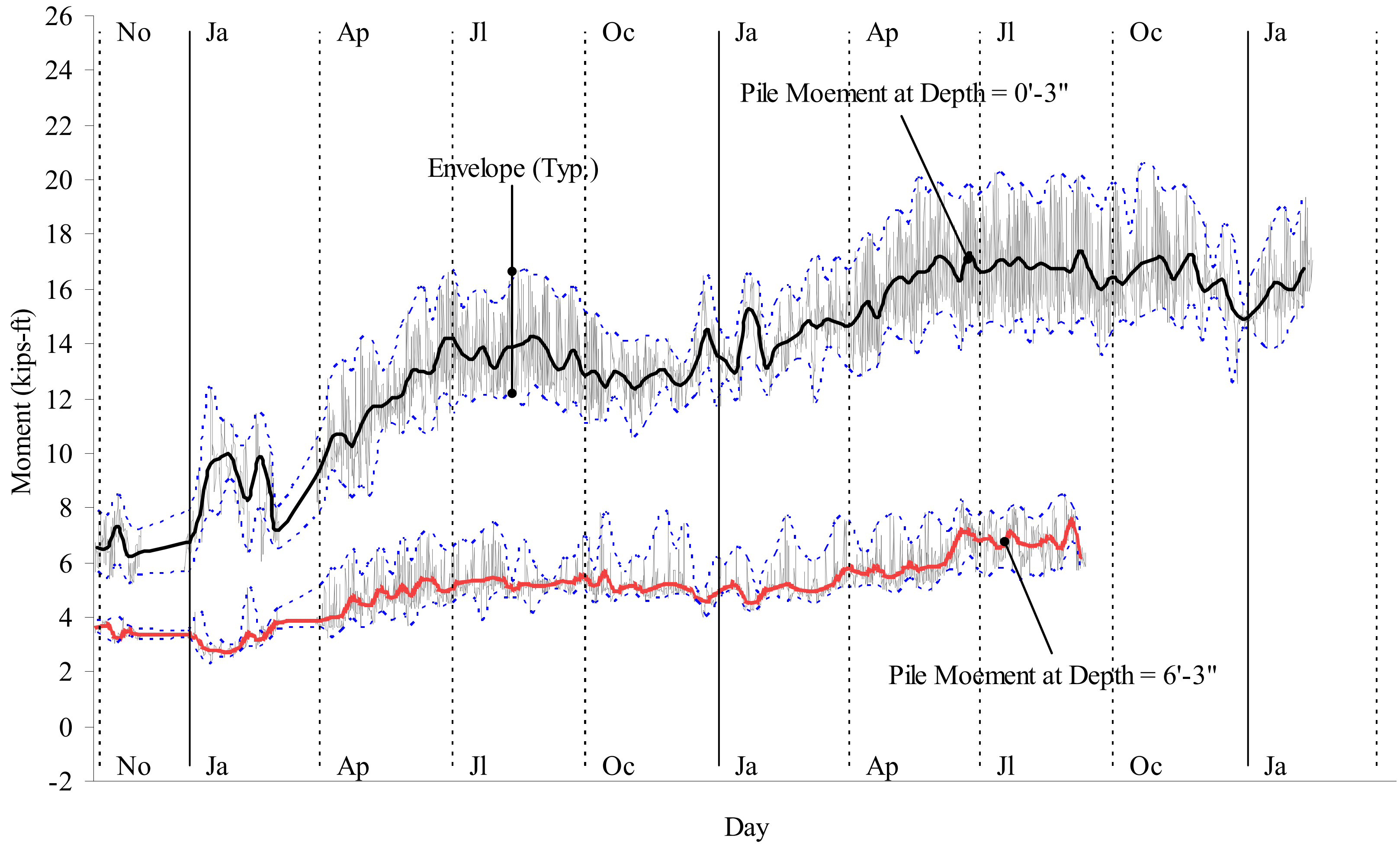

Figure 3.46. Bridge 222: Moments on South Pile (Abutment 2)

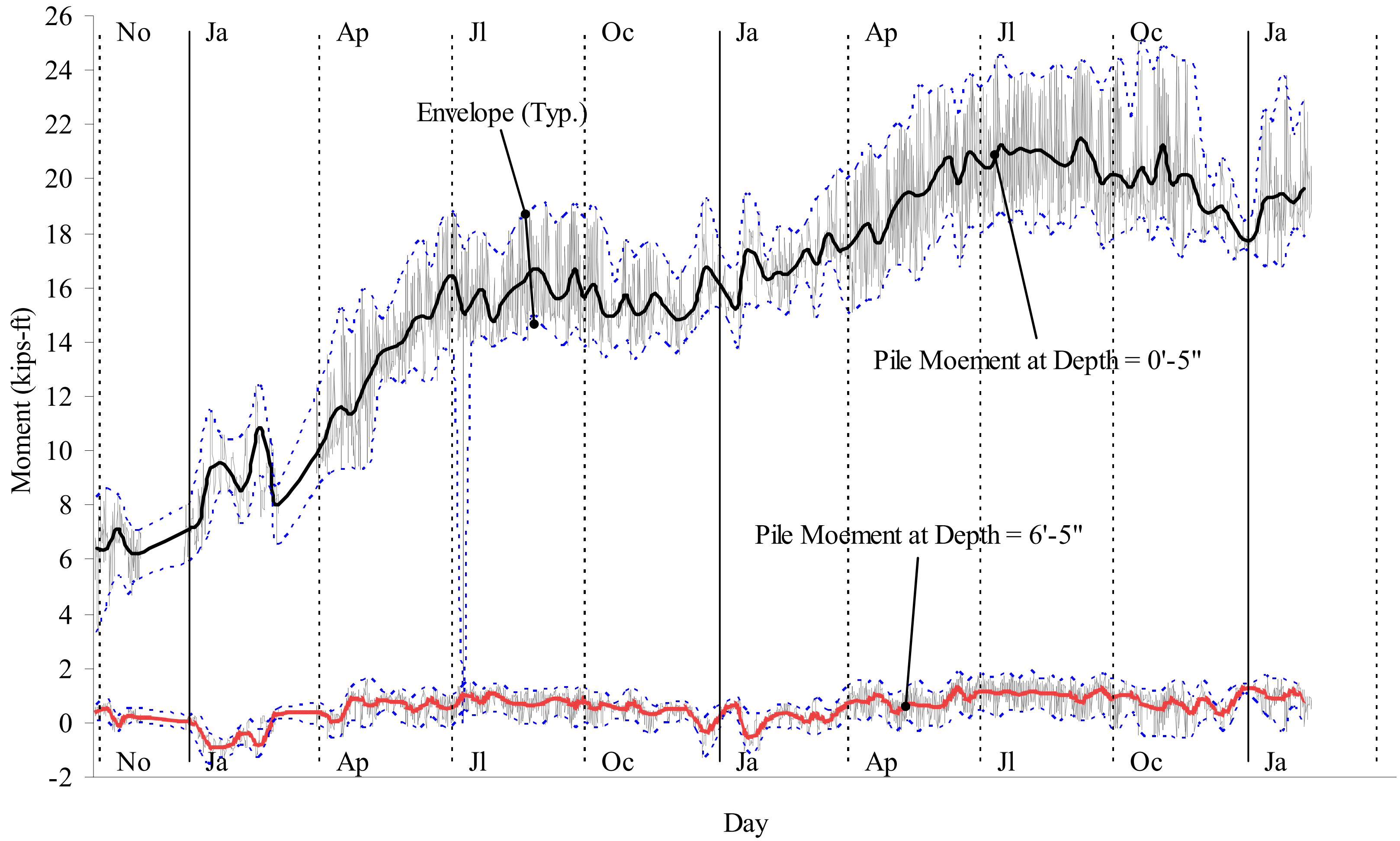

Figure 3.47. Bridge 222: Moments on North Pile (Abutment 2)

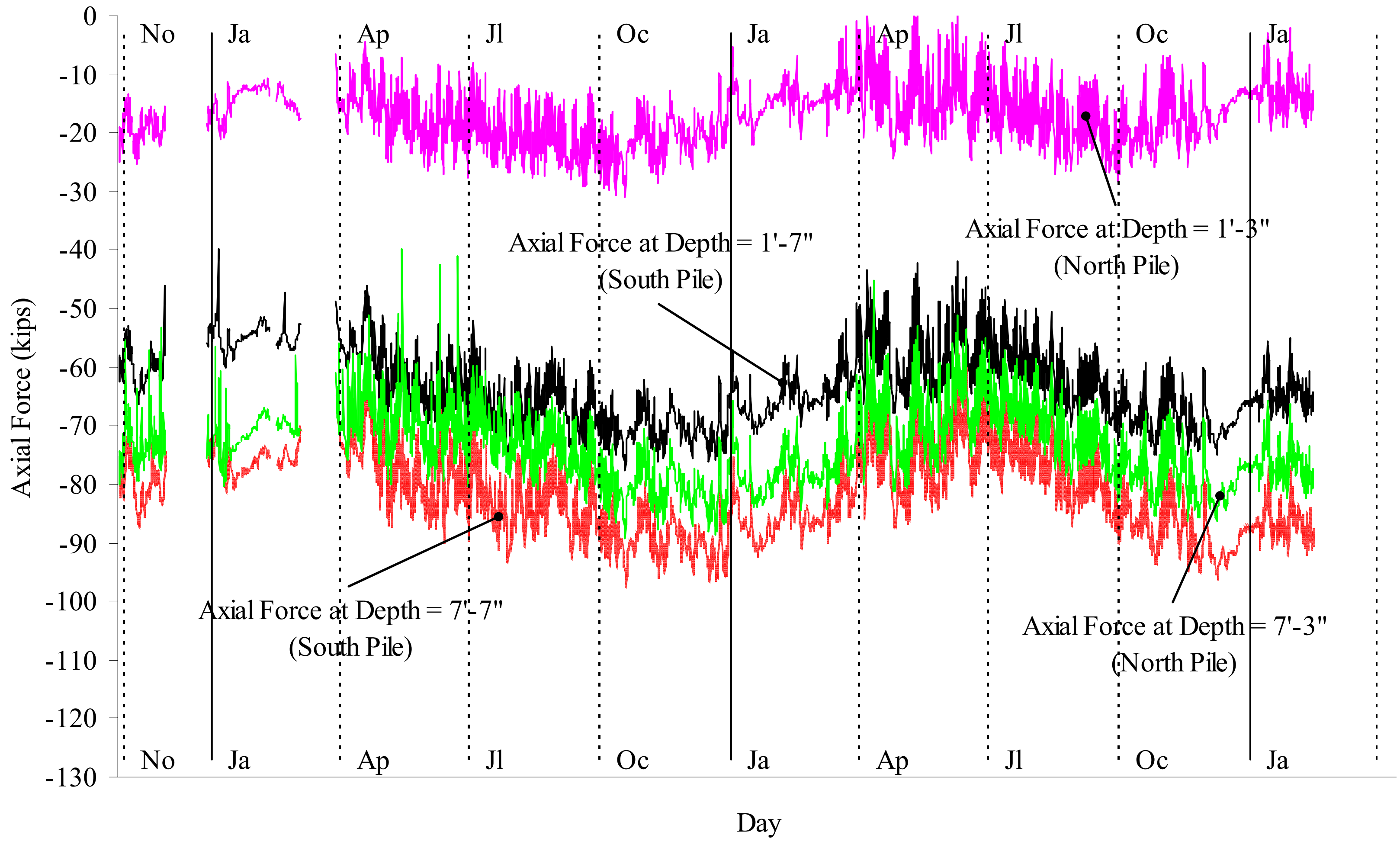

Figure 3.48. Bridge 222: Axial Forces on North and South Piles (Abutment 1)

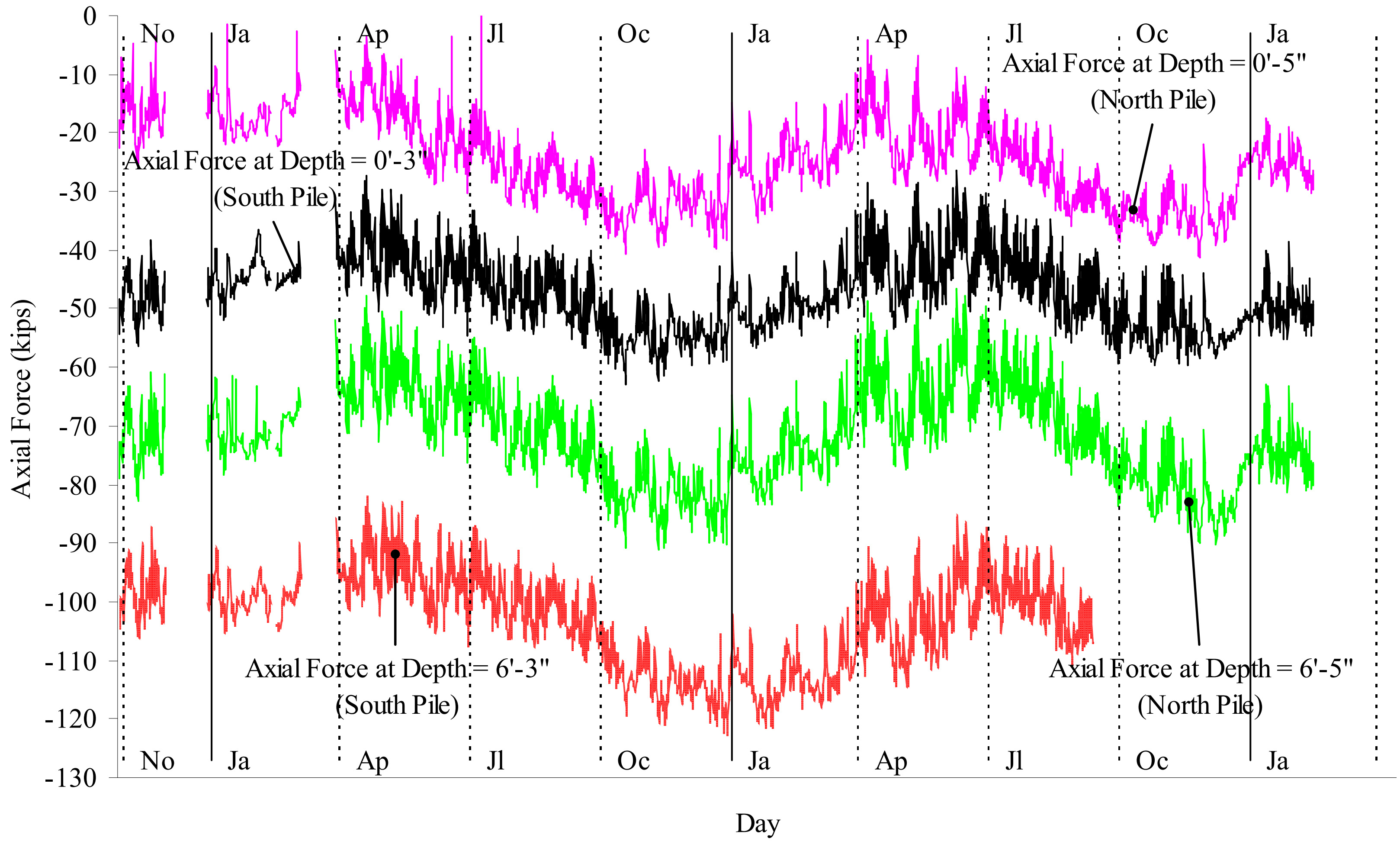

Figure 3.49. Bridge 222: Axial Forces on North and South Piles (Abutment 2)

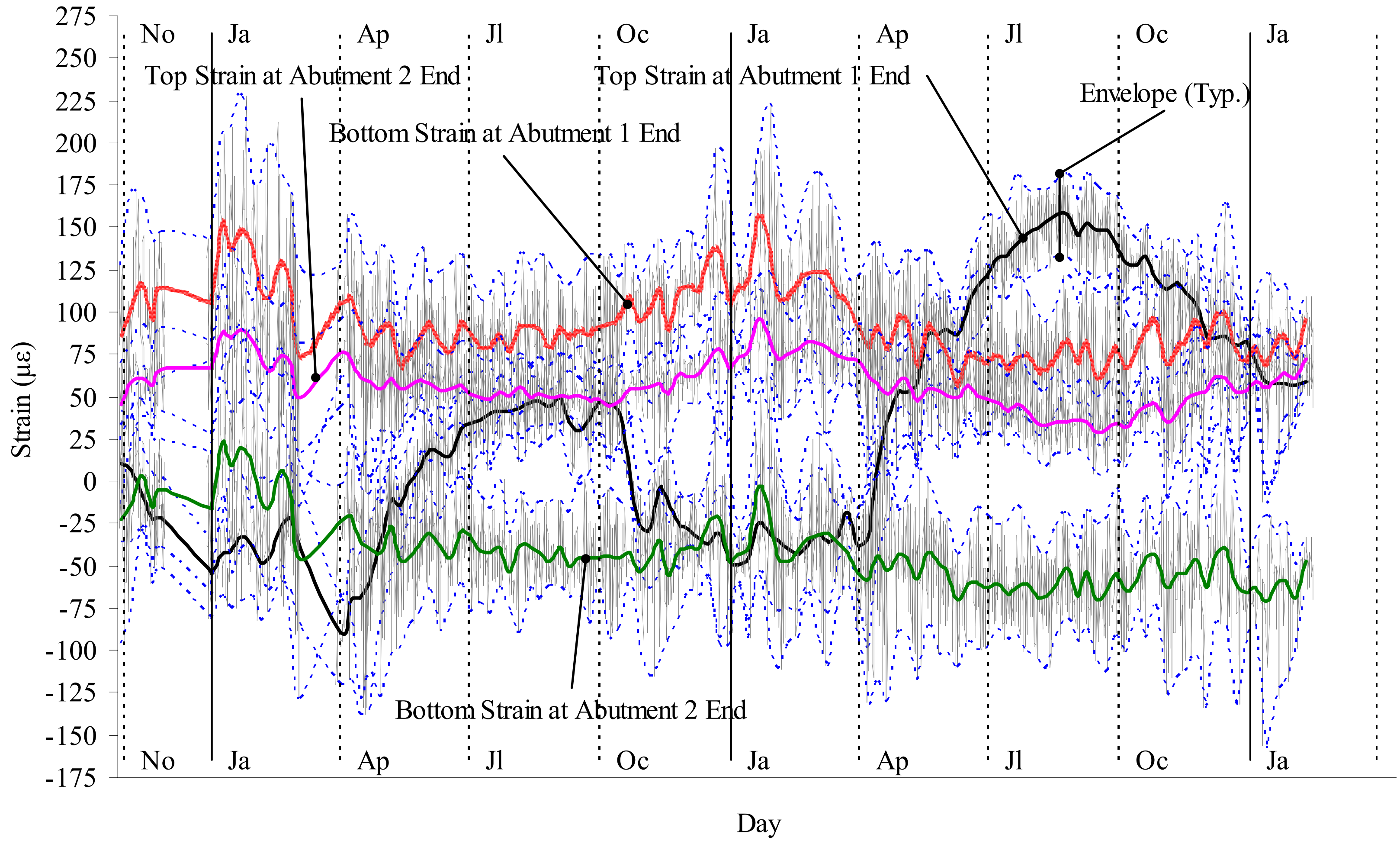

Figure 3.50. Bridge 222: Strain Gages on Girder 2

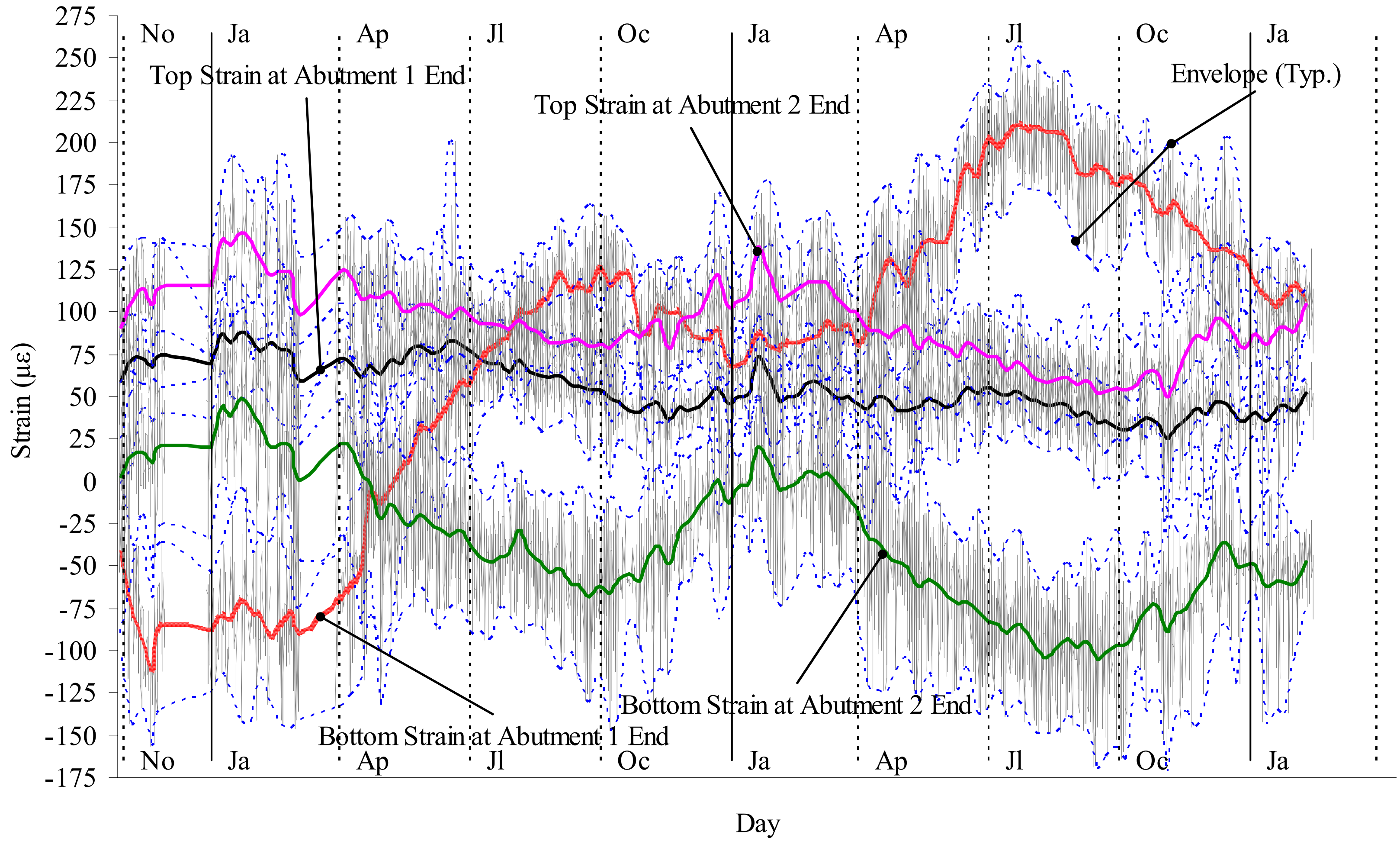

Figure 3.51. Bridge 222: Strain Gages on Girder 4

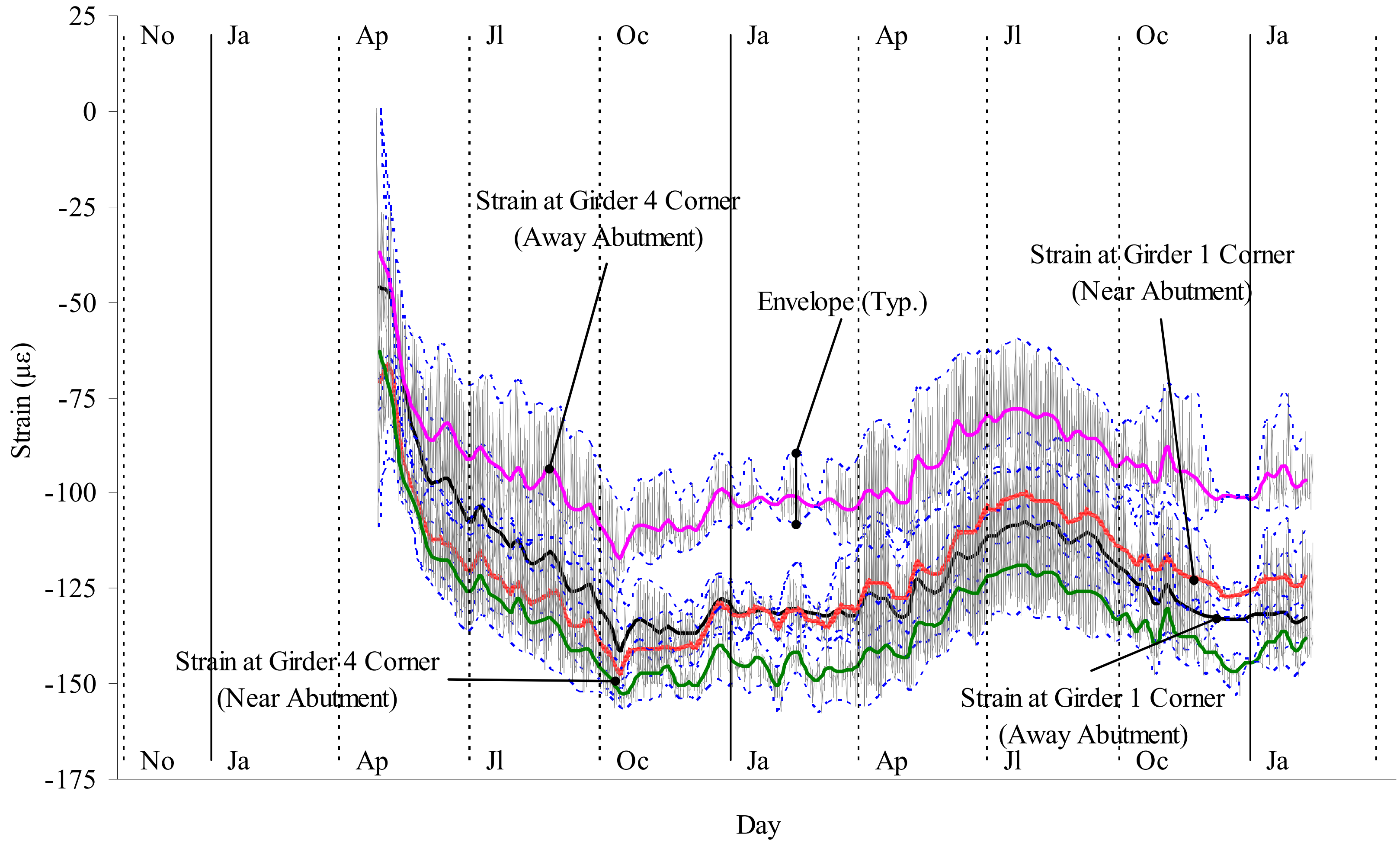

Figure 3.52. Bridge 222: Sister Bar Gages

3.5 BRIDGE 109 MONITORING RESULTS

This section presents field data obtained from bridge 109 instruments consisting of 5 extensometers, 5 pressure cells, 8 tilt meters, 24 strain gages on 4 piles, 16 strain gages on 4 prestressed concrete girders, and 6 sister bar gages. HP piles for abutment 2 were driven on September 2005 and strain gage measurements were regarded as initial zero values. Thus, east and west piles of abutment 2 were measured in September, October and November 2005. Piles for abutment 1 were driven on December 2005 and strain gages on the west and east piles of abutment 1 were read in December 2005 and February 2006. Axial forces and weak-axis bending moments for each pile were computed based on the strain gage measurements and presented in Table 3.1. It is noted that Channel 1-2 strain gage on the east pile of abutment 2 was damaged after driving and no moment data were available.

Table 3.1: Measured Data of Bridge 109

Abutment	Pile	Location	Depth	After Placing Abutment (1)		After Placing Abutment (2)	
				Axial Force (kips)	Weak-Axis Bending Moment (ft-kips)	Axial Force (kips)	Weak-Axis Bending Moment (ft-kips)
Abutment 1	West Pile	Bottom	7'-9"	8.12	5.95	N/A	N/A
		Top	0'-9"	10.13	3.45	N/A	N/A
	East Pile	Bottom	8'-8"	-4.55	0.32	N/A	N/A
		Top	1'-8"	-0.03	-0.78	N/A	N/A
Abutment 2	West Pile	Bottom	9'-3"	-7.15	0.83	-9.53	0.78
		Top	2'-3"	-3.25	-0.11	-4.45	0.04
	East Pile	Bottom	8'-3"	-5.41	N/A	-8.15	N/A
		Top	1'-3"	0.45	-0.80	-1.23	-0.84

3.6 CONCLUDING REMARKS

IA bridges 203, 211, 222 and 109 have been instrumented and monitored since November 2002, September 2004, November 2003, and September 2005, respectively. A total of 64 gages were mounted for bridges 203, 211 and 109 and a total of 48 gages were mounted for bridge 222 to investigate daily and seasonal thermal response of IA bridges. A general trend of extensometers had a ratcheting effect. Gage reads of top extensometers fluctuated widely compared to those of bottom extensometers. An obvious trend of pressure cells was for the top and bottom within an abutment to maintain a constant gap between top and bottom pressure results. The constant difference between pressure cells was not as large as expected. This may be because the upper backfill soil is subjected to higher pressure when a bridge expands. However, the lower backfill soil is subjected to higher pressure when a bridge contracts. Thus, pressures of top extensometers tend to fluctuate widely compared to those of bottom extensometers. Also, daily thermal expansion and contraction effect was very sensitive compared to other gage reads. The rotation of tilt meters on interior girders or abutments produced well-matched results to extensometers and strain gages. However, the rotation of tilt meters on exterior girders tended to vary in a narrow range but keep increasing. This tilt meter result was highly dependent on each bridge's geometries. Abutment rotations produced different rotations compared to girder rotations because the construction joint between the backwall and abutment below the girder seats was expected to rotate. Pile moments generally ranged within pile-moment capacity for bridges 203, 211 and 222. However, bridge 211 had the largest abutment displacement. The first year abutment displacement of bridge 211 was similar to third-year abutment displacement of bridge 203, although bridge 211 had a total 114-ft single-span length and bridge 203 had a total 172-ft three-span length. Also, pile moments are expected to be related to abutment height because bridge 222 (single span 62-ft length) produced the lowest abutment displacement and pile moments. Axial forces of foundation piles had well-matched trends to each other and fluctuated in a small range. Strain gages on girders produced well-matched results to abutment rotation and girder rotation. However, it is difficult to determine general behavior of exterior and interior girders and awkward variations of a strain gage that fluctuate widely while other gages on other girders do not range widely were observed. This fact implies that each girder is subjected to different backfill earth pressures or abutment distortions. Sister bar gages in approach slabs had a significant decrease at the beginning period due to creep and shrinkage and superstructure contraction. As observed in extensometers, the decrease of sister bar gages was not recovered to the original location.

CHAPTER 4

NUMERICAL MODELING

4.1 Introduction

This chapter presents details of the ANSYS numerical modeling for bridges 203, 211, 222, and 109. Due to the presence of structural continuity inherent to IA bridges, the complexity of numerical modeling commonly employed in conventional bridges is increased, requiring additional considerations:

- Time-dependent effects,
- Soil/structure interaction, and
- Abutment/backwall joint.

Methodologies to incorporate these three aspects are the primary focus of this chapter. Time-dependent effects consist of creep, shrinkage, and steel relaxation. Soil models are required to account for interaction between the soil and piles and soil and abutments. The abutment to backwall joint, depending on construction, may deform significantly into the inelastic region in the case of long length bridges. Model details of this particular joint were, therefore, incorporated into the numerical model here.

Chapter 4 is organized into three subsections with respect to the three issues listed above. Section 4.2 discusses the age-adjusted effective modulus (AAEM) method as an effective method of incorporating time-dependent effects. Section 4.3 describes soil models representing soil-structure interaction behaviors. And Section 4.4 presents a joint model representing abutment/backwall joint behavior.

4.2 TIME-DEPENDENT EFFECTS

Time-dependent effects in IA bridge analysis are the result of a combination of creep, shrinkage, and steel relaxation found in all prestressed concrete structures. These effects cause short- and long-term length instability of a superstructure component, producing secondary effects and displacements at the abutments and piles. Therefore, time-dependent effects must be included in numerical models for accurate movement predictions.

For the present research, ACI Committee 209 (2004) recommendations were utilized to predict creep and shrinkage of prestressed elements. In order to incorporate time-dependent effects into the numerical models, AAEM, based on a time-varying concrete modulus, was utilized because it is capable of solving all common time-dependent effect problems (Neville et al., 1983; Jirásek and Bažant, 2001). Creep and aging coefficients taken from ACI Committee 209 (2004) were used as a key parameter to obtain such a time-varying concrete modulus. In addition, time-dependent strains can be determined using the AAEM method and were consequently imposed on the superstructure component by means of an equivalent temperature loading. An equation of intrinsic relaxation in prestressing steel recommended by AASHTO LRFD (2004), was also incorporated into the numerical models.

Creep

Creep is a well-known phenomenon in concrete members, normally separated into two components: basic creep and drying creep. Basic creep occurs in a condition where moisture is constantly controlled. An uncontrolled condition leads to a drying creep that allows moisture in concrete to diffuse to the environment.

Most specifications, including ACI 209, use a dimensionless term referred to as the creep coefficient, $\varphi(t,t_o)$, to characterize creep (both basic and drying creep). The creep coefficient is defined as the ratio of load duration, $t-t_o$, to the initial elastic strain at time t_o. Therefore, the total strain can be expressed as (Jirásek and Bažant, 2001):

$$\varepsilon(t)=\frac{\sigma(t_o)}{E(t_o)}\left[1+\varphi(t,t_o)\right] \qquad 4.1$$

where $\varepsilon(t)$ is a total strain at time t, $\sigma(t_o)$ is an initial stress at time t_o, $E(t_o)$ is a concrete modulus of elasticity at time t_o, and $\varphi(t,t_o)$ is a creep coefficient at time t corresponding to the age at loading t_o. Figure 4.1 presents a sample creep coefficient curve based on bridge 222 girder properties.

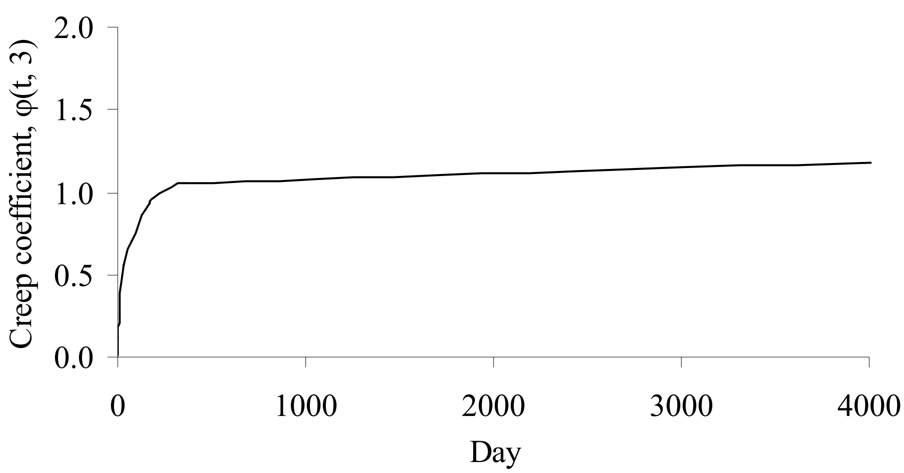

Figure 4.1. Creep Coefficient (Bridge 222)

Another important issue related to creep is the effect of varying stress on creep behavior. AAEM incorporates this effect by using a simplified aging coefficient $\chi(t, t_o)$. ACI Committee 209 (2004) includes a provision for computing this coefficient in a table format. Figure 4.2 presents a sample of the aging coefficient based on bridge 222 girder properties. The procedure used to incorporate creep and aging coefficients into numerical models is discussed later in this chapter.

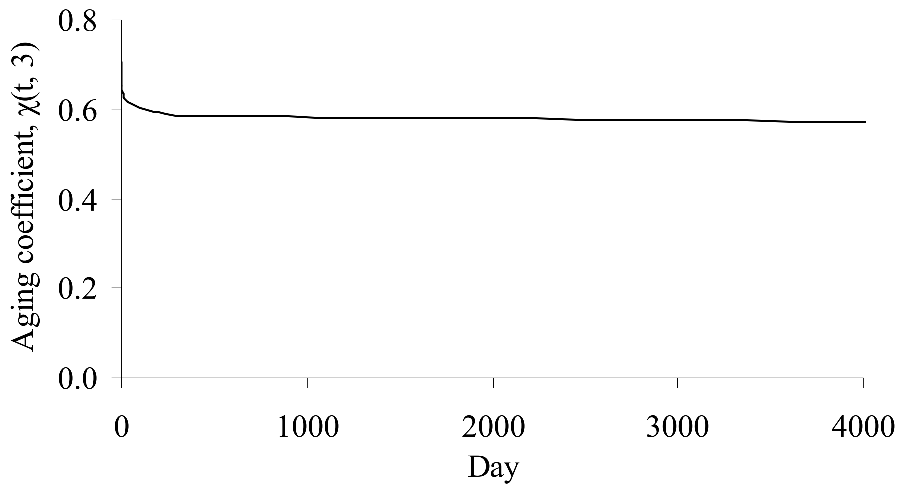

Figure 4.2. Aging coefficient (Bridge 222)

Shrinkage

Total shrinkage in concrete members is composed of four types: carbonation shrinkage, plastic shrinkage, autogenous shrinkage, and drying shrinkage. A detailed discussion of each shrinkage type is presented in Jirásek and Bažant (2001). Figure 4.3 presents shrinkage strain based on ACI Committee 209 (2004) and bridge 222 girder properties.

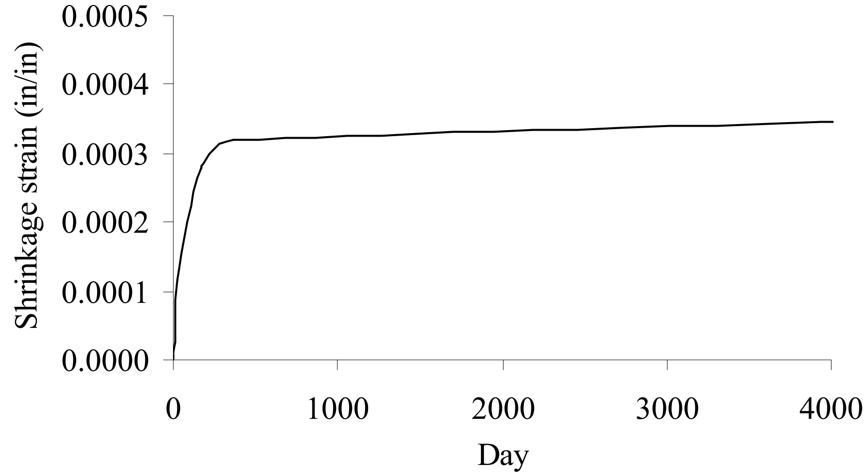

Figure 4.3. Shrinkage Strains (Bridge 222)

Relaxation of Prestressing Steel

Compared to creep and shrinkage, relaxation of prestressing steel is more readily predicted with accuracy. An equation of intrinsic relaxation in AASHTO LRFD (2004) for low-relaxation strand is expressed as:

$$\Delta f_{RE} = \frac{[\log(24t) - \log(24t_o)]}{40}\left[\frac{f_{pj}}{f_{py}} - 0.55\right] f_{pj} \qquad 4.2$$

where t is time at the end of the time interval in days, t_o is time at the beginning of the time interval (days), f_{pj} is stress in the prestressing steel at jacking (ksi), and f_{py} is a specified yield strength of prestressing steel (ksi).

The intrinsic relaxation occurs under a condition where constant strain is imposed to the strand. For a prestressed concrete member immediately after transfer, the condition of constant strain no longer holds due to the effects of elastic shortening, creep and shrinkage. As a result, reduction of the intrinsic relaxation must be made and can be simplified by applying a dimensionless coefficient of reduced relaxation, χ_r. The reduced relaxation Δf_R is given as:

$$\Delta f_R = \chi_r \Delta f_{RE} \tag{4.3}$$

An equation approximating χ_γ, taken from Ghali et al. (2002), is expressed as:

$$\chi_r = \exp\left[\left(-6.7 + 5.3\lambda\right)\Omega\right] \tag{4.4}$$

where $\lambda \quad = \dfrac{\text{steel stress immediately after transfer}}{\text{characteristic tensile stress}}$, and

$\Omega \quad = \dfrac{\text{total prestress change - intrinsic relaxation}}{\text{steel stress immediately after transfer}}$

It can be observed that the total prestress change is required for the calculation of χ_γ; however, this is not normally known in advance. Thus, it is imperative that an iterative procedure be employed in determining the coefficient of reduced relaxation.

Age-Adjusted Effective Modulus Method

There are several methods of analysis for time-dependent effects, including effective modulus method, rate of creep method, rate of flow method, improved Dischinger method, and age-adjusted effective modulus method (Neville et al., 1983). Among these methods, the AAEM method is the most widely accepted because it is capable of solving all common time-dependent problems with excellent agreement with more sophisticated step-by-step solutions (Neville et al., 1983; Jirásek and Bažant, 2001).

The derivative of aging coefficient, χ, and the basic equation of AAEM are taken from Jirásek and Bažant (2001). The basic AAEM equation is:

$$\varepsilon(t)=\frac{\sigma(t_o)}{E(t_o)}\left[1+\varphi(t,t_o)\right]+\frac{\left(\sigma(t)-\sigma(t_o)\right)}{\overline{E}(t,t_o)}+\varepsilon_{sh}\left(t,t_{sh,o}\right) \qquad 4.5$$

with notation consistent with Equation 1.1: $\overline{E}(t,t_o)$ is the age-adjusted effective modulus of concrete, $\sigma(t)$ is total applied stress at time *t*, χ is an aging coefficient at time *t* corresponding to the age at loading t_o, and $\varepsilon_{sh}\left(t,t_{sh,o}\right)$ is a total shrinkage strain at time *t*. A more detailed discussion of the AAEM method is available in Ghali et al. (2002). AAEM analyses for bridges 203, 211, 222, and 109 are presented in Appendix A.

The time-dependent strains at the top and bottom girder fibers for bridge 222 are presented in Figures 4.4 and 4.5, respectively. Three graphs corresponding to 174, 365, and 36,500 days after the concrete deck was poured are presented. For reference, the concrete bridge deck was placed at the 171st day.

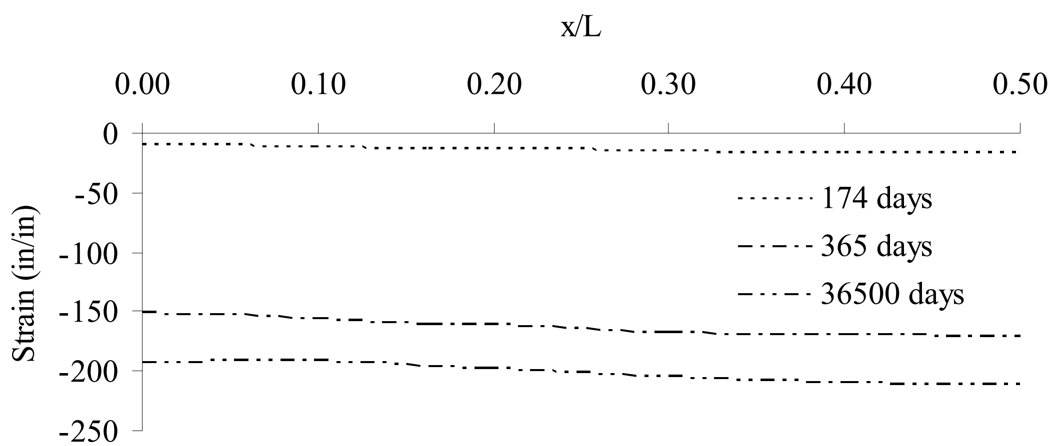

Figure 4.4. Strain at Top Fiber of Bridge 222 Girder

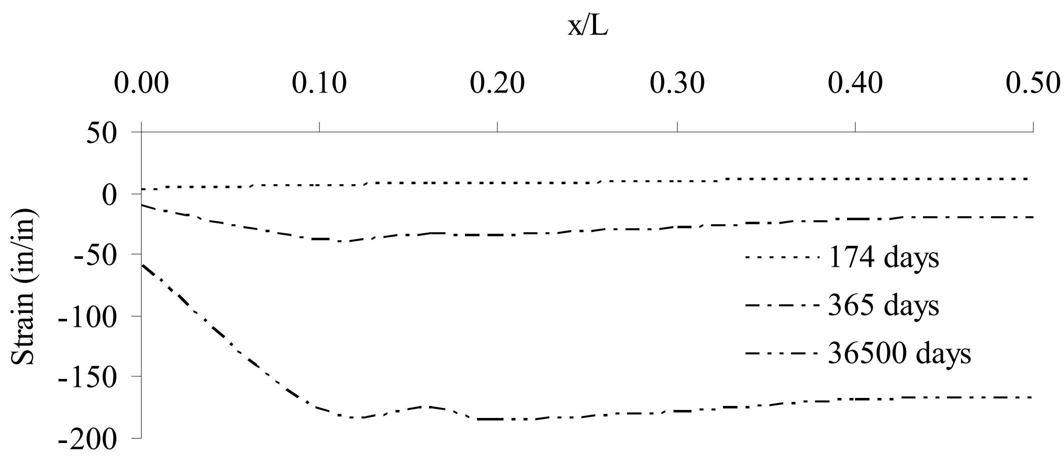

Figure 4.5. Strain at Bottom Fiber of Bridge 222 Girder

An unrestrained longitudinal boundary condition was assumed to analyze the time-dependent strains presented above. In order to account for effects of force redistribution due to structural continuity and support restraint to longitudinal movement, an analysis of time-dependent effect for statically indeterminate structures was investigated.

Time-Dependent Effects in Indeterminate Structures

Superstructure end restraint conditions prevent free contraction due to time-dependent effects. Longitudinal restraint causes time-dependent strains to develop in the girders. The force or displacement method is usually employed to solve this type of structural problem. The displacement method was used for the present study. The stiffness matrix based on the AAEM method is a time-dependent matrix as a result of replacing a typical elastic modulus by a time-dependent age-adjusted effective modulus $\overline{E}(t,t_o)$. In order to determine the force vector, an additional procedure is required. Time-dependent strains are converted to an equivalent temperature loading for constructing the force vector.

4.3 SOIL MODELS

Soil models are required to represent nonlinear and path-dependent responses of soil materials subjected to cyclic movement. In addition, compatibility of soil and structure deformations/strains to corresponding forces/stresses (soil-structure interaction) must be maintained in soil models at any instant of time. Soil-structure interaction is distinguished by two components: soil-pile interaction and soil-abutment interaction.

The modulus of subgrade reaction is widely used in analyzing a wide range of geotechnical applications such as foundations, retaining walls, and laterally loaded piles. A linear Winkler spring is usually employed for soil-abutment interaction. The *p-y* curve spring, known as a nonlinear Winkler spring, is more widely used for soil-pile interaction. In the present study, the p-y curve and a linear Winkler spring with upper and lower limits taken from classical earth pressure was adopted for soil-pile interaction and soil-abutment interaction, respectively.

Soil-Pile Interaction

Soil-pile interaction involves an interaction between piles and the surrounding soil. In the case of an IA bridge, soil resistance responding to bridge expansion is not the same as that of bridge contraction due to unsymmetrical soil geometry. Soil resistance developed under bridge contraction is generated by a small soil overburden and downhill slope on the bridge side of the abutment and is less than the soil resistance developed under expansion generated by a high soil overburden on the approach side of the abutment. These unequal soil resistances are one of the most important sources producing unequal structural responses between expansion and contraction cases.

A method based on *p*-*y* curves (Reese, 1984) was used for the soil-pile interaction modeling. This method was originally developed using finite difference techniques to solve an approximate solution of the 4^{th} order governing equation based on the modulus of subgrade reaction approach. The substitution of nonlinear *p*-*y* curve springs on the governing equation was performed herein rather than incorporating a traditional linear Winkler spring. An iterative solver was then implemented to achieve the transition.

In the present study, *p*-*y* curves were modeled using ANSYS element COMBIN39; therefore, validation against COM624P was completed to confirm the accuracy of this approach. Figures 4.6 and 4.7 present a sample of *p*-*y* curves (in dashed lines) generated from COM624P. Soil parameters were taken from the bridge 222 soil profile for clay above the water table and sand, respectively (See Chapter 5 for soil profile). The multi-linear curves (in solid lines) represent a nonlinear soil spring in ANSYS.

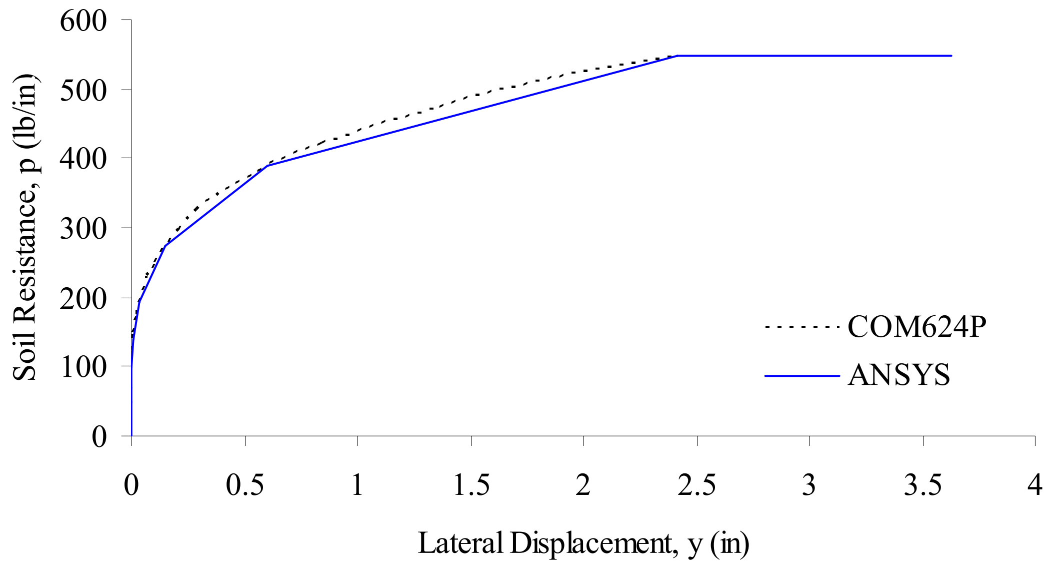

Figure 4.6. *p-y* Curve at Pile Head - Clay above Water Table (Bridge 222)

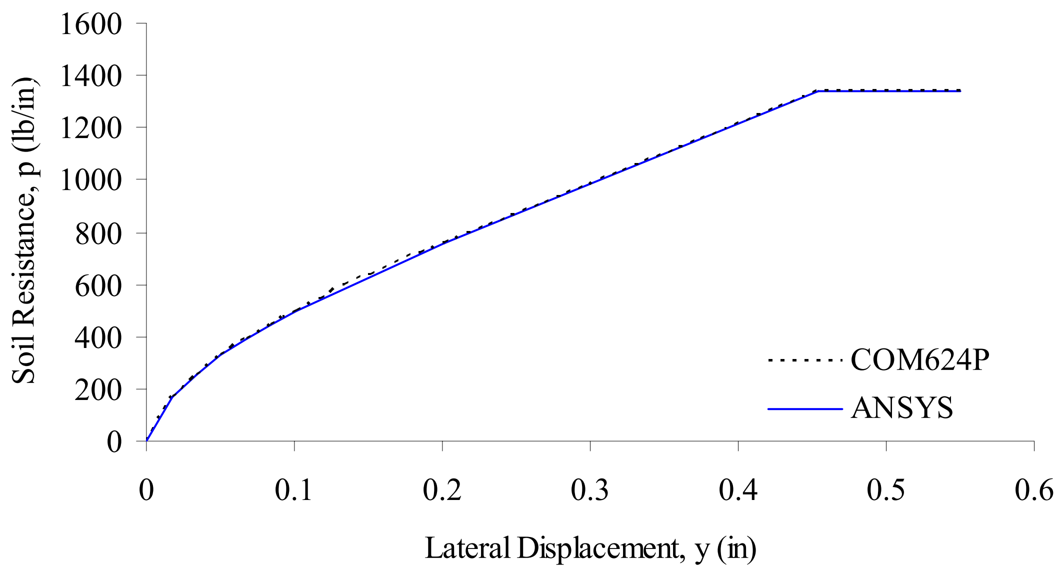

Figure 4.7. *p-y* Curve at 11.5 ft below Pile Head - Sand (Bridge 222)

An analysis test case was evaluated using the pile geometry and soil profile of bridge 222. A lateral force of 5 kips that produces a working displacement range of the actual structure and a free end boundary condition were applied at the pile head. COM624P and ANSYS comparisons of lateral displacements versus depth, bending moments versus depth, and shear forces versus depth are presented in Figures 4.8 through 11.

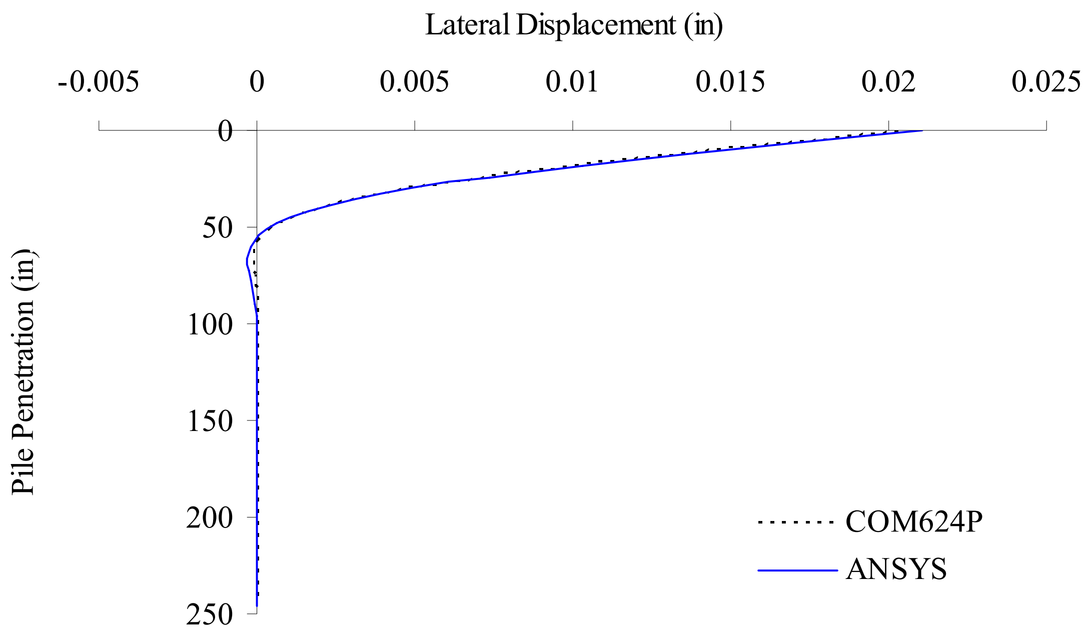

Figure 4.8. Lateral Displacement due to 5-kip Load at Pile Head (Bridge 222)

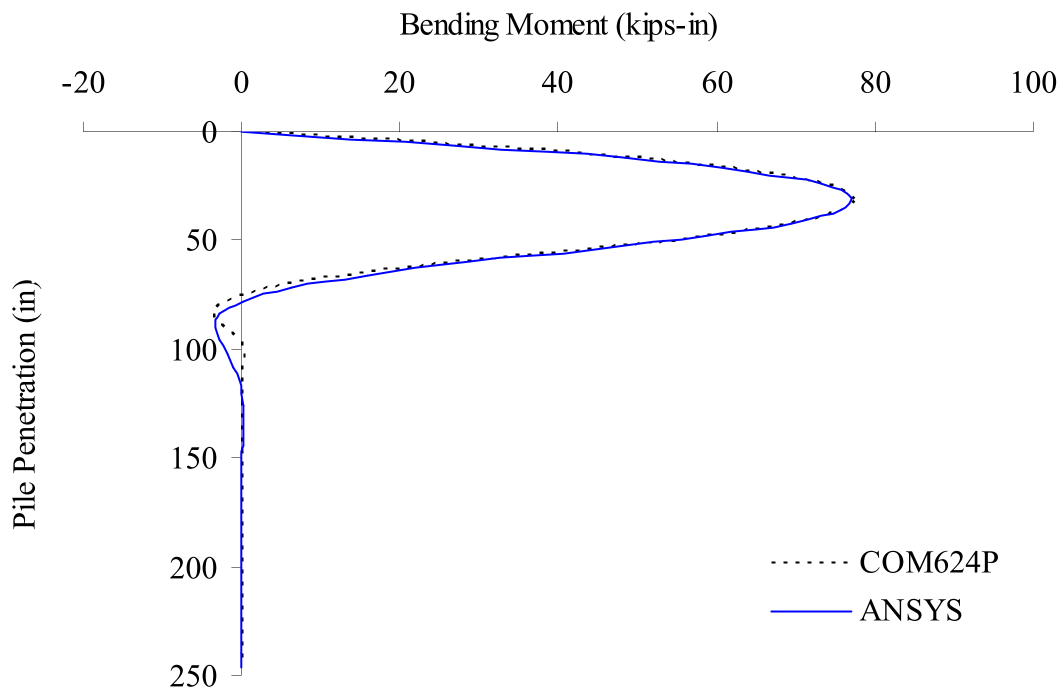

Figure 4.9. Pile Bending Moment due to 5 kip Load at Pile Head (Bridge 222)

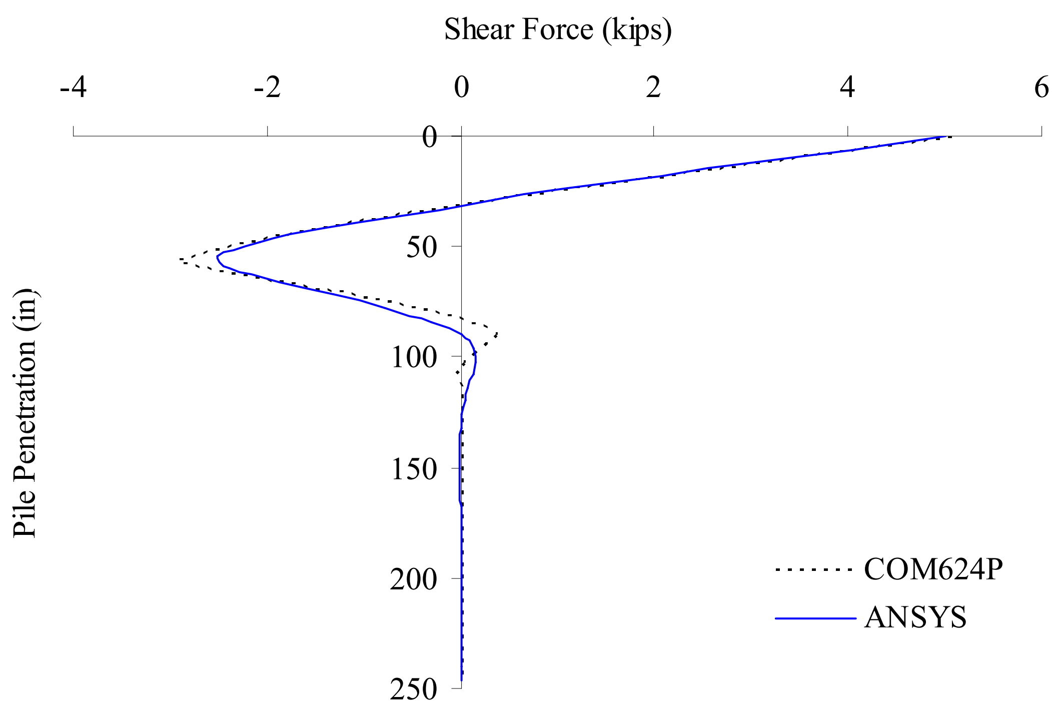

Figure 4.10. Pile Shear Force due to 5 kip Load at Pile Head (Bridge 222)

ANSYS predictions of pile behavior are similar to COM624P with a difference of 3.9, 0.1, and 1.5 percent for maximum lateral displacement (at the pile head), maximum bending moment (at about 30 inches below the pile head), and maximum shear (at the pile head), respectively. Element length in the ANSYS model is relatively coarse (6 inches) compared to the length used in COM624P (1.2 in). Therefore, differences in moments and shears at a depth of approximately 10 ft are expected to appear where a short distance of two adjacent inflection points occurs.

The unrecoverable characteristics of soil must also be considered when soil is subjected to cyclic loading. Modifications to the original *p-y* curves (Reese, 1984; and Wang and Reese, 1993) were proposed by several researchers (e.g., Boulanger, 1999; Lin and Liao, 1999; and Taciroglu et al., 2003). Among the proposed models, an elasto-plastic *p-y* curve proposed by Taciroglu et al. (2004) has proven to be numerically robust and was adopted herein. ANSYS COMBIN39 is capable of incorporating the elasto-plastic behavior by generating an unloading branch utilizing classical plasticity theory. A qualitative diagram of the elasto-plastic *p-y* curve is presented in Figure 4.11.

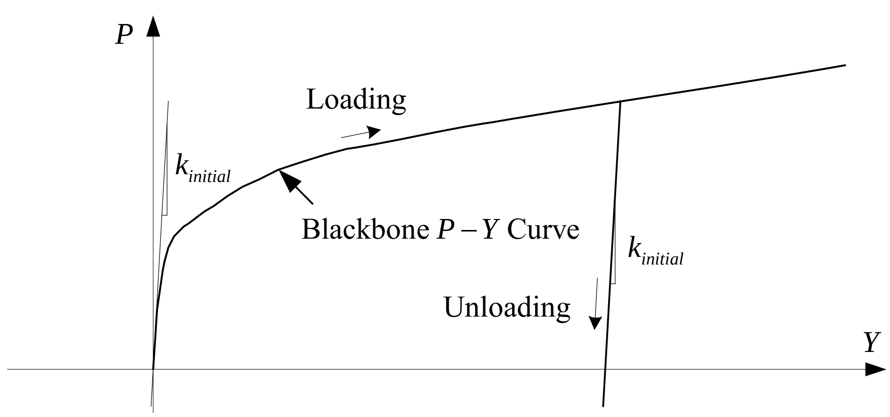

Figure 4.11. Qualitative Diagram of Elasto-Plastic *p-y* Curve

Soil-Abutment Interaction

The abutment backfill beneath the approach slab effectively interacts with the abutment and backwall. As the abutment and backwall moves away from the backfill (thermal contraction), active earth pressure will develop. When the abutment and backwall moves toward the backfill (thermal expansion), soil resistance gradually increases up to the passive earth pressure in the event of large displacements. Figure 4.12 presents a typical variation of earth pressures with respect to abutment and backwall displacement.

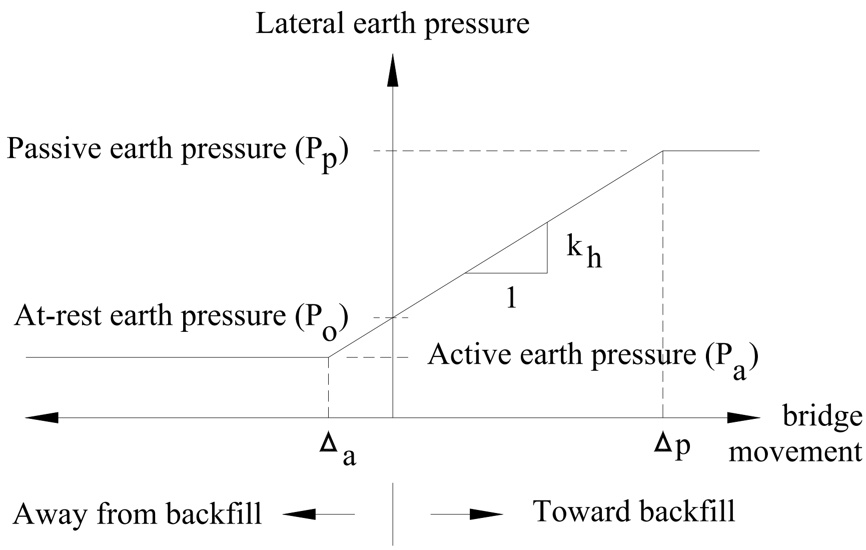

Figure 4.12. Qualitative Lateral Earth Pressure at the Abutment and Backwall

It is recognized that active earth pressure is reached rapidly (Delattre, 2001) and passive pressure will only occur with very large deformation. Therefore, upper and lower thresholds representing passive and active earth pressures are typically included, as depicted in Figure 4.12.

The prediction accuracy of soil-abutment interaction pressures relies primarily on the determination of the coefficient of lateral subgrade reaction, k_h. In the present study, the coefficient of lateral subgrade reaction was determined from the slope of lateral displacements versus pressures obtained from pressure cell data. According to Boulanger et al. (1999), stiffness of gravel soil material typically used as backfill is generally proportional to the square root of confinement. Thus, the equation of k_h at any depth z is expressed as:

$$k_h(z) = k_{ref}\left(\frac{z}{h_{ref}}\right)^{0.5} \qquad 4.6$$

where h_{ref} is a reference depth measured from soil surface to the pressure cell elevation and z is a depth of the interested elevation.

Figure 4.12 was used as the spring model in ANSYS COMBIN39 elements for numerical models. In addition, similar to the soil-pile interaction case, COMBIN39 also allows an unloading branch to be generated based on classical plasticity theory in order to represent unrecoverable soil properties.

4.4 ABUTMENT/BACKWALL JOINT

The joint at the abutment and backwall is a common detail found in IA bridge construction. Steel reinforcement bar details of this joint vary from state to state. The PennDOT standard IA joint detail specifies a U-shape #5 bar at 10 inches. This reinforcement is much less than the reinforcement provided in the abutment and will develop significant rotation between the two connected elements. Although the abutment/backwall joint is assumed to behave as a perfectly rigid connection, it has been observed to behave otherwise due the cold joint condition and the lack of rotational stiffness. Investigating the PennDOT standard abutment/backwall detail, Paul (2003) demonstrated that strength and initial joint stiffness obtained from calculated moment curvature are much lower than those calculated for abutments. An elasto-plastic model was also proposed by Paul.

In order to evaluate abutment/backwall joint and abutment stiffness, moment curvature relationships were developed, as presented in Figure 4.13. Strain compatibility and Whitney's equivalent stress block were used to compute all ultimate moment capacities. Due to restraint by girders, the reinforcement and the effective width of

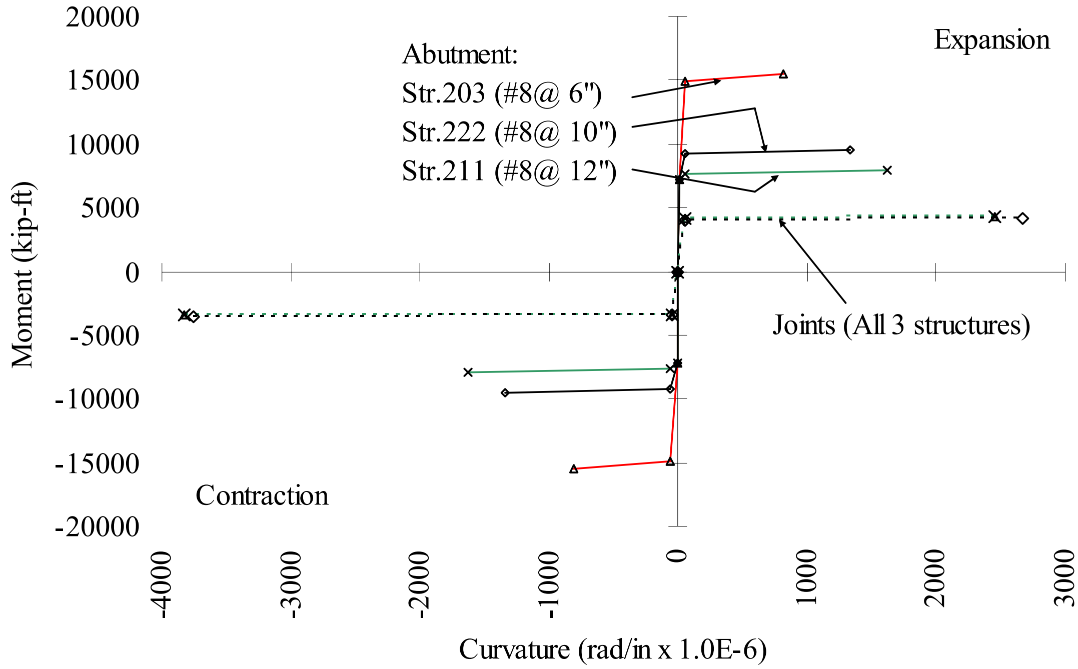

Figure 4.13. Moment-Curvatures of Abutment/Backwall Joints and Abutment Members

concrete, the expansion and contraction loading cases were not the same. The rotational strength and stiffness (by means of initial slopes) of the expansion case were greater than the contraction by about 20 percent. Additionally, abutment rotational stiffness was 16 to 20 times that of the joint.

To convert joint moment-curvature to moment-rotation for element stiffness properties in the numerical model, Equation 4.7, based small deformation and constant moment over a joint length *L*, was used (NEHRP Recommended Provisions, 2000; and Paul, 2003):

$$\theta = \int_0^L \frac{M}{EI} dx = \frac{M}{EI} L = \phi L \qquad 4.7$$

According to Paul (2003), a joint length *L* is associated with a development length of an epoxy-coated reinforcement, which is equal to 16 inches based on AASHTO LRFD (2004). By assuming a linear variation over the development length and fully mobilized tension on reinforcement at one end and zero at the other end, half of this length (i.e., L = 8 inches) was assumed in the present study.

CHAPTER 5

NUMERICAL MODELS

5.1 GENERAL MODEL DESCRIPTION

Numerical modeling of the four instrumented bridges was pursued in order to better develop IA behavior prediction and, therefore, more accurate designs. Numerical models were calibrated to the field-collected data and actual bridge responses. In addition, prediction of IA long-term behavior was desired. ANSYS version 10.0 was used to numerically model each of the four IA bridges. The three-dimensional (3D) numerical models included thermally induced loads and nonlinear behaviors caused by soil-structure interactions between abutments and foundation piles. In addition, the construction joint between backwall and abutment was modeled as a nonlinear element, as discussed in the previous chapter.

The material used in the numerical modeling was assumed to be homogeneous, isotropic. The critical behavior of IA bridges is significantly dependent on the numerical characterization of the soil. To accurately simulate the soil-structure interaction caused by backfill and soils around foundation piles, nonlinear stress-strain curves were adopted for soil models and construction joint between backwall and abutment, with linear elastic elements used for all other bridge components. The material properties used in the numerical modeling are presented in Table. 5.1.

Table 5.1. Material Properties

Material	Strength (f'_c or F_y) (ksi)	Young's Modulus (ksi)	Poisson's Ratio	Thermal Expansion Coefficient (in/in/ºF)
Concrete (Prestressed Girder)	8.0	5154	0.20	5.0 E-6
Concrete (Class AAA for Deck and Backwall)	4.0	3644	0.20	5.0 E-6
Concrete (Class AA for Parapet and Diaphragm)	3.5	3409	0.20	5.0 E-6
Concrete (Class A for Pier and Abutment)	3.0	3156	0.20	5.0 E-6
Steel (HP Piles)	50	29000	0.3	5.5 E-6
Elastomer Rubber	n/a	0.39	0.4985	n/a

5.1.2 Superstructure

A 3D numerical model of each bridge was developed to simulate actual IA bridge behavior over the life of the structure. In an effort to retain accuracy but limit model complexity, bridge girders, diaphragms, deck slab, and parapets were modeled using ANSYS SHELL63 elements, a 3D linear-elastic shell element. Rigid links using ANSYS BEAM4 elements, a 3D frame element, were incorporated into the 3D models to connect shell elements located in different planes but connected in the actual bridge. The model mesh density was approximately 12" x 12". Initial comparisons between a shell element model and a solid element model produced similar results.

5.1.3 Girder and Diaphragm

Girder and diaphragms were modeled with shell elements. Shell elements represent the bottom flange and the web of the girder, as shown in Figure 5.1. This element arrangement places a node at the bottom, extreme fiber of the girder, producing direct numerical results at strain gauge locations for direct comparison with measure results.

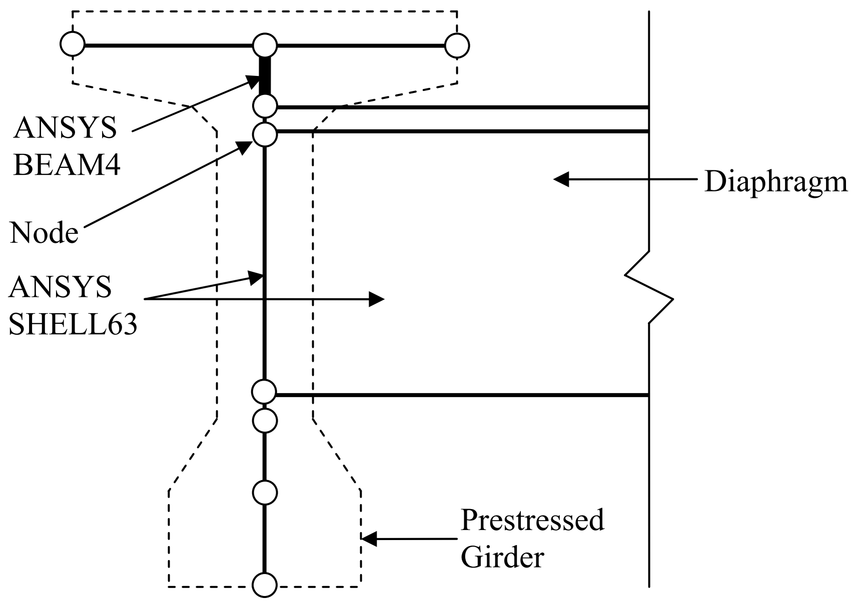

Figure 5.1: Cross Section of Bridge Girder (Structure 211)

Prestressing tendons were not included in the numerical models due to the low stress and strain levels induced and to limit model complexity to a reasonable level. In addition, prestressing is not a determining parameter for temperature-induced longitudinal displacement. Therefore, girders were modeled without prestressing tendons, as presented in Figure 5.2. Pretension force strongly influences creep and shrinkage, however, and this effect was included in the 3D numerical models.

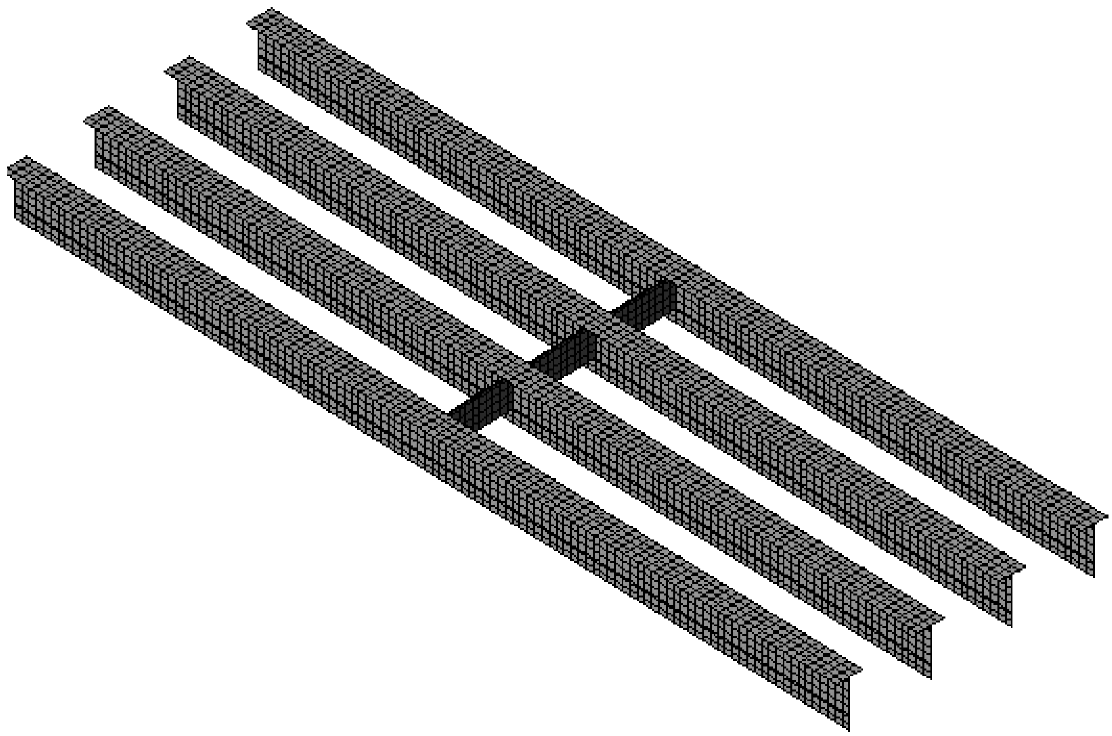

Figure 5.2: Mesh for Girder and Diaphragm (Structure 211)

5.1.4 Deck Slab and Parapet

Deck slab as-built transverse and longitudinal elevations were included in the numerical model SHELL63 elements. The deck transverse elevation changes result in abutment height changes that affect response. Longitudinal elevation changes between abutments also affect bridge response due to a vertical offset. The deck slab and parapet numerical mesh is presented in Figure 5.3. Parapets were included in the numerical model using SHELL63 elements because it has been widely reported that parapets provide longitudinal stiffness in the bridge as well as participation in thermal response. A rigid connection between parapets and deck slab was incorporated because an actual connection exists and thermal expansion strains are the same for both.

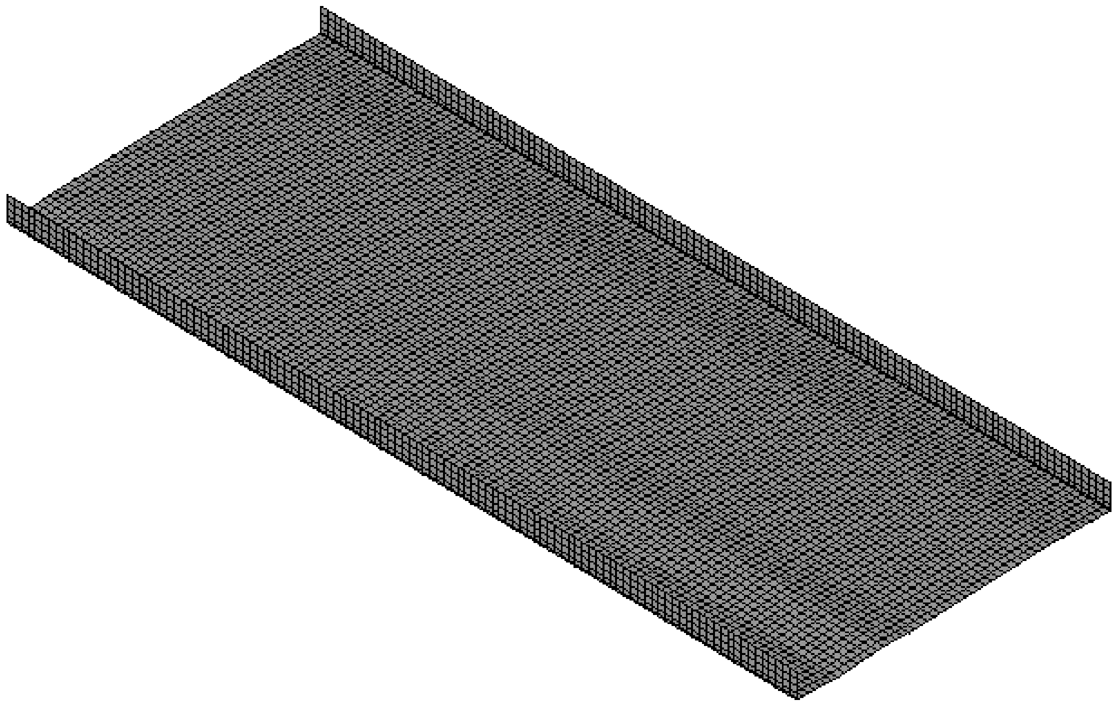

Figure 5.3: Deck Slab and Parapet Mesh

5.1.5 Backwall and Abutment

SHELL63 elements were used to model the backwall and the abutment, as shown in Figure 5.4. Nodes at the backwall-abutment joint were coupled for x, y, and z translations and x and y rotations. Z-axis rotation behavior was modeled at the backwall-abutment joint with a bi-linear, z-axis, rotational spring using ANSYS COMBIN39 with properties as presented in Figure 5.5. The bi-linear moment versus rotation relationship for the backwall-abutment joint was developed based on as-built reinforcement details and concrete strength (see Figure 5.6). The rotational property of this construction joint was determined based on the unit length property in Figure 5.7 and node spacings.

5.1.6 Soil-Abutment Interaction

To include soil-abutment interaction in the numerical model, a bi-linear, Winkler spring model was developed as described in Chapter 4. The Winkler spring model has been widely used to evaluate a range of soil-structure interaction problems such as structures on elastic foundations, retaining walls, and laterally loaded piles (Dicleli, 2000, 2003, 2004 and 2005; Faraji et al., 2001; Koskinen, 2003). The bi-linear Winkler spring is represented by the ANSYS COMBIN39 element. COMBIN39 is a one-dimensional element with characteristics of a nonlinear (multi-linear) force versus deflection diagram.

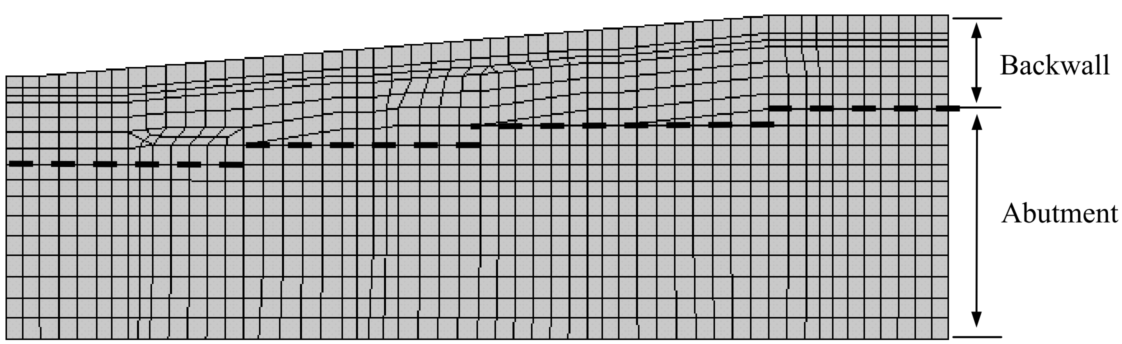

Figure 5.4: Abutment and Backwall Mesh (Bridge 222)

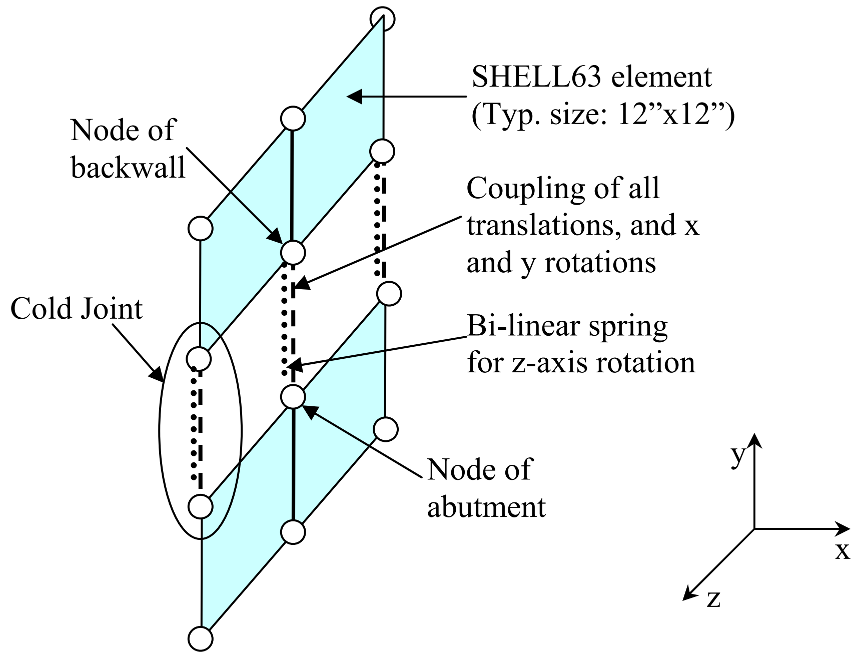

Figure 5.5: Backwall-Abutment Joint

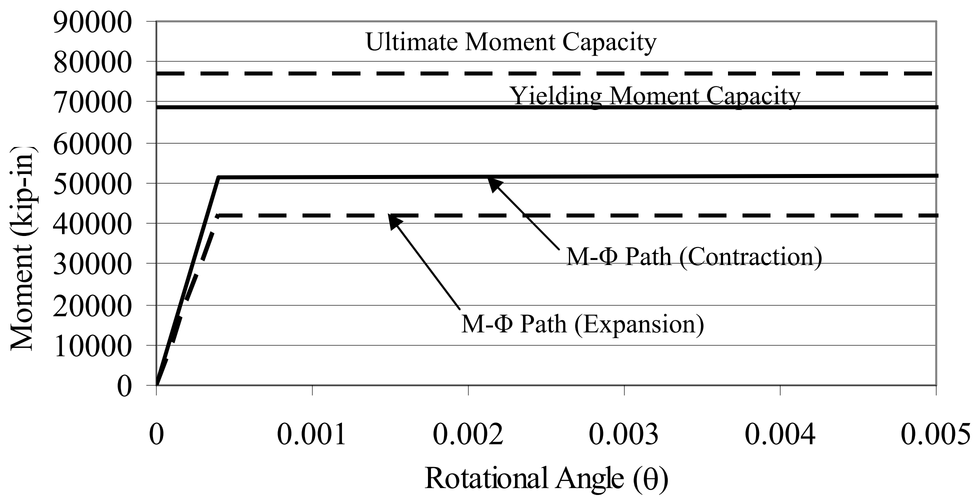

Figure 5.6: Abutment Joint Rotational Stiffness

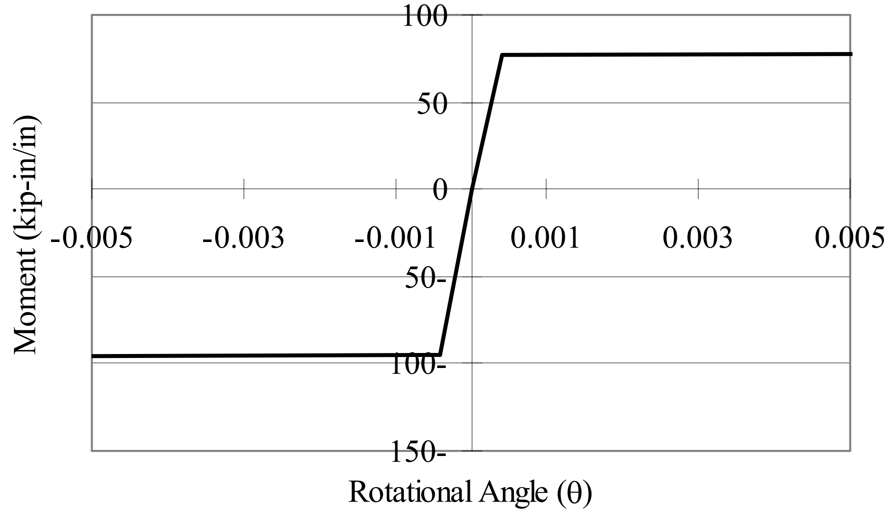

Figure 5.7: COMBIN39 Rotational Stiffness

An equivalent hydro-static pressure corresponding to the backfill depth was applied to the backwall and abutment to represent at-rest soil backfill pressure (see Figure 5.8). In numerical modeling, ANSYS COMBIN39 input properties require the lateral earth pressure variation diagram in Figure 4.13 to be represented in the first and third quadrants (i.e., from negative to positive pressures and displacements). Thus, execution of the numerical model analysis was completed in two analysis stages: (1) an initial analysis was performed to compute the displacements at each abutment-backfill interaction spring due to the at-rest pressure, and (2) the previously computed at-rest displacements were applied as initial displacements for abutment-backfill interaction springs and then at-rest soil pressure and temperature load applied. This procedure resulted in the abutment-backfill interaction spring being in the zero-force state but the abutment being subjected to the at-rest pressure. The abutment-backfill interaction spring property was computed based on the average area of SHELL63 elements that were connected to the interaction spring node. Four selected bi-linear abutment-backfill interaction spring properties are presented in Figure 5.9.

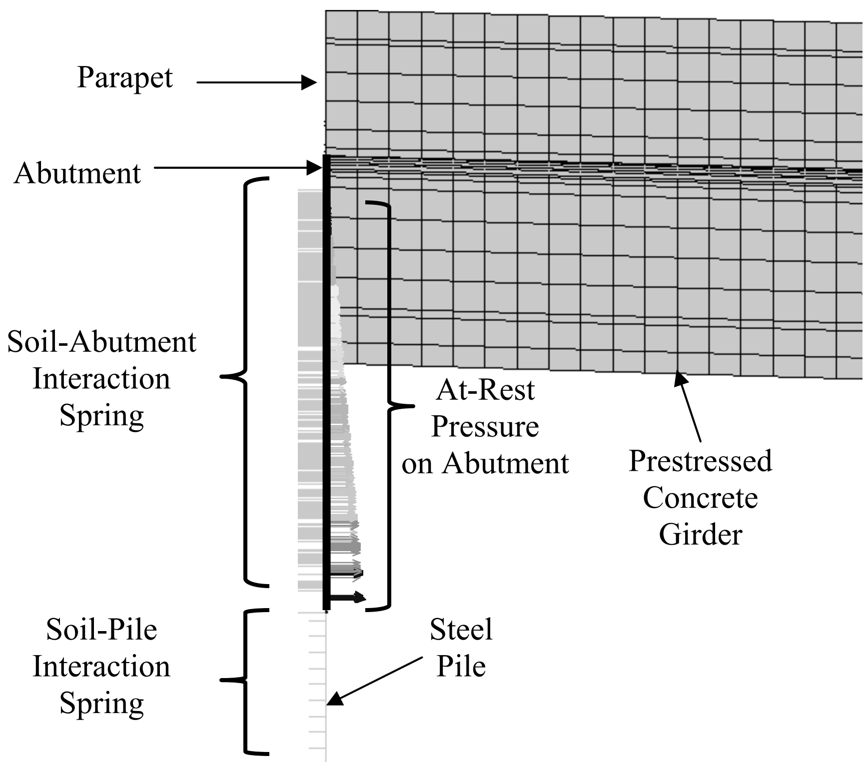

Figure 5.8: At-Rest Pressure Application (Bridge 211)

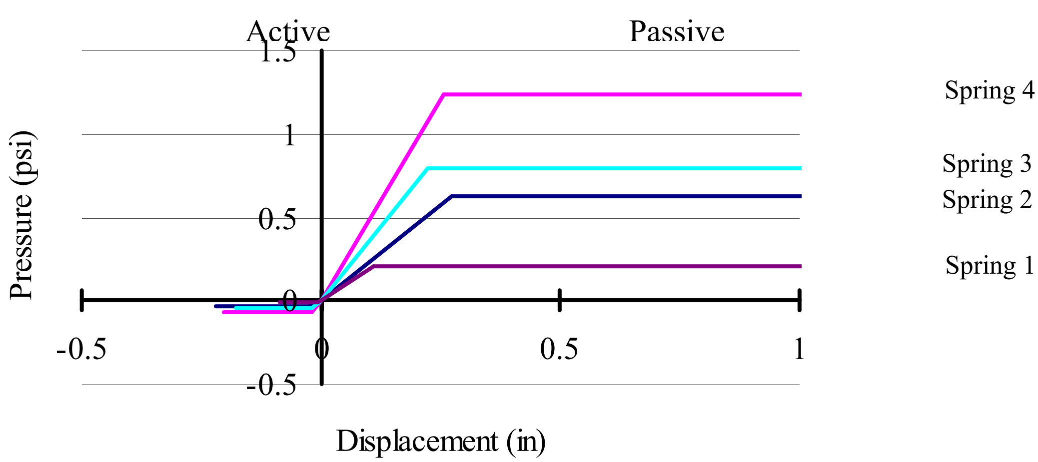

Figure 5.9: Soil-Abutment Spring

5.1.7 Foundation Piles

Piles and adjacent soil were modeled using BEAM4 and COMBIN39 elements, respectively. Nonlinear springs, developed based on p-y curves, were included as COMBIN39 elements to represent soil-pile interaction. Pile boundary conditions were rigid attachment to the abutment at the top and vertical translation restraint at the bottom bedrock layer. P-y curves were generated at each node position based on the American Petroleum Institute (API), with nonlinear soil springs at the pile function in the longitudinal direction only against superstructure expansion and contraction. However, different lateral earth pressures were induced depending on the expansion and contraction of the IA bridges because backfill behind the abutment was considered as overburden loads. Therefore, different spring properties were used for the cases: (1) a pile moves toward backfill and (2) a pile moves away backfill. An example p-y curve inputted in COMBIN39 is presented in Figure 5.10. Upper and middle pile elements were meshed in 3-inch and 6-inch segments, respectively, as the significant displacement and rotation gradiets were expected in this region. The lower pile elements were meshed at 12 inches. Also, the average pile length was modeled because pile behavior beyond approximately 20 ft did not affect the lateral resistance of the pile.

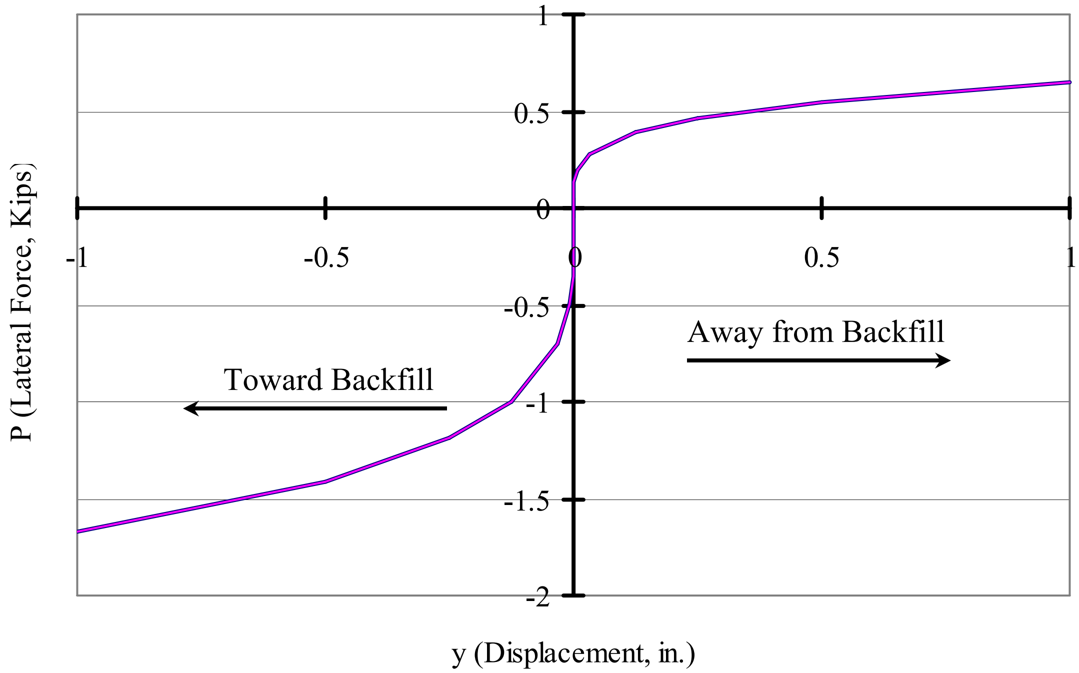

Figure 5.10: P-y Curve Example

5.2 THERMAL LOADS

Thermal loads are significant in determining IA bridge behavior and response because the expansion and contraction of the superstructure transfers large longitudinal forces to the abutments. The primary measure of thermal loading on IA bridges is the ambient air temperature (Emerson 1977). In addition, bridge component temperature is dependent on secondary factors such as solar radiation, wind, precipitation, and heat conductivity (Arsoy 1999).

Temperature variations applied to the numerical models were based on the ambient temperature collected at the weather station. Ambient temperature data collected from September 2002 to January 2006 are presented in Figure 5.11. Because the bridge represents a significant thermal mass, the diurnal ambient temperature is not reflective of the actual bridge temperatures. Hence, the 7-day mean temperature was computed and applied as the thermal load in the numerical models.

Temperature loading was mathematically represented as a sine function with a one-year period, defined as:

$$T(t) = T_m + A\sin(\omega t + \phi) \qquad 5.1$$

where T_m = mean temperature, A = amplitude of temperature fluctuation, ω = frequency, t = analysis time (days), and ϕ = phase lag (radians).

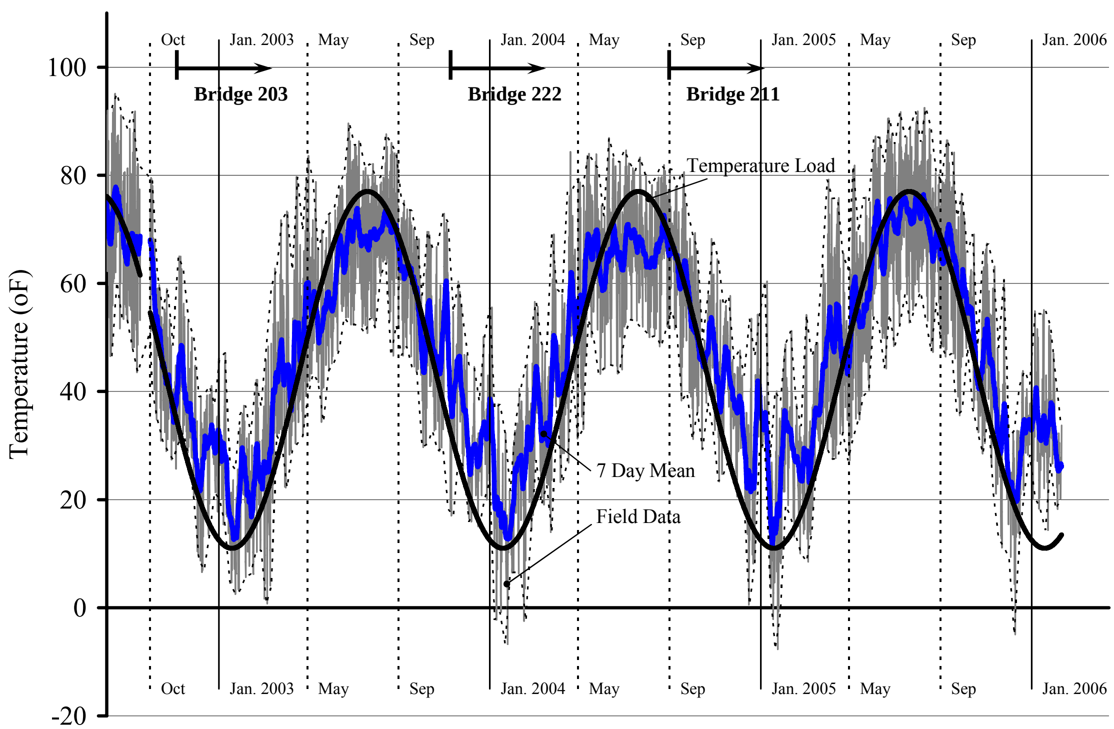

Figure 5.11: Weather Station Ambient Temperature

5.3 BRIDGE 109 MODEL

Numerical models were assembled using the elements described above. Prestressed concrete girders, deck, intermediate diaphragms, backwalls and abutments were modeled using SHELL63 elements and piles were modeled with BEAM4 elements. Each Winkler spring representing soil at the abutment and pile utilized COMBIN39 elements. The horizontal construction joint between the backwall and the abutment was included in the model using COMBIN39. A view of the completed bridge 109 numerical model is presented in Figure 5.13.

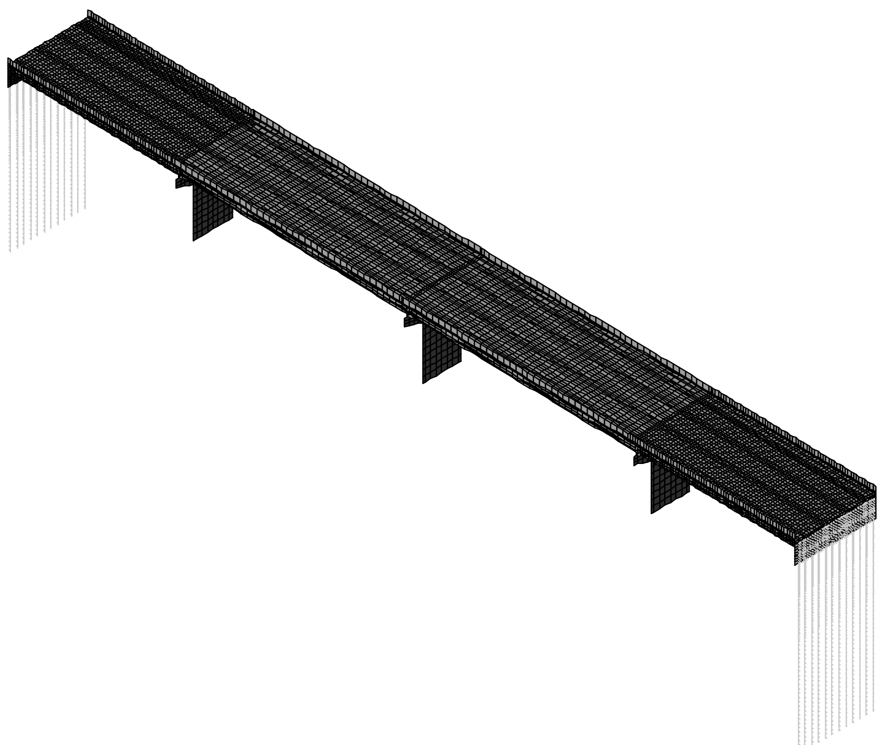

Figure 5.13: Completed Structure 109 Numerical Model

To limit the numerical model size for bridge 109, the middle two spans employed a larger element aspect ratio. Spans 2 and 3 element aspect ratios are approximately 13:1

for deck and girder elements. A larger aspect ratio may affect analysis results; however, the aspect ratio used did not produce significant differences in results when compared to more densely meshed models for the same bridge.

The numerical modeling of piles closely matches actual constructed conditions. Piles are rigidly attached to the abutment with a pin restraint at the pile tip. Soil-pile interaction springs were modeled using COMBIN39 based on active and passive soil pressure theory and traditional p-y relationships. The pile mesh for beam elements is 6" at the top soil layer and 12 inches below to the tip (see Figure 5.16).

Piers were modeled with SHELL63 elements and rotation and translation fixed at the base, as shown in Figure 5.17. Elastomeric pier bearings were modeled as 3-inch-long beam elements with assigned shear modulus of elasticity modified to represent the low shear stiffness of the bearing. The axial modulus was increased to an effective compressive modulus of elasticity (E_c) to include the effect of embedded steel shims, computed using Equation 5.2 (AASHTO):

$$E_c = 6GS^2 \qquad 5.2$$

A modification method to include E_c in a numerical analysis using equivalent area and moment of inertia and can be expressed as:

$$A_e = A_{bearing} \frac{E_c}{E} \qquad 5.3$$

$$I_e = \frac{GA_{bearing} H^2}{12E} \qquad 5.4$$

where A_e = equivalent area, $A_{bearing}$ = actual area of bearing pad, E = elastic modulus of bearing pad, G = shear modulus of bearing pad and H = thickness of bearing pad. Elastomeric bearing pad properties for Structure 109, including equivalent area and elastic modulus, are presented in Table 5.2.

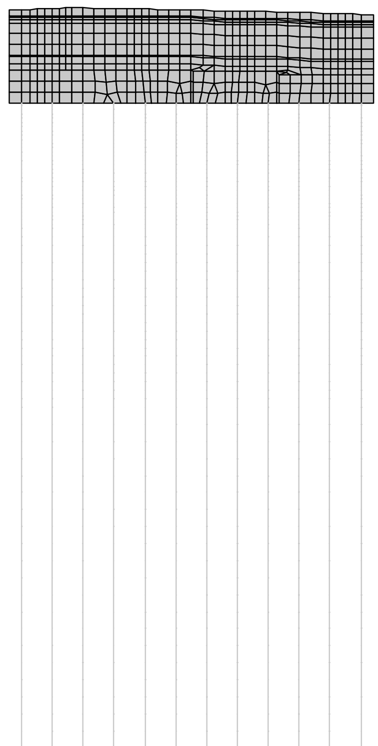

Figure 5.16: Bridge 109 Abutment and Piles

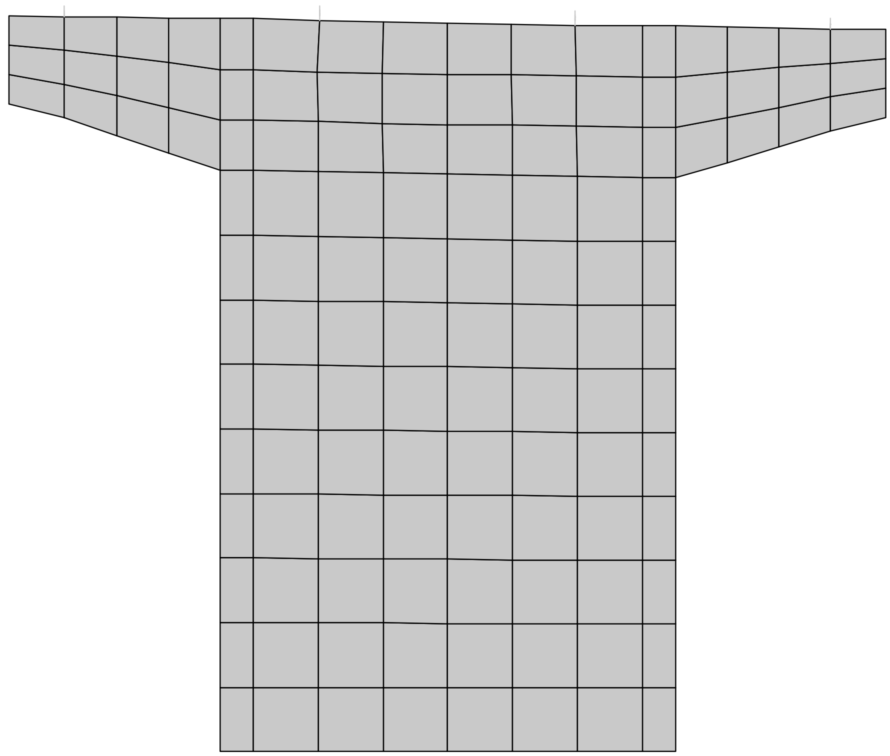

Figure 5.17: Bridge 109 Pier

Table 5.2 Bridge 109 Elastomeric Bearing Properties

Component	Elastic Modulus (ksi)	Poisson's Ratio	Thermal Expansion Coefficient (in/in/^{o}F)	Area (in^2)	Inertia (in^4)
Bearing at abutment 1 and 2 (Typ.)	0.39	0.4985	-	28,046	57.1
Bearing at piers (Typ.)	0.39	0.4985	-	42,108	70.4

5.4 BRIDGE 203 NUMERICAL MODEL

The numerical model developed for bridge 203 consists of three spans and follows the same element modeling scheme as bridge 109. Details of the numerical modeling can be found in Laman et al. (2003). Properties of SHELL63 elements used in piers, abutments and deck are presented in Table 5.3. Element material properties are as presented in Table 5.1.

Bridge 109 is unique among the four instrumented bridges in that abutment 1 is supported on rock and abutment 2 is supported on piles and constructed as a standard PennDOT integral abutment. Reflecting the actual construction, abutment 1 foundation element boundary conditions consist of restrained translation, effectively fixing the abutment against all rotations and translations. Abutment 2 is modeled in the same manner as the abutments for bridge 109.

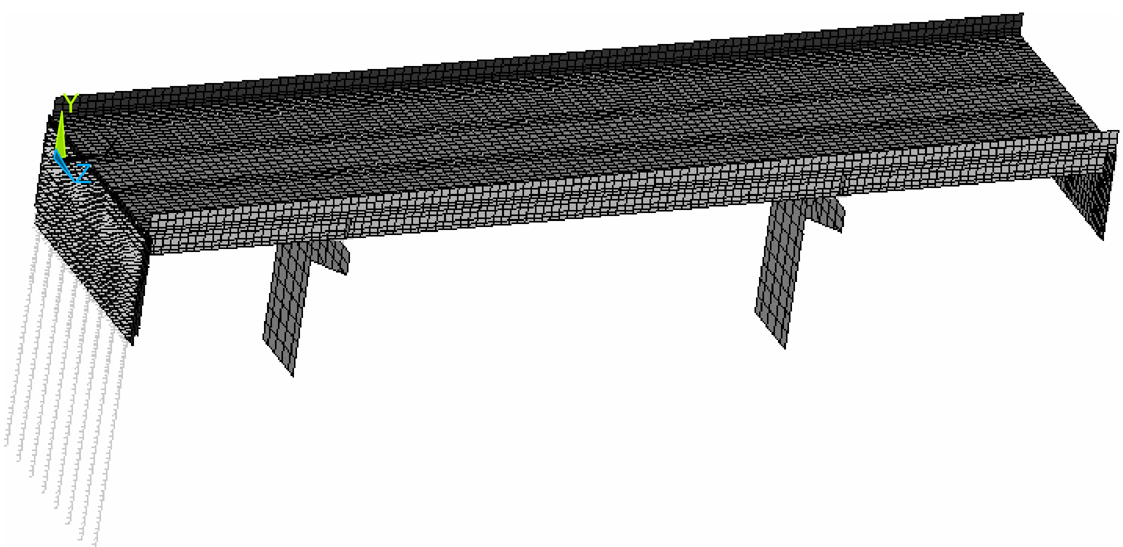

Figure 5.18: Complete Bridge 203 Numerical Model

5.5 BRIDGE 211 NUMERICAL MODEL

The numerical model developed for bridge 211 consists of one span and follows the same element modeling scheme as bridge 109. Details of the numerical modeling can be found in Laman et al. (2003). Element material properties are as presented in Table 5.1.

Figure 5.22: Complete Bridge 211 Numerical Model

5.6 BRIDGE 222 MODEL

The numerical model developed for bridge 222 consists of one span and also follows the same element modeling scheme as bridge 109. Details of the numerical modeling can be found in Laman et al. (2003). Element material properties are as presented in Table 5.1.

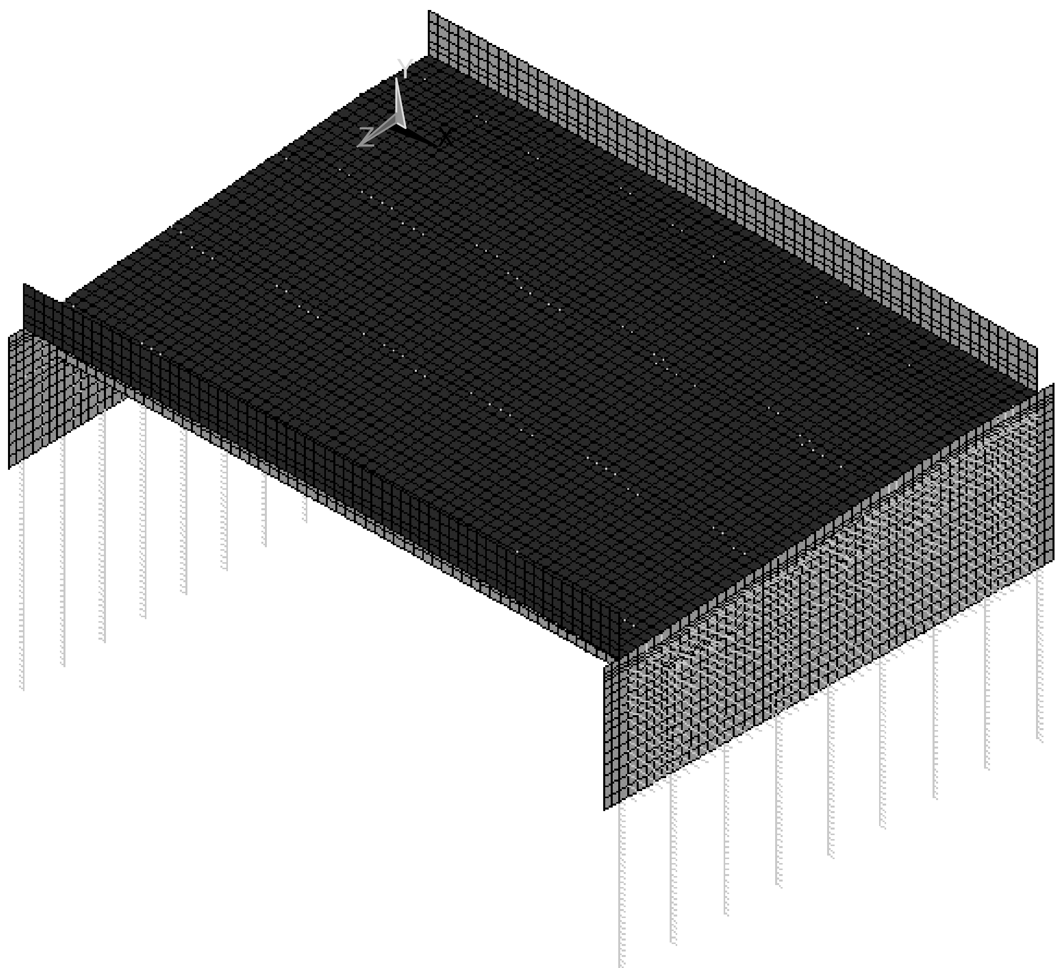

Figure 5.24: Structure 222 Numerical Model

4 Prestressed concrete girders were modeled with SHELL63 elements and rigidly connected to abutment backwalls. Deck and parapets were also modeled with SHELL63. Deck slabs were attached to girders using rigid link (BEAM4) and located at the mid-

thickness of deck slab. Parapets were rigidly connected to deck and each parapet segment was connected to the adjacent parapet with the restraint of all translation. Both abutments were composed of SHELL63 and located at the mid-thickness of the abutments (see Figure 5.25). Both abutments were rigidly connected and rested on nine steel HP piles. The back face of both abutments was laterally supported by soil-abutment interaction spring (see Figure 5.24). Steel HP12x74 piles were continuously modeled with 6-inch length for the top soil layer and 12-inch length for the rest of the soil layer using BEAM4 elements (see Figure 5.25). Nonlinear soil-pile springs attached to the piles laterally supported the HP piles and boundary conditions of vertical restrained translation were applied to supporting piles.

CHAPTER 6

NUMERICAL MODELING RESULTS AND DISCUSSION

Numerical model prediction results are an important aspect of the present study. Included herein are results of model predicted responses for bridges 203, 211, 222, and 109. A discussion of the numerically derived responses as compared to measured response is also presented. Comparisons between predicted and measured response were performed at all instrument locations for each instrumented bridge. (Field data were not available for bridge 109 at the time of publication of this report.) Measured pile axial strain and approach slab strain were not included due to the exclusion of dead load and approach slab components in the numerical models. Dead load effects have been omitted because this effect could not be recorded by the majority of the instruments that were installed after dead load deformations occurred. Also, strains observed from the approach slab indicate that the restraint offered by the slab was not significant relative to the forces developed in the backfill and the piles; therefore the complexity of numerically modeling the approach was not warranted.

Predicted and measured bridge response is presented in graphic format consistent with Chapter 3. All predicted responses derived from numerical models were taken directly from nodes/elements pre-placed at corresponding instrument locations. All graphical presentations of predicted and measured responses are superimposed so as to facilitate comparison and discussion.

6.1 BRIDGE 203 MODELING RESULTS AND DISCUSSION

Predicted and measured longitudinal abutment displacements at the three extensometers are presented in Figure 6.1. For the purposes of accurate comparison, the values of measured and predicted data were initialized with identical starting point established. This adjustment was required due to constraints on field instrumentation imposed by construction sequences that did not allow the measured data to have the same zero starting point and the numerical models.

It can be observed from Figure 6.1 that predicted displacements for the top corner and bottom extensometer locations were on the order of 0.918 and 0.821 R^2 values, respectively, compared to the corresponding observed displacements. A similar contraction trend of the abutment was observed from the predicted and observed displacements for the top corner and bottom extensometer locations. However, a different trend was observed from the predicted and observed displacements for the top center extensometer. The top center extensometer measured an expansion trend, while the corresponding predicted displacements showed a contraction trend with a calculated R^2 value of 0.702. As indicated from the predicted displacements for both top extensometer locations, the abutment behaved in a rigid body motion with respect to the transverse bridge dimension; however, the observed displacements imply the opposite abutment behavior.

Predicted earth pressures from the numerical model versus observed earth pressures from the three pressure cells are presented in Figure 6.2. As can be observed from Figure 6.2, all predicted pressures showed the same trend as the observed pressures with calculated R^2 values of 0.861, 0.915, and 0.897 for the top corner, top center, and bottom pressure cells, respectively. The predicted pressures for both top pressure cells were similar, indicating rigidity of the abutment in the transverse dimension. However, the amplitude of the observed pressures for the top center pressure cell was approximately 1.5 times greater than the amplitude of the observed pressures for the top center pressure cell. These differences in observed pressures indicate relatively flexible abutment in the transverse dimension.

Predicted relative rotations of the abutment-backwall connection from the numerical model versus relative rotations calculated from the four sets of collected tilt meter data are presented in Figure 6.3. A relative rotation is theoretically equal to zero if the abutment and backwall are rigidly connected. However, it can be observed from the tilt meter data that all relative rotations were not zero, indicating rotational flexibility of the abutment-backwall connection. For the purpose of trend comparisons, the initial relative rotations from both numerical model and tilt meters were set to zero in order to compare only changes in rotations. As can be derived from Figure 6.3, the predicted relative rotations for the four girder locations showed a similar trend and magnitudes of relative rotations. A result comparison between the predicted and observed relative rotations for girder 4 yields a similar trend. For result comparisons at the locations of girders 2 and 3, the difference trends and smaller predicted relative rotation variations at about 3 times are observed, indicating that the observed rotational stiffness of the abutment-backwall connection is more flexible than predictions at the center abutment section. For a result comparison at the girder 1 location, the difference trend and greater predicted relative rotation variation at about 2.3 times are observed, indicating that the predicted rotational stiffness of the abutment-backwall connection is more flexible than observation.

Predicted pile moments about the weak bending axis from the numerical model versus calculated moments from the three sets of collected strain gage data on the west pile and the one set of collected strain gage data on the east pile are presented in Figures 6.4 and 6.5, respectively. The predicted and observed moments on the west pile at depth = 2′-5″ showed a similar overall trend of continuous contraction; however, the initial value of the observed moments is greater than the initial value of the predicted moments because effects of geometry and material imperfections (pile crookedness, pile orientation, pile location, vertical pile alignment, and soil properties), which lead to additional eccentric and p-delta moments, were not considered in the numerical model. For a result comparison on the west pile at depth = 6′-5″, the predicted moments revealed an inflection point between depth = 2′-5″ and depth = 6′-5″ but the observed moments showed no moment reversal. For result comparisons on the west pile at depth = 11′-5″ and on the east pile at depth = 13′-3″, the very small variations of the predicted and observed moments were all observed due to the location near the fixity point.

Predicted girder strains from the numerical model versus observed girder strains from strain gages installed on all four girders are presented in Figure 6.6 through Figure 6.9. Similar to the extensometer case, the initial values of the observed strains did not account for effects of creep and shrinkage at the first 40 days due to constraints of the instrumentation schedule as well as effects of at-rest earth pressures. However, these effects are fully incorporated into the numerical model. As a result, it can be observed that the overall predicted strains showed compressive magnitudes greater than the overall strains obtained for the field data. For result comparisons of the predicted and observed strains at end-span top strain gages, the opposite trends but similar strain variations were observed for all four girders. For result comparisons at end-span bottom strain gages, the same trends were observed but the predicted strain variations averaged 3.9 times greater than the observed strain variations for all four girders. For result comparisons at mid-span top strain gages of girders 1 and 4 (exterior girders), the predicted strains and observed strains showed small variations, indicating the strain gage location near the elastic neutral axis of composite section. For result comparisons at mid-span top strain gages of girders 2 and 3 (interior girders), however, the strain gages measured magnitudes of strain variations much greater than the predicted strain variations. For result comparisons at mid-span bottom strain gages, magnitudes of strain variations predicted by the numerical model averaged 2.2 times greater than the observed data for all four girders. The overall trend of observed mid-span bottom strains at girders 1 and 3 was expansion, inconsistent with the overall contraction trend of the observed strains at girders 2 and 4. However, all predicted strains showed the overall contraction trend of girder strains.

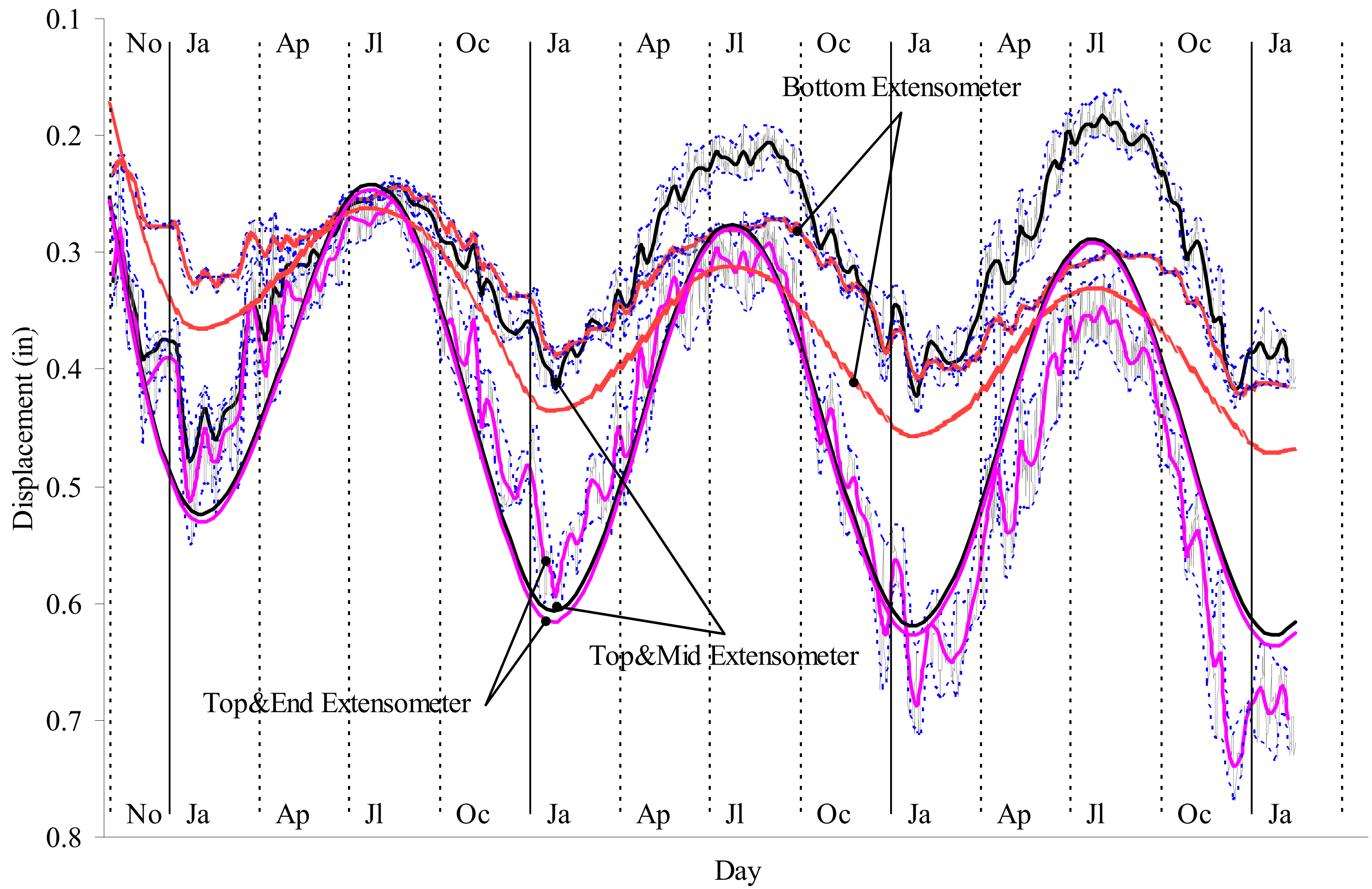

Figure 6.1. Bridge 203: Extensometers

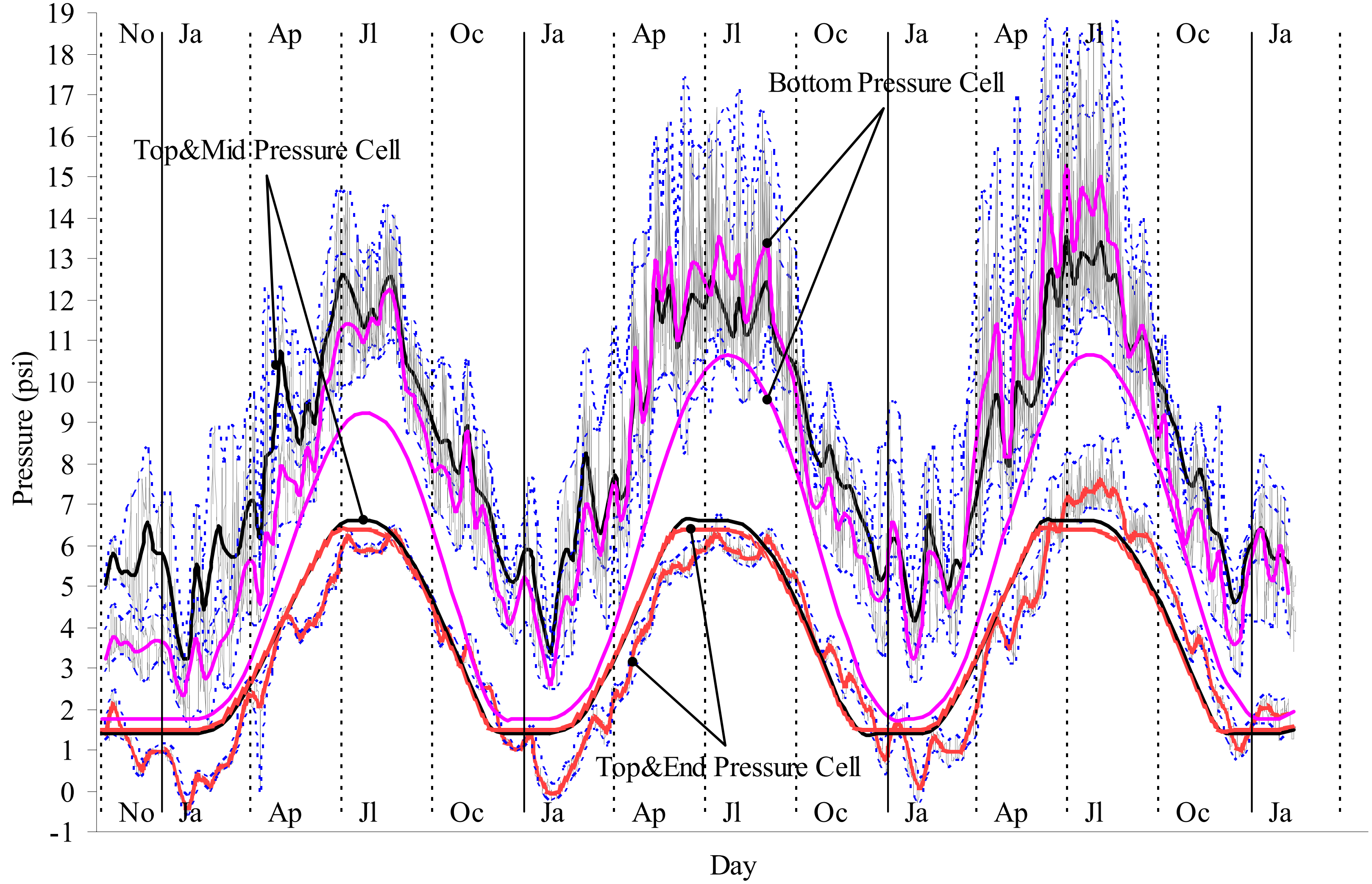

Figure 6.2. Bridge 203: Pressure Cells

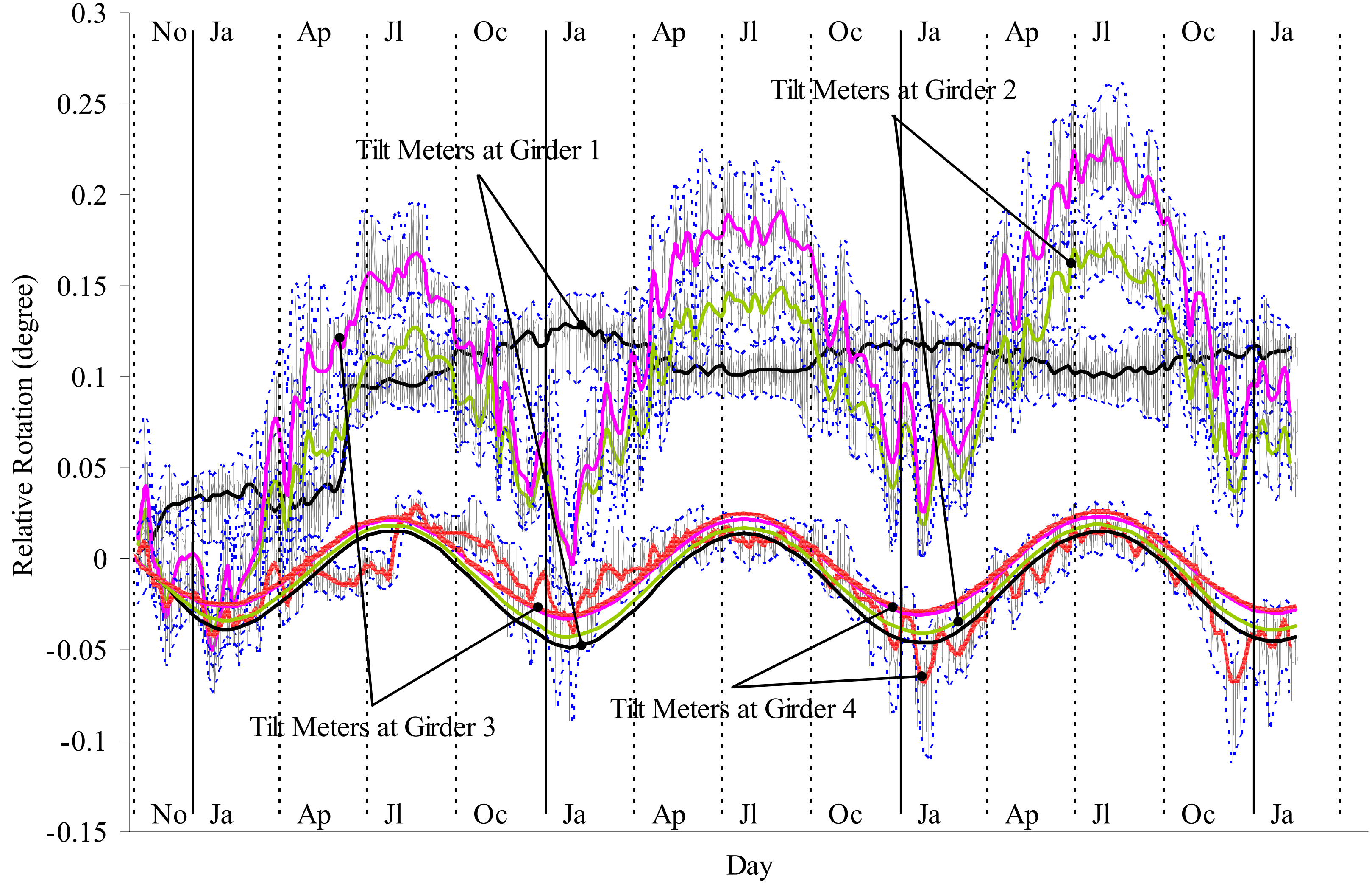

Figure 6.3. Bridge 203: Relative Rotations Between Girder and Abutment

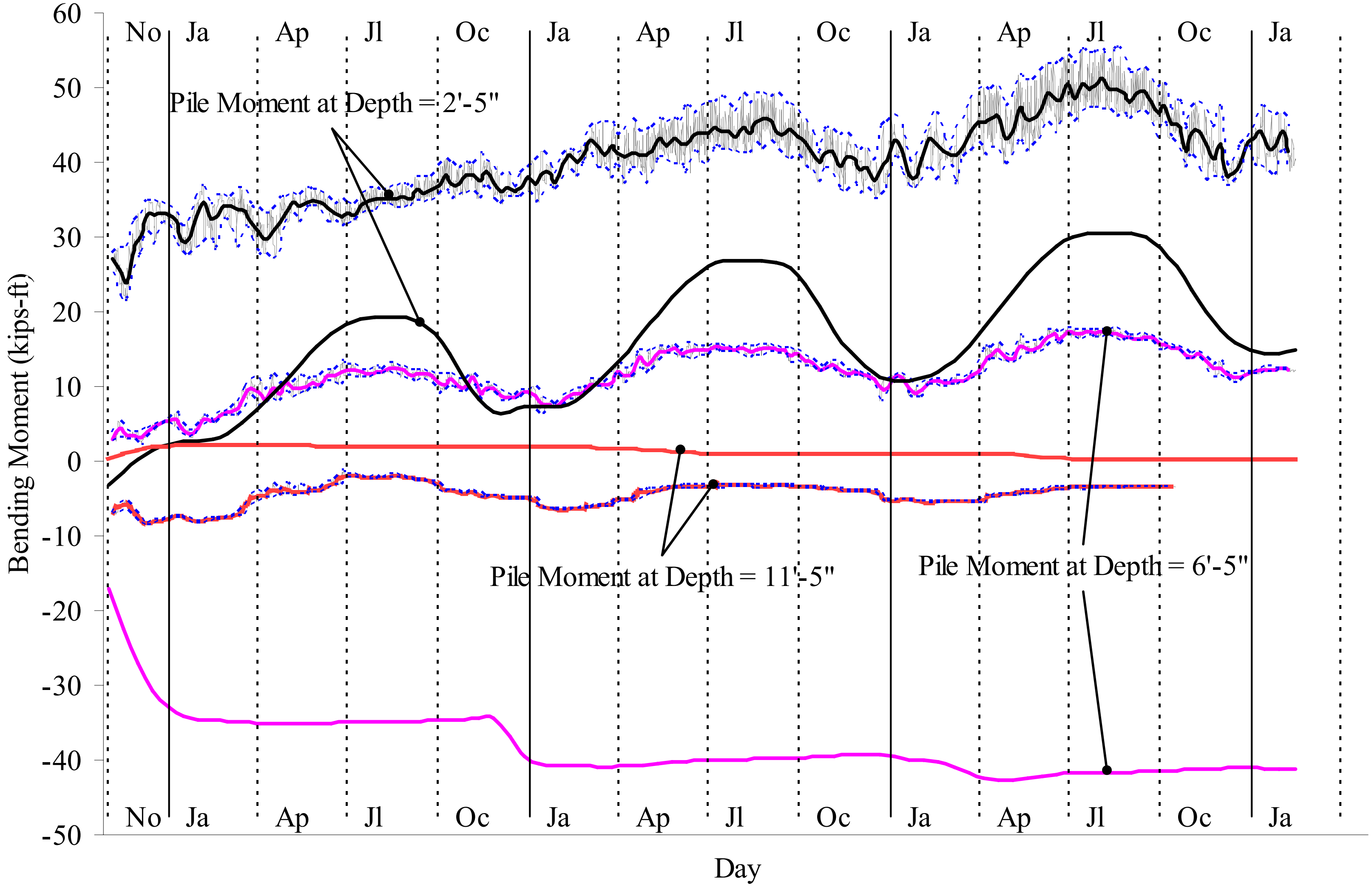

Figure 6.4. Bridge 203: Moments on West Pile

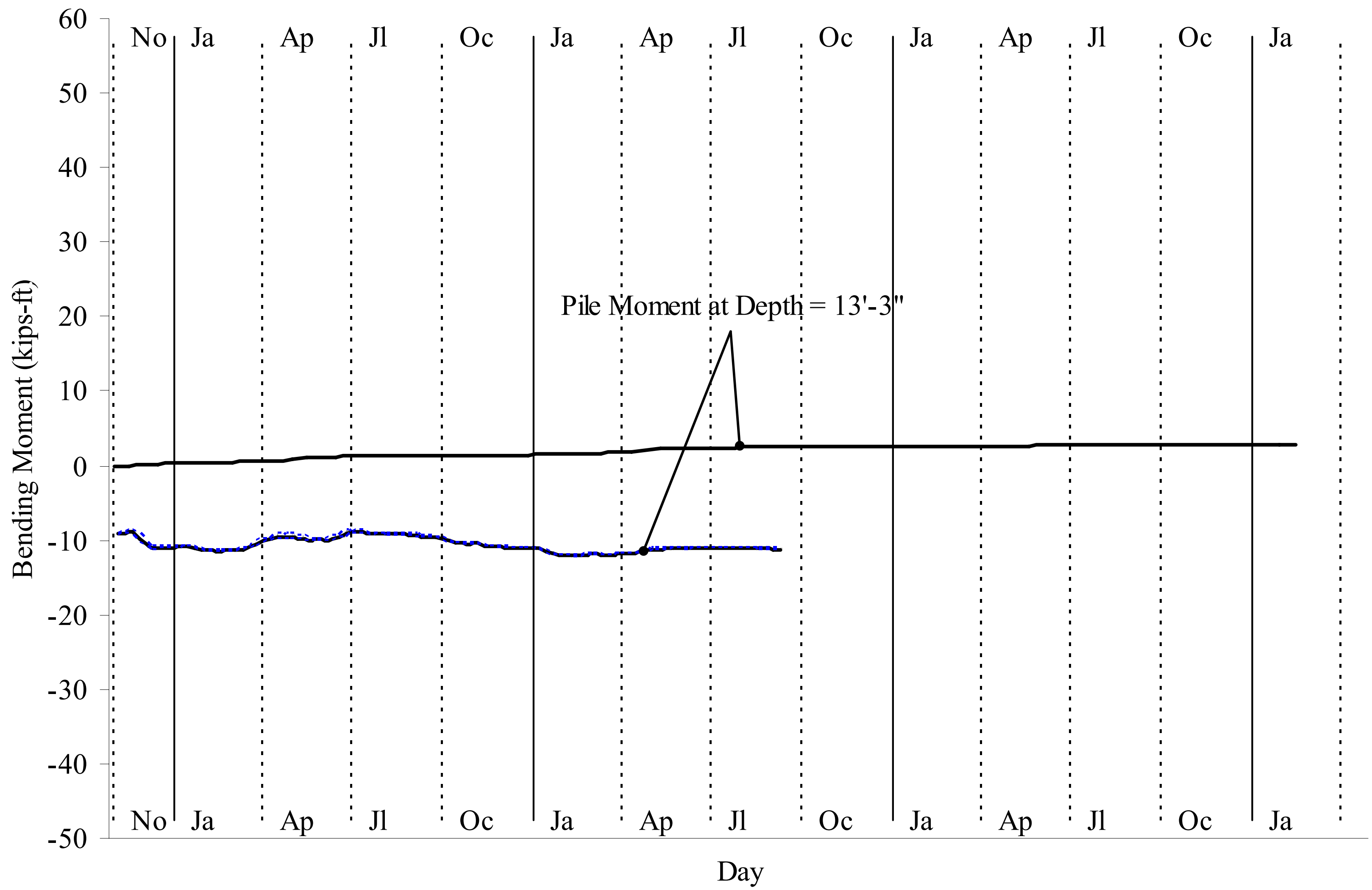

Figure 6.5. Bridge 203: Moments on East Pile

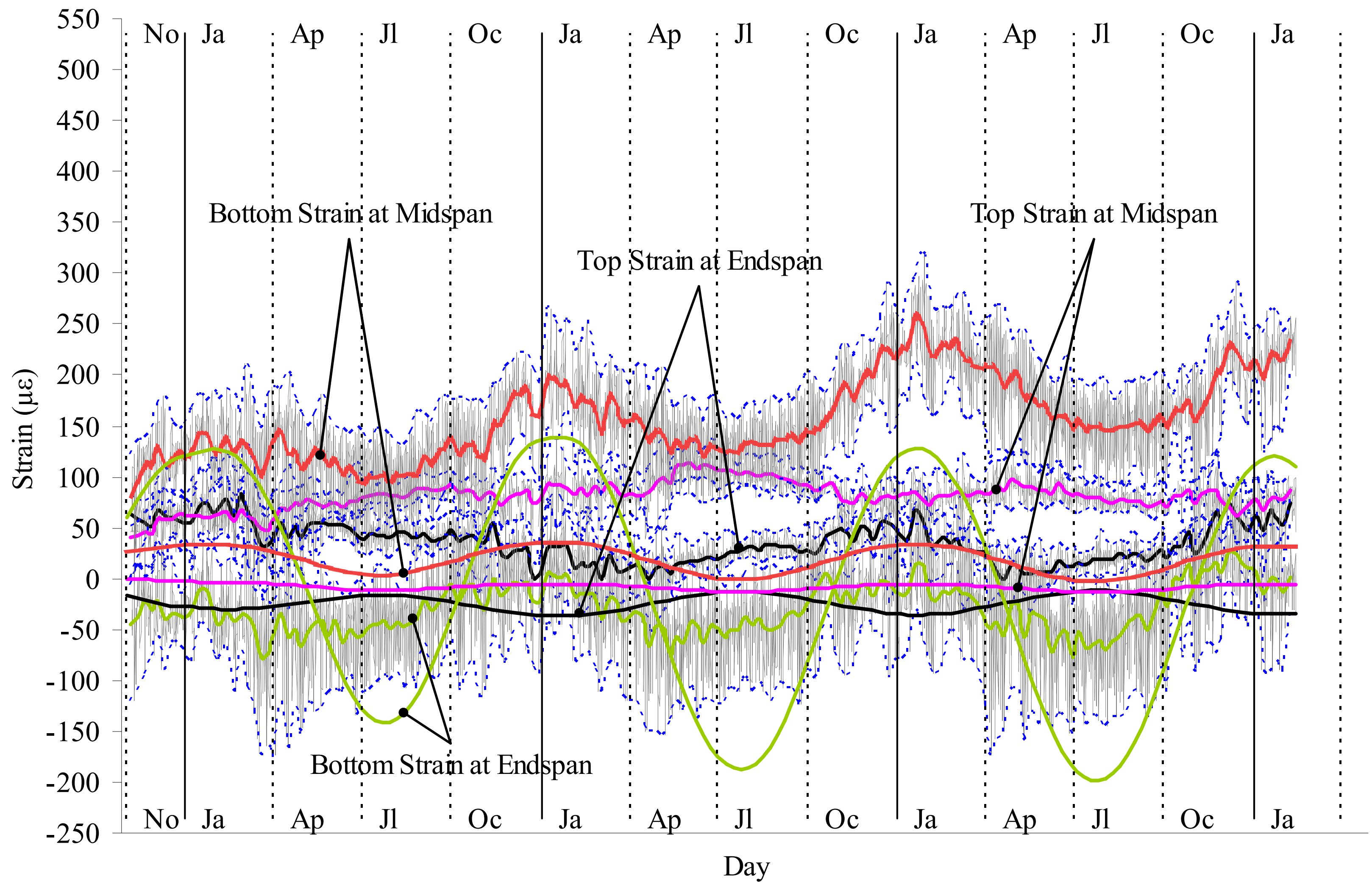

Figure 6.6. Bridge 203: Strain on Girder 1

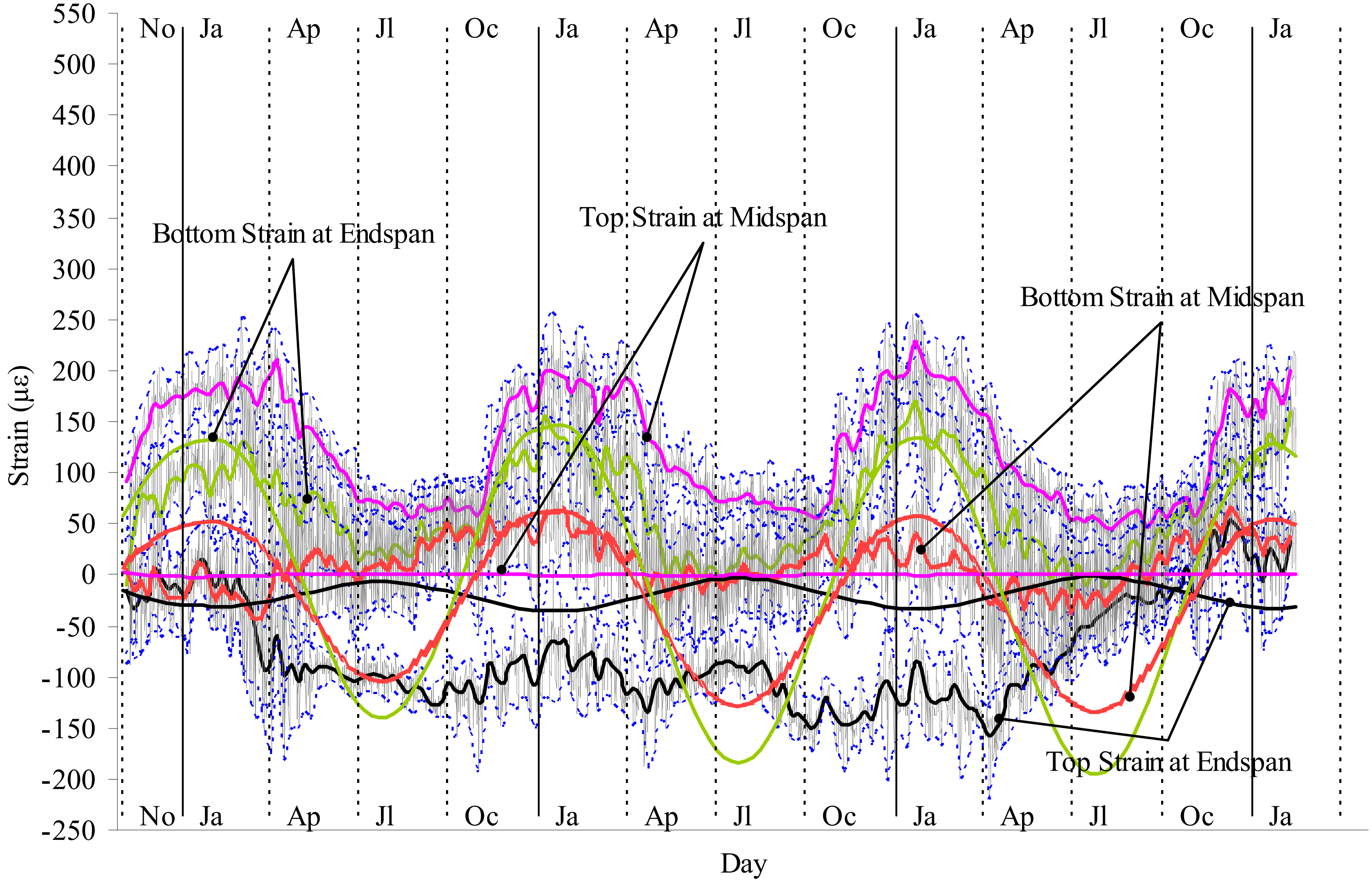

Figure 6.7. Bridge 203: Strain on Girder 2

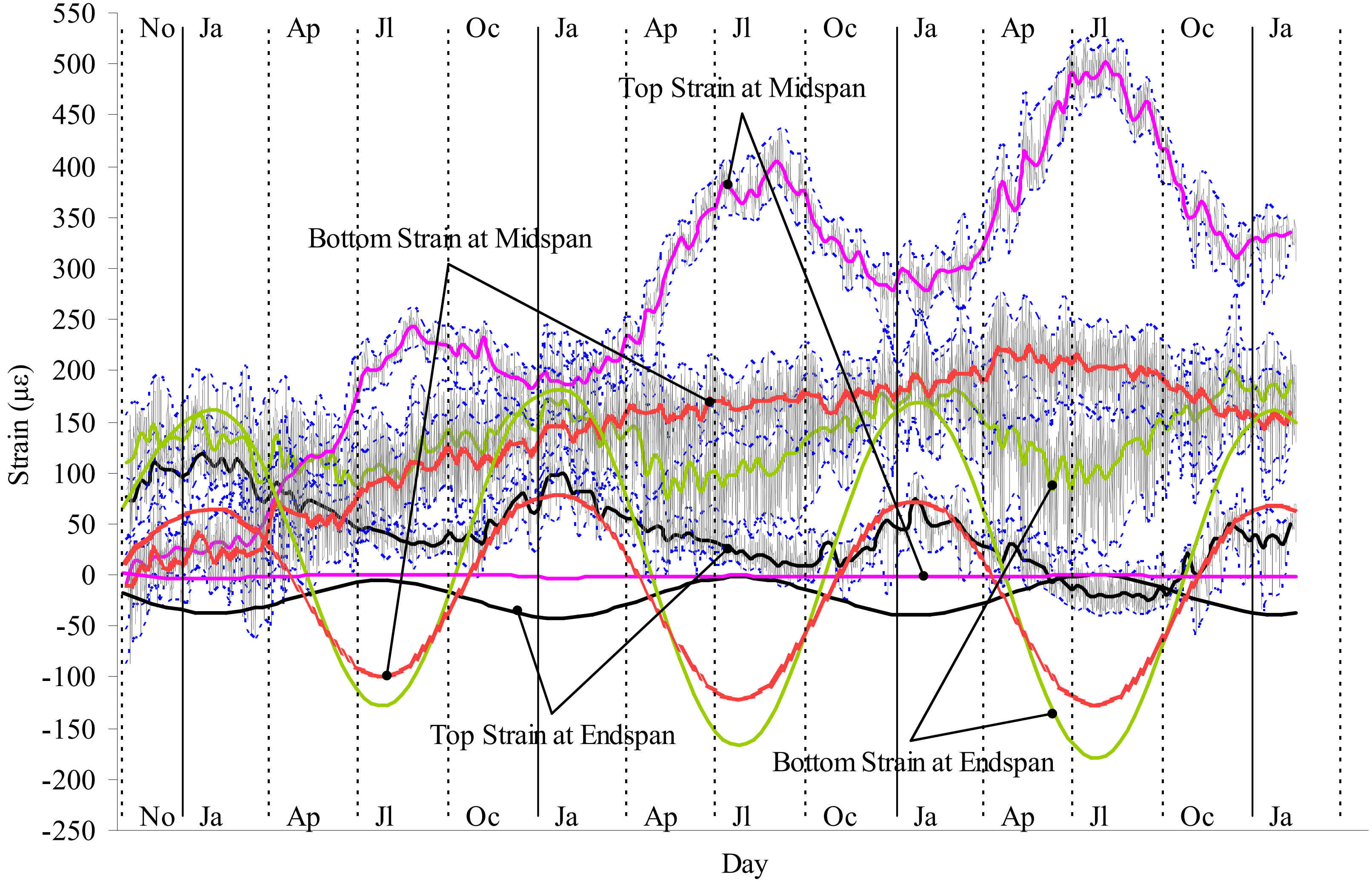

Figure 6.8. Bridge 203: Strain on Girder 3

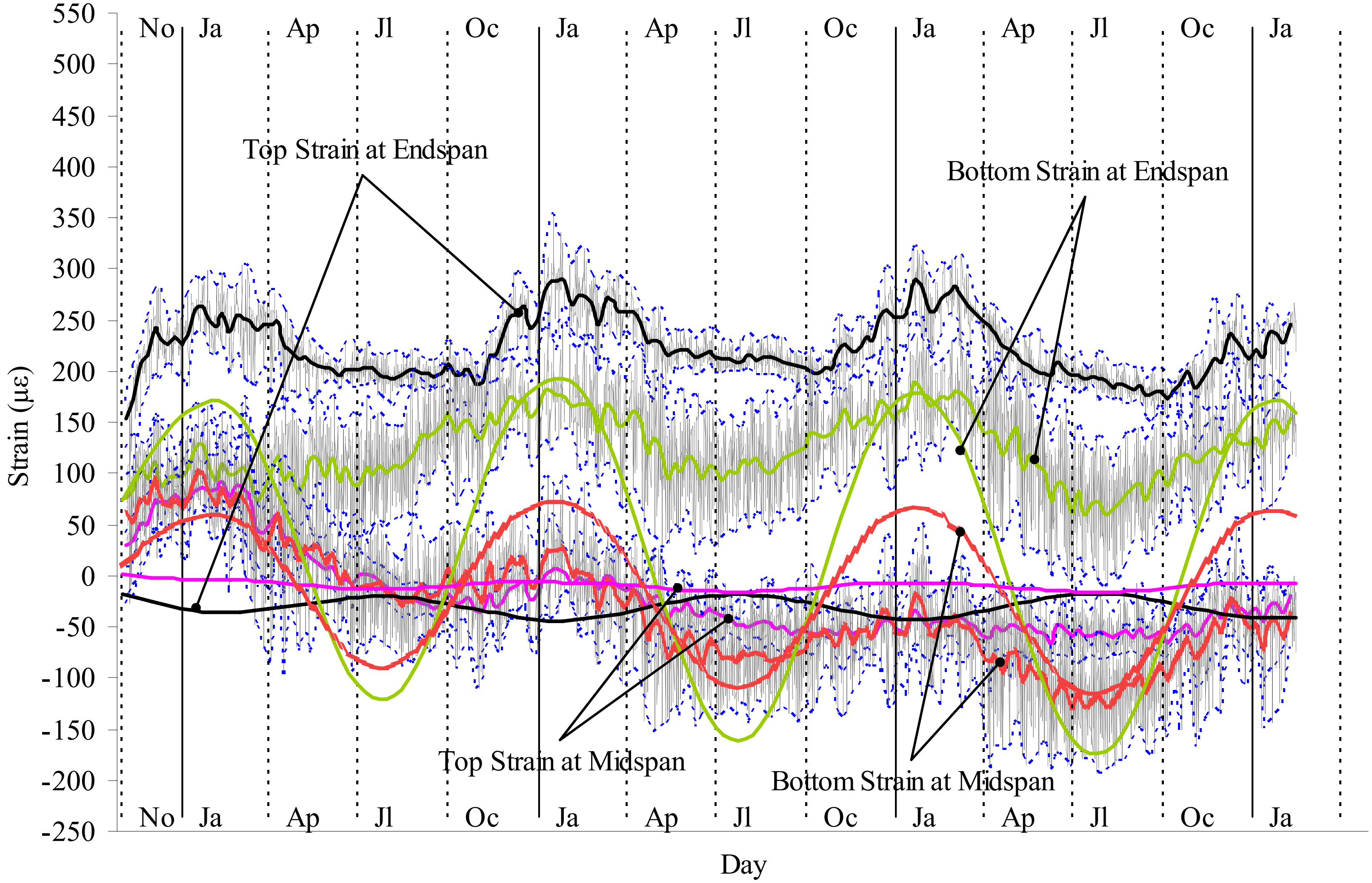

Figure 6.9. Bridge 203: Strain on Girder 4

6.2 BRIDGE 211 MODELING RESULTS AND DISCUSSION

Predicted and measured longitudinal abutment displacements at the two extensometers of abutment 1 and two extensometers of abutment 2 are presented in Figure 6.10 and 6.11, respectively. For the purpose of accurate comparison, the values of measured and predicted data have been adjusted as bridge 203.

It can be observed from Figure 6.10 that predicted displacements for the top and bottom extensometer locations of abutment 1 were in the range between 0.0 and 0.17. From Figure 6.11, the predicted displacements for the top and bottom extensometers of abutment 2 were in the range between 0.0 and 0.23. A similar contraction trend of the abutment was observed from the predicted and observed displacements for the top and bottom extensometer locations in both abutments. However, predicted displacements of both top extensometers exhibited more significant contraction and expansion displacements during winter 2004/2005 and summer 2005, compared to corresponding measured displacements.

Predicted earth pressures from the numerical model and observed lateral earth pressures from the two pressure cells on abutment 1 and two pressure cells on abutment 2 are presented in Figures 6.12 and 6.13, respectively. All predicted pressures produced a similar trend as the corresponding observed pressures. During bridge contraction, the predicted pressures for both abutments at the pressure cell locations are similar to field-observed pressures, indicating active failure behavior at each elevation. During bridge expansion, the observed pressures for both abutments at the top pressure cell locations exceeded even predicted passive failure pressures. This fact may imply that the passive pressure of the backfill soils is increased due to the daily bridge expansion and contraction and active failure of the backfill.

Predicted relative rotations of the abutment/girders from the four sets of collected tilt meter data and the numerical model results are presented in Figures 6.14 and 6.15. For the purpose of trend comparisons, the initial relative rotations from both numerical model and tilt meters have been set to zero in order to compare only changes in rotations. A relative rotation is theoretically equal to zero only if abutment and backwall are rigidly connected. However, it can be observed that the field observed data were not zero and were larger than the predicted, indicating a flexible connection of the abutment/backwall. The predicted relative rotations for the four girder locations produced the similar trend and magnitudes of relative rotations, except tilt meters at the centerline of girder 3 on abutment 1. Relative rotations on abutment 2 were very close to the predicted results as presented in Figure 6.15. The predicted relative rotations for girder 1 at both abutment ends yielded a similar trend to the observed. However, relative rotation at the centerline of girder 3 on the abutment 1 end produced very large and opposite rotation, though the predicted relative rotation for both abutment ends was almost zero (see Figure 6.14). This abnormal behavior was induced by abutment 1 and girder 3 rotations, as can be observed in Figures 3.22 and 3.23 in Chapter 3. This result implies a large distortion of abutment 1 while abutment 2 maintains its plane.

Predicted pile moments about the weak-axis bending from the numerical model and instrumented bending moments based on field-collected strain gage data on the north pile and south pile under abutment 1 and the north and south pile under abutment 2 are presented in Figures 6.16, 6.17, 6.18 and 6.19, respectively. Generally, pile moments at the shallow depth produced larger moments than those at the deeper depth, while piles experienced no rapid moment changes that tended to keep moderately increasing. Also, the north piles at both abutments produced larger moments than the south piles and the moment variations of the north and south pile under abutment 1 were very similar to those under abutment 2, respectively. This fact related to the previous rotational behavior of the abutment/backwall connection. The pile moments of the numerical model for the north pile at depth = 2′-7″ predicted a similar trend of the observed data though field observed moments included initial moments, due to the imperfections as discussed in Section 6.1. For the moments on the north pile at depth = 9′-7″ under abutment 1, the predicted moments revealed an inflection point between depth = 2′-7″ and depth = 9′-7″. In addition, the pile moments did not fluctuate along with bridge expansion and contraction though the field-observed data produced small moment changes. The south pile moments at both abutment sides yielded very small moments at both pile top and bottom locations. It should be noted that the strain gages on the south pile under abutment 2 were embedded 6 inches into the abutment concrete, and therefore the moments were very small compared to the predicted moments.

The predicted girder strains from the numerical model and the observed girder strains from the strain gages mounted on both ends of all four girders are presented in Figures 6.20, 6.21, 6.22 and 6.23. As discussed in Section 6.1, it can be observed that the overall predicted strains showed compressive magnitudes greater than the overall strains obtained for the field data. As a whole, results from girders 1 and 4 (exterior girders) matched with each other and results from girders 2 and 3 (interior girders) also matched with each other. The predicted strains and observed strains from the top strain gage location showed small variations, while bottom strain gage results maintained plane strain variations. As expected from the previous rotational results and pile moment variations, the bottom strain gages at abutment 1 varied within the widest range for all four girders and the bottom strain gages at abutment 2 had the second widest range. The top strain gages of girders 2 and 3 (interior girders) fluctuated along with bridge contraction and expansion as the bottom strain gages of all four girders but the top strain gages of girder 1 and 4 (exterior girders) tended to maintain their moments constantly.

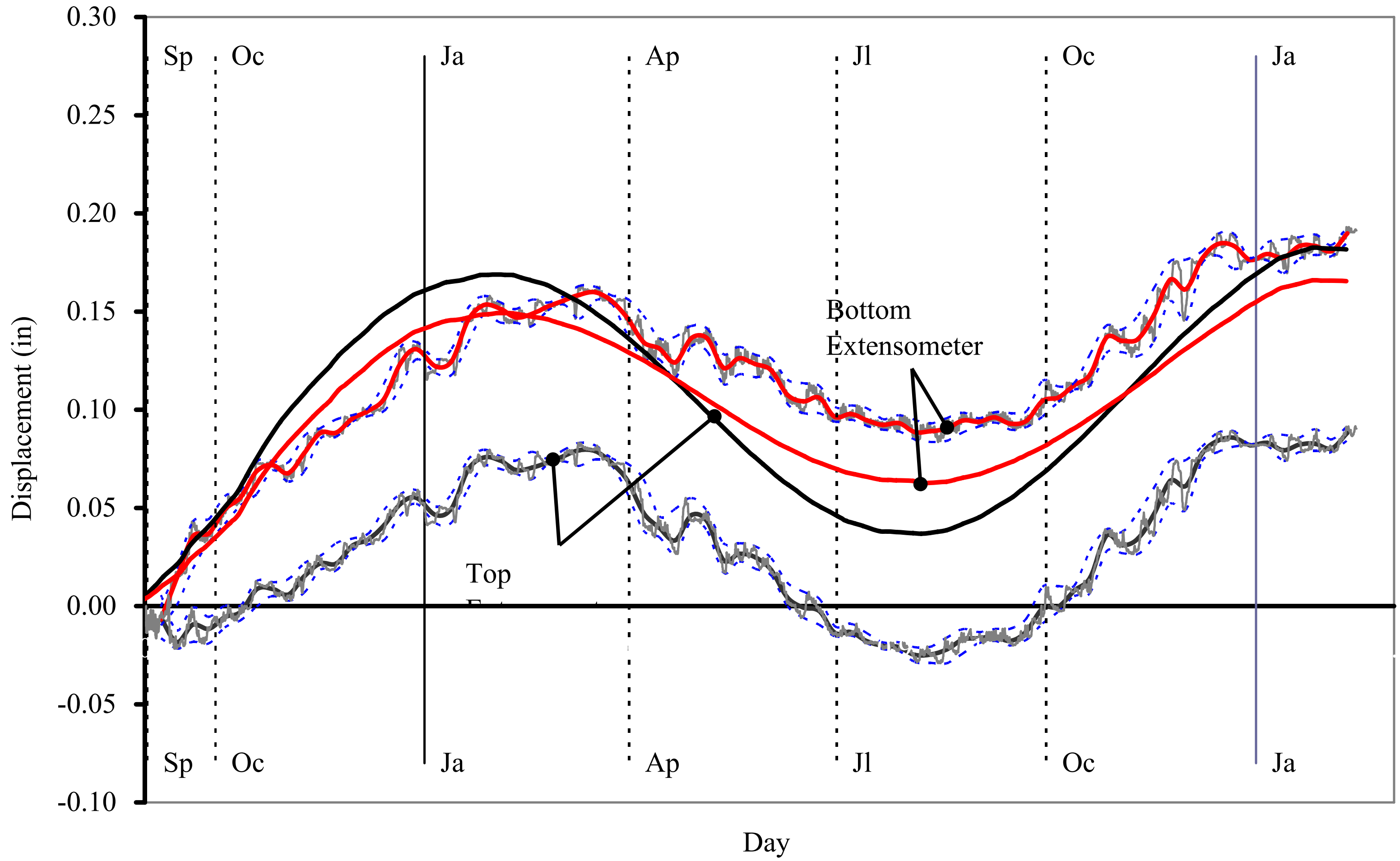

Figure 6.10. Bridge 211: Extensometers on Abutment 1

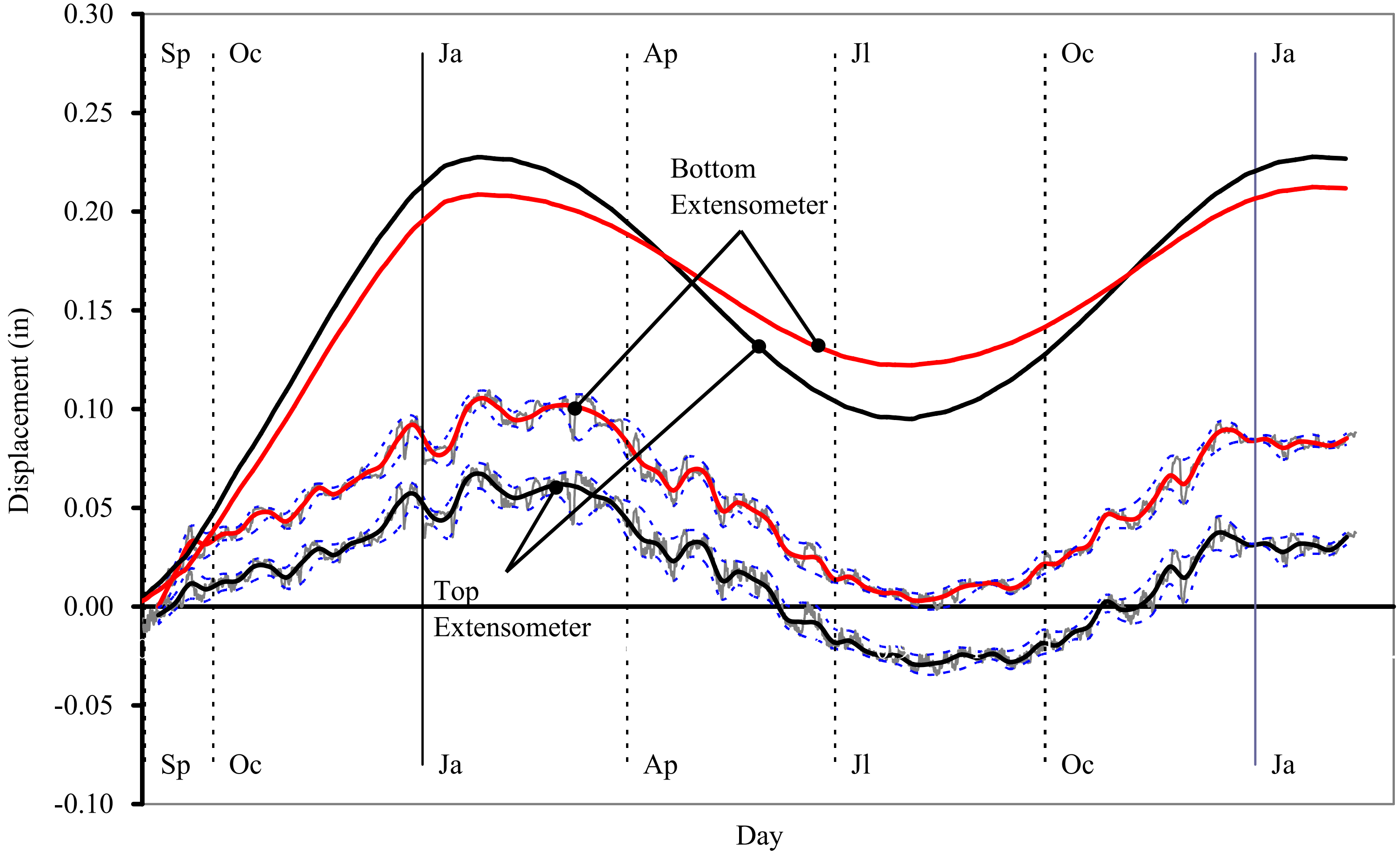

Figure 6.11. Bridge 211: Extensometers on Abutment 2

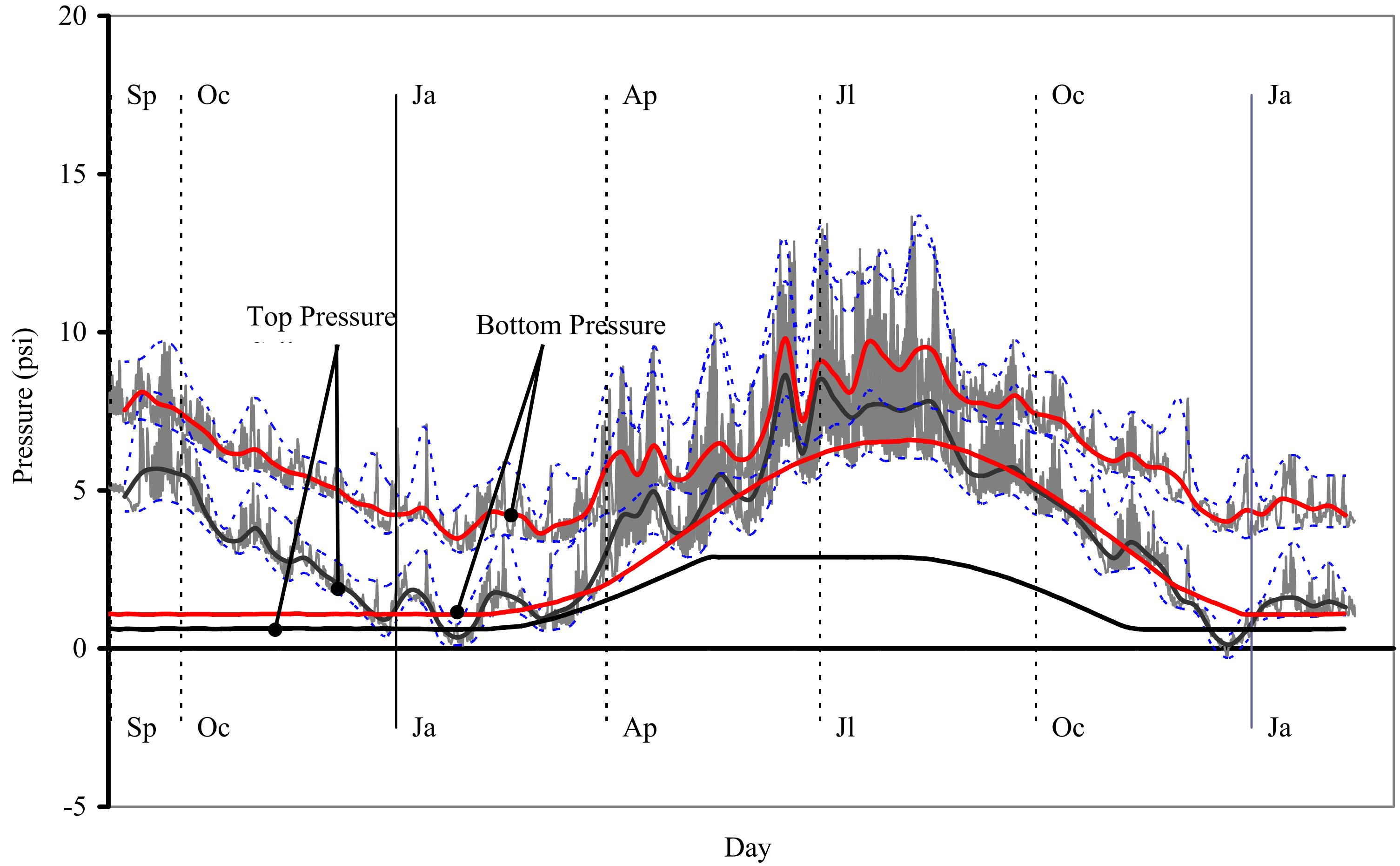

Figure 6.12. Bridge 211: Pressure Cells on Abutment 1

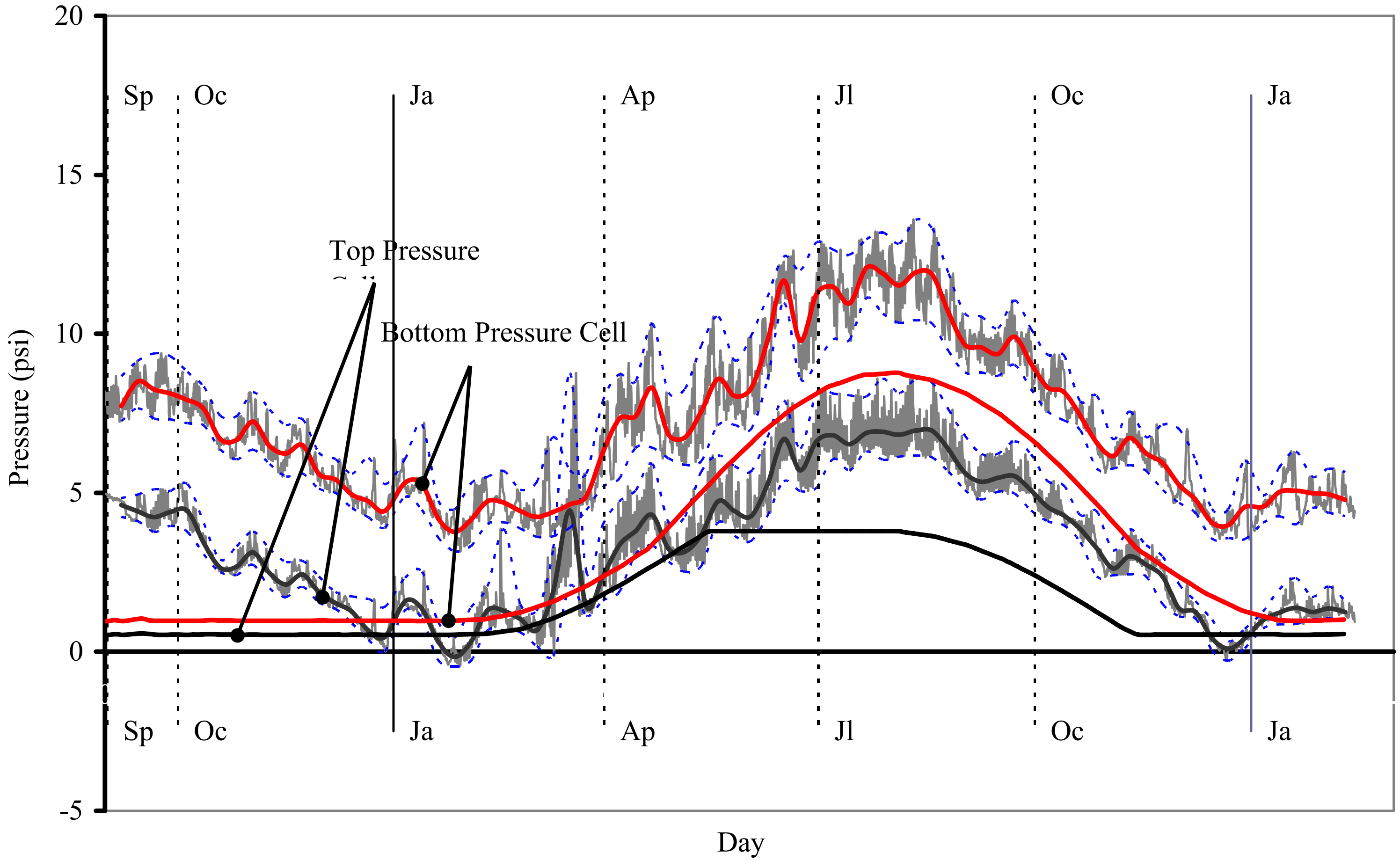

Figure 6.13. Bridge 211: Pressure Cells on Abutment 2

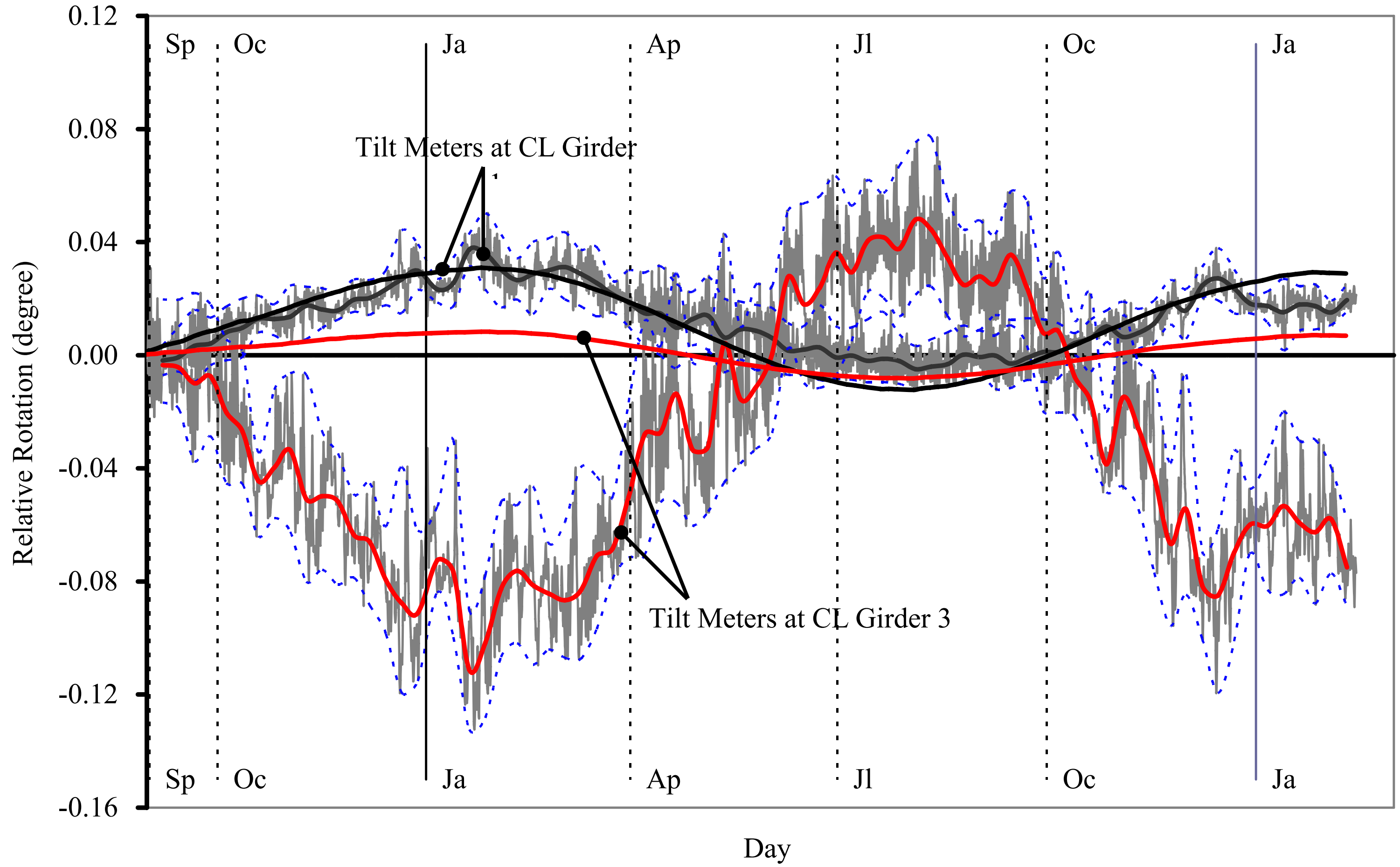

Figure 6.14. Bridge 211: Relative Rotations between girders and Abutment 1

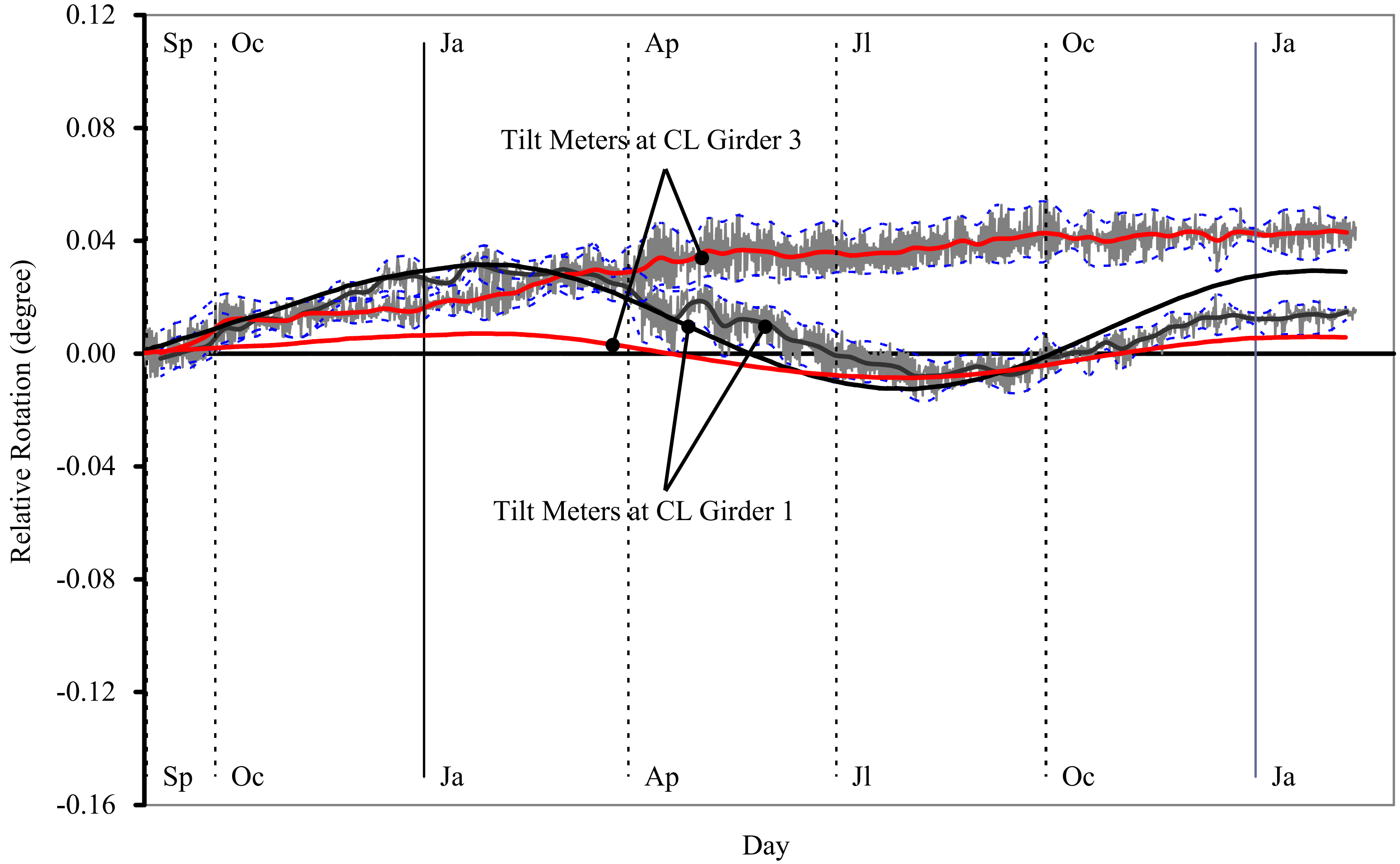

Figure 6.15. Bridge 211: Relative Rotations between girders and Abutment 2

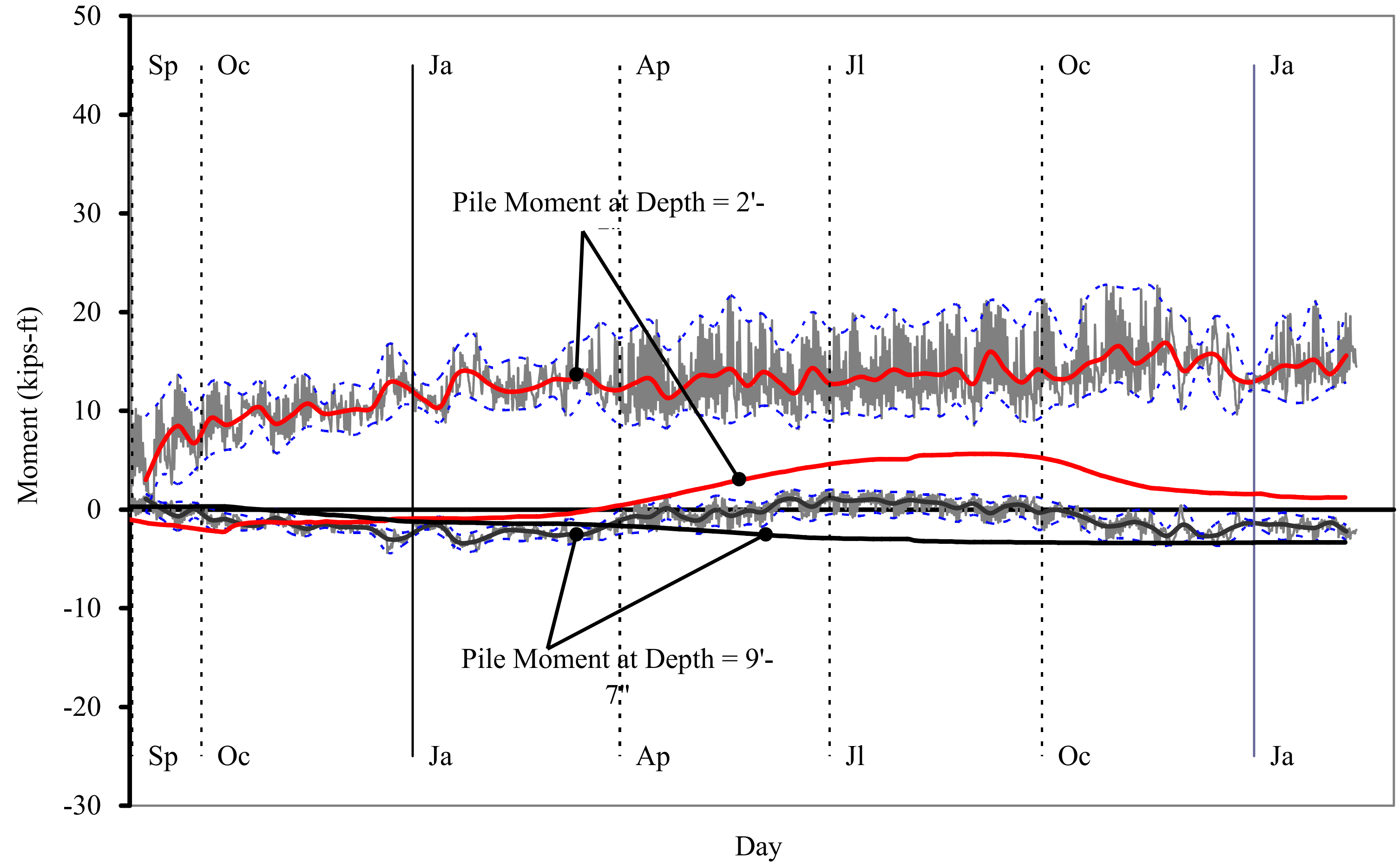

Figure 6.16. Bridge 211: Moments on North Pile of Abutment 1

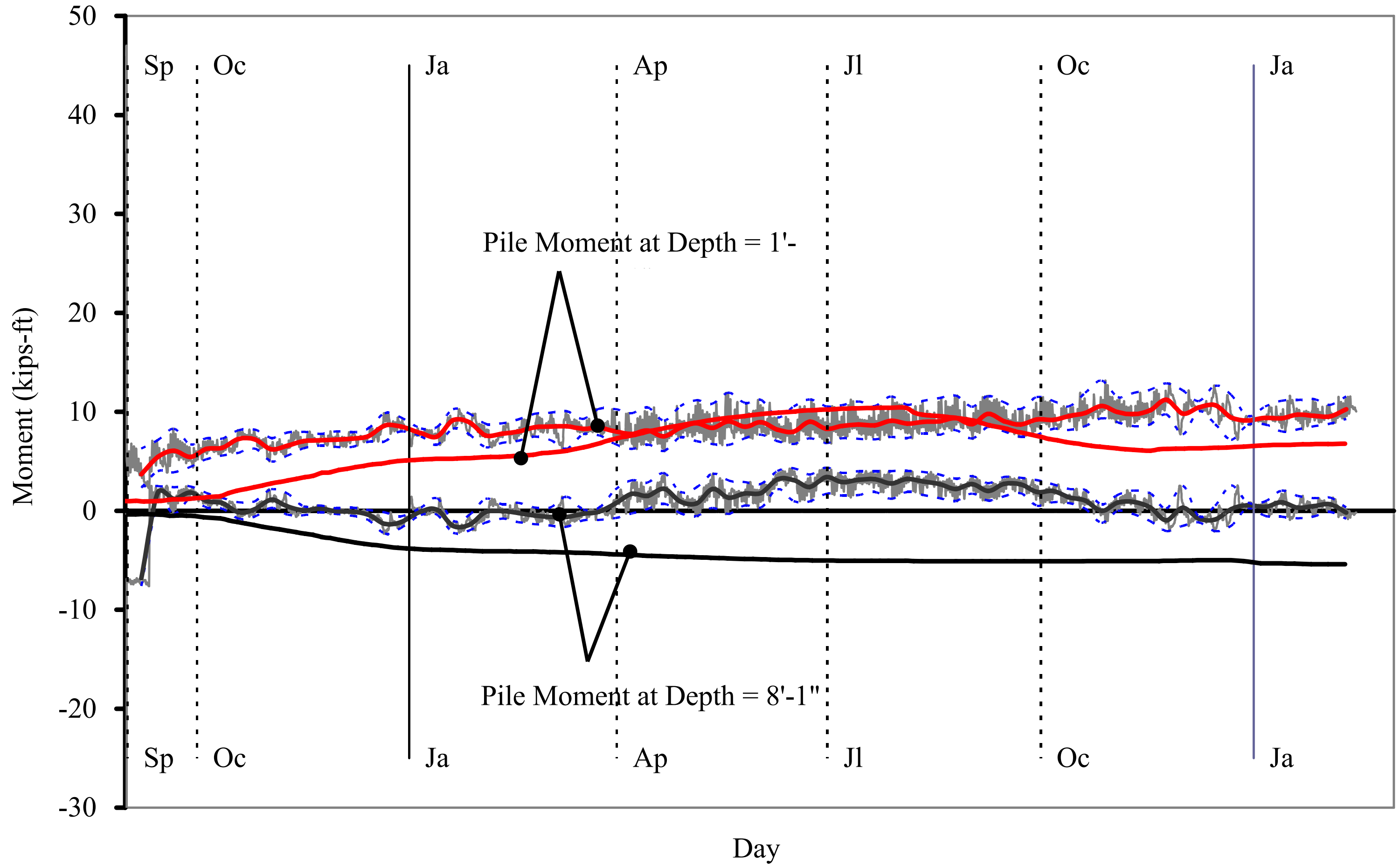

Figure 6.17. Bridge 211: Moments on South Pile of Abutment 1

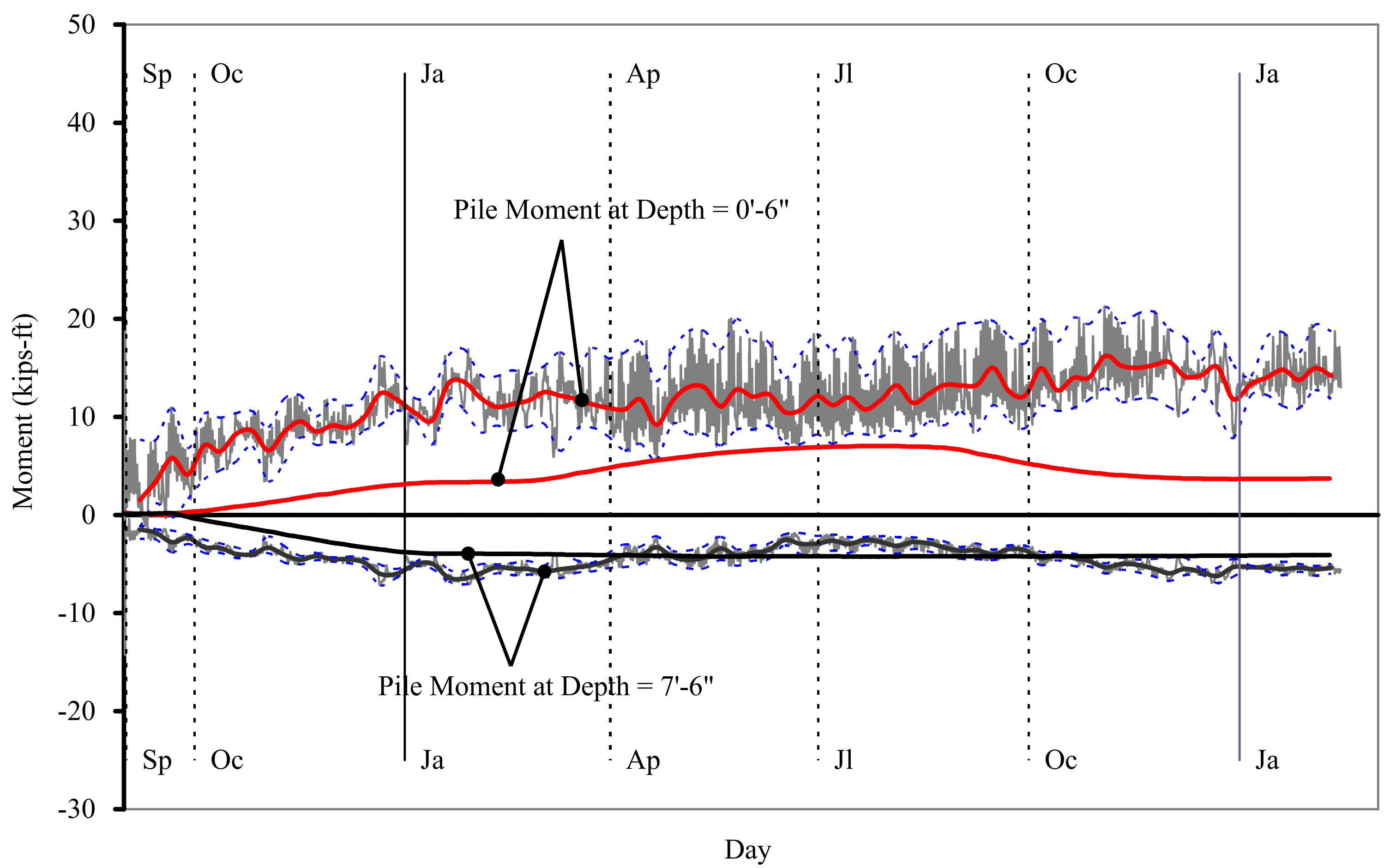

Figure 6.18. Bridge 211: Moments on North Pile of Abutment 2

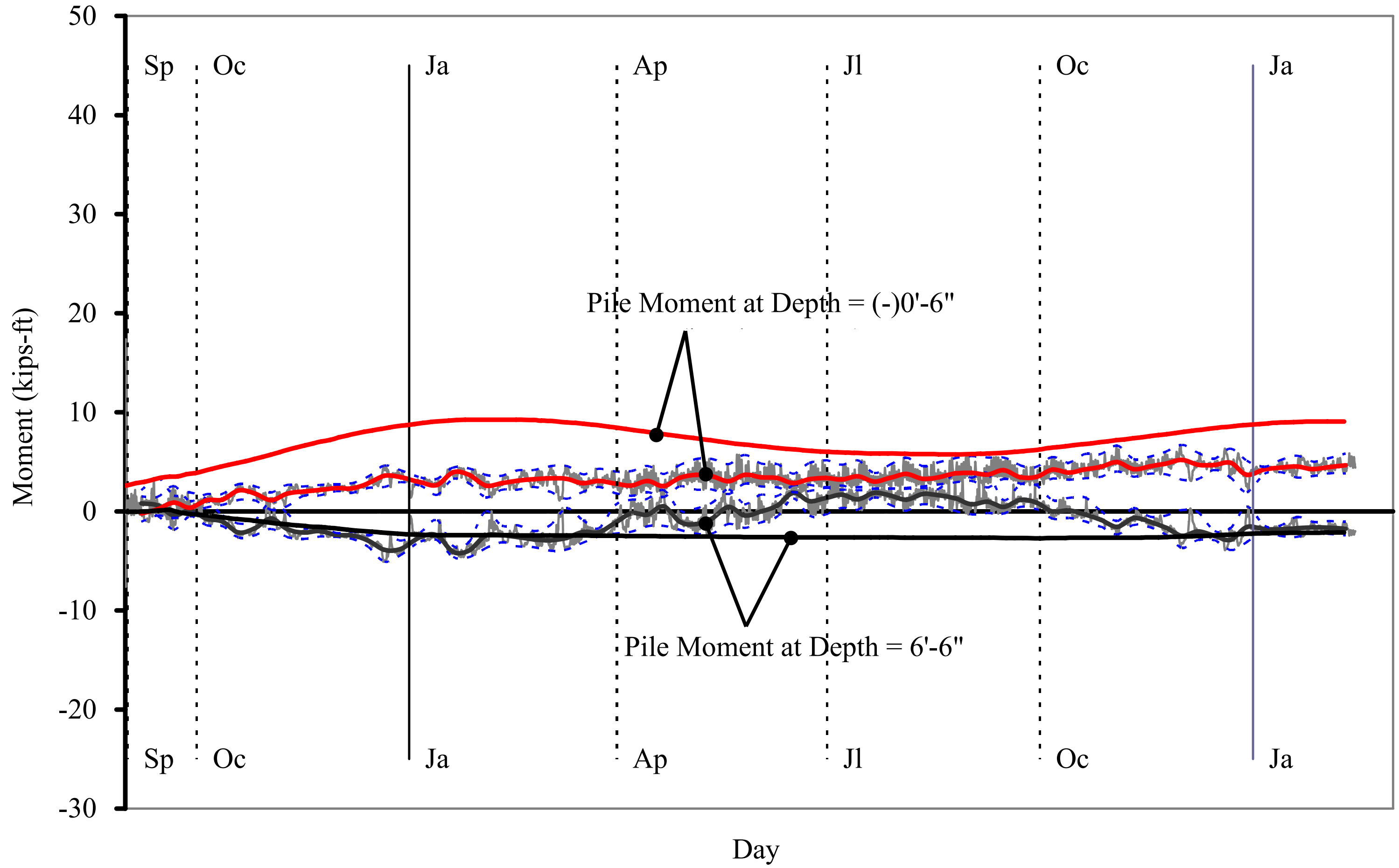

Figure 6.19. Bridge 211: Moments on South Pile of Abutment 2

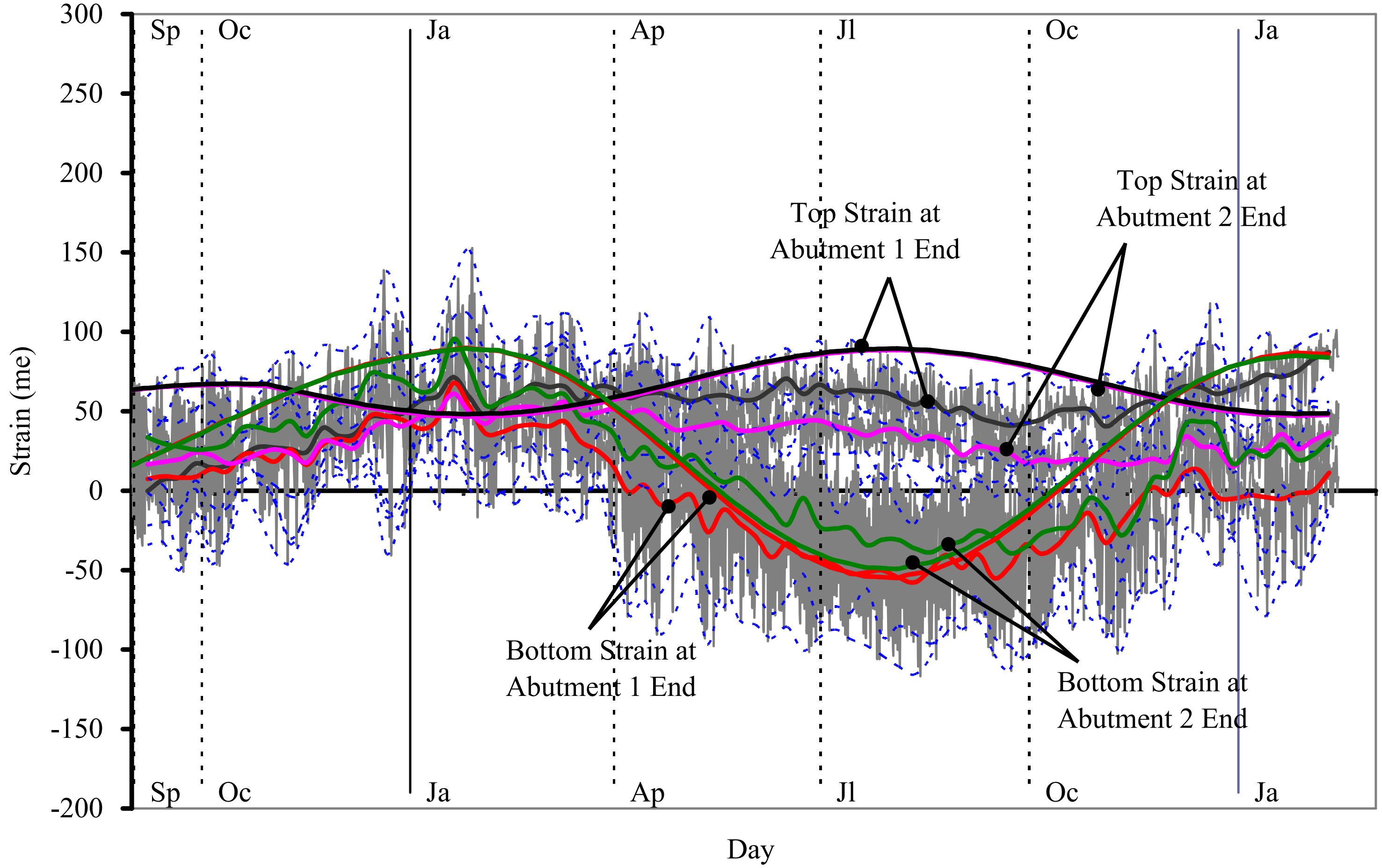

Figure 6.20. Bridge 211: Strain on Girder 1

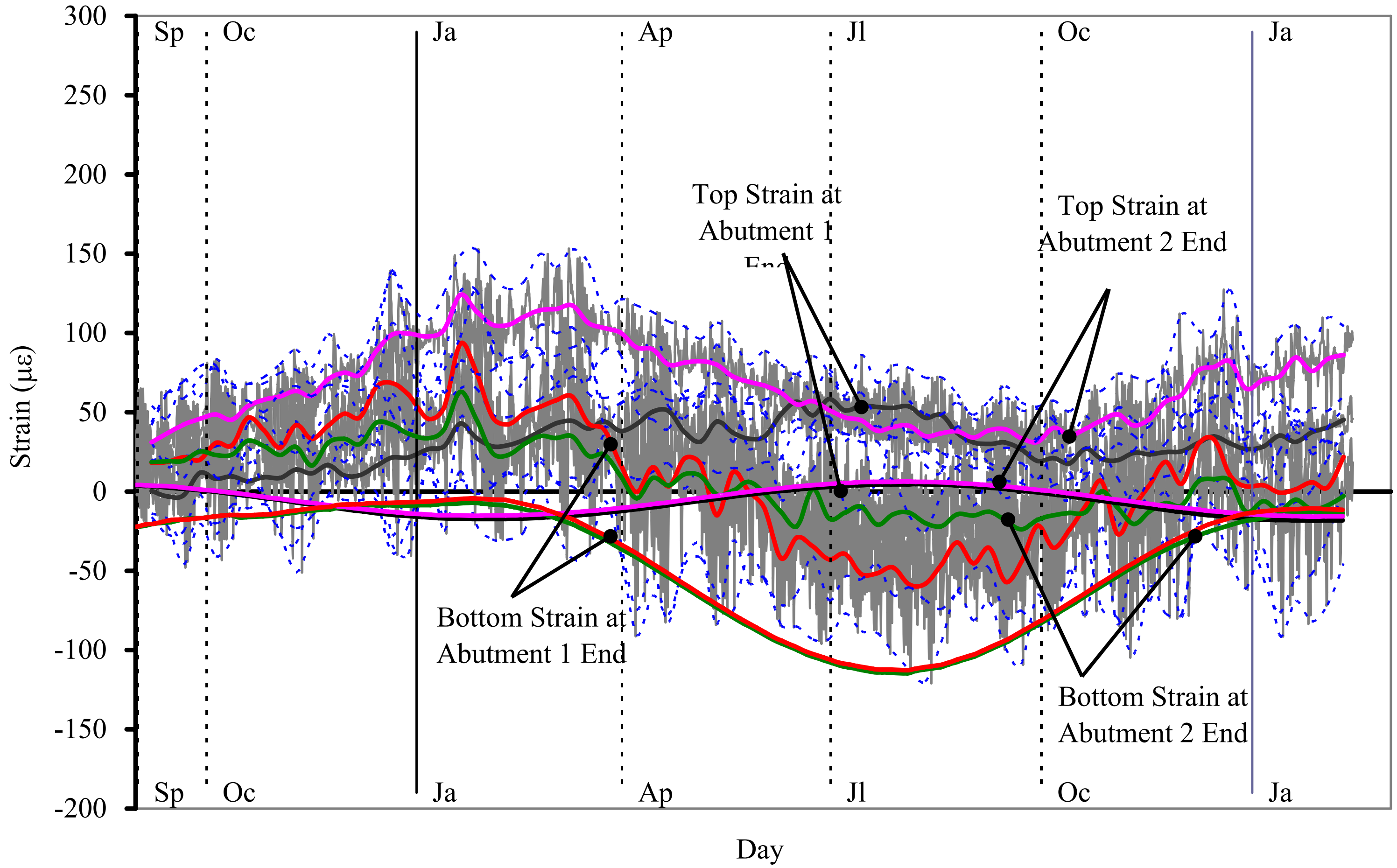

Figure 6.21. Bridge 211: Strain on Girder 2

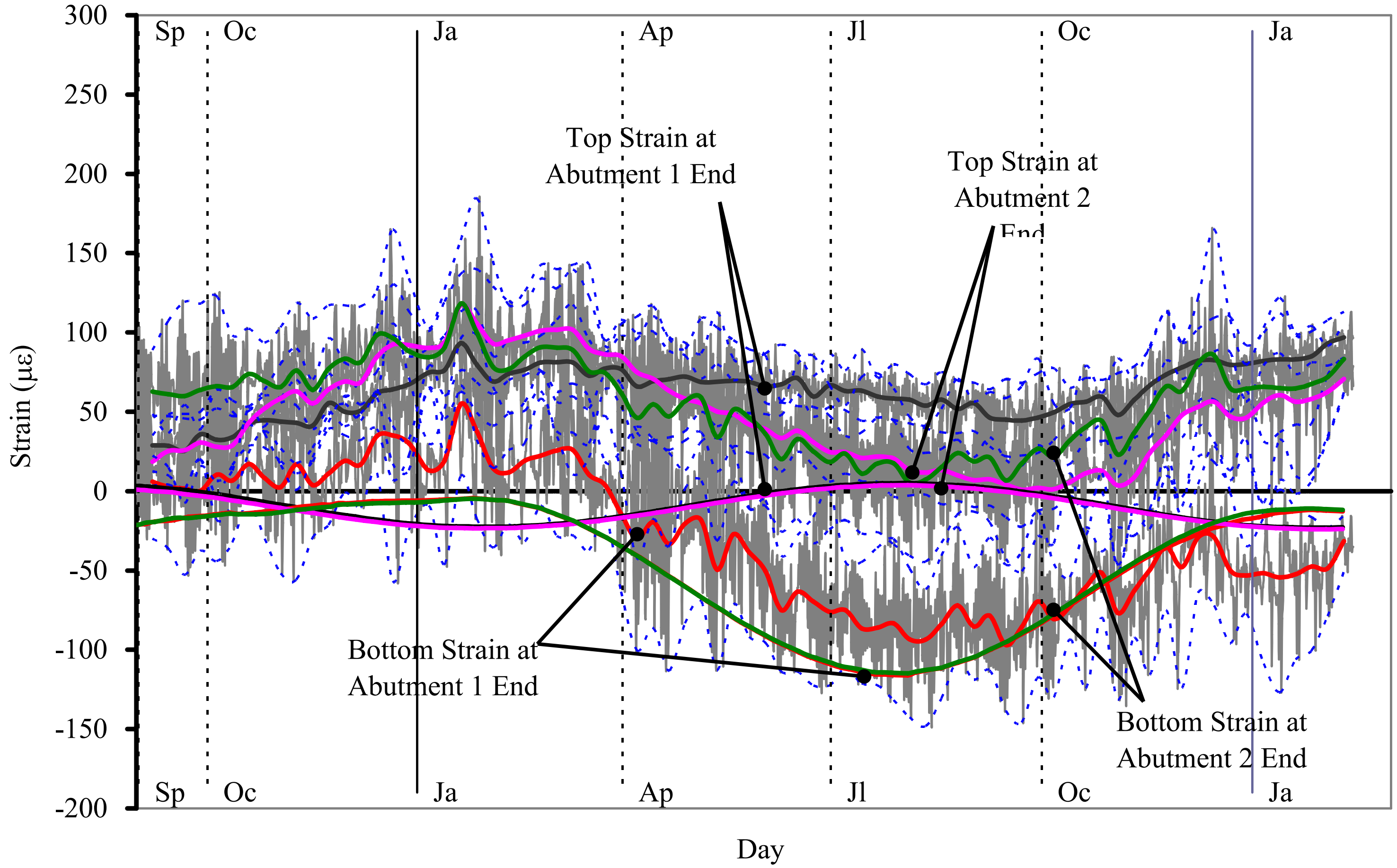

Figure 6.22. Bridge 211: Strain on Girder 3

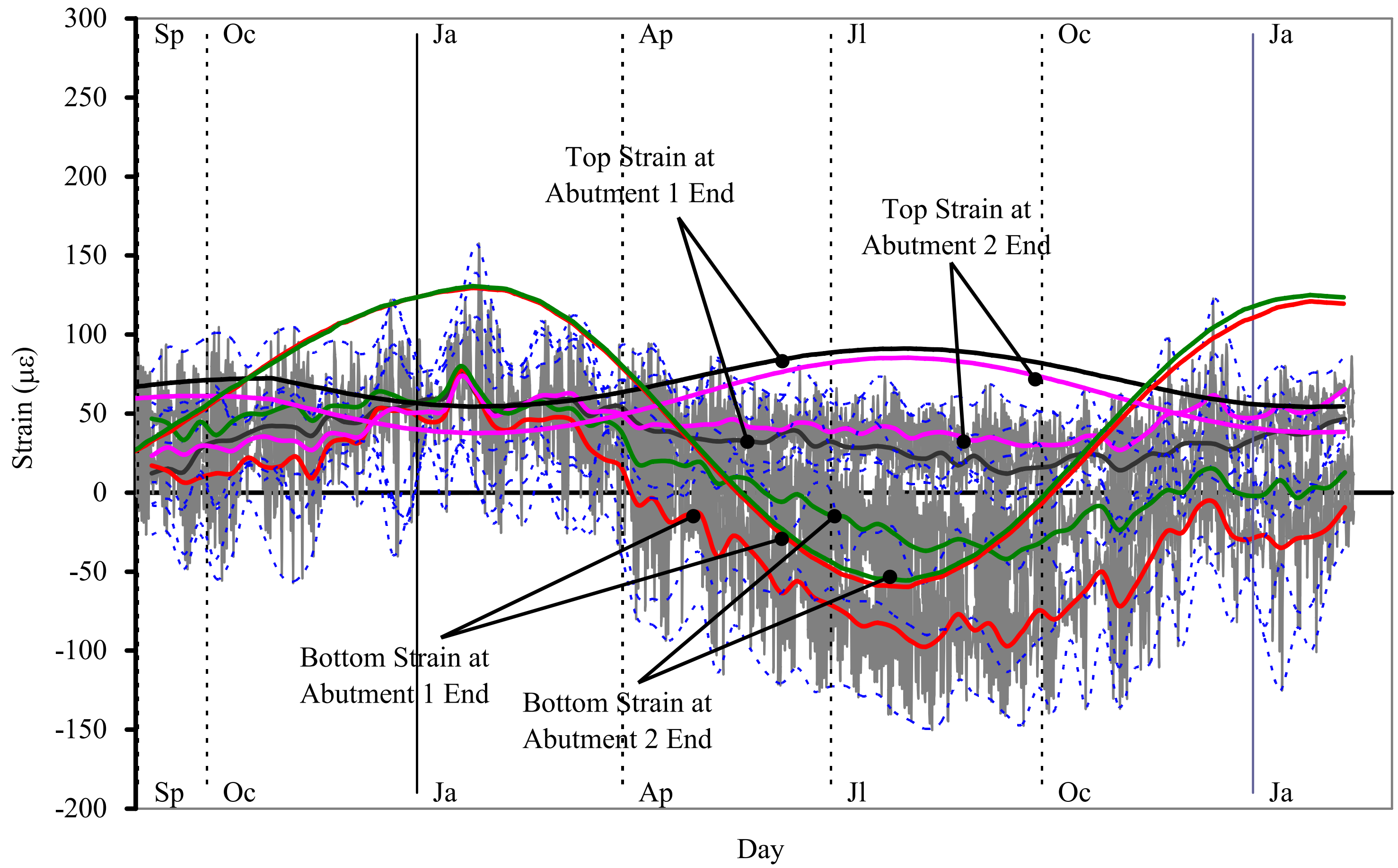

Figure 6.23: Bridge 211: Strain on Girder 4

6.3 BRIDGE 222 MODELING RESULTS AND DISCUSSION

Predicted and measured longitudinal abutment displacements at the two extensometers on abutment 1 are presented in Figure 6.24, and predicted and measured longitudinal abutment displacement at the two extensometers on abutment 2 are presented in Figure 6.25. It can be observed from Figure 6.24 that predicted displacements for the top and bottom extensometer locations were on the order of 0.617 and 0.240 R^2 values, respectively, compared to the corresponding observed displacements. It can also be observed from Figure 6.25 that predicted displacements for the top and bottom extensometer locations were on the order of 0.261 and 0.011 R^2 values, respectively, compared to the corresponding observed displacements. The predicted rates of overall displacement trends were generally different from the measured rates of overall displacement trends, because lag in peak magnitudes of the measured data exists.

Predicted earth pressures from the numerical model versus observed earth pressures at the two pressure cells on abutment 1 are presented in Figure 6.26, and predicted earth pressures from the numerical model versus observed earth pressures at the two pressure cells on abutment 2 are presented in Figure 6.27. As can be observed from Figure 6.26, all predicted pressures showed the same trend as the observed pressures with calculated R^2 values of 0.861 and 0.948 for the top and bottom pressure cells, respectively. As can also be observed from Figure 6.27, all predicted pressures showed the same trend as the observed pressures with calculated R^2 values of 0.859 and 0.934 for the top and bottom pressure cells, respectively.

Predicted relative rotations of the abutment-backwall connection from the numerical model versus relative rotations calculated from the two sets of collected tilt meter data are presented in Figure 6.28. As can be derived from Figure 6.28, the predicted relative rotations for the two girder locations showed the similar trend and magnitudes of relative rotations. The observed data indicate that the relative rotations at the interior section were greater than the relative rotations at the exterior section, which agrees with the observed data from bridge 203. However, the predicted relative rotation variations for bridge 222 are much smaller than the observed relative rotation variations, on the order of approximately 4 and 10 times for girders 2 and 4, respectively.

Predicted pile moments about the weak bending axis from the numerical model versus calculated moments from the two sets of collected strain gage data are presented in Figure 6.29 through Figure 6.32 for the south pile of abutment 1, the north pile of abutment 1, the south pile of abutment 2, and the north pile of abutment 2, respectively. Generally, the predicted moments at the depth near abutment bases (varied from depth = 0′-5″ to depth = 1′-7″) showed a similar trend but a difference in magnitude variations as compared to the observed moments. For deeper depth varied from depth = 6′-3″ to depth = 7′-7″, the predicted moments generally showed the opposite trend but similar magnitudes, as compared to the observed moments. In addition, geometry and material imperfections are a result of differences in initial moments between prediction and observation.

Predicted girder strains from the numerical model versus observed girder strains from strain gages installed on girders 2 and 4 girders are presented in Figure 6.33 and Figure 6.34, respectively. Similar to the bridge 203 case, it can be observed that the overall predicted strains showed compressive magnitudes greater than the overall strains obtained for the field data due to differences in initial strains. For a result comparison of all top strain gages except for the gage location of girder 2 near abutment 1, a similar trend was observed but the predicted strain variations averaged 4.5 times smaller than the observed strain variations for both girders. For a result comparison of all bottom strain gages except for the gage location of girder 4 near abutment 2, a similar trend was observed but the predicted strain variations averaged 1.6 times greater than the observed strain variations for both girders.

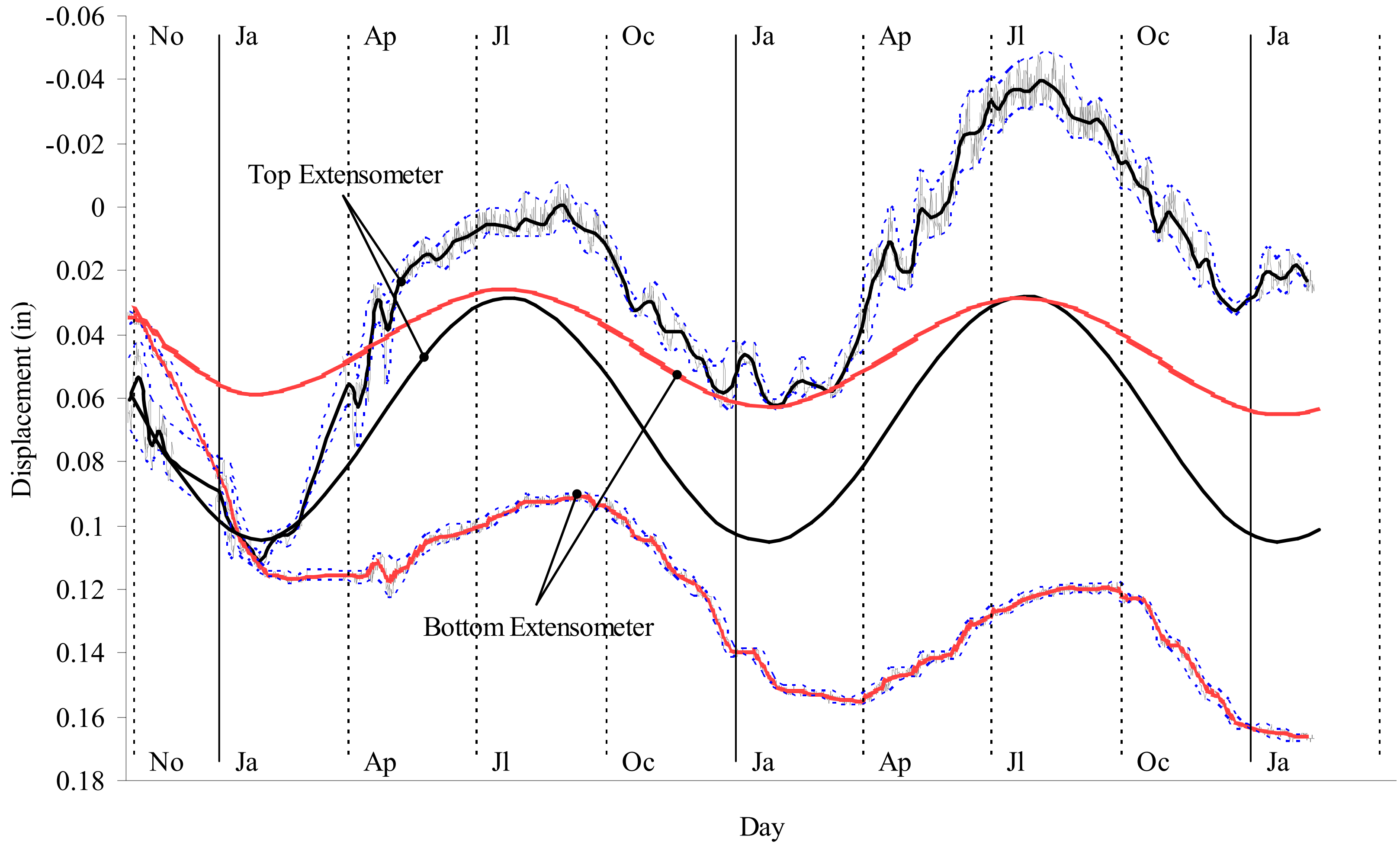

Figure 6.24 Bridge 222: Extensometers (Abutment 1)

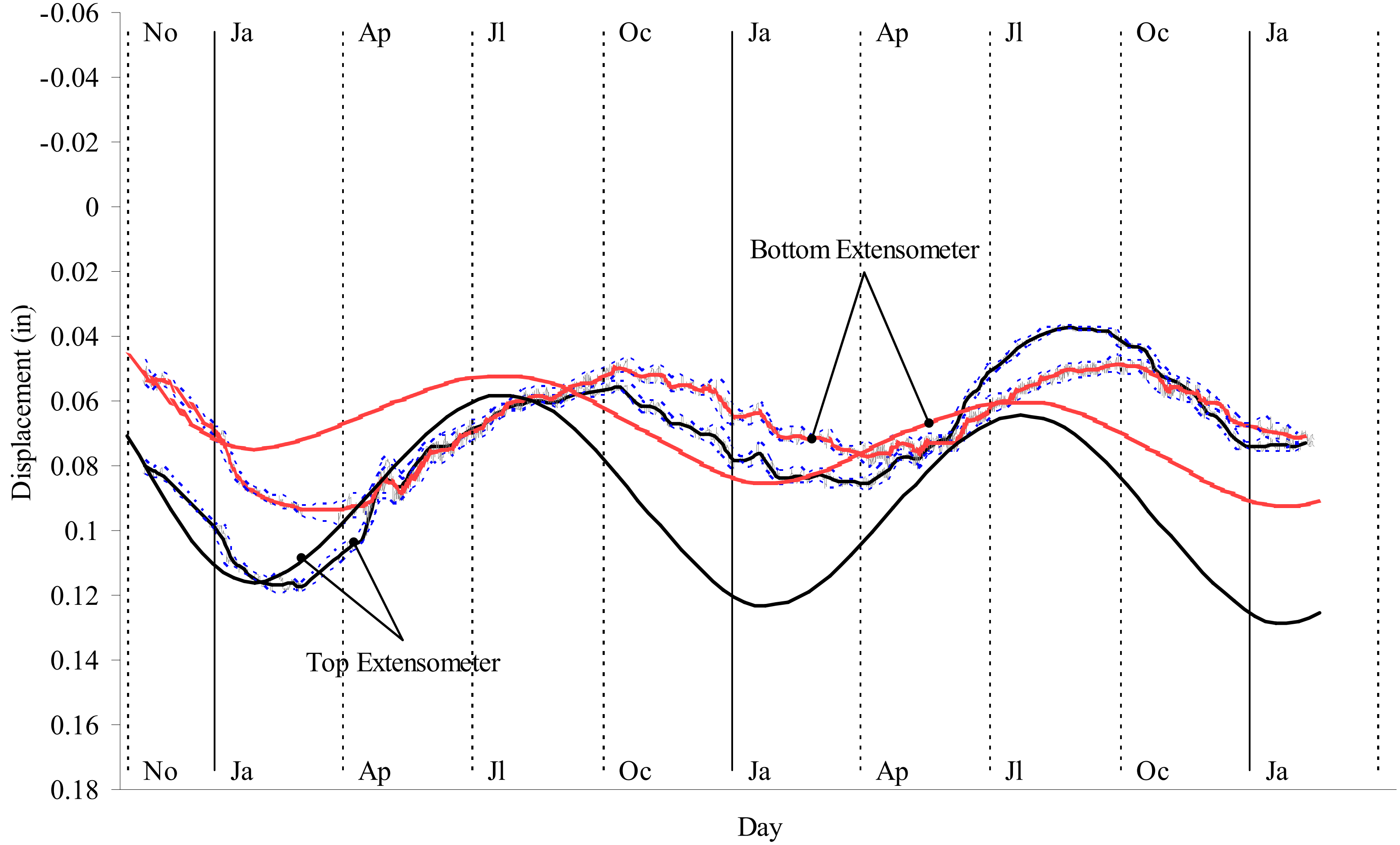

Figure 6.25 Bridge 222: Extensometers (Abutment 2)

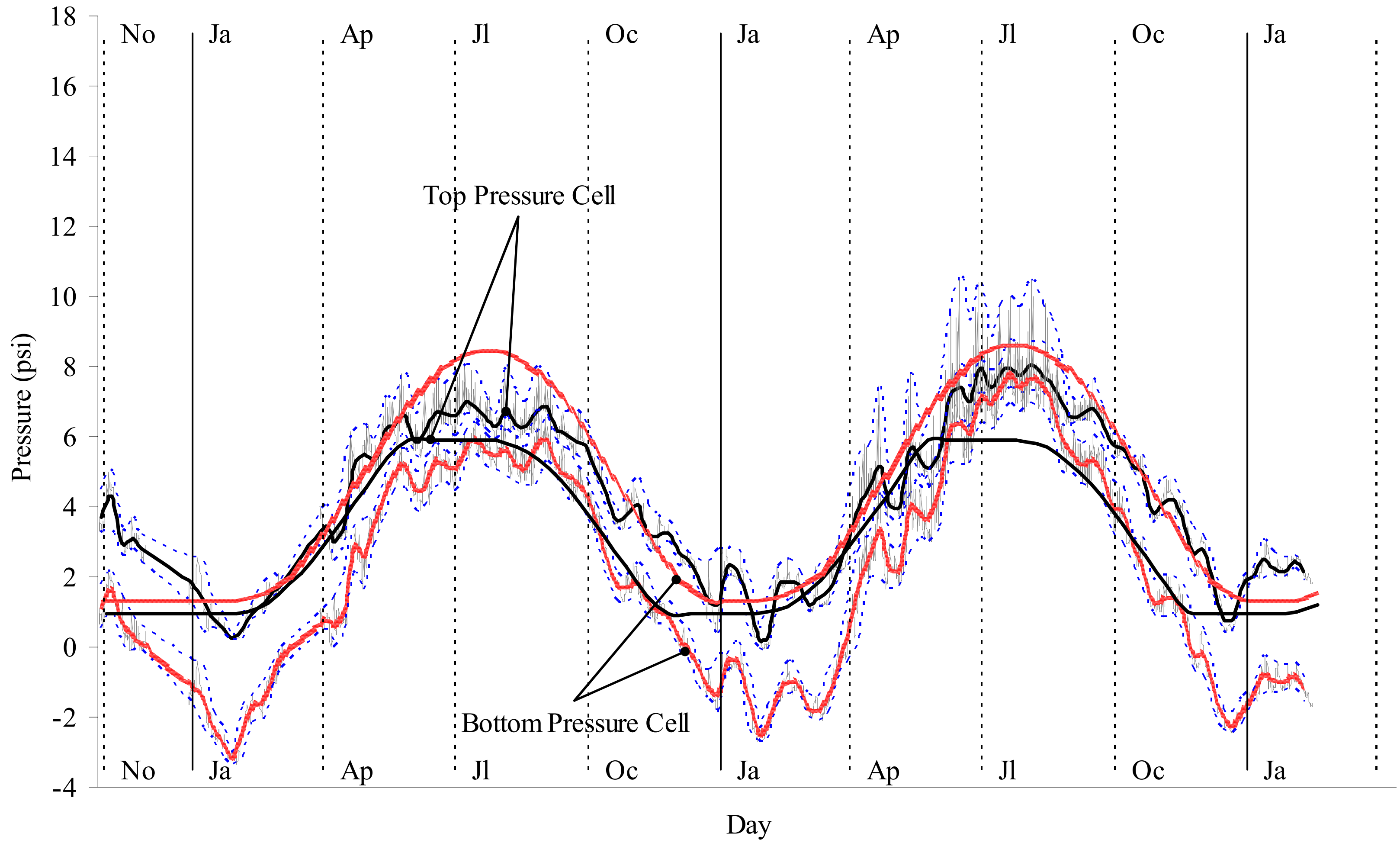

Figure 6.26 Bridge 222: Pressure Cells (Abutment 1)

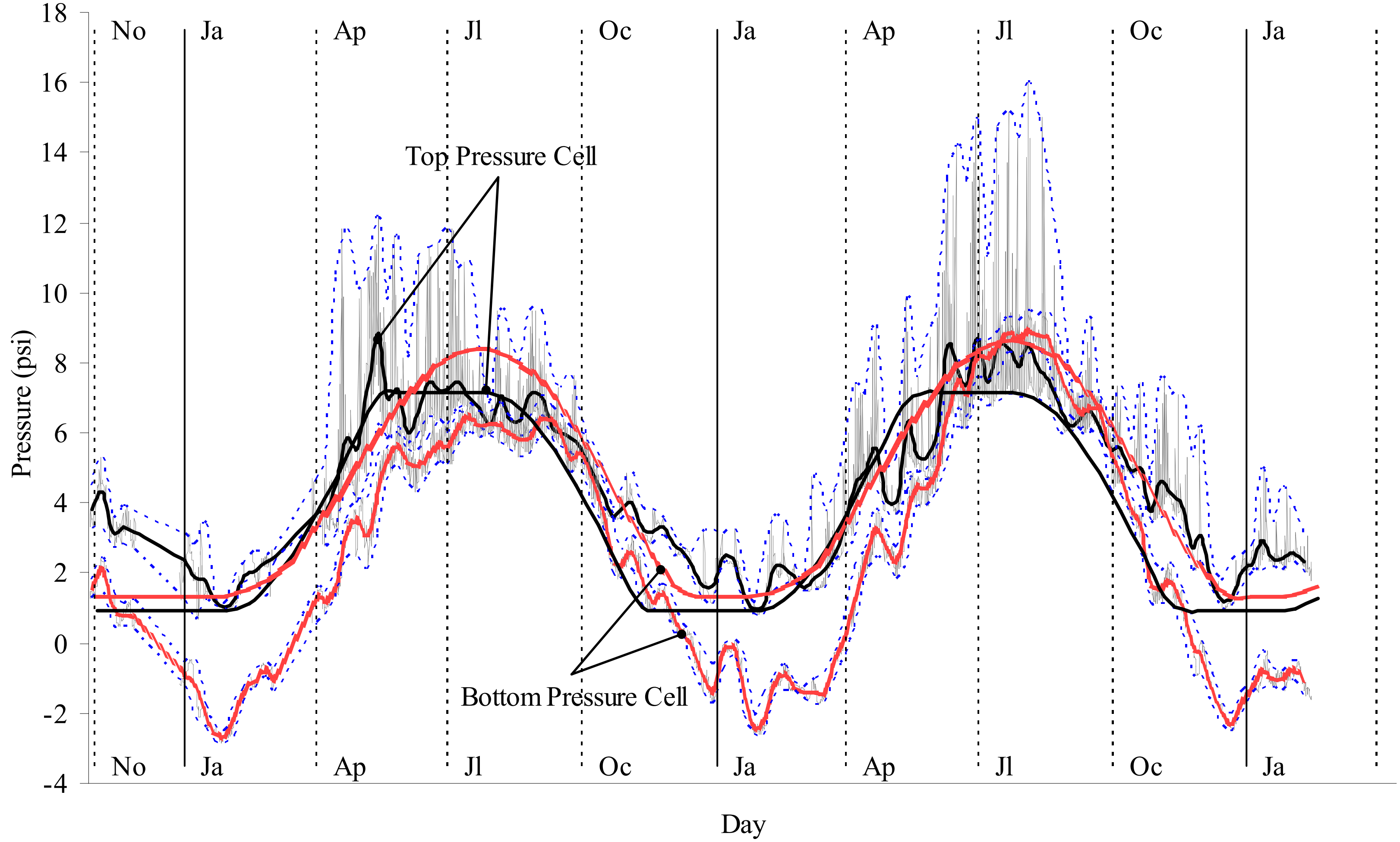

Figure 6.27 Bridge 222: Pressure Cells (Abutment 2)

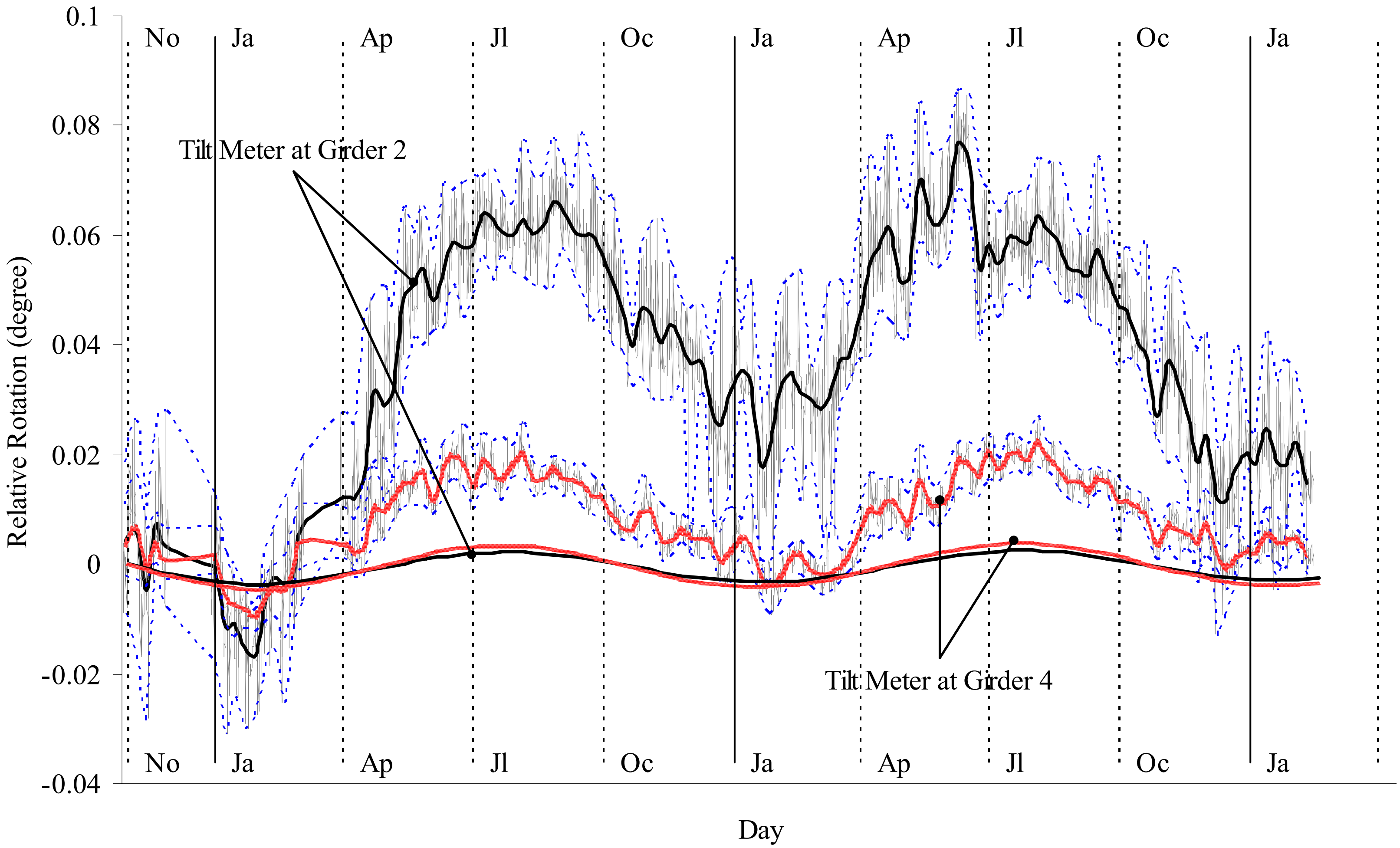

Figure 6.28 Bridge 222: Relative Rotations Between Girder and Abutment (Abutment 1)

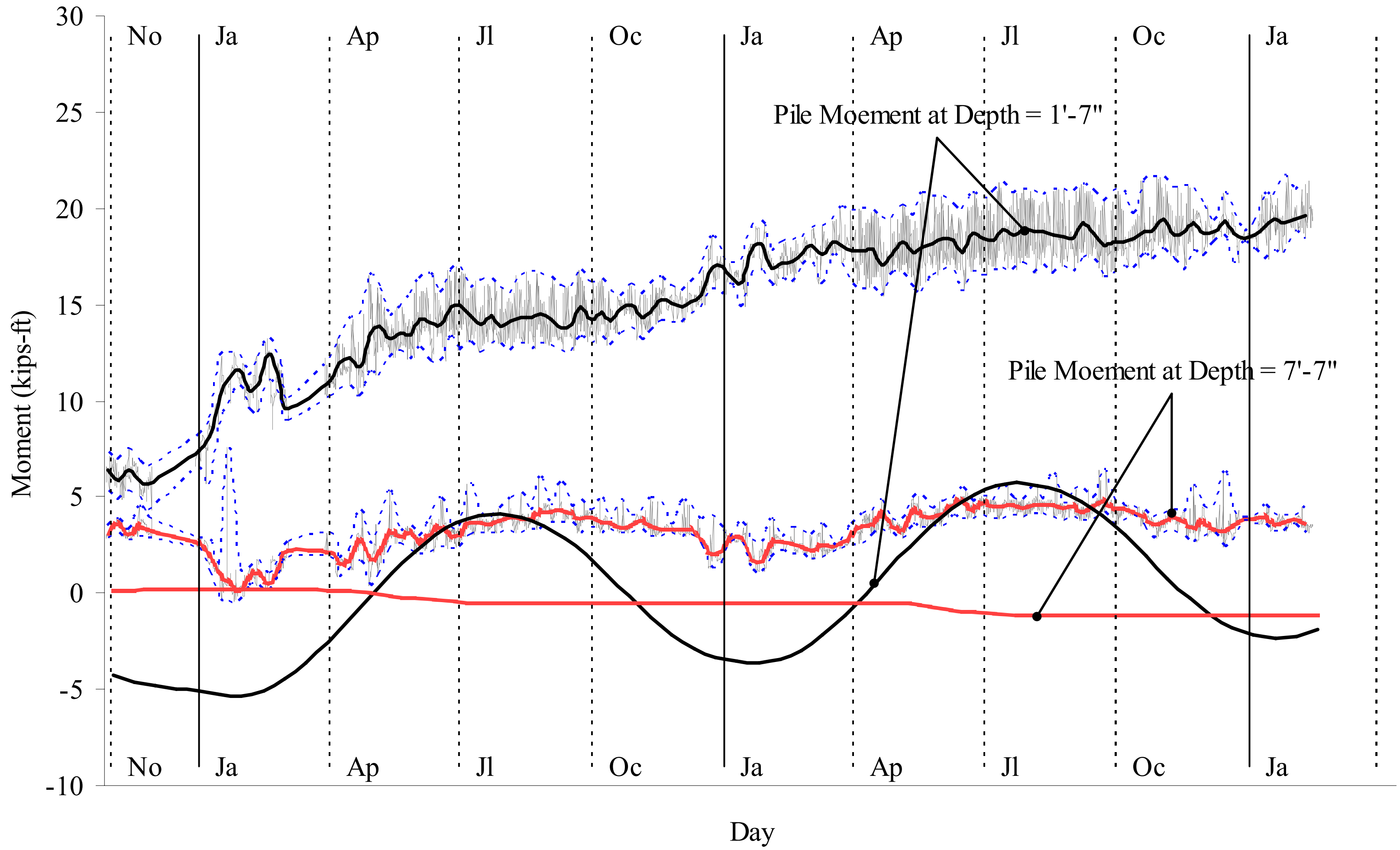

Figure 6.29 Bridge 222: Moments on South Pile (Abutment 1)

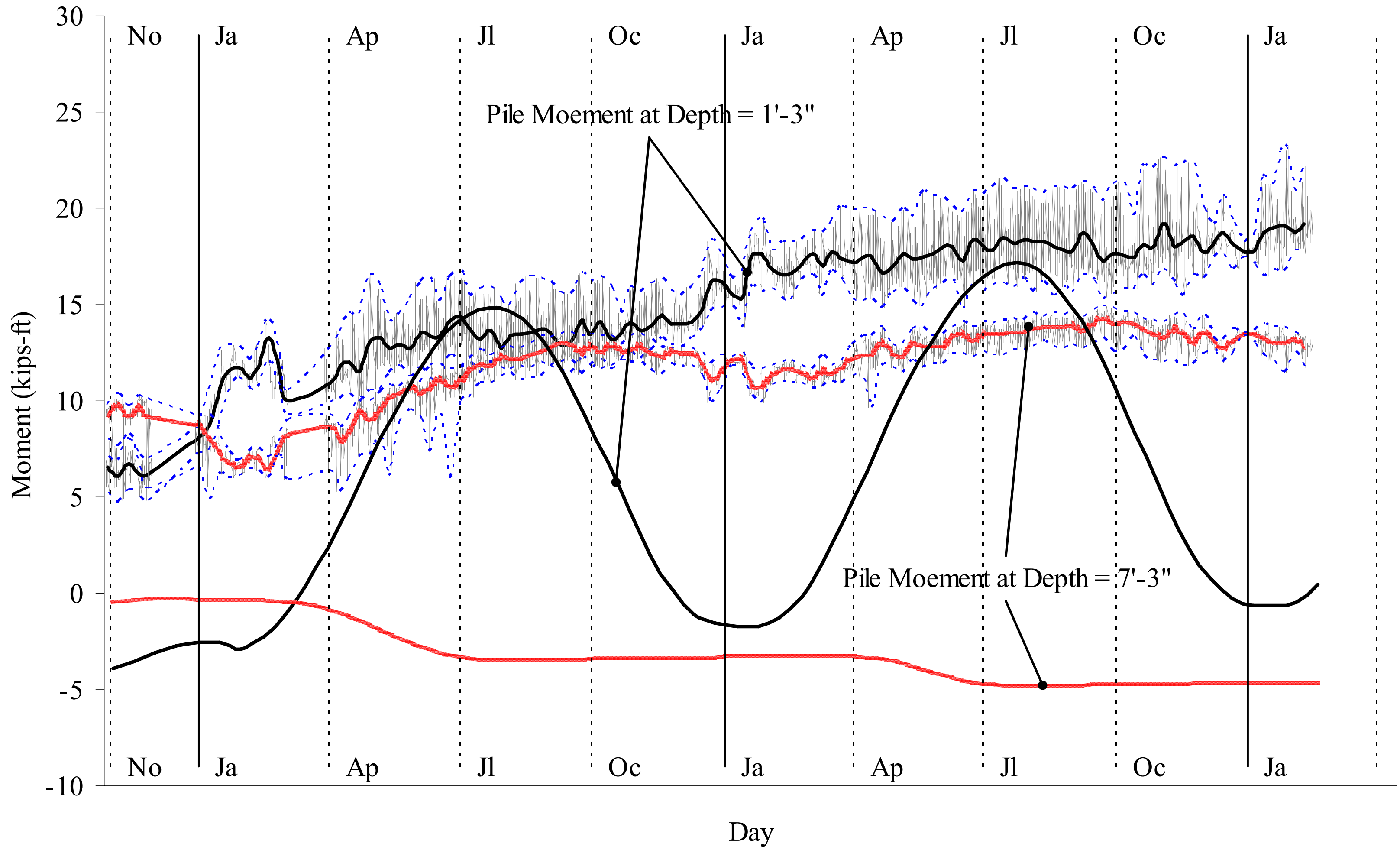

Figure 6.30 Bridge 222: Moments on North Pile (Abutment 1)

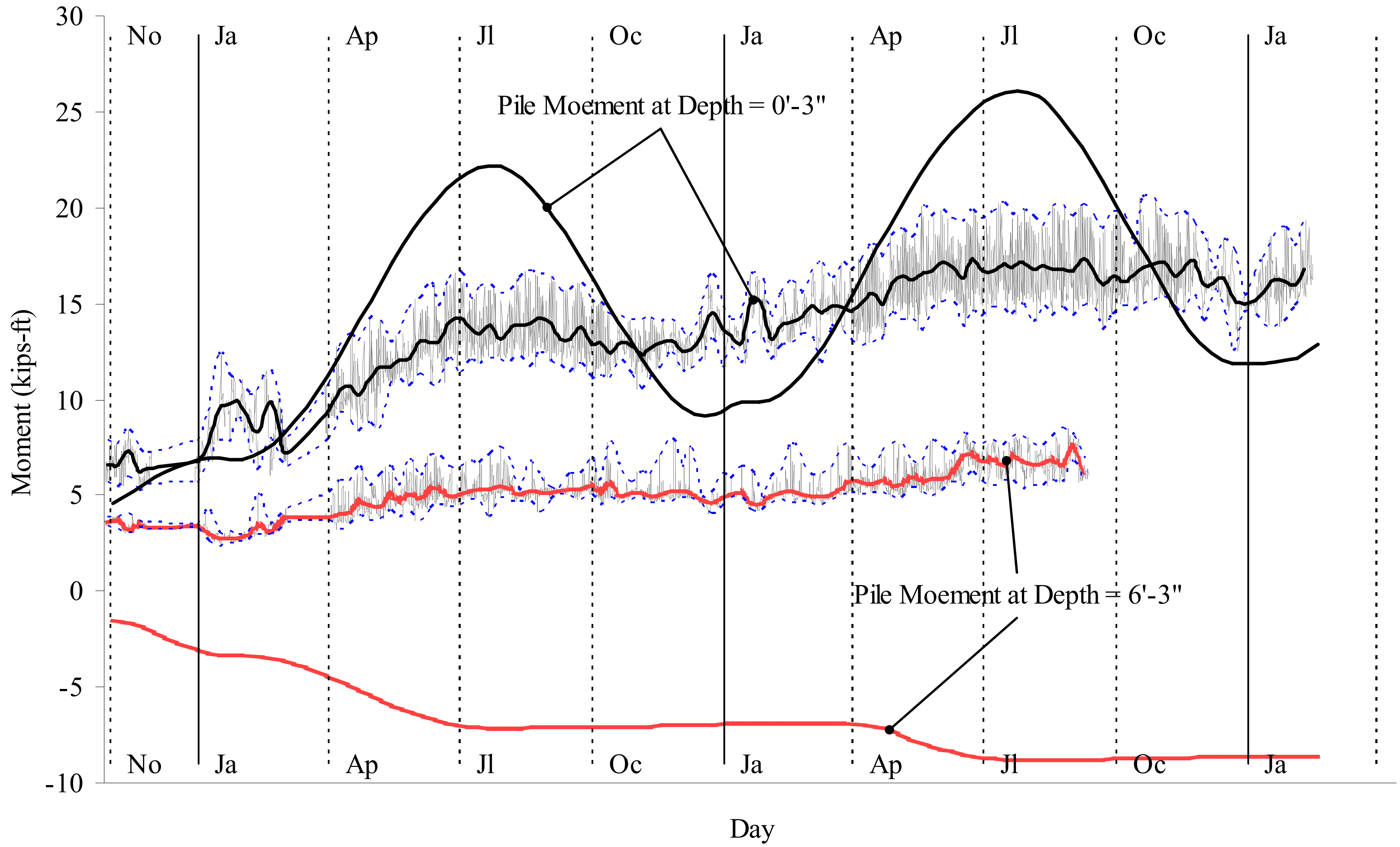

Figure 6.31 Bridge 222: Moments on South Pile (Abutment 2)

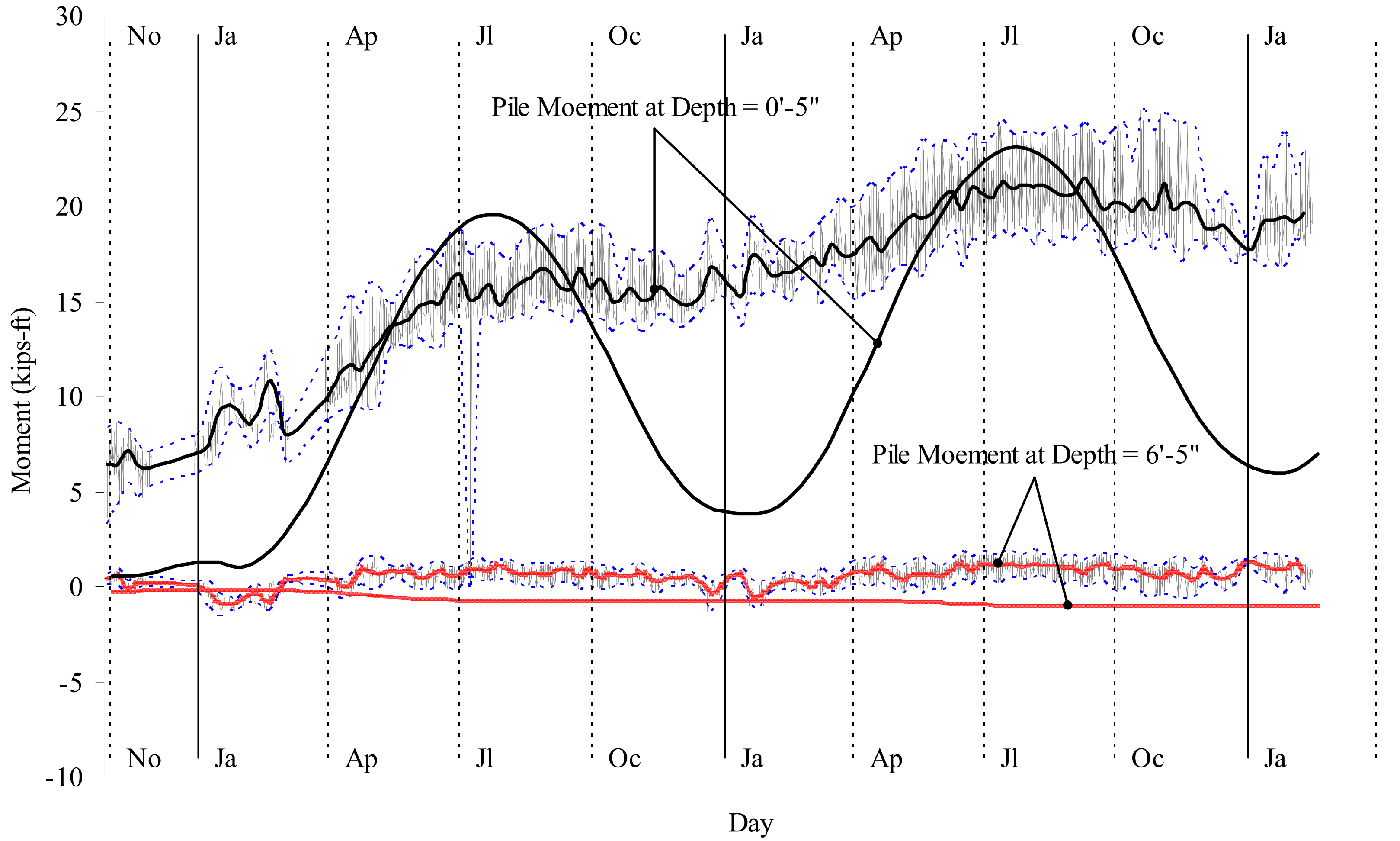

Figure 6.32 Bridge 222: Moments on North Pile (Abutment 2)

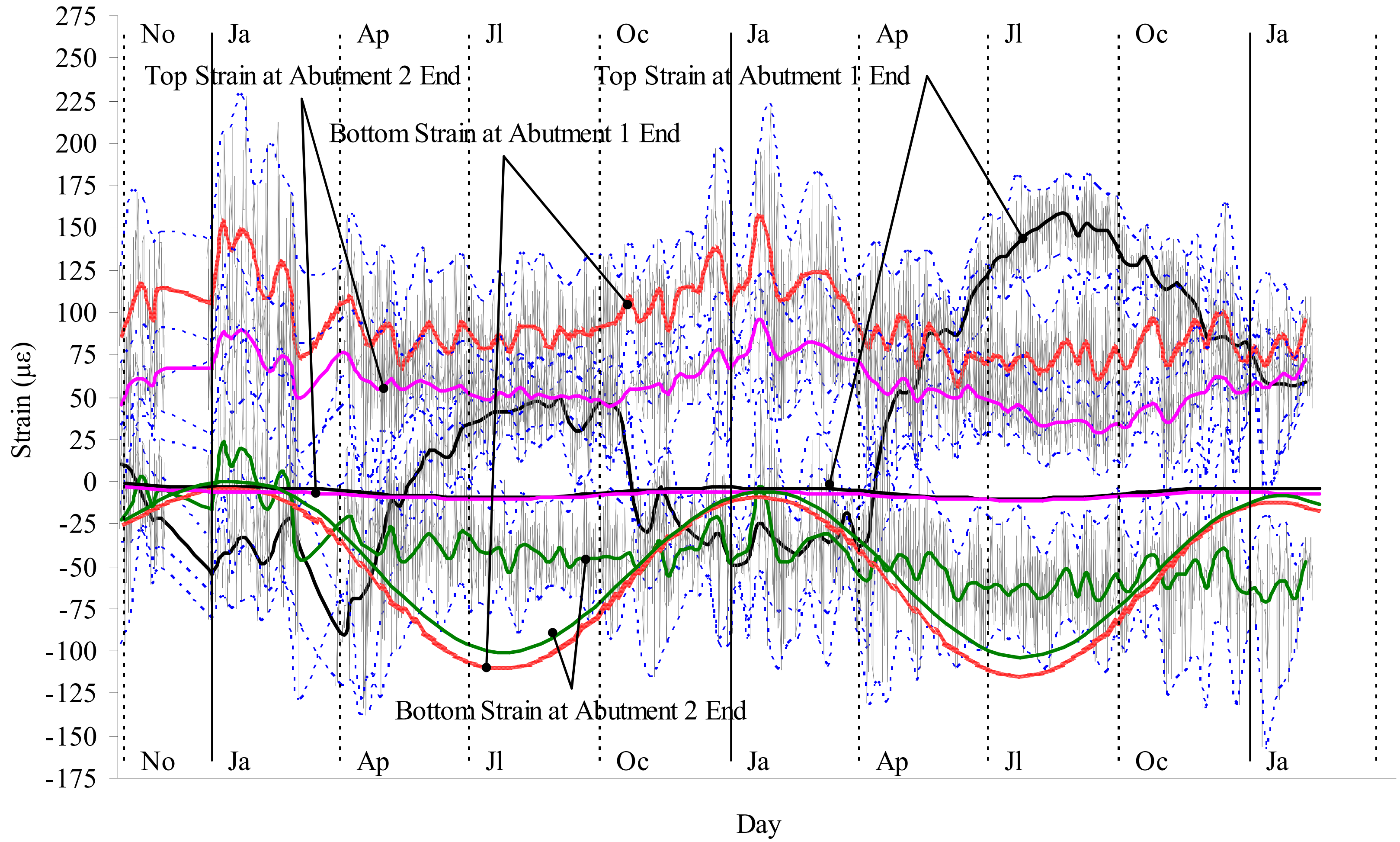

Figure 6.33 Bridge 222: Strain on Girder 2

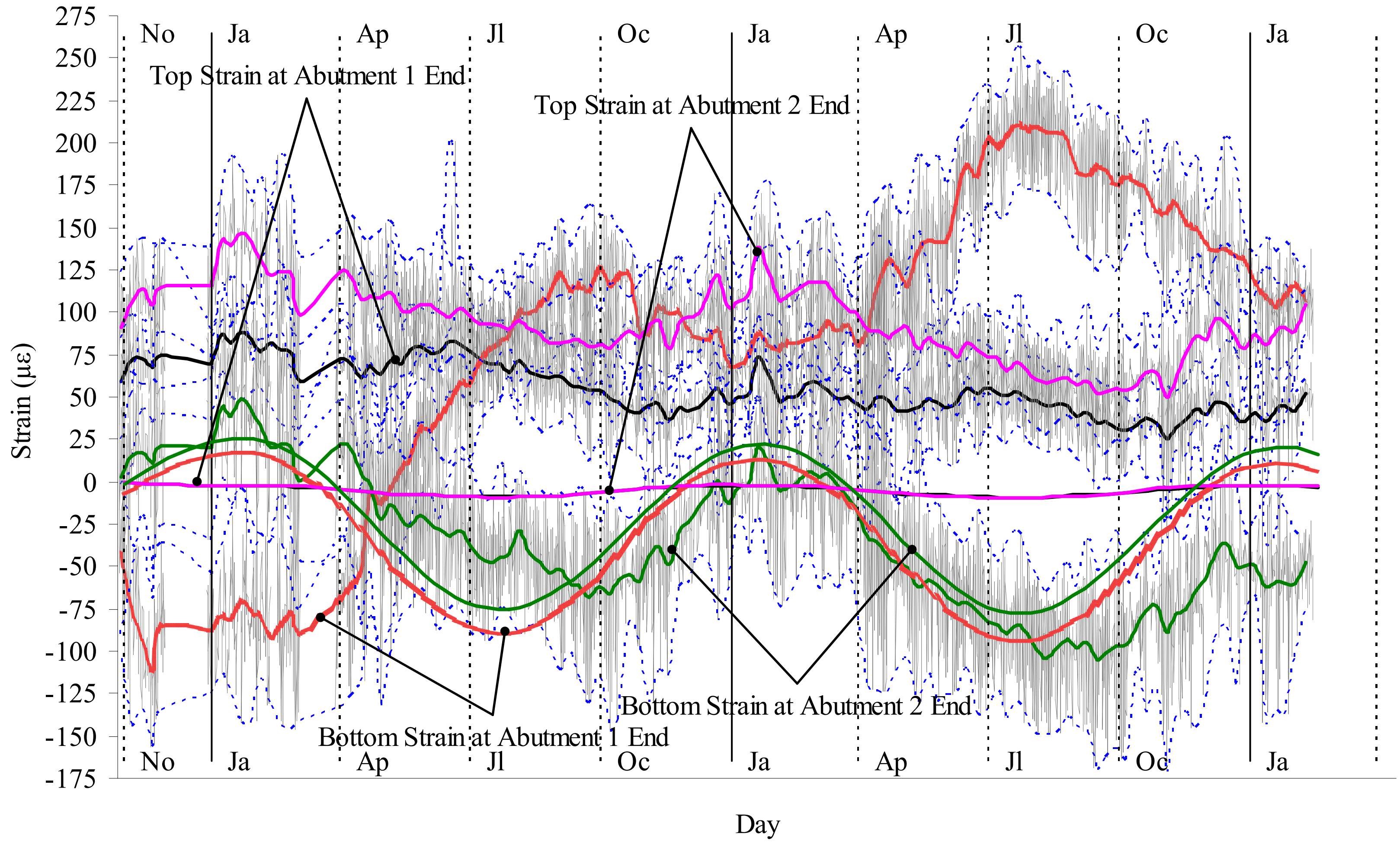

Figure 6.34 Bridge 222: Strain on Girder 4

6.4 CONCLUDING REMARKS

ANSYS numerical models of bridges 203, 211, 222, and 109 as well as the field-collected data for bridges 203, 211, 222 were presented as discussed in this chapter. The abutment displacements based on extensometer data from numerical model results and field collected data generally matched well. Bottom extensometers of predicted results and field data generally produced a contraction trend and larger than top extensometer displacements. All pressure cells from prediction and observation showed the same trend. However, the field collected data indicated that top pressure cells of all IA bridges experienced larger pressures than passive pressures when the IA bridges expanded. For relative rotations between girders and abutments, predicted results of exterior girders were very similar to the results of interior girders. However, observed data showed that interior girders have more relative rotation than exterior girders. Also, the abutment distortion was made to develop a general rotational behavior because the relative rotations were unexpected rotational behavior results. Pile moments at the depth close to abutment bases from prediction and observation showed all contraction trends with a similar overall rate of increasing in moments. For deeper depth, very small moment less than 5 kips-ft were observed and predicted. Also, a different inflection point location was implied because predicted and observed moment produced opposite sign of moment. Girder strains observed from field data were irregular. Generally, top strain gages produced constant strain while bottom strain gages yielded fluctuations of strain variation based on both predicted and observed data.

CHAPTER 7

EVALUATION OF PENNDOT IA DESIGN

Predicted behavior of the four instrumented bridges using the PennDOT IA design program was evaluated by comparison to the measured behavior obtained from the bridge monitoring program. Bridge parameters taken from design drawings, design calculations, and geotechnical reports provided by the engineer of record are used as input to the PennDOT program. All input and calculated output data of the program are presented herein for each of the four study bridges. A summary of the PennDOT program is described and evaluated on a design subsection basis. Comparisons are discussed and suggested program improvements are provided, where appropriate, on a bridge-by-bridge basis. Finally, summary comparisons and suggested improvements are provided.

7.1 PENNDOT IA DESIGN PROGRAM DESCRIPTION

The PennDOT IA design program was developed to aid analysis and design of IA bridge piles. AASHTO LRFD Bridge Design Specification (1994) and PennDOT Design Manual Part 4, DM-4 Appendix G (2000) were used for this design program development. There are two additional features incorporated into the PennDOT IA program: (1) design of abutment/pile cap reinforcement; and (2) pile design under scour conditions. Pile design for scour is not discussed or evaluated herein because the geotechnical reports of the four study bridges do not indicate scour problems.

The PennDOT IA program consists of five main sections: (1) bridge data, (2) integral abutment data, (3) load data, (4) pile data, and (5) analysis summary. The following descriptions of these five sections are limited to the design of abutment/pile cap reinforcement and piles under normal conditions.

The bridge data section allows users to specify girder material, type of girders, and bridge superstructure geometric data. Material options are steel and concrete. Where concrete is specified, an I-girder or spread box girder is listed. All descriptive geometric dimensions are required, including total bridge length, length of integral span, skew angle, bridge width, number of girders, girder spacing, girder depth, bearing pad thickness, deck and haunch thickness, and parapet height.

The integral abutment data section requires input of abutment height and wingwall length. Abutment length and width are automatically generated by the program based on the PennDOT Standard Drawing (BD-667M) and PennDOT Design Manual (DM-4) recommendations. Data input and generated information in this section are primarily used to determine abutment and wingwall dead loads.

The load data section requires the AASHTO LRFD load modifier, η_i, girder reactions due to dead loads and live loads, girder end rotations due to composite dead loads and live loads, wind pressure, and centrifugal force. Unfactored dead and live load girder reactions and rotations can be obtained from the PennDOT prestressed concrete girder design program PSLRFD for input to the program. Wind pressure and centrifugal force are also determined using AASHTO LRFD. Maximum and minimum factored dead load and live load girder reactions are calculated by the program using LRFD load combinations. Maximum and minimum unfactored girder reactions due to effects of wind and centrifugal force are also computed.

The pile data section requires pile properties, number of piles per abutment, pile spacing, pile length, soil resistance factors, pile resistance factors, and unit soil resistance. Soil and pile resistance factors are obtained from DM-4 while unit soil resistances must be obtained from geotechnical reports. In addition, a separate, iterative procedure to estimate depth to pile fixity must be performed to determine the moment arm and resulting axial pile force due to overturning moments of wind force on structure, wind force on live load, and centrifugal force. Normally, COM624P is utilized to determine these pile moments. The final design is performed by checking both geotechnical and structural pile axial force limits, axial-moment interaction, ductility, and abutment/pile cap reinforcements.

The analysis summary section repeats all input and reports warnings and errors to be addressed, if any. Critical design results including factored axial force versus axial capacities (both structural and geotechnical), and magnitude of axial-moment interaction evaluation are also provided.

7.2 BRIDGE 203 EVAUATION

The bridge 203 design was not based on the PennDOT IA program. The design philosophy used in the design of bridge 203 was based on load factor design (LFD). As a consequence, the analysis results obtained for this bridge through the LRFD based on the PennDOT IA program is not the same as the original design. In addition to a comparison between the PennDOT IA program and field data, a comparison is also presented between the original LFD method used and the PennDOT IA program.

The PennDOT IA program results, complete with input data, are presented below. Four sources were used to obtain bridge material and geometric information: (1) design drawings, (2) design calculations, (3) the geotechnical report, and (4) actual pile driving records. The design drawings, design calculations, and geotechnical report were obtained from HDR Inc., of Pittsburgh (the design consultant of this bridge). The average as-built pile length was used in the PennDOT IA program, as presented below.

Title: Bridge 203 - 52.43 m 3-Span Concrete Prestressed I-girder By: KP Date: 3/10/2006
90° skew, 3.594 m girder spacing Checked: ________ Date: ________

SPREADSHEET PROGRAM DESCRIPTION

This spreadsheet is intended to be used as an aid in designing and analyzing integral abutments. No users manual is provided, but explanations of input values are given throughout the spreadsheet. The spreadsheet is intended to be used in conjunction with the computer program COM624P, which analyzes the lateral behavior of piles, and with PennDOT's steel or prestressed concrete girder design programs. Design Specifications for integral abutments are available in PennDOT Design Manual Part 4 (DM-4), Appendix G. References to applicable provisions in the DM-4, as well as to the AASHTO LRFD Bridge Design Specifiction, 1994, are made near the right hand margin. Many dimensions for integral abutments are set forth in PennDOT's BD-667M Standard Drawings. The spreadsheet was written in SI units, although the English unit equivalents are also provided, such that either units can be used. Warning and Error messages are provided where possible. An Error message indicates an input value is incorrect and should be changed, a Warning message flags an input value that is suspect, and the user should verify the value, or in some cases, obtain the approval c
Different sheets (tabs), labeled along the bottom of the window, perform different tasks within the spreadsheet. The first tab in the spreadsheet summarizes the input values by providing a simple list which can be printed and filled in by hand, or used to insert the input values. The current tab is the Main tab where most of the analysis takes place. The Scour tab is available for cases where an additional scour check of the piles is required. The COM624P Input tab is used to generate an template for the COM624P computer program. The load factors for each load case are listed on the Load Factor tab. The Cap Reinforcement tab calculates the area of reinforcement needed for the pile cap. The Pile Data tab lists the properties of available H-pile sections, calculates the properties of concrete filled pipe piles, and lists the current pile properties for insertion into the Main tab.

[ ] - denotes input cells

BRIDGE DATA

Input all the geometric and material data for the proposed bridge. This information should be available from a superstructure design already performed independently, as well as a Type, Size, and Location (TS&L) Report, if available.

The girder material is required to determine the coefficient of thermal expansion of the bridge and the uniform temperature change.

Girder material (S - Steel, C - Concrete) [C]

There are three types of girders which can be used with integral abutments: Steel I-girders, concrete I-girders, or concrete spread box girders.

Girder type (I - I-girder, B - Box girder) [I]

Steel bridge lengths in excess of 120000 mm and concrete bridge lengths in excess of 180000 mm require the written approval of the Chief Bridge Engineer for use with integral abutments. In addition, bridges in excess of these limits require consideration of secondary forces such as those caused by creep, shrinkage, thermal gradient, or differential settlements. The methods of applying secondary forces also require the approval of the Chief Bridge Engineer. DM-4 Ap.G.1.2.1 DM-4 Ap.G.1.2.7.5

Total bridge length - centerline end bearing to centerline end bearing
[52425.6] mm 172.00 ft

The length of the span adjacent to the abutment is required to calculate the pedestrian loads and wind loads on the abutment. It is also used to assess whether the bridge is simply supported or continuous, and in the simplified procedure to determine axial forces induced in the piles in continuous bridges due to thermal movements. Input the total span length for single span bridges.

Length of span adjacent to abutment - centerline bearing to centerline bearing
[10820.4] mm 35.50 ft DM-4 Ap.G.1.2.1

Skews are limited to 70 degrees or more for continuous spans and single spans longer than 40000 mm. Skews of up to 60 degrees are allowed for single spans in excess of 27000 mm but not longer than 40000 mm. For single spans 27000 mm and less, skews up to 45 degrees are permitted. Only positive skew values >45 or <90 degrees can be used in the spreadsheet. DM-4 Ap.G.1.2.2

Skew [90] degrees 1.57 radians

The curb-to-curb roadway width, the sum of clear sidewalk widths, and the out-to-out superstructure widths are required input. Warnings will be supplied if these values plus conservative estimates of parapet widths are not consistent. It is the users responsibility to make sure these values are correct, however. The roadway and sidewalk widths are used in calculating live load reactions. The out-to-out superstructure width is used to determine both loadings and the length of the integral abutment.

Curb-to-curb (roadway) width	12192	mm	40.00 ft
Sum of clear widths of sidewalks on bridge	0	mm	0.00 ft
Out-to-out superstructure width	13072	mm	42.89 ft

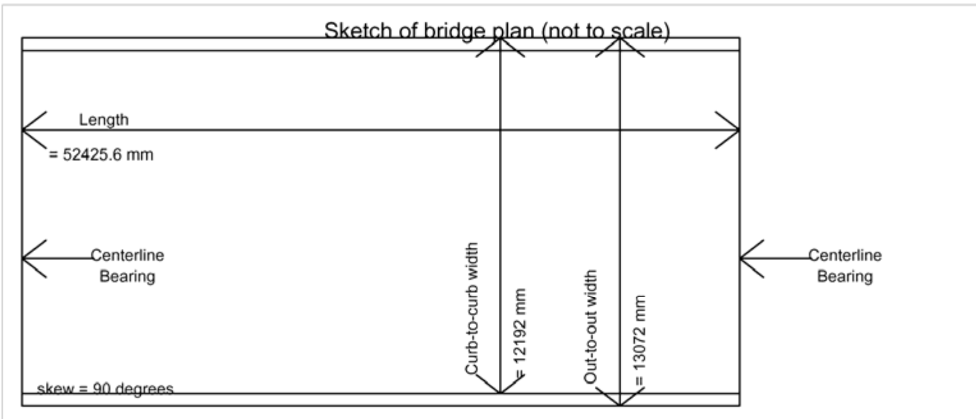

The maximum number of lanes with sidewalks is determined by dividing the width of available roadway (out-to-out of curbs) by the specified lane width (3600 mm) and rounding down to the nearest integer. Widths between 6000 and 7200 mm are assumed to carry two lanes, however. Similarly, the maximum number of lanes without sidewalks is determined by taking the out-to-out width of the structure minus two assumed 440 mm parapets, dividing by the specified lane width, and rounding down to the nearest integer. Again, widths between 6000 and 7200 mm are assumed to carry two lanes. A3.6.1.1.1

Curb-to-curb width of roadway divided by lane width = 12192/3600 = 3.39
Maximum number of lanes with sidewalks 3

Total bridge clear width divided by lane width = (13072 - 880)/3600 = 3.39
Maximum number of lanes without sidewalks 3

The number of girders and the girder spacing is needed to determine the maximum girder reaction for pile cap design. Other dimensions are used to determine various things such as end diaphragm height and lateral wind area of the span, which are utilized in calculating dead and wind loads.

Number of girders in the cross-section	4			
Girder spacing normal to longitudinal axis	3594.1	mm	11.79 ft	
Girder width (maximum of top or bottom flange width at the abutment)	1066.8	mm	3.50 ft	
Girder depth	1600.2	mm	5.25 ft	DM-4 Ap.G.1.2.8
Bearing pad thickness	20	mm	0.79 in	DM-4 Ap.G.1.7
Deck + haunch thickness	262.89	mm	10.35 in	
Parapet height	1143	mm	3.75 ft	

Total superstructure depth for wind analysis - top of parapet to bottom of girder

1600.2 + 262.89 + 1143 = 3006.09 mm 9.86 ft

The moment of inertia of the girders about the longitudinal axis of the bridge is calculated as illustrated in the figure below (five I-girders shown for illustrative purposes, the actual number of girders is used in the calculations). This value is used later to determine girder reactions due to transverse and overturning loadings.

Given a group of n girders, the second moment of inertia is calculated by summing the squares of the distances of the girders from the center of gravity of the girder group, or $I = \Sigma d_i^2$. For a single line of n equally spaced girders, the equation $I = n (n^2 - 1) L^2 / 12$ gives the same result, where n is the number of girders, and L is the girder spacing.

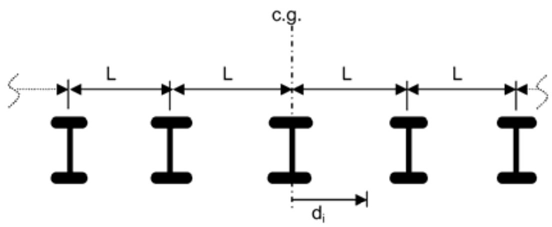

Moment of inertia of 4 I-girders about the longitudinal axis of the bridge:

4(4^2 - 1)(3594.1^2)/12 = 64587774.05 mm^2 100111 in^2

INTEGRAL ABUTMENT DATA

Given the geometry of the superstructure, the location of the proposed abutment, and the topography of the site, the geomety of the integral abutment can be calculated, and the wingwall lengths can be determined. Many of the dimensions are set in the PennDOT standards (see BD-667M Standard Drawing).

The abutment length is measured along the line of bearing. Note that specifying detached wingwalls later in the spreadsheet results in a slightly longer abutment (see BD-667M for detached wingwall details).

Abutment length	(13072+700)/sin(90) =	13772	mm	45.18 ft

The abutment width is set at 1200 mm so that for any potential skew angle the pile cap reinforcement can fit around the piles.

Abutment width	1200	mm	3.94 ft	DM-4 Ap.G.1.4.1

The minimum pile cap height is 1000 mm. The flexural design of the pile cap is based on the supplied minimum dimension. There are a number of factors which can affect the maximum pile cap height. These include, but are not limited to, bridge width and cross-slopes, superelevation, skew, etc. DM-4 Ap.G.1.4.1

Although PennDOT permits the opposite ends of integral abutments to vary up to 450 mm in height due to superelevation (300 mm for skews less than 80^o), sloping the bottom of the pile cap such that the ends are equal is recommended to simplify reinforcement details. DM-4 Ap.G.1.4.1

Left end pile cap height, d_{pc1}	4476.75	mm	14.69 ft
Pile cap height at the crown of the roadway, or at the bridge midwidth for a superelevated roadway, $d_{pc,cl}$	4391.787	mm	14.41 ft
Right end pile cap height, d_{pc2}	4306.824	mm	14.13 ft

Difference between the height of the cap at the ends, $|d_{pc1} - d_{pc2}|$ = | 4477 - 4307 | =

169.926 mm 0.56 ft

The previous three values are used to calculate an average pile cap height and assume a constantly sloping top of cap with a crown at the center, as illustrated in the figure below. Only the minimum value is used to design the pile cap, the average value is used for selfweight calculations. Note that if the cap does not have either a constant cross-slope or crown at the midwidth, the average pile cap height will not be precisely correct. If a more exact selfweight is required, the maximum height at midwidth can be adjusted until the desired average pile cap height is attained.

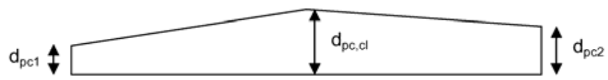

Average pile cap height
(4476.75+4306.824)/4 + 4391.787/2 = 4391.787 mm 14.41 ft
The end diaphragm height is equal to the deck and haunch thickness + girder depth + bearing pad depth.
End diaphragm height 262.89 + 1600.2 + 20 = 1883.09 mm 6.18 ft
The total average abutment height is equal to the end diaphragm height plus the average pile cap height.
Total average abutment height 1883 + 4392 = 6274.877 mm 20.59 ft

WINGWALLS

Attached wingwalls up to 2400 mm long (measured from the back face of the abutment) may be rectangular, extending the full depth of the abutment. Attached wingwalls over 2400 mm up to 4560 mm must be tapered. Wingwalls longer than 4560 mm will be detached. The standard location of the joint for a detached wingwall is 900 mm from the back face of the abutment, as shown in the figure below. The detached portion of the wingwall is to be designed independently. A 300 mm chamfer is provided in the interior corner of the wingwall/abutment connection (see figure). DM-4 Ap.G.1.4.4

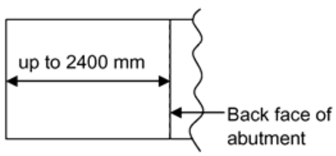

Rectangular wingwall

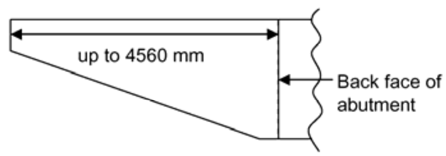

Tapered wingwall

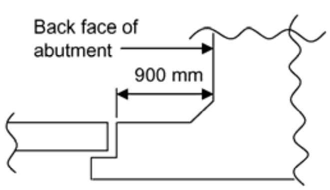

Detached wingwall

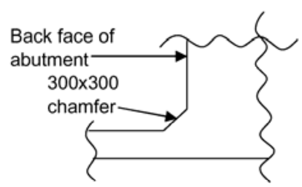

Abutment/wingwall corner chamfer

Type of wingwall (R - Rectangular, T - Tapered, D - Detached) D
Wingwall length (including 300mm chamfer) 900 mm 3.0 ft

The wingwall dimensions are required for dead load calculations.
The average wingwall height at the abutment back face is conservatively assumed to be equal to the average height of the abutment.
Wingwall height at back face of abutment 6274.877 mm 20.59 ft
The height at the end is assumed to be either equal to the height at the abutment for rectangular (R) or detached (D) wingwalls, or 600 mm for tapered (T) wingwalls DM-4 Ap.G.1.4.4
Wingwall height at end 6274.877 mm 20.59 ft
The attached wingwall thickness is assumed to be the same width as the typical concrete parapet. An effective average thickness is assumed for the abutment extension for detached wingwalls. To obtain the effective width, the 250x300 mm overlap section (see BD-667M Standard Drawing) is smeared over the length of the stub.
Wingwall width 440+350+[(250)(300)/900] = 873 mm 2.87 ft

Title: Bridge 203 - 52.43 m 3-Span Concrete Prestressed I-girder
90° skew, 3.594 m girder spacing
By: KP
Date: 3/10/2006
Checked:
Date:

LOAD DATA

LRFD design philosophy employs the equation $\Sigma\eta_i\gamma_i Q_i \leq \varphi R_n = R_r$. In this equation, γ_i is a load factor, Q_i is a load effect, φ is a resistance factor, R_n is a nominal resistance, and R_r is a factored resistance. This leaves the η_i (eta) factor, which is a load modifier used to account for ductility, redundancy, and operational importance. $\eta_{i,max}$ is used when maximizing loads. $\eta_{i,min}$ is used when minimizing loads. Penndot currently limits η_i to values greater than or equal to 1.00 and less than or equal to 1.16. A1.3.2.1 D1.3.2

η_i factor — 1.00

$\eta_{i,max} = \eta_i \geq 1.00$	1.00	D1.3.2
$\eta_{i,min} = 1/\eta_i \leq 1.00$	1.00	A1.3.2.1

The unfactored girder design loads are available from the superstructure design performed using PennDOT's prestressed concrete girder design program. Both the interior and exterior noncomposite girder design dead loads are required input, although if only the controlling value is known, it can be conservatively used for both. The remaining composite dead loads should be the same whether they come from an interior or exterior girder design. The maximum and minimum unfactored live loads, with impact and shear distribution factors included, are also required input. The shear distribution factor is required as well, so that it can be divided out of the given loads to get the reaction per traffic lane. These values are available directly from the PennDOT beam design programs. Either the exterior or interior girder design can be used for the live load values, as long as all the values (reactions and distribution factors) come from the same girder design. Additional loads are calculated later. DM-4 Ap.G.1.2.7

Dead Loads - Unfactored:

Non-composite DC1 loads - include girder, deck, haunch, interior diaphragms		
Interior girder, DC1	202.6 kN	45.55 k
Exterior girder, DC1	182.6 kN	41.05 k
Composite DC2 loads - include parapets,		
Interior girder, DC2	5.0 kN	1.12 k
Exterior girder, DC2	5 kN	1.12 k
Composite DW loads - include future wearing surface,		
Interior girder, DW	5.8 kN	1.30 k
Exterior girder, DW	5.8 kN	1.30 k

Live load shear distribution factor — 1.069

Live Loads - Unfactored from girder design program (distribution factor included):

PHL-93	max	424.5 kN	95.4 k
	min	-148.8 kN	-33.5 k
P-82	max	556.7 kN	125.2 k
	min	-252.0 kN	-56.7 k

Live Loads - Unfactored - distribution factor removed - reaction due to live load on one traffic lane:

PHL-93	max	(424.5)/(1.069) =	397.1 kN	89.3 k
	min	(-148.8)/(1.069) =	-139.2 kN	-31.3 k
P-82	max	(556.7)/(1.069) =	520.8 kN	117.1 k
	min	(-252)/(1.069) =	-235.7 kN	-53.0 k

The total pedestrian load reaction at the abutment is calculated assuming the approach slab and the first span are simply supported. The first span portion is calculated here, the approach slab portion is added in with the approach slab loads. The pedestrian load per unit area is as specified in the AASHTO LRFD Bridge specification, and the total width of sidewalk input earlier is used. This reaction is then distributed equally to all girders and piles. DM-4 Ap.G.1.2.7.2 A3.6.1.6 D3.6.1.6

Pedestrian	max	(0.0036)(0)(10820)/2000 =			
			0.0 kN	0.0 k	A3.6.1.6
	min		0.0 kN	0.0 k	

Choose the load factors to be used for the DW loads. For new construction or analysis of existing construction, where no future wearing surface is present, the DW load factors are taken as 1.50 max and 0.00 min. For bridges where a future wearing surface is present, the DW load factors are taken as 1.50 max and 0.65 min. Typically, the future wearing surface will not be currently present - N.

Future wearing surface currently present (Y or N)? N

DW load factors Maximum = 1.50 Minimum = 0.00

Title: Bridge 203 - 52.43 m 3-Span Concrete Prestressed I-girder
90° skew, 3.594 m girder spacing

By: KP
Checked:
Date: 3/10/2006
Date:

The extreme girder reactions, interior or exterior, are (conservatively) required for the design of the abutment pile cap. The total reaction with all lanes loaded, or the average pile reaction, is required for the pile design, which also requires both interior and exterior girder reactions. Note: The η_i factor is included here.

Factored Dead + Live reaction for interior girder:

Strength I	max	1.00[1.25(202.6+5) + 1.50(5.8) + 1.75(397.10)(3)/4] =	789.4 kN	177.5 k
	min	1.00[0.90(202.6+5) + 0.00(5.8)] + 1.00[1.75(-139.20)(3)/4] =	4.1 kN	0.9 k
Strength IP	max	1.00[1.25(202.6+5) + 1.50(5.8) + 1.75(0)/4 + 1.35(397.10)(3)/4] =	670.3 kN	150.7 k
	min	1.00[0.90(202.6+5) + 0.00(5.8) + 1.75(0.00)/4] + 1.00[1.35(-139.20)(3)/4] =	45.9 kN	10.3 k
Strength II	max	1.00[1.25(202.6+5) + 1.50(5.8) + 1.35[520.77+397.10(3-1)]/4] =	712.0 kN	160.1 k
	min	1.00[0.90(202.6+5) + 0.00(5.8)] + 1.35[(1.00)(-235.73)+(1.00)(-139.20)(3-1)]/4 =	13.3 kN	3.0 k
Strength III	max	1.00[1.25(202.6+5) + 1.50(5.8)] =	268.2 kN	60.3 k
	min	1.00[0.90(202.6+5) + 0.00(5.8)] =	186.8 kN	42.0 k
Strength V	max	1.00[1.25(202.6+5) + 1.50(5.8) + 1.35(397.10)(3)/4] =	670.3 kN	150.7 k
	min	1.00[0.90(202.6+5) + 0.00(5.8)] + 1.00[1.35(-139.20)(3)/4] =	45.9 kN	10.3 k

Factored Dead + Live reaction for exterior girder:

Strength I	max	1.00[1.25(182.6+5) + 1.50(5.8) + 1.75(397.10)(3)/4] =	764.4 kN	171.8 k
	min	1.00[0.90(182.6+5) + 0.00(5.8)] + 1.00[1.75(-139.20)(3)/4] =	-13.9 kN	-3.1 k
Strength IP	max	1.00[1.25(182.6+5) + 1.50(5.8) + 1.75(0)/4 + 1.35(397.10)(3)/4] =	645.3 kN	145.1 k
	min	1.00[0.90(182.6+5) + 0.00(5.8) + 1.75(0.00)/4] + 1.00[1.35(-139.20)(3)/4] =	27.9 kN	6.3 k
Strength II	max	1.00[1.25(182.6+5) + 1.50(5.8) + 1.35[520.77+397.10(3-1)]/4] =	687.0 kN	154.4 k
	min	1.00[0.90(182.6+5) +0.00(5.8)] + 1.35[(1.00)(-235.73)+(1.00)(-139.20)(3-1)]/4 =	-4.7 kN	-1.1 k
Strength III	max	1.00[1.25(182.6+5) + 1.50(5.8)] =	243.2 kN	54.7 k
	min	1.00[0.90(182.6+5) + 0.00(5.8)] =	168.8 kN	38.0 k
Strength V	max	1.00[1.25(182.6+5) + 1.50(5.8) + 1.35(397.10)(3)/4] =	645.3 kN	145.1 k
	min	1.00[0.90(182.6+5) + 0.00(5.8)] + 1.00[1.35(-139.20)(3)/4] =	27.9 kN	6.3 k

When designing integral abutments, only the girder rotations that are transferred to the piles are needed. Most dead load rotations occur prior to pouring the end diaphragm, and therefore will not be transferred to the piles. The exception to this is any composite dead loads such as future wearing surface or parapets. The extreme live load and composite dead load girder rotations are conservatively used as the design rotations for the piles. The unfactored live load and composite dead load rotations are available from the girder design.

Unfactored Live Load rotations per girder (including distribution factor):

PHL-93	max	0.018 degrees	0.0003	radians
	min	-0.017 degrees	-0.0003	radians
P-82	max	0.024 degrees	0.0004	radians
	min	-0.029 degrees	-0.0005	radians

Title: Bridge 203 - 52.43 m 3-Span Concrete Prestressed I-girder
90° skew, 3.594 m girder spacing
By: KP Date: 3/10/2006
Checked: Date:

The rotations above are the single girder unfactored rotations. To get the average girder rotations required for the design of integral abutments, the maximum number of traffic lanes on the bridge are loaded and the loads are assumed equally distributed to all girders. To accomplish this using the above results from the girder design program, the distribution factor is divided out to get the rotation of the full traffic lane applied to one girder. Then, the result is multiplied by the number of lanes and divided by the number of girders in the bridge.

Average Live Load rotations per girder:

PHL-93	max	(0.0003/1.069)(3/4) =		
		0.013 degrees	0.0002 radians	
	min	(-0.0003/1.069)(3/4) =		
		-0.012 degrees	-0.0002 radians	
P-82	max	(0.0004/1.069)(3/4) =		
		0.017 degrees	0.0003 radians	
	min	(-0.0005/1.069)(3/4) =		
		-0.020 degrees	-0.0004 radians	

The total rotation of any composite dead load rotations (unfactored), e.g. future wearing surface and parapets, can be input here. This value will be factored using the maximum DW load factor, 1.50.

0.000 degrees 0.0000 radians

Maximum factored rotations are calculated here. The DM-4 allows the P-82 permit load to be placed in only one lane, with PHL-93 load in the remaining lanes. If the P-82 rotation controls the girder design the abutment design rotations are adjusted accordingly to account for P-82 on one lane and PHL-93 on all other lanes. The maximum load factor is used for both the maximum (positive) and minimum (negative) values.

Average factored live load + future dead load rotations (including eta factor):

	Controlling load			
max	PHL-93 all lanes	(1.00)[(1.75)(0.0002) + (1.50)(0.0000)] =		
		0.022 degrees	0.0004 radians	
min	PHL-93 all lanes	(1.00)[(1.75)(-0.0002) + (1.50)(0.0000)] =		
		-0.021 degrees	-0.0004 radians	

Additional Loads

Additional loads due to wind and centrifugal force are calculated here. The approach slab dead and live loads, and wingwall and abutment dead loads are calculated in the next section.

Wind Loads — DM-4 Ap.G.1.2.7.3
The appropriate wind pressure on the structure is input here. — A3.8
Wind on structure pressure = 0.0024 MPa 0.000348 ksi — A3.8.1.2

The wind forces on the abutment are calculated assuming only the bridge span adjacent to the abutment contributes to the load, and that the span is simply supported laterally (half of the wind force on the end span is resisted by the abutment).
lateral force = (0.0024)(10820.4)(3006.09)/2000 = 39.03 kN 8.77 k

Uplift pressure is defined as a constant 0.00096 MPa. The force from this pressure is assumed to act as a line load at a distance of 1/4 of the out-to-out width of the bridge from the edge of the bridge. — A3.8.2
Uplift force (acts @ 1/4 point) pressure = 0.00096 MPa 0.000139 ksi
uplift = (-0.00096)(10820.4)(13072)/2000 = -67.89 kN -15.26 k
moment about the longitudinal axis of the bridge = -(-67.89)(13072)/4000 =
221.88 kN-m 163.65 k-ft

Wind on live load is taken as 1.46 kN/m acting at 1800 mm above the deck — A3.8.1.3
Wind on live load distributed force = 1.46 kN/m 0.10 k/ft
lateral force = (1.46)(10820.4)/2000 = 7.90 kN 1.78 k

Centrifugal force — DM-4 Ap.G.1.2.3
Integral abutments are permitted for curved bridges as long as the girders are straight and parallel within each span, and approval is obtained from the Chief Bridge Engineer. Despite the limited curvature this allows, centrifugal forces can be generated. The centrifugal force and any other lateral forces other than wind forces contributing to overturning moments can be input here. This force will be assumed to act perpendicular to the longitudinal axis of the bridge at a distance 1800 mm above the roadway surface. — A3.6.3
Centrifugal force 0 kN 0.00 k

Girder and Pile Reactions

Girder and pile reactions are calculated assuming overturning moments are resisted by vertical forces only.
Girder reactions due to wind and centrifugal forces:
The top of deck to the top of the pile cap is equal to the end diaphragm height.

Top of deck to the top of the pile cap =	1883.09 mm	6.18 ft

The moment due to the wind on the superstructure is equal to the wind force times half the depth of the structure plus the bearing pad depth.

Wind on structure

moment = (39.03)[(3006.09/2)+20]/1000 =	59.45 kN-m	43.85 k-ft

The moment of the wind on the live load is equal to the force times the moment arm which is equal to the distance from the top of the pile cap to the top of the deck plus 1800 mm.

Wind on live load

moment = (7.90)(1883.09+1800)/1000 =	29.09 kN-m	21.46 k-ft

The moment of the centrifugal force is equal to the centrifugal force times the moment arm which is also equal to the distance from the top of the pile cap to the top of the deck plus 1800 mm.

Centrifugal

moment = (0.00)(1883+1800)/1000 =	0.00 kN-m	0.00 k-ft

The unfactored extreme reactions per girder for wind loads are calculated assuming the vertical wind forces are distributed equally to all girders, and the moments are resisted by vertical reactions of the girders (see figure below - note that five I-girders are used for illustrative purposes only - actual number of girders used in calculations). Forces due to the moments are calculated assuming the superstructure acts as a rigid member transversely, and the vertical force is proportional to the distance from the center of gravity of the girder group. The force at any girder is equal to the moment times the distance from the midwidth of the bridge divided by the second moment of inertia. The extreme overturning reactions are therefore at the exterior girders.

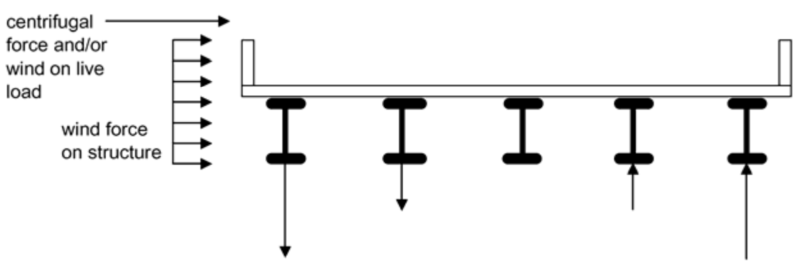

Extreme girder reactions due to wind on the structure

WS	max	(59.45)(1000)(4-1)(3594.1)/(2*64587774.05) =		
			4.96 kN/girder	1.12 k/girder
	min	-(59.45)(1000)(4-1)(3594.1)/(2*64587774.05) =		
			-4.96 kN/girder	-1.12 k/girder

Extreme forces due to uplift

Uplift	max	-67.89/4 + (221.88)(1000)(4-1)(3594.1)/(2*64587774.05) =		
			1.55 kN/girder	0.35 k/girder
	min	-67.89/4 - (221.88)(1000)(4-1)(3594.1)/(2*64587774.05) =		
			-35.49 kN/girder	-7.98 k/girder

Extreme forces due to wind on live load

WL	max	(29.09)(1000)(4-1)(3594.1)/(2*64587774.05) =		
			2.43 kN/girder	0.55 k/girder
	min	-(29.09)(1000)(4-1)(3594.1)/(2*64587774.05) =		
			-2.43 kN/girder	-0.55 k/girder

Extreme forces due to centrifugal forces

CE	max	(0.00)(1000)(4-1)(3594.1)/(2*64587774.05) =		
			0.00 kN/girder	0.00 k/girder
	min	-(0.00)(1000)(4-1)(3594.1)/(2*64587774.05) =		
			0.00 kN/girder	0.00 k/girder

Choose a trial pile section at this point. The pile dimensions are needed for the pile location check. The pile

moment of inertia is used to calculate the thermally induced forces in the piles. The pile properties are also required to run the COM624P computer program. Two types of piles are permitted for integral abutments, steel H-piles or concrete filled pipe piles.

Type of piles H - HP shape, P - pipe H

For H-piles, the yield stress of the steel and the metric designation of the pile is required input. A list of available H-pile sections is provided. The user may then input the additional section properties manually, or press the button to the right, and the properties will be automatically retrieved.

Import Pile Properties

Pile Properties					HP Shapes
Pile designation	HP310x110		(HP12x74)		HP360x174
Yield stress of pile steel, F_y	345	MPa	50	ksi	HP360x152
Pile section depth, d	308	mm	12.1	in	HP360x132
Flange width, bf	310	mm	12.2	in	HP360x108
Flange thickness, tf	15.50	mm	0.610	in	HP310x125
Pile Area, Ap	14100	mm^2	21.9	in^2	HP310x110
Moment of inertia, $I_{y\text{-}y}$	77.1E+6	mm^4	185	in^4	HP310x94
Elastic section modulus, $S_{y\text{-}y}$	49.7E+4	mm^3	30.3	in^3	HP310x79
Radius of gyration, $r_{y\text{-}y}$	73.9	mm	2.91	in	HP250x85
Plastic section modulus, $Z_{y\text{-}y}$	76.3E+4	mm^3	46.6	in^3	HP250x62
					HP200x54

PILE DATA

Choose a pile layout. If a geotechnical report is available with a calculated pile capacity, a preliminary number of piles can be found by dividing the total factored dead + live girder reactions by the given pile capacity and rounding up to the next highest integer. If no pile load capacity is available, use an estimate of the load capacity based on the soil conditions. The maximum pile spacing is 3000 mm. The minimum pile spacing is the larger of 900 mm, or 2.5 times the diameter of round piles, or 2 times the diagonal dimension of H-piles (The 2x criteria only controls for HP360 piles). Note that the approximate range of allowed pile spacing calculated below assumes 900 mm is the minimum pile spacing, and may suggest a range which is not permitted based on pile dimensions. The pile location check made below should flag any erroneous spacings attempted, however.

DM-4 Ap.G.1.4.2
D10.7.1.5

Maximum total factored dead + live girder reactions
(764.39)(2) + (789.39)(2) = 3107.58 kN 698.61 k
Number of piles 8
Approximate range of allowed pile spacing for 8 piles is about 1760 to 1830 mm
Chosen pile spacing along abutment 1676.4 mm 5.50 ft
Total pile length, L_{tot} = 12192 mm 40.00 ft

The minimum and maximum edge distance for the end piles is intended to keep the piles close to the end of the integral abutment in order to provide support for the attached wingwalls, without getting too close to the end of the abutment.

Minimum edge distance to centerline of piles	450	mm	17.72	in	D10.7.1.5
Maximum edge distance to centerline of piles	750	mm	29.53	in	DM-4 Ap.G.1.4.2.1

Pile location check ***Error - edge distance of piles is greater than the 750 mm allowable***
Pile spacing normal to the longitudinal axis of span
1676.4sin(90) = 1676 mm 5.50 ft

The moment of inertia of the pile group is calculated similarly to the girders above and is used to determine the axial forces in the piles due to overturning moments.
Moment of inertia of pile group about the longitudinal axis of the bridge
8(8^2 - 1)(1676^2)/12 = 118033312 mm^2 182952 in^2

Title: Bridge 203 - 52.43 m 3-Span Concrete Prestressed I-girder
90° skew, 3.594 m girder spacing

By: KP
Date: 3/10/2006
Checked:
Date:

Pile loads due to wind and centrifugal forces

At this point, an iterative procedure is initiated to determine the loads on the piles. Initially, a depth to fixity of the piles is assumed. Later, the actual depth to fixity is calculated using the computer program COM624P, and this value is adjusted as necessary. The procedure is repeated until the estimated value is within 10% of the value obtained from the COM624P computer program. An initial choice of 5000-6000 mm to the point of fixity is reasonable.

Assume depth to pile fixity of 3657.6 mm 12.00 ft

The overturning moment resisted by the piles is calculated similarly to the overturning moments resisted by the girders, except the moment arm extends to the point of assumed pile fixity (see figure below - note that five I-girders and six H-piles are used for illustration purposes only). Wind uplift forces result in the same overturning moments on the piles as calculated earlier for the girders.

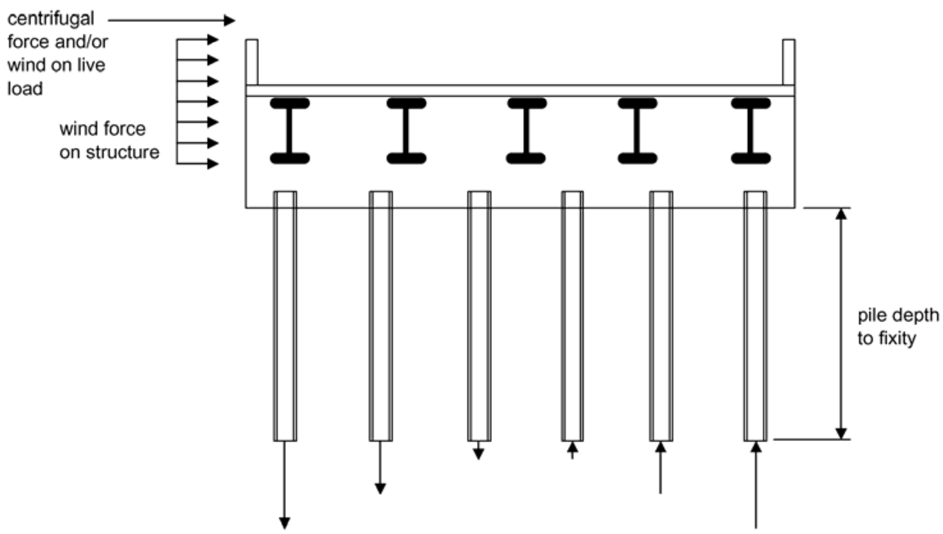

Wind on structure	moment = (39.03)(3658+4391.787+20+3006.09/2)/1000 =		
		373.64 kN-m	275.58 k-ft
Wind on live load	moment = (7.90)(1800+3658+4391.787+1883.09)/1000 =		
		92.67 kN-m	68.35 k-ft
Centrifugal forces	moment = (0.00)(1800+3658+4391.787+1883.09)/1000 =		
		0.00 kN-m	0.00 k-ft

The unfactored extreme loads per pile for wind cases are calculated similar to the girder reactions

Extreme forces due to wind on the structure

WS	max	(373.64)(1000)(8-1)(1676)/(2*118033312) =		
			18.57 kN/pile	4.18 k/pile
	min	-(373.64)(1000)(8-1)(1676)/(2*118033312) =		
			-18.57 kN/pile	-4.18 k/pile

Extreme forces due to uplift

Uplift	max	-67.89/8 + (221.88)(1000)(8-1)(1676)/(2*118033312) =		
			2.54 kN/pile	0.57 k/pile
	min	-67.89/8 - (221.88)(1000)(8-1)(1676)/(2*118033312) =		
			-19.52 kN/pile	-4.39 k/pile

Extreme forces due to wind on live load

WL	max	(92.67)(1000)(8-1)(1676)/(2*118033312) =		
		4.61 kN/pile	1.04 k/pile	
	min	-(92.67)(1000)(8-1)(1676)/(2*118033312) =		
		-4.61 kN/pile	-1.04 k/pile	

Extreme forces due to centrifugal force

CE	max	(0.00)(1000)(8-1)(1676)/(2*118033312) =		
		0.00 kN/pile	0.00 k/pile	
	min	-(0.00)(1000)(8-1)(1676)/(2*118033312) =		
		0.00 kN/pile	0.00 k/pile	

Additional Dead + Live Loads (Approach Slab, Wingwalls, and Abutment)

The approach slab live load is calculated assuming the slab is simply supported at the ends, the lane load only is present in all lanes, and the total reaction is distributed equally to all piles. The truck load is not included here because it was already included in the bridge loads. As previously, the multiple presence factor is not used. Dead loads from the approach slab are also distributed equally to all piles.

Approach slab dimensions

Approach slab thickness =	450 mm	18 in	DM-4 App. G 1.5
Approach slab length =	7500 mm	25 ft	

Approach slab loads

Approach Slab Load = (2.4)(9.81)(12192)(7500)(0.45)/2000000 =			
	484.39 kN	108.90 k	
Approach Slab Future Wearing Surface = (0.15)(9.81)(12192)(7500)/2000000 =			D3.5.1
	67.28 kN	15.12 k	
Approach Slab Lane Load (1 lane) = (9.3)(7500)/2000 =			A3.6.1.2.4
	34.88 kN	7.84 k	
Approach Slab Pedestrian Live Load (total reaction) = (0.0036)(0)(7500)/2000 =			
	0.00 kN	0.00 k	
Abutment self-weight Dead Load = (2.4)(9.81)(13772)(1200)(6275)/1000000000 =			
	2441.54 kN	548.88 k	

Wingwalls and parapet load

The parapet weight/length can be input for wingwall dead load calculations. A typical 440 mm wide concrete parapet weighs about 7.60 N/mm. Any other miscellaneous loads can also be included in this number, but note that the value will be multiplied by the length of the wingwall plus abutment (900 + 1200/SIN(90) = 2100 mm) times two since parapets are assumed to be on both sides of the bridge.

Parapet weight/length $\boxed{7.60}$ N/mm 0.521 k/ft

Weight of two wingwalls = (2)(2.4)(9.81){(6274.877)(300)(873+300sin(90)/2)+[(900-300)(873)(6274.877+6274.877)/2)]/100000000

Weight of two parapets = (2)(7.60)(900+1200/sin(90))/1000

Total weight of wingwalls and parapets = 277.46 kN 62.37 k

Thermal Expansion

The thermal expansion of the bridge is calculated assuming the entire superstructure length, L, is unrestrained, and undergoes a uniform thermal expansion. This ignores the pier stiffnesses (if any) and passive soil pressure against the backwalls. For design purposes, a percentage of this thermal expansion can be assigned to take place at the abutment under consideration. It is the responsibility of the designer to determine the percentage of expansion. In some cases, such as single spans with identical abutments, simply assigning 50% of the movement to each end may be appropriate. In other cases, such as for continuous structures with unsymmetrical piers, a more in-depth thermal analysis taking pier and abutment stiffnesses into account is required. See DM-4 Ap.G.1.2.7.4 for thermal movement requirements.

The coefficient of thermal expansion and temperature range are assigned based on the girder material, concrete or steel.

Coefficient of thermal expansion, α	10.8E-6 /°C	(concrete girders)	D5.4.2.2
Temperature range, Δ_T ($\pm$)	44 °C		DM-4 Ap.G.1.2.7.4
Load factor, ϕ_T	1.0		DM-4 Ap.G.1.2.7.6

Total $\pm$change in length of the bridge, $\phi_T\alpha\Delta_T L$ = (1.0)(0.0000108)(44)(52425.6) =

24.9 mm 0.98 in

Title: Bridge 203 - 52.43 m 3-Span Concrete Prestressed I-girder
90^{o} skew, 3.594 m girder spacing

By: KP
Checked:
Date: 3/10/2006
Date:

The percentage of thermal expansion that occurs at the abutment being designed is input here. The value should be between 0 and 100%. For symmetrical structures, 50% of the expansion occurs at each abutment. For unsymmetrical structures, use the procedure described in DM-4 Ap.G1.2.7.4 to determine the percentage of movement at each end.

Percentage of expansion at abutment being designed $\boxed{100}$ %

Maximum movement (expansion or contraction) at abutment ($\pm$), Δ

(1.00)(24.9) = 24.9 mm 0.98 in

The thermal expansion of continuous bridges induces an axial force in the piles, P_T, which is estimated using the simplified elastic procedure illustrated below (see figure on following page). This procedure assumes that the full passive pressure of the soil is acting on the abutment. Note that the additional pile axial force is zero in a simple span with passive pressure acting at the same height on both abutments.

The coefficient of passive earth pressure has been found to vary from about 3.0 for loose sand to about 6 for dense sand. PennDOT requires that the region immediately adjacent to the abutment be only nominally compacted, so 3.0 is an acceptable value. DM-4 Ap.G.1.2.7.4

Coefficient of passive earth pressure, k_p = 3.0

The density of loose sand given in the AASHTO-LRFD Bridge Design Specification is 1600 kg/m^3. Multiplying by 9.81 m/s^2 converts this value to weight. A3.5.1

Soil unit weight, γ = (1600)(9.81) = 15.70 kN/m^3 100 lb/ft^3

Using the coefficient of passive earth pressure, the soil density, and the depth of the abutment, the force per unit length on the abutment can be calculated.

Force from soil on abutment, $F=1/2\ k_p\gamma H^2$ = (1/2)(3.0)(15.70)(6274.877/1000)^2 =
927.0 kN/m 63.5 k/ft

The total longitudinal force on the abutment can be found by multiplying by the projected length of the abutment on a line perpendicular to the longitudinal axis of the bridge, which is equal to the out-to-out width of the bridge.

Total passive earth pressure force on abutment, F = (927.0)(13072)/1000 =
12118.0 kN 2724.2 k

The previously assumed depth to pile fixity, L_p = 3657.6 mm 12.00 ft

Using simple equilibrium by taking the moment about point A, the axial reaction per pile due to the force, F, and the displacement, Δ, can be calculated as:

F_p = 2FH / 3L / number of piles = (2)(12118.0)(6274.877)/[(3)(10820.4)]/8 =
585.6 kN/pile 131.7 k/pile

The moment induced in the piles by the thermal movement can be determined using the following equation. The top of the pile is assumed to be fixed.

The moment, $M_T = 6E_pI_p\Delta/L_p^2$ = (6)(200)(77100000)(24.9)/(3657.6^2)/1000 =
172.3 kN-m/pile 127.08 k-ft/pile

Check to make sure the moment, M_T, does not exceed the plastic moment, M_p. Even though the maximum flexural resistance of the pile may be lower, the plastic moment is conservatively used here as an upper bound.

Plastic moment, $M_p = F_yZ_{y\text{-}y}$ = (345)(763000)/1000000 = 263.2 kN-m 194.15 k-ft

since 172.3 < 263.2 - use M_T = 172.3 kN-m 127.08 k-ft

The horizontal force induced in the pile by the thermal deformation can be determined using the following equation. The top of the pile is assumed to be fixed.

The horizontal force, $H_T = 2M_T/L_p$ = (2)(172.3)(1000)/3657.6 =
94.2 kN/pile 21.2 k/pile

The total axial force induced in the pile due to these three components is equal to:

$2FH/3L+H_TH/L+M_T/L$ = 585.6 + (94.2)(6274.877)/10820.4 + 172.3/(10820.4/1000) = 656.2 kN (147.5 k) /pile

Axial force induced in piles, P_T = 656.2 kN/pile 147.5 k/pile

L

Title: Bridge 203 - 52.43 m 3-Span Concrete Prestressed I-girder
90° skew, 3.594 m girder spacing

By: KP
Checked:
Date: 3/10/2006
Date:

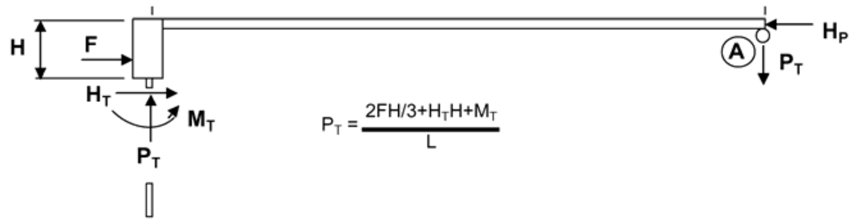

Calculate the maximum factored load on the most heavily loaded pile (see Load Factors tab for load factors for each load combination). Since the factored dead and live loads from the interior and exterior girders have already been calculated, the sum of the girder loads is calculated assuming two exterior girders and the remaining ones interior. These loads, as well as any additional vertical loads, are distributed equally to all piles. The factored extreme overturning loads, which occur on the exterior piles are added. The η_i modifier is also included.

Extreme Factored Dead + Live Loads per pile

Strength I	max	[(789.4)(2)+(764.4)(2)]/8 + 1.00{[1.25(484.4+2441.5+277.5)+1.50(67.3)+1.75(3)(34.9)]/8 + 1.75(0.0) + 1.00(656.2)} =	1580.65 kN/pile	355.34 k/pile
	min	[(4.1)(2)+(-13.9)(2)]/8 + 1.00{[0.90(484.4+2441.5+277.5)+0.00(67.3)+1.75(3)(0.0)]/8} + 1.00[1.75(0.0) + 1.00(0.0)] =	357.95 kN/pile	80.47 k/pile
Strength IP	max	[(670.3)(2)+(645.3)(2)]/8 + 1.00{[1.25(484.4+2441.5+277.5)+1.50(67.3)+1.35(3)(34.9)+1.75(0.0)]/8 + 1.35(0.0) + 1.00(656.2)} =	1515.85 kN/pile	340.78 k/pile
	min	[(45.9)(2)+(27.9)(2)]/8 + 1.00{[0.90(484.4+2441.5+277.5)+0.00(67.3)+1.35(3)(0.0)+1.75(0.0)]/8} + 1.00[1.35(0.0) + 1.00(0.0)] =	378.83 kN/pile	85.17 k/pile
Strength II	max	[(712.0)(2)+(687.0)(2)]/8 + 1.00{[1.25(484.4+2441.5+277.5)+1.5(67.3)+1.35(3-1)(34.9)]/8 + 1.35(0.0) + 1.0(656.2)} =	1530.84 kN/pile	344.15 k/pile
	min	[(13.3)(2)+(-4.7)(2)]/8 + 1.00{[0.9(484.4+2441.5+277.5)+0(67.3)+1.35(2)(0.0)]/8} + 1.00[1.35(0.0) + 1.0(0.0)] =	362.54 kN/pile	81.50 k/pile
Strength III	max	[(268.2)(2)+(243.2)(2)]/8 + 1.00{[1.25(484.4+2441.5+277.5)+1.50(67.3)]/8 + 1.40(18.6) + + 1.00(656.2)} + 1.00(1.40)(2.5) =	1326.73 kN/pile	298.26 k/pile
	min	[(186.8)(2)+(168.8)(2)]/8 + 1.00{[0.90(484.4+2441.5+277.5)+0.00(67.3)]/8} + 1.00[1.40(-18.6) + 1.00(0.0) + 1.40(-19.5)] =	395.98 kN/pile	89.02 k/pile
Strength V	max	[(670.3)(2)+(645.3)(2)]/8 + 1.00{[1.25(484.4+2441.5+277.5)+1.50(67.3)+1.35(3)(34.9)]/8 + 0.40(18.6) + 1.00(4.6) + 1.35(0.0) + 1.00(656.2)} =	1527.89 kN/pile	343.48 k/pile
	min	[(45.9)(2)+(27.9)(2)]/8 + 1.00{[0.90(484.4+2441.5+277.5)+0.00(67.3)+1.35(3)(0.0)]/8} + 1.00{0.40(-18.6) + 1.00(-4.6) + 1.35(0.0) + 1.00(0.0)} =	366.80 kN/pile	82.46 k/pile

Controlling Loads	max STR I	1580.65 kN/pile	355.34 k/pile
	min STR I	357.95 kN/pile	80.47 k/pile

Lateral Pile Analysis

Knowing the soil properties at the abutment (taken from the geotechnical report), and the properties of the piles, and using the calculated design values for maximum factored axial load, live load rotation, and thermal expansion, the computer program COM624P can be used to determine the depth to pile fixity, the depth to the first inflection point of the pile, the unbraced length of the pile, the depth at which the lateral pile deflection is equal to 2% of the pile diameter (needed for friction piles only), and the maximum moment in the pile below the first point of inflection. Since a pre-augered hole, 3000 mm minimum depth, filled with loose sand, is present at the top of the piles, the COM624P analysis should use the properties of the weaker of either the loose sand or the actual soil for the depth of the pre-augered hole. The procedure for running COM624P is as follows:

Run COM624P using the top of pile boundary condition which permits a specified lateral deflection along with an applied moment. Apply the maximum pile vertical axial load to the pile simultaneously with the abutment maximum thermal movement. The axial load and deflection should be input as positive values. Apply the negative plastic moment at the head of the pile and run the analysis.
1 - If the calculated pile head rotation (positive value) is less than the end rotation of the pile due to live loads and composite dead loads, the analysis is complete.
2 - If the calculated pile head rotation is greater than the end rotation of the pile due to live loads and composite dead loads, iteratively reduce the moment at the head of the pile until the rotations are equal (within tolerance).

Title: Bridge 203 - 52.43 m 3-Span Concrete Prestressed I-girder
90° skew, 3.594 m girder spacing

By: KP
Checked:

Date: 3/10/2006
Date:

Design values for COM624P:

Pile Section	HP310x110	HP12x74
Pile width or diameter	0.308 m	12.1 in
Pile moment of inertia	0.0000771 m^4	185 in^4
Pile area	0.0141 m^2	21.9 in^2
Vertical axial load	1580.7 kN	355.3 k
Design rotation	0.0004 radians	0.022 degrees
Design thermal movement	0.0249 m	0.98 in
Plastic moment (if required)	-263.2 kN-m	-194.2 k-ft

At this point COM624P should be run. COM624P is run using a text file as input. There are two ways to develop this text input file. The first is to use the input file editor program supplied with COM624P. The second method is to use any text editor to develop the input file using the COM624P users manual as a guide. If this second method is chosen, a template file for COM624P can be created from the COM624P Input tab. Once the template is created, it can be edited using any text editor.

Results from COM624P (See figures below for illustrations of the data required from the program).

The depth to fixity is defined as the shallowest depth at which the pile deflection is equal to zero.

Depth to fixity, L_p = 3655.1 mm 143.90 in

The depth to the uppermost point of inflection is the depth measured from the bottom of the abutment to the first point of zero moment on the pile moment diagram.

Depth to first point of inflection, L_{i1} = 1358.9 mm 53.50 in

The depth to the second point of inflection is the depth measured from the bottom of the abutment to the second point of zero moment on the pile moment diagram. For a short pile with only one point of inflection, input the total pile length

Depth to second point of inflection, L_{i2} = 4541.5 mm 178.80 in

The depth above which friction is ineffective is input here. For a laterally deflected pile, this depth is defined as the point where the deflection is 2% of the pile diameter. For the present pile (see section properties above), this deflection value is (0.02)(308) = 6.16 mm (0.24 in). The length of pile above this point is considered ineffective in the design of friction piles. If the pile is driven through an embankment fill which is to be neglected in calculating pile friction resistance, input the depth of fill. This value is not required for end bearing piles.

DM-4 Ap.G.1.4.2.2

Depth to 2% deflection, L_n = 3317.2 mm 130.60 in

The maximum bending moment in the pile is the maximum moment below the uppermost point of inflection and neglects the moment at the pile-pile cap interface.

Maximum bending moment in pile, M_u = 91.2 kN-m 67.27 k-ft

Lateral pile deflection vs depth

Pile moment vs depth

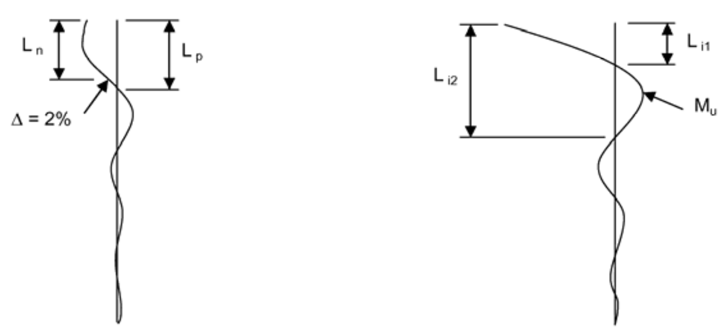

Typical COM624P results (exaggerated)

Title: Bridge 203 - 52.43 m 3-Span Concrete Prestressed I-girder
90^o skew, 3.594 m girder spacing

By: KP
Checked:
Date: 3/10/2006
Date:

Pile Capacity Analysis

Check the geotechnical resistance of the pile
The geotechnical resistance can be supplied by skin friction, end bearing, or both. The easiest way to eliminate one or the other from contributing to the resistance is to simply put zero in for the unit resistance of the one to be neglected. The resistance factors for bearing capacity and skin friction should be chosen according to the provisions of DM-4.

Shaft and tip resistance factors

Tip (bearing) resistance factor, ϕ_{qp}	0.50		D10.5.4-2
Shaft (skin friction) resistance factor, ϕ_{qs}	0.55		D10.5.4-2

Tip resistance

Unit tip resistance, q_p	113 MPa	16 ksi	
Nominal pile tip resistance, $Q_p = q_pA_p$ =	(113)(14100)/1000 =		
	1593.30 kN	358.2 k	

The effective shaft length is the total shaft length minus a length at the top of the pile which is ineffective due to the lateral movement which occurs. Using a displacement of 2% of the pile diameter as the boundary above which skin friction becomes ineffective has been found to be reasonable. The depth, L_n, at which the displacement reaches this critical value was determined previously using the computer program COM624P.

Shaft resistance (skin friction)

Depth to 2% deflection, L_n =	3317.20 mm	10.88 ft
Effective shaft length, $L_e = L_{tot} - L_n$ =	12192 - 3317.2 =	
	8874.8 mm	29.12 ft

The unit shaft resistance (skin friction) is required for friction piles. For layered soils, a weighted average unit shaft resistance should be used.

Unit shaft resistance, q_s	0.1 MPa	14.50 psi
Nominal pile shaft resistance, $Q_s = q_sA_s$	= (0.1)(1825)(8874.8)/1000 =	
	1619.83 kN	364.2 k

Total factored resistance per pile, $Q_R = \phi_{qp}Q_p + \phi_{qs}Q_s$
(0.50)(1593.30) + (0.55)(1619.83) = 1687.56 kN 379.4 k
1687.6 kN (379.4 k) > 1580.7 kN (355.3 k) - OK

Check the capacity of the pile as a structural member

The pile resistance factors in DM-4 are to be applied assuming only axial forces are present at the tip of the pile, where any driving damage is likely to occur. At the top of the pile, where axial forces and bending are present, the piles are generally undamaged. For these reasons a lower load factor is used when the axial force only is considered. The combined flexure and axial force resistance factors are higher. The calculated nominal axial resistances are also different, as the pile is assumed fully supported at the tip, but an unbraced length is assumed between the top two points of inflection.

Pile resistance factors

Axial compression only, ϕ_c	0.45		D6.5.4.2
Axial compression, ϕ_c plus	0.60	(used together)	D6.5.4.2
Flexure, ϕ_f	0.85		

Compressive resistance (lower portion of pile - axial loads only)
Nominal axial resistance, P_n = FyAs = (345)(14100)/1000 =
4864.5 kN 1093.6 k

Title: Bridge 203 - 52.43 m 3-Span Concrete Prestressed I-girder By: KP Date: 3/10/2006
90^o skew, 3.594 m girder spacing Checked: ________ Date: ________

For the check of axial capacity, the entire axial load is considered for end bearing piles. For friction piles, the load at the pile tip is assumed to be the total pile load minus 50% of the factored friction resistance of the pile.

Check axial capacity
Axial load at tip of pile, P_u = (≥ 0.0)
1580.65 kN 355.3 k
Factored axial resistance, $P_r = \phi\ P_n$ = (0.45)(4864.50) =
2189.03 kN 492.1 k
2189.03 kN (492.1 k) > 1580.65 kN (355.3 k) - OK

The unbraced length is defined as the distance between the top two points of inflection (zero moment) on the pile moment diagram.
(4542) - (1359) = 3182.6 mm 125.30 in
As a structural member, the pile length between the top two inflection points is assumed to be a pinned-pinned member. The effective length factor, K, of a pinned-pinned member = 1.0.

Compressive resistance (upper portion of pile - under combined axial load and moment)

For steel H-piles
F_e = Fy = 345 MPa
E_e = Est = 200000 MPa
$\lambda = (KL_b/r_s\pi)^2\ (F_e/E_e)$ = [(1.0*3182.6)/(74*3.142)]^2 (345/200000) = 0.324 A6.9.4.1
if $\lambda \leq 2.25$, $P_n = 0.66^{\lambda}F_eA_s$, if $\lambda > 2.25$, $P_n = 0.88F_eA_s / \lambda$

Nominal axial resistance, P_n = 0.66^0.324 (345)(14100)/1000 =
4251.5 kN 955.8 k
Factored axial resistance, $P_r = \phi\ P_n$ = (0.6)(4251.5) =
2550.9 kN 573.5 k

Flexural resistance of steel H-piles
Plastic Moment, $M_p = F_y\ Z_y$ = (345)(763000)/1000000 =
263.2 kN-m 194.2 k-ft
Yield Moment, $M_y = F_y\ S_y$ = (345)(497000)/1000000 =
171.5 kN-m 126.5 k-ft

For H-piles, if the width-to-thickness ratio of the flanges is not sufficient to consider the section compact, an interaction formula from AISC is used to interpolate between the plastic moment resistance and the yield moment resistance.

$M_n = M_p - (M_p - M_y)(\lambda - \lambda_p)/(\lambda_r - \lambda_p) \leq M_p$ AISC-LRFD, Ap.F F1., 1994

For pipe piles, if the diameter-to-thickness ratio of the pipe is not sufficient to consider the section compact, then the section is considered non-compact. A6.12.2.3.2

Width-to-thickness ratio of projecting flange element
λ = bf / 2tf = 310/(2*15.5) = 10.00
Width-to-thickness criteria for flange element to reach plastic moment
λ_p = 0.38 * $(E / F_y)^{1/2}$ = 0.382*(200000/345)^0.5 = 9.20 A6.10.5.2.3c
Width-to-thickness criteria for flange element to reach yield stress
λ_r = 0.56 * $(E / F_y)^{1/2}$ = 0.56*(200000/345)^0.5 = 13.48 A6.9.4.2
Nominal flexural resistance, M_n = Mp
Use M_n = 246.05 kN-m 181.48 k-ft

Pile factored flexural resistance, $M_r = \phi\ M_n$ = (0.85)(246.1) =
209.1 kN-m 154.26 k-ft
Check moment-axial interaction
P_u / P_r = 1580.7/2550.9 = 0.62 A6.9.2.2
if $P_u / P_r < 0.2$ then $P_u / 2.0P_r + M_u / M_r \leq 1.0$
if $P_u / P_r \geq 0.2$ then $P_u / P_r + (8.0 / 9.0)\ M_u / M_r \leq 1.0$
Moment - axial interaction = 1580.7/2550.9 + (8.0/9.0)(91.2/209.1) = 1.01
Error - 1.01 > 1.00 - Increase the number of piles or change the pile section - push ctrl-a

Title: Bridge 203 - 52.43 m 3-Span Concrete Prestressed I-girder
90^o skew, 3.594 m girder spacing

By: KP
Checked:
Date: 3/10/2006
Date:

Pile Ductility Requirement

Since the top of the pile will often have to undergo inelastic rotations, a check is performed based on a method contained in Greimann et. al. (1987) for determining whether the pile has enough ductility to undergo the required calculated deflections. DM-4 Ap.G.1.4.2.5

Ductility Criterion, $\Delta \leq \Delta_i$, where
Δ = design displacement
Δ_i = allowable displacement

The design displacement is the total displacement due to the full range of thermal expansion / contraction at the abutment being designed. Most of the data for thermal displacements was listed previously, and the percentage of the total displacement of the bridge is denoted by k.

Temperature range, Δ_T = 50 ^{o}C Concrete girders D3.12.2.1

Design displacement, $\Delta = k\phi_T\alpha\Delta_T L$ = (1.00)(1.0)(0.0000108)(50)(52425.6) =
28.3 mm 1.11 in

The design rotation is the total factored rotation at the support due to live load and composite dead loads which is equal to the sum of the absolute values of the maximum and minimum factored rotations.

Total design rotation, $\theta_w = \theta_{min} + \theta_{max}$ = 0.0004 + 0.0004 =
0.0008 radians 0.043 degrees

Pile yield stress, F_y 345 MPa 50 ksi

The plastic rotation is the rotation required to form a plastic hinge in the pile.

Plastic rotation, $\theta_p = F_y Z L_i / 3EI$ = (345)(763000)(1358.9)/(3*200000*77100000) =
0.0077 radians 0.443 degrees

Inelastic rotation capacity reduction factor, C_i ($0 \leq C_i \leq 1.0$)

$C_i = 3.17 - 5.68 \cdot (F_y / E)^{1/2} \ (bf / 2tf)$ = 3.17 - 5.68 * (345/200000)^0.5 [310/(2*15.5)] = 0.81
Use C_i = 0.81

Inelastic rotation capacity, $\theta_{inel} = (K^*C_iM_pL_i)/EI$ For H-piles, K = 1.500
[(1.500)(0.81)(263.24)(1000)(1358.9)]/[(200)(77100000)] =
0.0282 radians 1.617 degrees

Allowable displacement, $\Delta_i = 4^*L_i^*[(\theta_{inel} - \theta_w)/2 + \theta_p]$ = (4)(1358.9)[(0.0282 - 0.0008)/2 + 0.0077] =
116.7 mm 4.59 in

28.3 mm (1.11 in) < 116.7 mm (4.59 in) - OK

Pile Cap Reinforcing Design

Extreme Factored Dead + Live Loads per girder.

The extreme interior and exterior vertical girder reactions are listed below. When combined with the extreme wind and centrifugal reactions for an exterior girder, the result is a conservative maximum girder reaction for pile cap design.

Strength I	maximum of 789.39 and 764.39 =	789.39 kN	177.46 k
	minimum of 4.15 and -13.85 =	-13.85 kN	-3.11 k
Strength IP	maximum of 670.26 and 645.26 =	670.26 kN	150.68 k
	minimum of 45.90 and 27.90 =	27.90 kN	6.27 k
Strength II	maximum of 712.00 and 687.00 =	712.00 kN	160.06 k
	minimum of 13.32 and -4.68 =	-4.68 kN	-1.05 k
Strength III	maximum of 268.20 and 243.20 =	268.20 kN	60.29 k
	minimum of 186.84 and 168.84 =	168.84 kN	37.96 k
Strength V	maximum of 670.26 and 645.26 =	670.26 kN	150.68 k
	minimum of 45.90 and 27.90 =	27.90 kN	6.27 k

Title: Bridge 203 - 52.43 m 3-Span Concrete Prestressed I-girder
90^o skew, 3.594 m girder spacing

By: KP
Checked:
Date: 3/10/2006
Date:

The following reactions are the extreme factored dead and live load girder reaction calculated previously, plus the extreme reactions on the exterior girder due to wind, centifugal, and thermal forces. It is recognized that the extreme reactions due to lateral forces occur on the exterior girders, while the extreme gravity reaction may occur on the interior girders, but combining the two should not be overly conservative. The η_i modifier is included here as well.

Strength I	max	789.39 + 1.00[1.75(0.00) + 1.00(656.17)(8/4)] =		
			2101.74 kN/girder	472.49 k/girder
	min	-13.85 + 1.00[1.75(0.00) + 1.00(0.00)(8/4)] =		
			-13.85 kN/girder	-3.11 k/girder
Strength IP	max	670.26 + 1.00[1.35(0.00) + 1.00(656.17)(8/4)] =		
			1982.61 kN/girder	445.71 k/girder
	min	27.90 + 1.00[1.35(0.00) + 1.00(0.00)(8/4)] =		
			27.90 kN/girder	6.27 k/girder
Strength II	max	712.00 + 1.00[1.35(0.00) + 1.00(656.17)(8/4)] =		
			2024.35 kN/girder	455.09 k/girder
	min	-4.68 + 1.00[1.35(0.00) + 1.00(0.00)(8/4)] =		
			-4.68 kN/girder	-1.05 k/girder
Strength III	max	268.20 + 1.00[1.40(1.55)] + 1.00[1.40(4.96) + 1.00(656.17)(8/4)] =		
			1589.66 kN/girder	357.37 k/girder
	min	168.84 + 1.00[1.40(-35.49+ -4.96) + 1.00(0.00)(8/4)] =		
			112.20 kN/girder	25.22 k/girder
Strength V	max	670.26 + 1.00[0.40(4.96) + 1.00(2.43) + 1.35(0.00) + 1.00(656.17)(8/4)] =		
			1987.02 kN/girder	446.70 k/girder
	min	27.90 + 1.00[0.40(-4.96) + 1.00(-2.43) + 1.35(0.00) + 1.00(0.00)(8/4)] =		
			23.49 kN/girder	5.28 k/girder

Controlling Loads	max STR I	2101.74 kN/girder	472.49 k/girder
	min STR I	-13.85 kN/girder	-3.11 k/girder

Pile Cap Reinforcing

Knowing the maximum girder reaction, the pile spacing, the dimensions of the cap and diaphragm, and the material properties, the pile cap reinforcing can be calculated. The loads used for design are the maximum simply supported beam moments reduced by 20% to account for the continuity over the piles. Calculations for reinforcement are performed on the Cap Reinforcement tab.

Concrete compressive strength, f'_c	20.7	MPa	3.0	ksi
Reinforcing steel yield strength, F_y	413.7	MPa	60	ksi
Maximum factored girder reaction, R_u	2101.7	kN	472.5	k
Pile Spacing	1676	mm	5.50	ft

Pile cap reinforcement - use 4 # 25 bars top and bottom of cap beam

Title: Bridge 203 - 52.43 m 3-Span Concrete Prestressed I-girder
90° skew, 3.594 m girder spacing

By: KP
Checked:
Date: 3/10/2006
Date:

ANALYSIS SUMMARY PAGE

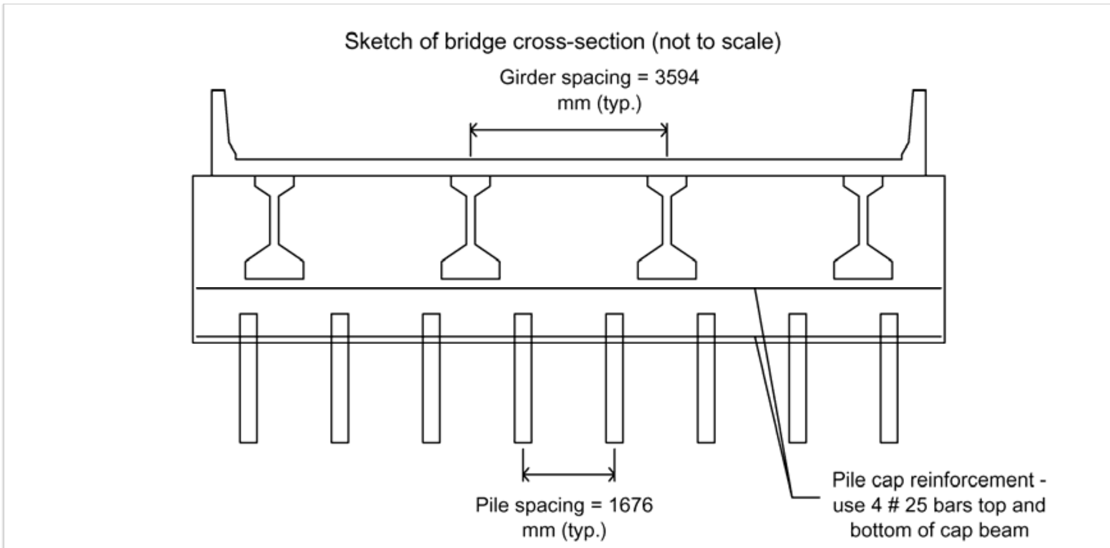

Bridge Description
Bridge length: 52425.6 mm (172.00 ft) continuous span.
Skew: 90 degrees.
Maximum number of traffic lanes: 3.
Curb-to-curb roadway width: 12192 mm (40.00 ft).
Total width of sidewalk(s): 0 mm (0.00 ft).
Out-to-out superstructure width: 13072 mm (42.89 ft).
Maximum number of traffic lanes with no sidewalks: 3.
Number of girders: 4 prestressed concrete I-girders
Girder spacing: 3594.1 mm (11.79 ft).
Moment of inertia of the girders about the longitudinal axis of the bridge: 64587774 mm^2 (100111 in^2).
Girders depth: 1600.2 mm (11.79 ft).
Girder width: 1066.8 mm (3.50 ft).
Bearing pad thickness 20 mm (0.8 in).
Average deck + haunch thickness: 262.89 mm (10.35 in).
Parapet height: 1143 mm (3.75 ft).

Integral Abutment Description
Abutment width: 1200 mm (3.94 ft).
Abutment length: 13772 mm (45.18 ft).
Pile cap depth: 4476.75 mm (14.69 ft) at the left end.
4391.787 mm (14.41 ft) at the center.
4306.824 mm (14.13 ft) at the right end.
Average pile cap depth: 4391.787 mm (14.41 ft).
Pile cap reinforcement: 4 # 25 bars top and bottom.
End diaphragm height (equal to the deck + haunch + girder + bearing pad depth): 1883.09 mm (6.18 ft).
Total average abutment height: 6274.877 mm (20.59 ft).
Wingwall length: 900 mm (2.95 ft) long stubs for detached wingwalls at each end of the abutment.

Pile Description
Number of piles: 8 - HP310x110 (HP12x74) piles.
Pile spacing: 1676.4 mm (5.50 ft) in a single row along the centerline of bearing of the abutment.
Moment of inertia of the piles about the longitudinal axis of the bridge: 118033312 mm^2 (182952 in^2).
Design pile length: 12192 mm (40.00 ft).
Depth to fixity: 3655.1 mm (143.90 in).
Unbraced length: 3182.6 mm (125.30 in).
Depth to the first point of inflection: 4541.5 mm (178.80 in).
Depth to the point where the lateral deflection is 2% of the pile width (friction engaged): 3317.2 mm (130.60 in).
Pile yield moment, My: 171.5 kN-m (126.5 k-ft).
Pile plastic moment, Mp: 263.2 kN-m (194.2 k-ft).

Title: Bridge 203 - 52.43 m 3-Span Concrete Prestressed I-girder
90° skew, 3.594 m girder spacing

By: KP Date: 3/10/2006
Checked: ______ Date: ______

Total factored geotechnical capacity of the pile: 1687.6 kN (379.4 k).
Factored axial resistance of the pile at the tip: 2189.0 kN (492.1 k).
Factored axial resistance of upper portion of pile for use in interaction equation: 2550.9 kN (573.46 k).
Factored flexural resistance of upper portion of pile for use in interaction equation: 209.1 kN-m (154.3 k-ft).

Loads and Deformations
Maximum girder reaction: 2101.7 kN (472.5 k) due to the STR I load case
Maximum axial force in the pile: 1580.7 kN (355.3 k) due to the STR I load case.
Maximum bending moment in the pile (other than at the pile-abutment connection): 91.2 kN-m (67.3 k-ft).
Total maximum design movement for the abutment: 56.6 mm (2.23 in).
Maximum movement in one direction: 24.9 mm (0.98 in).
Maximum design rotation: 0.0004 radians (0.022 degrees).
Axial load-moment interaction equation result for the pile (maximum allowable is 1.00): 1.01.

Warnings and Errors
The spreadsheet generated 0 warning(s) and 2 error(s).

The 2 error(s) must be addressed to satisfy design requirements.

An evaluation of the above presented PennDOT IA program output was performed through comparisons with field data and bridge 203 original design. The five program design sections were evaluated individually and are summarized in Table 7.1. Page numbers presented in the first column correspond to the program page numbers.

Table 7.1. Bridge 203: Program Evaluation

Design Section	Discussion	Suggested Improvements
1) Bridge Data (pp. 1-3)	Input data sequence and explanations are clearly presented.	-
2) Integral Abutment Data (pp. 3-4)	Input data sequence and explanations are clearly presented.	-
3) Load Data (pp. 5-8)		
• Dead and live load girder reactions (p. 6)	Calculation in the program strictly follows DM-4 App. G 1.2.7.2, which is based on the assumptions of equally distributed loads to all piles and removal of the multiple presence provision. The original design calculation presented girder reactions based on two cases: with and without using these assumptions. The former case exceeded the latter by 1.4 times.	More study is required to ensure that this assumption does not produce either over- or underestimated results for both narrow and wide bridges.
• Girder end rotation due to composite dead and live loads (pp. 6-7)	The original design calculation assumed integral abutment rigid-body movement and did not consider effects of girder-end rotations on the pile head rotations. Discussion of this issue is continued in section 4.	See design section 4 under *iterative procedure interacting with COM624P*.
4) Pile Data (pp. 9-18)		

• Pile properties (p. 9)	The geotechnical report recommends that a 1/16-inch loss in pile thickness (all around) due to corrosion be incorporated. This corrosion effect has been considered in the original design calculation. The pile properties used in the PennDOT IA program above did not consider this effect -- only short-term results are shown.	Input of the anticipated pile thickness loss as well as an option to automatically compute deteriorated pile properties are suggested.
• Edge distance of piles (p. 9)	The program reported an error due to excessive pile edge distance according to DM-4 App. G 1.4.2.1. The actual abutment width at only the lower portion was reduced to meet this provision.	-
• Temperature range (p. 11)	The structural continuity of bridge 203 was established during mid Sept. 2002 with an average ambient temperature of 68 ^{o}F. Measured extreme maximum and minimum ambient temperatures were 95 ^{o}F and -8 ^{o}F, respectively, over the 43-month period, below the design value of $\pm$80 ^{o}F.	Modification of the design temperature range as specified in DM-4 Ap.G 1.2.7.4 for U.S. customary units (111 ^{o}F) is required to eliminate inconsistent conversion between Fahrenheit and Celsius.
• Maximum abutment movement (p. 12)	Maximum measured abutment thermal displacements are 0.2 inch and 0.42 inch for expansion and contraction movements, respectively. This is compared to the PennDOT IA program design value of 0.98 inch.	IA program abutment displacement was overestimated due to the extremely large design temperature range and large thermal mass of the bridge. A modification of the temperature range is possible to allow more accurate predictions of displacements.
• Coefficient of passive earth	The maximum measured earth pressure was 19 psi. The	-

pressure (p. 12)	calculated effective vertical stress at this pressure cell location was 6.2 psi, indicating a maximum equivalent coefficient of earth pressure of 3.1, which is very close to the design value of 3.0. The measured earth pressures were high at the abutment mid-height and relatively low at the top and bottom.	
• Axial load per pile (p. 13)	The maximum measured pile axial dead load was 107 k/pile as compared to the total predicted unfactored axial dead load of 112 k/pile, a difference of 4.7%.	Excellent agreement.
• Iterative procedure interacting with COM624P (p. 14)	Measured girder and abutment rotations, pile strains, and abutment displacements all indicate that the abutment-to-backwall connection is not rigid and the abutment rotates away from the backfill. Assumption of a rigid connection by the PennDOT IA program leads to excessively conservative results. Measured pile moments were 55 ft-kip as compared to predicted 194 ft-kip, nearly 4 times larger.	The PennDOT IA program poorly predicts the behavior of the abutment and backwall movement and program assumptions are not valid. A behavior model that incorporates rotational flexibility of the structure needs to be incorporated.
• Axial load-moment interaction (p. 16)	The PennDOT IA program reported an axial load-moment interaction value greater than 1.0, indicating insufficient design pile strength. This results from differences between LRFD and LFD where load factors are smaller. Neither design accounts for x-axis pile bending under wind loads and thermally induced abutment movements in the transverse direction.	Corrections of structure flexibility as described above and the inclusion of wind and transverse thermal behavior are required to more accurately predict behavior.

• Abutment/pile cap reinforcement (p. 18)	The PennDOT IA program is limited to design of longitudinal reinforcement for abutment/pile cap.	The design of vertical reinforcement for the abutment/pile cap is suggested.
5) Analysis Summary (pp. 19-20)	Analysis summary is concisely and clearly presented.	-

In addition to the issues discussed in Table 7.1, creep and shrinkage of prestressed concrete members were identified as producing a significant and adverse effect on the long-term behavior of IA bridges, including longitudinal abutment movement and pile stresses. As can be observed from extensometer and pile strain gage data (see Chapter 3), the abutment longitudinal displacement in the 3rd year was about two times greater than the initial displacement and, similarly, the pile moment at the depth near the abutment of the 3rd year was about two times greater than the initial moment. This behavior is largely due to the effects of concrete creep and shrinkage, which should also be considered in IA bridge design.

Thermally induced loads on the abutment and pier result in additional, redistributed bending moments at both the superstructure and abutment from vertical movements. Bridge 203 is a three-span continuous consisting of two abutments and two intermediate piers. Abutment and pier heights are 8.9, 31.3, 29, and 14.1 ft for abutment 1, pier 1, pier 2, and abutment 2, respectively. Relative thermal vertical displacement of piers 1 and 2 under ±80 ^{o}F temperature load are determined as ±0.12 inch and ±0.09 inch, respectively. This relative vertical thermal displacement is equivalent to differential settlement effects and results in moments as high as 10 percent of the moments caused by abutment longitudinal displacement, which are anticipated to produce significant magnitudes of redistributed bending moments on the superstructure and integral abutment.

7.3 BRIDGE 211 EVAUATION

Similar to bridge 203, the bridge 211 design is not based on the PennDOT IA program. The design philosophy used in the design of bridge 211 was based on load factor design (LFD). As a consequence, the analysis results obtained for this bridge through the LRFD-based PennDOT IA program are not the same as the original design. In addition to a comparison between the PennDOT IA program and field data, a comparison is also presented between the original LFD method used and the PennDOT IA program.

The PennDOT program results, complete with input data, are presented below. Four sources were used to obtain bridge material and geometric information: (1) design drawings, (2) design calculations, (3) the geotechnical report, and (4) actual pile driving records. The design drawings, design calculations, and geotechnical report were obtained from HDR Inc., of Pittsburgh (the design consultant of this bridge). The average as-built pile length was used in the PennDOT IA program, as presented below.

Title: Birdge 211 - 34.7 m Single Span Concrete Prestressed I-girder
90° skew, 3.39 m girder spacing

By: WS Date: 3/10/2003
Checked: ________ Date: ________

SPREADSHEET PROGRAM DESCRIPTION

This spreadsheet is intended to be used as an aid in designing and analyzing integral abutments. No users manual is provided, but explanations of input values are given throughout the spreadsheet. The spreadsheet is intended to be used in conjunction with the computer program COM624P, which analyzes the lateral behavior of piles, and with PennDOT's steel or prestressed concrete girder design programs. Design Specifications for integral abutments are available in PennDOT Design Manual Part 4 (DM-4), Appendix G. References to applicable provisions in the DM-4, as well as to the AASHTO LRFD Bridge Design Specifiction, 1994, are made near the right hand margin. Many dimensions for integral abutments are set forth in PennDOT's BD-667M Standard Drawings. The spreadsheet was written in SI units, although the English unit equivalents are also provided, such that either units can be used. Warning and Error messages are provided where possible. An Error message indicates an input value is incorrect and should be changed, a Warning message flags an input value that is suspect, and the user should verify the value, or in some cases, obtain the approval c
Different sheets (tabs), labeled along the bottom of the window, perform different tasks within the spreadsheet. The first tab in the spreadsheet summarizes the input values by providing a simple list which can be printed and filled in by hand, or used to insert the input values. The current tab is the Main tab where most of the analysis takes place. The Scour tab is available for cases where an additional scour check of the piles is required. The COM624P Input tab is used to generate an template for the COM624P computer program. The load factors for each load case are listed on the Load Factor tab. The Cap Reinforcement tab calculates the area of reinforcement needed for the pile cap. The Pile Data tab lists the properties of available H-pile sections, calculates the properties of concrete filled pipe piles, and lists the current pile properties for insertion into the Main tab.

[ ] - denotes input cells

BRIDGE DATA

Input all the geometric and material data for the proposed bridge. This information should be available from a superstructure design already performed independently, as well as a Type, Size, and Location (TS&L) Report, if available.

The girder material is required to determine the coefficient of thermal expansion of the bridge and the uniform temperature change.

Girder material (S - Steel, C - Concrete) [C]

There are three types of girders which can be used with integral abutments: Steel I-girders, concrete I-girders, or concrete spread box girders.

Girder type (I - I-girder, B - Box girder) [I]

Steel bridge lengths in excess of 120000 mm and concrete bridge lengths in excess of 180000 mm require the written approval of the Chief Bridge Engineer for use with integral abutments. In addition, bridges in excess of these limits require consideration of secondary forces such as those caused by creep, shrinkage, thermal gradient, or differential settlements. The methods of applying secondary forces also require the approval of the Chief Bridge Engineer. DM-4 Ap.G.1.2.1 DM-4 Ap.G.1.2.7.5

Total bridge length - centerline end bearing to centerline end bearing
[34747.2] mm 114.00 ft

The length of the span adjacent to the abutment is required to calculate the pedestrian loads and wind loads on the abutment. It is also used to assess whether the bridge is simply supported or continuous, and in the simplified procedure to determine axial forces induced in the piles in continuous bridges due to thermal movements. Input the total span length for single span bridges.

Length of span adjacent to abutment - centerline bearing to centerline bearing
[34747.2] mm 114.00 ft DM-4 Ap.G.1.2.1

Skews are limited to 70 degrees or more for continuous spans and single spans longer than 40000 mm. Skews of up to 60 degrees are allowed for single spans in excess of 27000 mm but not longer than 40000 mm. For single spans 27000 mm and less, skews up to 45 degrees are permitted. Only positive skew values >45 or <90 degrees can be used in the spreadsheet. DM-4 Ap.G.1.2.2

Skew [90] degrees 1.57 radians

Title: Birdge 211 - 34.7 m Single Span Concrete Prestressed I-girder
90° skew, 3.39 m girder spacing

By: WS
Checked:
Date: 3/10/2003
Date:

The curb-to-curb roadway width, the sum of clear sidewalk widths, and the out-to-out superstructure widths are required input. Warnings will be supplied if these values plus conservative estimates of parapet widths are not consistent. It is the users responsibility to make sure these values are correct, however. The roadway and sidewalk widths are used in calculating live load reactions. The out-to-out superstructure width is used to determine both loadings and the length of the integral abutment.

Curb-to-curb (roadway) width	12192	mm	40.00 ft
Sum of clear widths of sidewalks on bridge	0	mm	0.00 ft
Out-to-out superstructure width	13072	mm	42.89 ft

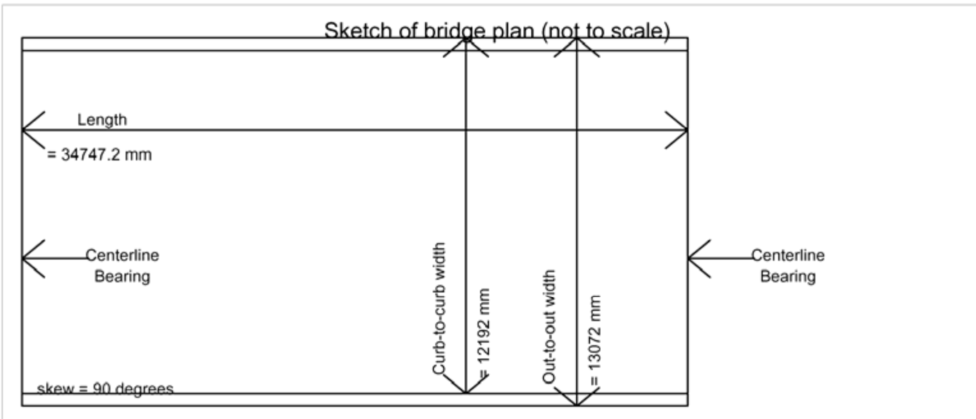

The maximum number of lanes with sidewalks is determined by dividing the width of available roadway (out-to-out of curbs) by the specified lane width (3600 mm) and rounding down to the nearest integer. Widths between 6000 and 7200 mm are assumed to carry two lanes, however. Similarly, the maximum number of lanes without sidewalks is determined by taking the out-to-out width of the structure minus two assumed 440 mm parapets, dividing by the specified lane width, and rounding down to the nearest integer. Again, widths between 6000 and 7200 mm are assumed to carry two lanes. A3.6.1.1.1

Curb-to-curb width of roadway divided by lane width = 12192/3600 = 3.39
Maximum number of lanes with sidewalks 3

Total bridge clear width divided by lane width = (13072 - 880)/3600 = 3.39
Maximum number of lanes without sidewalks 3

The number of girders and the girder spacing is needed to determine the maximum girder reaction for pile cap design. Other dimensions are used to determine various things such as end diaphragm height and lateral wind area of the span, which are utilized in calculating dead and wind loads.

Number of girders in the cross-section	4			
Girder spacing normal to longitudinal axis	3390.9	mm	11.13 ft	
Girder width (maximum of top or bottom flange width at the abutment)	1066.8	mm	3.50 ft	
Girder depth	1981.2	mm	6.50 ft	DM-4 Ap.G.1.2.8

Warning - girders deeper than 1825 mm (6.0 ft.) require the written approval of the Chief Bridge Engineer as per DM-4 Ap. G1.2.8

Bearing pad thickness	20	mm	0.79 in	DM-4 Ap.G.1.7
Deck + haunch thickness	277.749	mm	10.94 in	
Parapet height	1016	mm	3.33 ft	

Total superstructure depth for wind analysis - top of parapet to bottom of girder

1981.2 + 277.749 + 1016 = 3274.949 mm 10.74 ft

The moment of inertia of the girders about the longitudinal axis of the bridge is calculated as illustrated in the figure below (five I-girders shown for illustrative purposes, the actual number of girders is used in the calculations). This value is used later to determine girder reactions due to transverse and overturning loadings.

Given a group of n girders, the second moment of inertia is calculated by summing the squares of the distances of the girders from the center of gravity of the girder group, or $I = \Sigma d_i^2$. For a single line of n equally spaced girders, the equation $I = n(n^2 - 1)L^2 / 12$ gives the same result, where n is the number of girders, and L is the girder spacing.

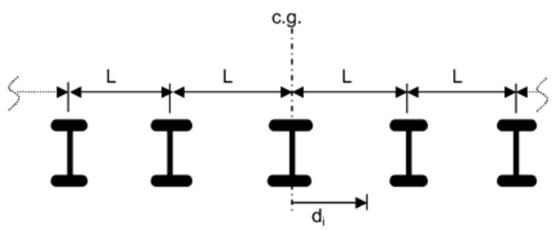

Moment of inertia of 4 I-girders about the longitudinal axis of the bridge:

4(4^2 - 1)(3390.9^2)/12 = 57491014.05 mm² 89111 in²

INTEGRAL ABUTMENT DATA

Given the geometry of the superstructure, the location of the proposed abutment, and the topography of the site, the geomety of the integral abutment can be calculated, and the wingwall lengths can be determined. Many of the dimensions are set in the PennDOT standards (see BD-667M Standard Drawing).

The abutment length is measured along the line of bearing. Note that specifying detached wingwalls later in the spreadsheet results in a slightly longer abutment (see BD-667M for detached wingwall details).

Abutment length	(13072+700)/sin(90) =	13772 mm	45.18 ft	

The abutment width is set at 1200 mm so that for any potential skew angle the pile cap reinforcement can fit around the piles.

Abutment width	1200 mm	3.94 ft	DM-4 Ap.G.1.4.1

The minimum pile cap height is 1000 mm. The flexural design of the pile cap is based on the supplied minimum dimension. There are a number of factors which can affect the maximum pile cap height. These include, but are not limited to, bridge width and cross-slopes, superelevation, skew, etc. DM-4 Ap.G.1.4.1

Although PennDOT permits the opposite ends of integral abutments to vary up to 450 mm in height due to superelevation (300 mm for skews less than 80°), sloping the bottom of the pile cap such that the ends are equal is recommended to simplify reinforcement details. DM-4 Ap.G.1.4.1

Left end pile cap height, d_{pc1}	2374.392 mm	7.79 ft
Pile cap height at the crown of the roadway, or at the bridge midwidth for a superelevated roadway, $d_{pc,cl}$	2563.368 mm	8.41 ft
Right end pile cap height, d_{pc2}	2606.04 mm	8.55 ft

Difference between the height of the cap at the ends, $|d_{pc1} - d_{pc2}|$ = | 2374 - 2606 | =

231.648 mm 0.76 ft

The previous three values are used to calculate an average pile cap height and assume a constantly sloping top of cap with a crown at the center, as illustrated in the figure below. Only the minimum value is used to design the pile cap, the average value is used for selfweight calculations. Note that if the cap does not have either a constant cross-slope or crown at the midwidth, the average pile cap height will not be precisely correct. If a more exact selfweight is required, the maximum height at midwidth can be adjusted until the desired average pile cap height is attained.

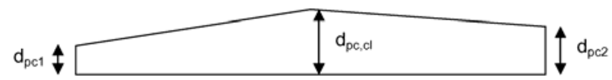

Average pile cap height			
99999+2606.03999999999)/4 + 2563.36800000002/2 =	2526.792	mm	8.29 ft

The end diaphragm height is equal to the deck and haunch thickness + girder depth + bearing pad depth.

End diaphragm height 277.749 + 1981.2 + 20 =	2278.949	mm	7.48 ft

The total average abutment height is equal to the end diaphragm height plus the average pile cap height.

Total average abutment height 2279 + 2527 =	4805.741	mm	15.77 ft

WINGWALLS

Attached wingwalls up to 2400 mm long (measured from the back face of the abutment) may be rectangular, extending the full depth of the abutment. Attached wingwalls over 2400 mm up to 4560 mm must be tapered. Wingwalls longer than 4560 mm will be detached. The standard location of the joint for a detached wingwall is 900 mm from the back face of the abutment, as shown in the figure below. The detached portion of the wingwall is to be designed independently. A 300 mm chamfer is provided in the interior corner of the wingwall/abutment connection (see figure). DM-4 Ap.G.1.4.4

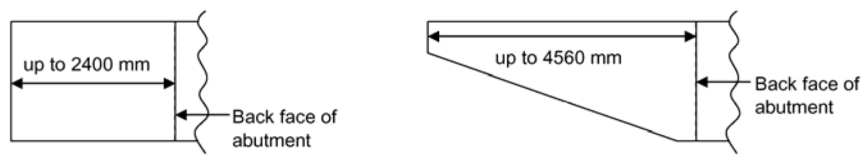

Rectangular wingwall Tapered wingwall

Detached wingwall Abutment/wingwall corner chamfer

Type of wingwall (R - Rectangular, T - Tapered, D - Detached)	D		
Wingwall length (including 300mm chamfer)	900	mm	3.0 ft

The wingwall dimensions are required for dead load calculations.
The average wingwall height at the abutment back face is conservatively assumed to be equal to the average height of the abutment.

Wingwall height at back face of abutment	4805.741	mm	15.77 ft

The height at the end is assumed to be either equal to the height at the abutment for rectangular (R) or detached (D) wingwalls, or 600 mm for tapered (T) wingwalls DM-4 Ap.G.1.4.4

Wingwall height at end	4805.741	mm	15.77 ft

The attached wingwall thickness is assumed to be the same width as the typical concrete parapet. An effective average thickness is assumed for the abutment extension for detached wingwalls. To obtain the effective width, the 250x300 mm overlap section (see BD-667M Standard Drawing) is smeared over the length of the stub.

Wingwall width 440+350+[(250)(300)/900] =	873	mm	2.87 ft

Title: Birdge 211 - 34.7 m Single Span Concrete Prestressed I-girder
90° skew, 3.39 m girder spacing

By: WS
Checked:
Date: 3/10/2003
Date:

LOAD DATA

LRFD design philosophy employs the equation $\Sigma\eta_i\gamma_i Q_i \le \varphi R_n = R_r$. In this equation, γ_i is a load factor, Q_i is a load effect, φ is a resistance factor, R_n is a nominal resistance, and R_r is a factored resistance. This leaves the η_i (eta) factor, which is a load modifier used to account for ductility, redundancy, and operational importance. $\eta_{i,max}$ is used when maximizing loads. $\eta_{i,min}$ is used when minimizing loads. Penndot currently limits η_i to values greater than or equal to 1.00 and less than or equal to 1.16. — A1.3.2.1, D1.3.2

η_i factor	1.00	
$\eta_{i,max} = \eta_i \ge 1.00$	1.00	D1.3.2
$\eta_{i,min} = 1/\eta_i \le 1.00$	1.00	A1.3.2.1

The unfactored girder design loads are available from the superstructure design performed using PennDOT's prestressed concrete girder design program. Both the interior and exterior noncomposite girder design dead loads are required input, although if only the controlling value is known, it can be conservatively used for both. The remaining composite dead loads should be the same whether they come from an interior or exterior girder design. The maximum and minimum unfactored live loads, with impact and shear distribution factors included, are also required input. The shear distribution factor is required as well, so that it can be divided out of the given loads to get the reaction per traffic lane. These values are available directly from the PennDOT beam design programs. Either the exterior or interior girder design can be used for the live load values, as long as all the values (reactions and distribution factors) come from the same girder design. Additional loads are calculated later. — DM-4 Ap.G.1.2.7

Dead Loads - Unfactored:

Non-composite DC1 loads - include girder, deck, haunch, interior diaphragms		
Interior girder, DC1	661.5 kN	148.71 k
Exterior girder, DC1	633.3 kN	142.37 k
Composite DC2 loads - include parapets,		
Interior girder, DC2	141.7 kN	31.86 k
Exterior girder, DC2	141.7 kN	31.86 k
Composite DW loads - include future wearing surface,		
Interior girder, DW	76.1 kN	17.11 k
Exterior girder, DW	76.1 kN	17.11 k

Live load shear distribution factor: 1.026

Live Loads - Unfactored from girder design program (distribution factor included):

PHL-93	max	567.8 kN	127.6 k
	min	0.0 kN	0.0 k
P-82	max	987.4 kN	222.0 k
	min	0.0 kN	0.0 k

Live Loads - Unfactored - distribution factor removed - reaction due to live load on one traffic lane:

PHL-93	max	(567.8)/(1.026) =	553.4 kN	124.4 k
	min	(0)/(1.026) =	0.0 kN	0.0 k
P-82	max	(987.4)/(1.026) =	962.4 kN	216.4 k
	min	(0)/(1.026) =	0.0 kN	0.0 k

The total pedestrian load reaction at the abutment is calculated assuming the approach slab and the first span are simply supported. The first span portion is calculated here, the approach slab portion is added in with the approach slab loads. The pedestrian load per unit area is as specified in the AASHTO LRFD Bridge specification, and the total width of sidewalk input earlier is used. This reaction is then distributed equally to all girders and piles. — DM-4 Ap.G.1.2.7.2, A3.6.1.6, D3.6.1.6

Pedestrian	max	(0.0036)(0)(34747)/2000 =	0.0 kN	0.0 k	A3.6.1.6
	min		0.0 kN	0.0 k	

Choose the load factors to be used for the DW loads. For new construction or analysis of existing construction, where no future wearing surface is present, the DW load factors are taken as 1.50 max and 0.00 min. For bridges where a future wearing surface is present, the DW load factors are taken as 1.50 max and 0.65 min. Typically, the future wearing surface will not be currently present - N.

Future wearing surface currently present (Y or N)? N

DW load factors Maximum = 1.50 Minimum = 0.00

Title: Birdge 211 - 34.7 m Single Span Concrete Prestressed I-girder
90° skew, 3.39 m girder spacing

By: WS
Checked: ______
Date: 3/10/2003
Date: ______

The extreme girder reactions, interior or exterior, are (conservatively) required for the design of the abutment pile cap. The total reaction with all lanes loaded, or the average pile reaction, is required for the pile design, which also requires both interior and exterior girder reactions. Note: The η_i factor is included here.

Factored Dead + Live reaction for interior girder:

Strength I	max	1.00[1.25(661.5+141.7) + 1.50(76.1) + 1.75(553.41)(3)/4] =	1844.5 kN	414.7 k
	min	1.00[0.90(661.5+141.7) + 0.00(76.1)] + 1.00[1.75(0.00)(3)/4] =	722.9 kN	162.5 k
Strength IP	max	1.00[1.25(661.5+141.7) + 1.50(76.1) + 1.75(0)/4 + 1.35(553.41)(3)/4] =	1678.5 kN	377.3 k
	min	1.00[0.90(661.5+141.7) + 0.00(76.1) + 1.75(0.00)/4] + 1.00[1.35(0.00)(3)/4] =	722.9 kN	162.5 k
Strength II	max	1.00[1.25(661.5+141.7) + 1.50(76.1) + 1.35[962.38+553.41(3-1)]/4] =	1816.5 kN	408.4 k
	min	1.00[0.90(661.5+141.7) + 0.00(76.1)] + 1.35[(1.00)(0.00)+(1.00)(0.00)(3-1)]/4 =	722.9 kN	162.5 k
Strength III	max	1.00[1.25(661.5+141.7) + 1.50(76.1)] =	1118.2 kN	251.4 k
	min	1.00[0.90(661.5+141.7) + 0.00(76.1)] =	722.9 kN	162.5 k
Strength V	max	1.00[1.25(661.5+141.7) + 1.50(76.1) + 1.35(553.41)(3)/4] =	1678.5 kN	377.3 k
	min	1.00[0.90(661.5+141.7) + 0.00(76.1)] + 1.00[1.35(0.00)(3)/4] =	722.9 kN	162.5 k

Factored Dead + Live reaction for exterior girder:

Strength I	max	1.00[1.25(633.3+141.7) + 1.50(76.1) + 1.75(553.41)(3)/4] =	1809.3 kN	406.7 k
	min	1.00[0.90(633.3+141.7) + 0.00(76.1)] + 1.00[1.75(0.00)(3)/4] =	697.5 kN	156.8 k
Strength IP	max	1.00[1.25(633.3+141.7) + 1.50(76.1) + 1.75(0)/4 + 1.35(553.41)(3)/4] =	1643.2 kN	369.4 k
	min	1.00[0.90(633.3+141.7) + 0.00(76.1) + 1.75(0.00)/4] + 1.00[1.35(0.00)(3)/4] =	697.5 kN	156.8 k
Strength II	max	1.00[1.25(633.3+141.7) + 1.50(76.1) + 1.35[962.38+553.41(3-1)]/4] =	1781.3 kN	400.4 k
	min	1.00[0.90(633.3+141.7) +0.00(76.1)] + 1.35[(1.00)(0.00)+(1.00)(0.00)(3-1)]/4 =	697.5 kN	156.8 k
Strength III	max	1.00[1.25(633.3+141.7) + 1.50(76.1)] =	1082.9 kN	243.4 k
	min	1.00[0.90(633.3+141.7) + 0.00(76.1)] =	697.5 kN	156.8 k
Strength V	max	1.00[1.25(633.3+141.7) + 1.50(76.1) + 1.35(553.41)(3)/4] =	1643.2 kN	369.4 k
	min	1.00[0.90(633.3+141.7) + 0.00(76.1)] + 1.00[1.35(0.00)(3)/4] =	697.5 kN	156.8 k

When designing integral abutments, only the girder rotations that are transferred to the piles are needed. Most dead load rotations occur prior to pouring the end diaphragm, and therefore will not be transferred to the piles. The exception to this is any composite dead loads such as future wearing surface or parapets. The extreme live load and composite dead load girder rotations are conservatively used as the design rotations for the piles. The unfactored live load and composite dead load rotations are available from the girder design.

Unfactored Live Load rotations per girder (including distribution factor):

PHL-93	max	0.123 degrees	0.0021	radians
	min	0.000 degrees	0.0000	radians
P-82	max	0.206 degrees	0.0036	radians
	min	0.000 degrees	0.0000	radians

The rotations above are the single girder unfactored rotations. To get the average girder rotations required for the design of integral abutments, the maximum number of traffic lanes on the bridge are loaded and the loads are assumed equally distributed to all girders. To accomplish this using the above results from the girder design program, the distribution factor is divided out to get the rotation of the full traffic lane applied to one girder. Then, the result is multiplied by the number of lanes and divided by the number of girders in the bridge.

Average Live Load rotations per girder:

PHL-93	max	(0.0021/1.026)(3/4) =	
		0.090 degrees	0.0016 radians
	min	(0.0000/1.026)(3/4) =	
		0.000 degrees	0.0000 radians
P-82	max	(0.0036/1.026)(3/4) =	
		0.151 degrees	0.0026 radians
	min	(0.0000/1.026)(3/4) =	
		0.000 degrees	0.0000 radians

The total rotation of any composite dead load rotations (unfactored), e.g. future wearing surface and parapets, can be input here. This value will be factored using the maximum DW load factor, 1.50.

0.033 degrees $\boxed{0.0006}$ radians

Maximum factored rotations are calculated here. The DM-4 allows the P-82 permit load to be placed in only one lane, with PHL-93 load in the remaining lanes. If the P-82 rotation controls the girder design the abutment design rotations are adjusted accordingly to account for P-82 on one lane and PHL-93 on all other lanes. The maximum load factor is used for both the maximum (positive) and minimum (negative) values.

Average factored live load + future dead load rotations (including eta factor):

	Controlling load		
max	PHL-93 all lanes	(1.00)[(1.75)(0.0016) + (1.50)(0.0006)] =	
		0.207 degrees	0.0036 radians
min		(1.00)[(1.75)(0.0000) + (1.50)(0.0000)] =	
		0.000 degrees	0.0000 radians

Additional Loads

Additional loads due to wind and centrifugal force are calculated here. The approach slab dead and live loads, and wingwall and abutment dead loads are calculated in the next section.

Wind Loads — DM-4 Ap.G.1.2.7.3

The appropriate wind pressure on the structure is input here. — A3.8

Wind on structure pressure = $\boxed{0.0024}$ MPa 0.000348 ksi — A3.8.1.2

The wind forces on the abutment are calculated assuming only the bridge span adjacent to the abutment contributes to the load, and that the span is simply supported laterally (half of the wind force on the end span is resisted by the abutment).

lateral force = (0.0024)(34747.2)(3274.949)/2000 136.55 kN 30.70 k

Uplift pressure is defined as a constant 0.00096 MPa. The force from this pressure is assumed to act as a line load at a distance of 1/4 of the out-to-out width of the bridge from the edge of the bridge. — A3.8.2

Uplift force (acts @ 1/4 point)	pressure =	0.00096 MPa	0.000139 ksi
uplift = (-0.00096)(34747.2)(13072)/2000 =		-218.02 kN	-49.01 k
moment about the longitudinal axis of the bridge = -(-218.02)(13072)/4000 =			
		712.50 kN-m	525.51 k-ft

Wind on live load is taken as 1.46 kN/m acting at 1800 mm above the deck — A3.8.1.3

Wind on live load	distributed force =	1.46 kN/m	0.10 k/ft
	lateral force = (1.46)(34747.2)/2000 =	25.37 kN	5.70 k

Centrifugal force — DM-4 Ap.G.1.2.3

Integral abutments are permitted for curved bridges as long as the girders are straight and parallel within each span, and approval is obtained from the Chief Bridge Engineer. Despite the limited curvature this allows, centrifugal forces can be generated. The centrifugal force and any other lateral forces other than wind forces contributing to overturning moments can be input here. This force will be assumed to act perpendicular to the longitudinal axis of the bridge at a distance 1800 mm above the roadway surface. — A3.6.3

Centrifugal force $\boxed{0}$ kN 0.00 k

Girder and Pile Reactions

Girder and pile reactions are calculated assuming overturning moments are resisted by vertical forces only.
Girder reactions due to wind and centrifugal forces:
The top of deck to the top of the pile cap is equal to the end diaphragm height.

Top of deck to the top of the pile cap =	2278.949 mm	7.48 ft

The moment due to the wind on the superstructure is equal to the wind force times half the depth of the structure plus the bearing pad depth.

Wind on structure

moment = (136.55)[(3274.949/2)+20]/1000 =	226.34 kN-m	166.94 k-ft

The moment of the wind on the live load is equal to the force times the moment arm which is equal to the distance from the top of the pile cap to the top of the deck plus 1800 mm.

Wind on live load

moment = (25.37)(2278.949+1800)/1000 =	103.46 kN-m	76.31 k-ft

The moment of the centrifugal force is equal to the centrifugal force times the moment arm which is also equal to the distance from the top of the pile cap to the top of the deck plus 1800 mm.

Centrifugal

moment = (0.00)(2279+1800)/1000 =	0.00 kN-m	0.00 k-ft

The unfactored extreme reactions per girder for wind loads are calculated assuming the vertical wind forces are distributed equally to all girders, and the moments are resisted by vertical reactions of the girders (see figure below - note that five I-girders are used for illustrative purposes only - actual number of girders used in calculations). Forces due to the moments are calculated assuming the superstructure acts as a rigid member transversely, and the vertical force is proportional to the distance from the center of gravity of the girder group. The force at any girder is equal to the moment times the distance from the midwidth of the bridge divided by the second moment of inertia. The extreme overturning reactions are therefore at the exterior girders.

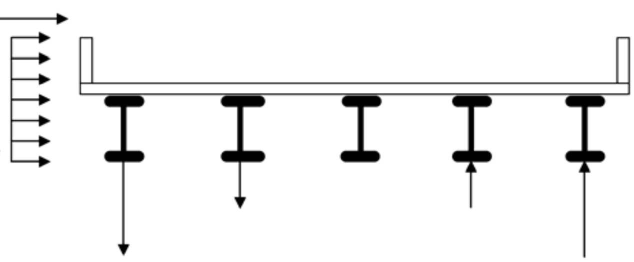

Extreme girder reactions due to wind on the structure

WS	max	(226.34)(1000)(4-1)(3390.9)/(2*57491014.05) =		
			20.02 kN/girder	4.50 k/girder
	min	-(226.34)(1000)(4-1)(3390.9)/(2*57491014.05) =		
			-20.02 kN/girder	-4.50 k/girder

Extreme forces due to uplift

Uplift	max	-218.02/4 + (712.50)(1000)(4-1)(3390.9)/(2*57491014.05) =		
			8.53 kN/girder	1.92 k/girder
	min	-218.02/4 - (712.50)(1000)(4-1)(3390.9)/(2*57491014.05) =		
			-117.54 kN/girder	-26.42 k/girder

Extreme forces due to wind on live load

WL	max	(103.46)(1000)(4-1)(3390.9)/(2*57491014.05) =		
			9.15 kN/girder	2.06 k/girder
	min	-(103.46)(1000)(4-1)(3390.9)/(2*57491014.05) =		
			-9.15 kN/girder	-2.06 k/girder

Extreme forces due to centrifugal forces

CE	max	(0.00)(1000)(4-1)(3390.9)/(2*57491014.05) =		
			0.00 kN/girder	0.00 k/girder
	min	-(0.00)(1000)(4-1)(3390.9)/(2*57491014.05) =		
			0.00 kN/girder	0.00 k/girder

Choose a trial pile section at this point. The pile dimensions are needed for the pile location check. The pile

moment of inertia is used to calculate the thermally induced forces in the piles. The pile properties are also required to run the COM624P computer program. Two types of piles are permitted for integral abutments, steel H-piles or concrete filled pipe piles.

Type of piles H - HP shape, P - pipe | H |

For H-piles, the yield stress of the steel and the metric designation of the pile is required input. A list of available H-pile sections is provided. The user may then input the additional section properties manually, or press the button to the right, and the properties will be automatically retrieved.

Import Pile Properties

Pile Properties				HP Shapes
Pile designation	HP310x110		(HP12x74)	HP360x174
Yield stress of pile steel, F_y	245	MPa	36 ksi	HP360x152
Pile section depth, d	308	mm	12.1 in	HP360x132
Flange width, bf	310	mm	12.2 in	HP360x108
Flange thickness, tf	15.50	mm	0.610 in	HP310x125
Pile Area, Ap	14100	mm^2	21.9 in^2	HP310x110
Moment of inertia, $I_{y\text{-}y}$	77.1E+6	mm^4	185 in^4	HP310x94
Elastic section modulus, $S_{y\text{-}y}$	49.7E+4	mm^3	30.3 in^3	HP310x79
Radius of gyration, $r_{y\text{-}y}$	73.9	mm	2.91 in	HP250x85
Plastic section modulus, $Z_{y\text{-}y}$	76.3E+4	mm^3	46.6 in^3	HP250x62
				HP200x54

PILE DATA

Choose a pile layout. If a geotechnical report is available with a calculated pile capacity, a preliminary number of piles can be found by dividing the total factored dead + live girder reactions by the given pile capacity and rounding up to the next highest integer. If no pile load capacity is available, use an estimate of the load capacity based on the soil conditions. The maximum pile spacing is 3000 mm. The minimum pile spacing is the larger of 900 mm, or 2.5 times the diameter of round piles, or 2 times the diagonal dimension of H-piles (The 2x criteria only controls for HP360 piles). Note that the approximate range of allowed pile spacing calculated below assumes 900 mm is the minimum pile spacing, and may suggest a range which is not permitted based on pile dimensions. The pile location check made below should flag any erroneous spacings attempted, however.

DM-4 Ap.G.1.4.2
D10.7.1.5

Maximum total factored dead + live girder reactions
(1809.25)(2) + (1844.50)(2) = 7307.51 kN 1642.79 k
Number of piles | 11 |
Approximate range of allowed pile spacing for 11 piles is about 1230 to 1280 mm
Chosen pile spacing along abutment | 1244.6 | mm 4.08 ft
Total pile length, L_{tot} = | 11277.6 | mm 37.00 ft

The minimum and maximum edge distance for the end piles is intended to keep the piles close to the end of the integral abutment in order to provide support for the attached wingwalls, without getting too close to the end of the abutment.

Minimum edge distance to centerline of piles	450	mm	17.72 in	D10.7.1.5
Maximum edge distance to centerline of piles	750	mm	29.53 in	DM-4 Ap.G.1.4.2.1

Pile location check OK
Pile spacing normal to the longitudinal axis of span
1244.6sin(90) = 1245 mm 4.08 ft

The moment of inertia of the pile group is calculated similarly to the girders above and is used to determine the axial forces in the piles due to overturning moments.
Moment of inertia of pile group about the longitudinal axis of the bridge
11(11^2 - 1)(1245^2)/12 = 170393208 mm^2 264110 in^2

Title: Birdge 211 - 34.7 m Single Span Concrete Prestressed I-girder
90° skew, 3.39 m girder spacing

By: WS
Checked:
Date: 3/10/2003
Date:

Pile loads due to wind and centrifugal forces

At this point, an iterative procedure is initiated to determine the loads on the piles. Initially, a depth to fixity of the piles is assumed. Later, the actual depth to fixity is calculated using the computer program COM624P, and this value is adjusted as necessary. The procedure is repeated until the estimated value is within 10% of the value obtained from the COM624P computer program. An initial choice of 5000-6000 mm to the point of fixity is reasonable.

Assume depth to pile fixity of 3657.6 mm 12.00 ft

The overturning moment resisted by the piles is calculated similarly to the overturning moments resisted by the girders, except the moment arm extends to the point of assumed pile fixity (see figure below - note that five I-girders and six H-piles are used for illustration purposes only). Wind uplift forces result in the same overturning moments on the piles as calculated earlier for the girders.

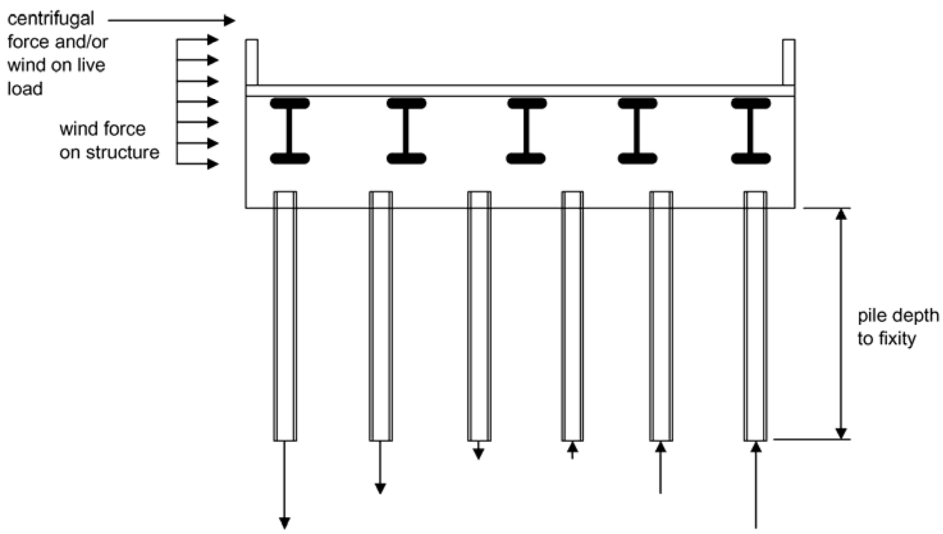

Wind on structure	moment = (136.55)(3658+2563.36800000002+20+3274.949/2)/1000 =		
		1075.84 kN-m	793.50 k-ft
Wind on live load	moment = (25.37)(1800+3658+2563.36800000002+2278.949)/1000 =		
		261.26 kN-m	192.70 k-ft
Centrifugal forces	moment = (0.00)(1800+3658+2563.36800000002+2278.949)/1000 =		
		0.00 kN-m	0.00 k-ft

The unfactored extreme loads per pile for wind cases are calculated similar to the girder reactions

Extreme forces due to wind on the structure

WS	max	(1075.84)(1000)(11-1)(1245)/(2*170393208) =		
			39.29 kN/pile	8.83 k/pile
	min	-(1075.84)(1000)(11-1)(1245)/(2*170393208) =		
			-39.29 kN/pile	-8.83 k/pile

Extreme forces due to uplift

Uplift	max	-218.02/11 + (712.50)(1000)(11-1)(1245)/(2*170393208) =		
			6.20 kN/pile	1.39 k/pile
	min	-218.02/11 - (712.50)(1000)(11-1)(1245)/(2*170393208) =		
			-45.84 kN/pile	-10.31 k/pile

Extreme forces due to wind on live load

WL	max	(261.26)(1000)(11-1)(1245)/(2*170393208) =		
		9.54 kN/pile	2.15 k/pile	
	min	-(261.26)(1000)(11-1)(1245)/(2*170393208) =		
		-9.54 kN/pile	-2.15 k/pile	

Extreme forces due to centrifugal force

CE	max	(0.00)(1000)(11-1)(1245)/(2*170393208) =		
		0.00 kN/pile	0.00 k/pile	
	min	-(0.00)(1000)(11-1)(1245)/(2*170393208) =		
		0.00 kN/pile	0.00 k/pile	

Additional Dead + Live Loads (Approach Slab, Wingwalls, and Abutment)

The approach slab live load is calculated assuming the slab is simply supported at the ends, the lane load only is present in all lanes, and the total reaction is distributed equally to all piles. The truck load is not included here because it was already included in the bridge loads. As previously, the multiple presence factor is not used. Dead loads from the approach slab are also distributed equally to all piles.

Approach slab dimensions

Approach slab thickness =	450 mm	18 in	DM-4 App. G 1.5
Approach slab length =	7500 mm	25 ft	

Approach slab loads

Approach Slab Load = (2.4)(9.81)(12192)(7500)(0.45)/2000000 =			
	484.39 kN	108.90 k	
Approach Slab Future Wearing Surface = (0.15)(9.81)(12192)(7500)/2000000 =			D3.5.1
	67.28 kN	15.12 k	
Approach Slab Lane Load (1 lane) = (9.3)(7500)/2000 =			A3.6.1.2.4
	34.88 kN	7.84 k	
Approach Slab Pedestrian Live Load (total reaction) = (0.0036)(0)(7500)/2000 =			
	0.00 kN	0.00 k	
Abutment self-weight Dead Load = (2.4)(9.81)(13772)(1200)(4806)/1000000000 =			
	1869.90 kN	420.37 k	

Wingwalls and parapet load

The parapet weight/length can be input for wingwall dead load calculations. A typical 440 mm wide concrete parapet weighs about 7.60 N/mm. Any other miscellaneous loads can also be included in this number, but note that the value will be multiplied by the length of the wingwall plus abutment (900 + 1200/SIN(90) = 2100 mm) times two since parapets are assumed to be on both sides of the bridge.

Parapet weight/length $\boxed{7.60}$ N/mm 0.521 k/ft

Weight of two wingwalls = (2)(2.4)(9.81){(4805.74100000001)(300)(873+300sin(90)/2)+[(900-300)(873)(4805.74100000001+4805

Weight of two parapets = (2)(7.60)(900+1200/sin(90))/1000

Total weight of wingwalls and parapets = 219.97 kN 49.45 k

Thermal Expansion

The thermal expansion of the bridge is calculated assuming the entire superstructure length, L, is unrestrained, and undergoes a uniform thermal expansion. This ignores the pier stiffnesses (if any) and passive soil pressure against the backwalls. For design purposes, a percentage of this thermal expansion can be assigned to take place at the abutment under consideration. It is the responsibility of the designer to determine the percentage of expansion. In some cases, such as single spans with identical abutments, simply assigning 50% of the movement to each end may be appropriate. In other cases, such as for continuous structures with unsymmetrical piers, a more in-depth thermal analysis taking pier and abutment stiffnesses into account is required. See DM-4 Ap.G.1.2.7.4 for thermal movement requirements.

The coefficient of thermal expansion and temperature range are assigned based on the girder material, concrete or steel.

Coefficient of thermal expansion, α	10.8E-6 /°C	(concrete girders)	D5.4.2.2
Temperature range, Δ_T ($\pm$)	44 °C		DM-4 Ap.G.1.2.7.4
Load factor, ϕ_T	1.0		DM-4 Ap.G.1.2.7.6
Total $\pm$change in length of the bridge, $\phi_T\alpha\Delta_T L$ =	(1.0)(0.0000108)(44)(34747.2) =		
	16.5 mm	0.65 in	

Title: Birdge 211 - 34.7 m Single Span Concrete Prestressed I-girder By: WS Date: 3/10/2003
90° skew, 3.39 m girder spacing Checked: ________ Date: ________

The percentage of thermal expansion that occurs at the abutment being designed is input here. The value should be between 0 and 100%. For symmetrical structures, 50% of the expansion occurs at each abutment. For unsymmetrical structures, use the procedure described in DM-4 Ap.G1.2.7.4 to determine the percentage of movement at each end.

Percentage of expansion at abutment being designed 50 %

Maximum movement (expansion or contraction) at abutment (±), Δ

(0.50)(16.5) = 8.3 mm 0.33 in

The thermal expansion of continuous bridges induces an axial force in the piles, P_T, which is estimated using the simplified elastic procedure illustrated below (see figure on following page). This procedure assumes that the full passive pressure of the soil is acting on the abutment. Note that the additional pile axial force is zero in a simple span with passive pressure acting at the same height on both abutments.

The coefficient of passive earth pressure has been found to vary from about 3.0 for loose sand to about 6 for dense sand. PennDOT requires that the region immediately adjacent to the abutment be only nominally compacted, so 3.0 is an acceptable value. DM-4 Ap.G.1.2.7.4

Coefficient of passive earth pressure, k_p = 3.0

The density of loose sand given in the AASHTO-LRFD Bridge Design Specification is 1600 kg/m^3. Multiplying by 9.81 m/s^2 converts this value to weight. A3.5.1

Soil unit weight, γ = (1600)(9.81) = 15.70 kN/m^3 100 lb/ft^3

Using the coefficient of passive earth pressure, the soil density, and the depth of the abutment, the force per unit length on the abutment can be calculated.

Force from soil on abutment, $F=1/2\, k_p\gamma H^2$ = (1/2)(3.0)(15.70)(4805.74100000001/1000)^2 =
543.8 kN/m 37.3 k/ft

The total longitudinal force on the abutment can be found by multiplying by the projected length of the abutment on a line perpendicular to the longitudinal axis of the bridge, which is equal to the out-to-out width of the bridge.

Total passive earth pressure force on abutment, F = (543.8)(13072)/1000 =
7107.9 kN 1597.9 k

The previously assumed depth to pile fixity, L_p = 3657.6 mm 12.00 ft

Using simple equilibrium by taking the moment about point A, the axial reaction per pile due to the force, F, and the displacement, Δ, can be calculated as:

F_p = 2FH / 3L / number of piles = (2)(7107.9)(4805.74100000001)/[(3)(34747.2)]/11 =
59.6 kN/pile 13.4 k/pile

The moment induced in the piles by the thermal movement can be determined using the following equation. The top of the pile is assumed to be fixed.

The moment, $M_T = 6E_pI_p\Delta/L_p^2$ = (6)(200)(77100000)(8.3)/(3657.6^2)/1000 =
57.1 kN-m/pile 42.11 k-ft/pile

Check to make sure the moment, M_T, does not exceed the plastic moment, M_p. Even though the maximum flexural resistance of the pile may be lower, the plastic moment is conservatively used here as an upper bound.

Plastic moment, $M_p = F_yZ_{y\text{-}y}$ = (245)(763000)/1000000 = 186.9 kN-m 137.88 k-ft
since 57.1 < 186.9 - use M_T = 57.1 kN-m 42.11 k-ft

The horizontal force induced in the pile by the thermal deformation can be determined using the following equation. The top of the pile is assumed to be fixed.

The horizontal force, $H_T = 2M_T/L_p$ = (2)(57.1)(1000)/3657.6 =
31.2 kN/pile 7.0 k/pile

The total axial force induced in the pile due to these three components is equal to:

$2FH/3L+H_TH/L+M_T/L$ = 59.6 + (31.2)(4805.74100000001)/34747.2 + 57.1/(34747.2/1000) = 65.5 kN (14.7 k) /pile

Axial force induced in piles, P_T = 0.0 kN/pile 0.0 k/pile

(Note: = 0 is used for single spans because the lateral loads on the two abutments will balance each other and no net vertical load on the piles will exist)

L

Title: Birdge 211 - 34.7 m Single Span Concrete Prestressed I-girder
90° skew, 3.39 m girder spacing

By: WS Date: 3/10/2003
Checked: ______ Date: ______

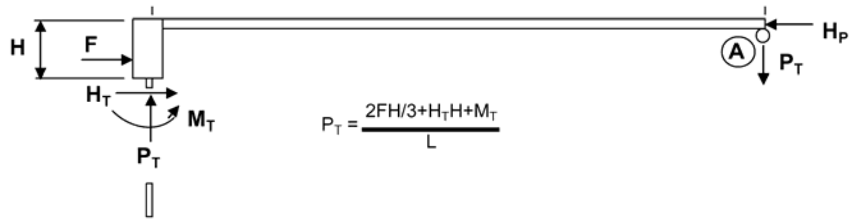

Calculate the maximum factored load on the most heavily loaded pile (see Load Factors tab for load factors for each load combination). Since the factored dead and live loads from the interior and exterior girders have already been calculated, the sum of the girder loads is calculated assuming two exterior girders and the remaining ones interior. These loads, as well as any additional vertical loads, are distributed equally to all piles. The factored extreme overturning loads, which occur on the exterior piles are added. The η_i modifier is also included.

Extreme Factored Dead + Live Loads per pile

Strength I	max	[(1844.5)(2)+(1809.3)(2)]/11 + 1.00{[1.25(484.4+1869.9+220.0)+1.50(67.3)+1.75(3)(34.9)]/11 + 1.75(0.0) + 1.00(0.0)} =	982.67 kN/pile	220.91 k/pile
	min	[(722.9)(2)+(697.5)(2)]/11 + 1.00{[0.90(484.4+1869.9+220.0)+0.00(67.3)+1.75(3)(0.0)]/11} + 1.00[1.75(0.0) + 1.00(0.0)] =	468.87 kN/pile	105.41 k/pile
Strength IP	max	[(1678.5)(2)+(1643.2)(2)]/11 + 1.00{[1.25(484.4+1869.9+220.0)+1.50(67.3)+1.35(3)(34.9)+1.75(0.0)]/11 + 1.35(0.0) + 1.00(0.0)} =	918.49 kN/pile	206.49 k/pile
	min	[(722.9)(2)+(697.5)(2)]/11 + 1.00{[0.90(484.4+1869.9+220.0)+0.00(67.3)+1.35(3)(0.0)+1.75(0.0)]/11} + 1.00[1.35(0.0) + 1.00(0.0)] =	468.87 kN/pile	105.41 k/pile
Strength II	max	[(1816.5)(2)+(1781.3)(2)]/11 + 1.00{[1.25(484.4+1869.9+220.0)+1.5(67.3)+1.35(3-1)(34.9)]/11 + 1.35(0.0) + 1.0(0.0)} =	964.40 kN/pile	216.81 k/pile
	min	[(722.9)(2)+(697.5)(2)]/11 + 1.00{[0.9(484.4+1869.9+220.0)+0(67.3)+1.35(2)(0.0)]/11} + 1.00[1.35(0.0) + 1.0(0.0)] =	468.87 kN/pile	105.41 k/pile
Strength III	max	[(1118.2)(2)+(1082.9)(2)]/11 + 1.00{[1.25(484.4+1869.9+220.0)+1.50(67.3)]/11 + 1.40(39.3) + + 1.00(0.0)} + 1.00(1.40)(6.2) =	765.58 kN/pile	172.11 k/pile
	min	[(722.9)(2)+(697.5)(2)]/11 + 1.00{[0.90(484.4+1869.9+220.0)+0.00(67.3)]/11} + 1.00[1.40(-39.3) + 1.00(0.0) + 1.40(-45.8)] =	349.69 kN/pile	78.61 k/pile
Strength V	max	[(1678.5)(2)+(1643.2)(2)]/11 + 1.00{[1.25(484.4+1869.9+220.0)+1.50(67.3)+1.35(3)(34.9)]/11 + 0.40(39.3) + 1.00(9.5) + 1.35(0.0) + 1.00(0.0)} =	943.75 kN/pile	212.16 k/pile
	min	[(722.9)(2)+(697.5)(2)]/11 + 1.00{[0.90(484.4+1869.9+220.0)+0.00(67.3)+1.35(3)(0.0)]/11} + 1.00{0.40(-39.3) + 1.00(-9.5) + 1.35(0.0) + 1.00(0.0)} =	443.61 kN/pile	99.73 k/pile

Controlling Loads	max STR I	982.67 kN/pile	220.91 k/pile
	min STR III	349.69 kN/pile	78.61 k/pile

Lateral Pile Analysis

Knowing the soil properties at the abutment (taken from the geotechnical report), and the properties of the piles, and using the calculated design values for maximum factored axial load, live load rotation, and thermal expansion, the computer program COM624P can be used to determine the depth to pile fixity, the depth to the first inflection point of the pile, the unbraced length of the pile, the depth at which the lateral pile deflection is equal to 2% of the pile diameter (needed for friction piles only), and the maximum moment in the pile below the first point of inflection. Since a pre-augered hole, 3000 mm minimum depth, filled with loose sand, is present at the top of the piles, the COM624P analysis should use the properties of the weaker of either the loose sand or the actual soil for the depth of the pre-augered hole. The procedure for running COM624P is as follows:

Run COM624P using the top of pile boundary condition which permits a specified lateral deflection along with an applied moment. Apply the maximum pile vertical axial load to the pile simultaneously with the abutment maximum thermal movement. The axial load and deflection should be input as positive values. Apply the negative plastic moment at the head of the pile and run the analysis.
1 - If the calculated pile head rotation (positive value) is less than the end rotation of the pile due to live loads and composite dead loads, the analysis is complete.
2 - If the calculated pile head rotation is greater than the end rotation of the pile due to live loads and composite dead loads, iteratively reduce the moment at the head of the pile until the rotations are equal (within tolerance).

Title: Birdge 211 - 34.7 m Single Span Concrete Prestressed I-girder
90° skew, 3.39 m girder spacing

By: WS
Date: 3/10/2003
Checked:
Date:

Design values for COM624P:

Pile Section	HP310x110	HP12x74
Pile width or diameter	0.308 m	12.1 in
Pile moment of inertia	0.0000771 m^4	185 in^4
Pile area	0.0141 m^2	21.9 in^2
Vertical axial load	982.7 kN	220.9 k
Design rotation	0.0036 radians	0.207 degrees
Design thermal movement	0.0083 m	0.33 in
Plastic moment (if required)	-186.9 kN-m	-137.9 k-ft

At this point COM624P should be run. COM624P is run using a text file as input. There are two ways to develop this text input file. The first is to use the input file editor program supplied with COM624P. The second method is to use any text editor to develop the input file using the COM624P users manual as a guide. If this second method is chosen, a template file for COM624P can be created from the COM624P Input tab. Once the template is created, it can be edited using any text editor.

Results from COM624P (See figures below for illustrations of the data required from the program).

The depth to fixity is defined as the shallowest depth at which the pile deflection is equal to zero.

Depth to fixity, L_p = 3733.8 mm 147.00 in

The depth to the uppermost point of inflection is the depth measured from the bottom of the abutment to the first point of zero moment on the pile moment diagram.

Depth to first point of inflection, L_{i1} = 1625.6 mm 64.00 in

The depth to the second point of inflection is the depth measured from the bottom of the abutment to the second point of zero moment on the pile moment diagram. For a short pile with only one point of inflection, input the total pile length

Depth to second point of inflection, L_{i2} = 4554.22 mm 179.30 in

The depth above which friction is ineffective is input here. For a laterally deflected pile, this depth is defined as the point where the deflection is 2% of the pile diameter. For the present pile (see section properties above), this deflection value is (0.02)(308) = 6.16 mm (0.24 in). The length of pile above this point is considered ineffective in the design of friction piles. If the pile is driven through an embankment fill which is to be neglected in calculating pile friction resistance, input the depth of fill. This value is not required for end bearing piles. DM-4 Ap.G.1.4.2.2

Depth to 2% deflection, L_n = 3111.5 mm 122.50 in

The maximum bending moment in the pile is the maximum moment below the uppermost point of inflection and neglects the moment at the pile-pile cap interface.

Maximum bending moment in pile, M_u = 39.3 kN-m 28.99 k-ft

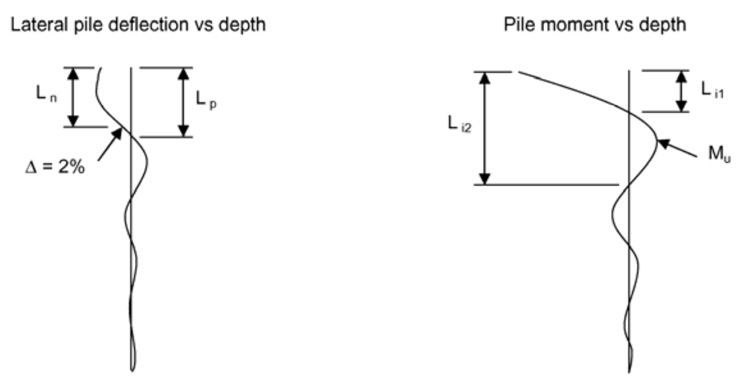

Typical COM624P results (exaggerated)

Title: Birdge 211 - 34.7 m Single Span Concrete Prestressed I-girder
90° skew, 3.39 m girder spacing

By: WS
Date: 3/10/2003
Checked:
Date:

Pile Capacity Analysis

Check the geotechnical resistance of the pile

The geotechnical resistance can be supplied by skin friction, end bearing, or both. The easiest way to eliminate one or the other from contributing to the resistance is to simply put zero in for the unit resistance of the one to be neglected. The resistance factors for bearing capacity and skin friction should be chosen according to the provisions of DM-4.

Shaft and tip resistance factors

Tip (bearing) resistance factor, ϕ_{qp}	0.50		D10.5.4-2
Shaft (skin friction) resistance factor, ϕ_{qs}	0.55		D10.5.4-2

Tip resistance

Unit tip resistance, q_p	140 MPa	20 ksi	
Nominal pile tip resistance, $Q_p = q_pA_p$ =	(140)(14100)/1000 =		
	1974.00 kN	443.8 k	

The effective shaft length is the total shaft length minus a length at the top of the pile which is ineffective due to the lateral movement which occurs. Using a displacement of 2% of the pile diameter as the boundary above which skin friction becomes ineffective has been found to be reasonable. The depth, L_n, at which the displacement reaches this critical value was determined previously using the computer program COM624P.

Shaft resistance (skin friction)

Depth to 2% deflection, L_n =	3111.50 mm	10.21 ft
Effective shaft length, $L_e = L_{tot} - L_n$ =	11277.6 - 3111.5 =	
	8166.1 mm	26.79 ft

The unit shaft resistance (skin friction) is required for friction piles. For layered soils, a weighted average unit shaft resistance should be used.

Unit shaft resistance, q_s	0.065 MPa	9.43 psi
Nominal pile shaft resistance, $Q_s = q_sA_s$	= (0.065)(1825)(8166.1)/1000 =	
	968.81 kN	217.8 k

Total factored resistance per pile, $Q_R = \phi_{qp}Q_p + \phi_{qs}Q_s$

(0.50)(1974.00) + (0.55)(968.81) = 1519.85 kN 341.7 k

1519.8 kN (341.7 k) > 982.7 kN (220.9 k) - OK

Check the capacity of the pile as a structural member

The pile resistance factors in DM-4 are to be applied assuming only axial forces are present at the tip of the pile, where any driving damage is likely to occur. At the top of the pile, where axial forces and bending are present, the piles are generally undamaged. For these reasons a lower load factor is used when the axial force only is considered. The combined flexure and axial force resistance factors are higher. The calculated nominal axial resistances are also different, as the pile is assumed fully supported at the tip, but an unbraced length is assumed between the top two points of inflection.

Pile resistance factors

Axial compression only, ϕ_c	0.45		D6.5.4.2
Axial compression, ϕ_c plus	0.60	(used together)	D6.5.4.2
Flexure, ϕ_f	0.85		

Compressive resistance (lower portion of pile - axial loads only)

Nominal axial resistance, P_n = FyAs = (245)(14100)/1000 =

3454.5 kN 776.6 k

For the check of axial capacity, the entire axial load is considered for end bearing piles. For friction piles, the load at the pile tip is assumed to be the total pile load minus 50% of the factored friction resistance of the pile.

Check axial capacity
Axial load at tip of pile, P_u = (≥ 0.0)
982.67 kN 220.9 k
Factored axial resistance, $P_r = \phi P_n$ = (0.45)(3454.50) =
1554.53 kN 349.5 k
1554.53 kN (349.5 k) > 982.67 kN (220.9 k) - OK

The unbraced length is defined as the distance between the top two points of inflection (zero moment) on the pile moment diagram.
(4554) - (1626) = 2928.62 mm 115.30 in
As a structural member, the pile length between the top two inflection points is assumed to be a pinned-pinned member. The effective length factor, K, of a pinned-pinned member = 1.0.

Compressive resistance (upper portion of pile - under combined axial load and moment)

For steel H-piles
F_e = Fy = 245 MPa
E_e = Est = 200000 MPa
$\lambda = (KL_b/r_s\pi)^2 (F_e/E_e)$ = [(1.0*2928.62)/(74*3.142)]^2 (245/200000) = 0.195 A6.9.4.1
if $\lambda \le 2.25$, $P_n = 0.66^{\lambda}F_eA_s$, if $\lambda > 2.25$, $P_n = 0.88F_eA_s / \lambda$

Nominal axial resistance, P_n = 0.66^0.195 (245)(14100)/1000 =
3185.7 kN 716.2 k
Factored axial resistance, $P_r = \phi P_n$ = (0.6)(3185.7) =
1911.4 kN 429.7 k

Flexural resistance of steel H-piles
Plastic Moment, $M_p = F_y Z_y$ = (245)(763000)/1000000 =
186.9 kN-m 137.9 k-ft
Yield Moment, $M_y = F_y S_y$ = (245)(497000)/1000000 =
121.8 kN-m 89.8 k-ft

For H-piles, if the width-to-thickness ratio of the flanges is not sufficient to consider the section compact, an interaction formula from AISC is used to interpolate between the plastic moment resistance and the yield moment resistance.

$M_n = M_p - (M_p - M_y)(\lambda - \lambda_p)/(\lambda_r - \lambda_p) \le M_p$ AISC-LRFD, Ap.F F1., 1994

For pipe piles, if the diameter-to-thickness ratio of the pipe is not sufficient to consider the section compact, then the section is considered non-compact. A6.12.2.3.2

Width-to-thickness ratio of projecting flange element
λ = bf / 2tf = 310/(2*15.5) = 10.00
Width-to-thickness criteria for flange element to reach plastic moment
λ_p = 0.38 * $(E / F_y)^{1/2}$ = 0.382*(200000/245)^0.5 = 10.91 A6.10.5.2.3c
Width-to-thickness criteria for flange element to reach yield stress
λ_r = 0.56 * $(E / F_y)^{1/2}$ = 0.56*(200000/245)^0.5 = 16.00 A6.9.4.2
Nominal flexural resistance, M_n = Mp
Use M_n = 186.94 kN-m 137.88 k-ft

Pile factored flexural resistance, $M_r = \phi M_n$ = (0.85)(186.9) =
158.9 kN-m 117.19 k-ft
Check moment-axial interaction
P_u / P_r = 982.7/1911.4 = 0.51 A6.9.2.2
if $P_u / P_r < 0.2$ then $P_u / 2.0P_r + M_u / M_r \le 1.0$
if $P_u / P_r \ge 0.2$ then $P_u / P_r + (8.0 / 9.0) M_u / M_r \le 1.0$
Moment - axial interaction = 982.7/1911.4 + (8.0/9.0)(39.3/158.9) = 0.73 ≤ 1.00 OK

Title: Birdge 211 - 34.7 m Single Span Concrete Prestressed I-girder By: WS Date: 3/10/2003
90° skew, 3.39 m girder spacing Checked: ________ Date: ________

Pile Ductility Requirement

Since the top of the pile will often have to undergo inelastic rotations, a check is performed based on a method contained in Greimann et. al. (1987) for determining whether the pile has enough ductility to undergo the required calculated deflections. DM-4 Ap.G.1.4.2.5

Ductility Criterion, $\Delta \le \Delta_i$, where
Δ = design displacement
Δ_i = allowable displacement

The design displacement is the total displacement due to the full range of thermal expansion / contraction at the abutment being designed. Most of the data for thermal displacements was listed previously, and the percentage of the total displacement of the bridge is denoted by k.

Temperature range, Δ_T = 50 °C Concrete girders D3.12.2.1

Design displacement, $\Delta = k\phi_T\alpha\Delta_T L$ = (0.50)(1.0)(0.0000108)(50)(34747.2) =
9.4 mm 0.37 in

The design rotation is the total factored rotation at the support due to live load and composite dead loads which is equal to the sum of the absolute values of the maximum and minimum factored rotations.

Total design rotation, $\theta_w = \theta_{min} + \theta_{max}$ = 0.0036 + 0.0000 =
0.0036 radians 0.207 degrees

Pile yield stress, F_y 245 MPa 36 ksi

The plastic rotation is the rotation required to form a plastic hinge in the pile.

Plastic rotation, $\theta_p = F_y Z L_i / 3EI$ = (245)(763000)(1625.6)/(3*200000*77100000) =
0.0066 radians 0.376 degrees

Inelastic rotation capacity reduction factor, C_i ($0 \le C_i \le 1.0$)

$C_i = 3.17 - 5.68 \cdot (F_y / E)^{1/2}$ (bf / 2tf) = 3.17 - 5.68 * (245/200000)^0.5 [310/(2*15.5)] = 1.18
Use C_i = 1.00

Inelastic rotation capacity, $\theta_{inel} = (K^*C_i M_p L_i)/EI$ For H-piles, K = 1.500
[(1.500)(1.00)(186.94)(1000)(1625.6)]/[(200)(77100000)] =
0.0296 radians 1.694 degrees

Allowable displacement, $\Delta_i = 4^*L_i^*[(\theta_{inel} - \theta_w)/2 + \theta_p]$ = (4)(1625.6)[(0.0296 - 0.0036)/2 + 0.0066] =
127.1 mm 5.00 in

9.4 mm (0.37 in) < 127.1 mm (5.00 in) - OK

Pile Cap Reinforcing Design

Extreme Factored Dead + Live Loads per girder.

The extreme interior and exterior vertical girder reactions are listed below. When combined with the extreme wind and centrifugal reactions for an exterior girder, the result is a conservative maximum girder reaction for pile cap design.

Strength I	maximum of 1844.50 and 1809.25 =	1844.50 kN	414.66 k
	minimum of 722.88 and 697.50 =	697.50 kN	156.80 k
Strength IP	maximum of 1678.48 and 1643.23 =	1678.48 kN	377.34 k
	minimum of 722.88 and 697.50 =	697.50 kN	156.80 k
Strength II	maximum of 1816.51 and 1781.26 =	1816.51 kN	408.37 k
	minimum of 722.88 and 697.50 =	697.50 kN	156.80 k
Strength III	maximum of 1118.15 and 1082.90 =	1118.15 kN	251.37 k
	minimum of 722.88 and 697.50 =	697.50 kN	156.80 k
Strength V	maximum of 1678.48 and 1643.23 =	1678.48 kN	377.34 k
	minimum of 722.88 and 697.50 =	697.50 kN	156.80 k

Title: Birdge 211 - 34.7 m Single Span Concrete Prestressed I-girder
90^{o} skew, 3.39 m girder spacing

By: WS Date: 3/10/2003
Checked: ________ Date: ________

The following reactions are the extreme factored dead and live load girder reaction calculated previously, plus the extreme reactions on the exterior girder due to wind, centifugal, and thermal forces. It is recognized that the extreme reactions due to lateral forces occur on the exterior girders, while the extreme gravity reaction may occur on the interior girders, but combining the two should not be overly conservative. The η_i modifier is included here as well.

Strength I	max	1844.50 + 1.00[1.75(0.00) + 1.00(0.00)(11/4)] =	1844.50 kN/girder	414.66 k/girder
	min	697.50 + 1.00[1.75(0.00) + 1.00(0.00)(11/4)] =	697.50 kN/girder	156.80 k/girder
Strength IP	max	1678.48 + 1.00[1.35(0.00) + 1.00(0.00)(11/4)] =	1678.48 kN/girder	377.34 k/girder
	min	697.50 + 1.00[1.35(0.00) + 1.00(0.00)(11/4)] =	697.50 kN/girder	156.80 k/girder
Strength II	max	1816.51 + 1.00[1.35(0.00) + 1.00(0.00)(11/4)] =	1816.51 kN/girder	408.37 k/girder
	min	697.50 + 1.00[1.35(0.00) + 1.00(0.00)(11/4)] =	697.50 kN/girder	156.80 k/girder
Strength III	max	1118.15 + 1.00[1.40(8.53)] + 1.00[1.40(20.02) + 1.00(0.00)(11/4)] =	1158.13 kN/girder	260.36 k/girder
	min	697.50 + 1.00[1.40(-117.54+ -20.02) + 1.00(0.00)(11/4)] =	504.91 kN/girder	113.51 k/girder
Strength V	max	1678.48 + 1.00[0.40(20.02) + 1.00(9.15) + 1.35(0.00) + 1.00(0.00)(11/4)] =	1695.64 kN/girder	381.20 k/girder
	min	697.50 + 1.00[0.40(-20.02) + 1.00(-9.15) + 1.35(0.00) + 1.00(0.00)(11/4)] =	680.34 kN/girder	152.95 k/girder

Controlling Loads	max STR I	1844.50 kN/girder	414.66 k/girder
	min STR III	504.91 kN/girder	113.51 k/girder

Pile Cap Reinforcing

Knowing the maximum girder reaction, the pile spacing, the dimensions of the cap and diaphragm, and the material properties, the pile cap reinforcing can be calculated. The loads used for design are the maximum simply supported beam moments reduced by 20% to account for the continuity over the piles. Calculations for reinforcement are performed on the Cap Reinforcement tab.

Concrete compressive strength, f'_c	20.7	MPa	3.0	ksi
Reinforcing steel yield strength, F_y	413.7	MPa	60	ksi
Maximum factored girder reaction, R_u	1844.5	kN	414.7	k
Pile Spacing	1245	mm	4.08	ft

Pile cap reinforcement - use 4 # 25 bars top and bottom of cap beam

Title: Birdge 211 - 34.7 m Single Span Concrete Prestressed I-girder
90° skew, 3.39 m girder spacing

By: WS
Checked: ________
Date: 3/10/2003
Date: ________

ANALYSIS SUMMARY PAGE

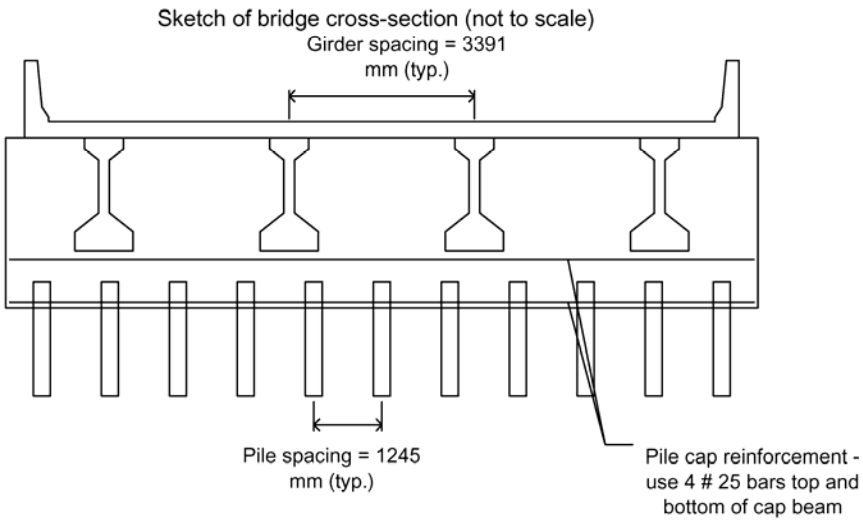

Bridge Description
Bridge length: 34747.2 mm (114.00 ft) simple span.
Skew: 90 degrees.
Maximum number of traffic lanes: 3.
Curb-to-curb roadway width: 12192 mm (40.00 ft).
Total width of sidewalk(s): 0 mm (0.00 ft).
Out-to-out superstructure width: 13072 mm (42.89 ft).
Maximum number of traffic lanes with no sidewalks: 3.
Number of girders: 4 prestressed concrete I-girders
Girder spacing: 3390.9 mm (11.13 ft).
Moment of inertia of the girders about the longitudinal axis of the bridge: 57491014 mm^2 (89111 in^2).
Girders depth: 1981.2 mm (11.13 ft).
Girder width: 1066.8 mm (3.50 ft).
Bearing pad thickness 20 mm (0.8 in).
Average deck + haunch thickness: 277.749 mm (10.94 in).
Parapet height: 1016 mm (3.33 ft).

Integral Abutment Description
Abutment width: 1200 mm (3.94 ft).
Abutment length: 13772 mm (45.18 ft).
Pile cap depth: 2374.39199999999 mm (7.79 ft) at the left end.
2563.36800000002 mm (8.41 ft) at the center.
2606.03999999999 mm (8.55 ft) at the right end.
Average pile cap depth: 2526.79200000001 mm (8.29 ft).
Pile cap reinforcement: 4 # 25 bars top and bottom.
End diaphragm height (equal to the deck + haunch + girder + bearing pad depth): 2278.949 mm (7.48 ft).
Total average abutment height: 4805.74100000001 mm (15.77 ft).
Wingwall length: 900 mm (2.95 ft) long stubs for detached wingwalls at each end of the abutment.

Pile Description
Number of piles: 11 - HP310x110 (HP12x74) piles.
Pile spacing: 1244.6 mm (4.08 ft) in a single row along the centerline of bearing of the abutment.
Moment of inertia of the piles about the longitudinal axis of the bridge: 170393208 mm^2 (264110 in^2).
Design pile length: 11277.6 mm (37.00 ft).
Depth to fixity: 3733.8 mm (147.00 in).
Unbraced length: 2928.62 mm (115.30 in).
Depth to the first point of inflection: 4554.22 mm (179.30 in).
Depth to the point where the lateral deflection is 2% of the pile width (friction engaged): 3111.5 mm (122.50 in).
Pile yield moment, My: 121.8 kN-m (89.8 k-ft).
Pile plastic moment, Mp: 186.9 kN-m (137.9 k-ft).

Title: Birdge 211 - 34.7 m Single Span Concrete Prestressed I-girder
90° skew, 3.39 m girder spacing

By: WS
Checked:
Date: 3/10/2003
Date:

Total factored geotechnical capacity of the pile: 1519.8 kN (341.7 k).
Factored axial resistance of the pile at the tip: 1554.5 kN (349.5 k).
Factored axial resistance of upper portion of pile for use in interaction equation: 1911.4 kN (429.71 k).
Factored flexural resistance of upper portion of pile for use in interaction equation: 158.9 kN-m (117.2 k-ft).

Loads and Deformations
Maximum girder reaction: 1844.5 kN (414.7 k) due to the STR I load case
Maximum axial force in the pile: 982.7 kN (220.9 k) due to the STR I load case.
Maximum bending moment in the pile (other than at the pile-abutment connection): 39.3 kN-m (29.0 k-ft).
Total maximum design movement for the abutment: 18.8 mm (0.74 in).
Maximum movement in one direction: 8.3 mm (0.33 in).
Maximum design rotation: 0.0036 radians (0.207 degrees).
Axial load-moment interaction equation result for the pile (maximum allowable is 1.00): 0.73.

Warnings and Errors
The spreadsheet generated 1 warning(s) and 0 error(s).
The 1 warning(s) should should be checked to make sure requirements are satisfied.

An evaluation of the above-presented PennDOT program output was performed through comparisons with field data and the bridge 211 original design. The five program design sections were evaluated individually and are summarized in Table 7.2.

Table 7.2. Bridge 211: Program Evaluation

Design Part	Discussion	Suggested Improvements
1) Bridge Data (pp. 1-3)	Minor warning concerning girder depth greater than the specified value by DM-4 is reported.	-
2) Integral Abutment Data (pp. 3-4)	Input data sequence and explanations are clearly presented.	-
3) Load Data (pp. 5-8)		
• Dead and live load girder reactions (p. 6)	Calculation in the program strictly follows DM-4 Ap.G 1.2.7.2, which is based on the assumption of equally distributed loads to all piles and removal of the multiple-presence provision. However, this assumption was not applied to the original design calculation.	More study is required to ensure that this assumption does not produce either over- or underestimated results for both narrow and wide bridges.
• Girder end rotation due to composite dead and live loads (pp. 6-7)	The original design calculation assumed integral abutment rigid-body movement and did not consider effects of girder-end rotations on the pile head rotations. Discussion of this issue is continued in section 4.	See design section 4 under *iterative procedure interacting with COM624P*.
4) Pile Data (pp.9-18)		
• Pile properties (p. 9)	The geotechnical report recommends that a 1/16-inch loss in pile thickness (all around) due to corrosion be incorporated.	Input of the anticipated pile thickness loss as well as an option to automatically compute

	This corrosion effect was considered in the original design calculation. The pile properties used in the PennDOT IA program above did not consider this effect - only short-term results are shown.	deteriorated pile properties are suggested.
• Temperature range (p. 11)	The structural continuity of bridge 211 was established during mid Aug. 2004 with an average ambient temperature of 65 ºF. Measured extreme maximum and minimum ambient temperatures were 95 ºF and -8 ºF, respectively, over the 43-month period, below the design value of ±80 ºF.	Modification of the design temperature range as specified in DM-4 Ap.G 1.2.7.4 for U.S. customary units (111 ºF) is required to eliminate inconsistent conversion between Fahrenheit and Celsius.
• Maximum abutment movement (p. 12)	Maximum measured abutment thermal displacements were 0.03 inch and 0.19 inch for expansion and contraction movements, respectively. This is compared to the PennDOT IA program design value of 0.33 inch.	IA program abutment displacement was overestimated due to the extremely large design temperature range and large thermal mass of the bridge. A modification of the temperature range is possible to allow more accurate predictions of displacements.
• Coefficient of passive earth pressure (p. 12)	The maximum measured earth pressure was 8.0 psi. The calculated effective vertical stress at this pressure cell location was 2.5 psi, indicating a maximum equivalent coefficient of earth pressure of 3.25, which is very close to the design value of 3.0.	-
• Axial load per pile (p. 13)	The maximum measured pile axial dead load was 120 k/pile, as compared to the total predicted unfactored axial dead load of 117 k/pile, a difference of -2.5%.	Excellent agreement.

• Iterative procedure interacting with COM624P (p. 14)	Measured girder and abutment rotations, pile strains, and abutment displacements all indicate that the abutment-to-backwall connection is not rigid and the abutment rotates away from the backfill. Assumption of a rigid connection by the PennDOT IA program leads to excessively conservative results. Measured pile moments were 22.5 ft-kip as compared to predicted 121 ft-kip, nearly 5 times larger.	The PennDOT IA program poorly predicts the behavior of the abutment and backwall movement and program assumptions are not valid. A behavior model that incorporates rotational flexibility of the structure needs to be incorporated.
• Axial load-moment interaction (p. 16)	Neither the original design nor the PennDOT IA program design accounts for x-axis pile bending under wind loads and thermally induced abutment movements in the transverse direction.	Corrections of structure flexibility as described above and the inclusion of wind and transverse thermal behavior are required to more accurately predict behavior.
• Abutment/pile cap reinforcement (p. 18)	The PennDOT IA program is limited to design of longitudinal reinforcement for abutment/pile cap.	The design of vertical reinforcement for the abutment/pile cap is suggested.
5) Analysis Summary (pp. 19-20)	Analysis summary is concisely and clearly presented.	-

In addition to the issues discussed in Table 7.2, creep and shrinkage of prestressed concrete members were identified as producing a significant and adverse effect on the long-term behavior of IA bridges, including longitudinal abutment movement and pile stresses. Creep and shrinkage effects are suggested to be incorporated into the analysis and design of IA bridges.

7.4 BRIDGE 222 EVAUATION

Similar to bridges 203 and 211, the bridge 222 design was not based on the PennDOT IA program. The design philosophy used in the design of bridge 222 was based on load factor design. As a consequence, the analysis results obtained for this bridge through the LRFD-based PennDOT IA program are not the same as the original design. In addition to a comparison between the PennDOT IA program and field data, a comparison is also presented between the original LFD method used and the PennDOT IA program.

The PennDOT program results, complete with input data, are presented below. Four sources were used to obtain bridge material and geometric information: (1) design drawings, (2) design calculations, (3) the geotechnical report, and (4) actual pile driving records. The design drawings, design calculations, and geotechnical report were obtained from HDR Inc., of Pittsburgh (the design consultant of this bridge). The average as-built pile length was used in the PennDOT IA program, as presented below.

Title: Bridge 222 - 18.9 m Single Span Concrete Prestressed I-girder
90° skew, 3.594 m girder spacing

By: KP Date: 3/10/2006
Checked: Date:

SPREADSHEET PROGRAM DESCRIPTION

This spreadsheet is intended to be used as an aid in designing and analyzing integral abutments. No users manual is provided, but explanations of input values are given throughout the spreadsheet. The spreadsheet is intended to be used in conjunction with the computer program COM624P, which analyzes the lateral behavior of piles, and with PennDOT's steel or prestressed concrete girder design programs. Design Specifications for integral abutments are available in PennDOT Design Manual Part 4 (DM-4), Appendix G. References to applicable provisions in the DM-4, as well as to the AASHTO LRFD Bridge Design Specifiction, 1994, are made near the right hand margin. Many dimensions for integral abutments are set forth in PennDOT's BD-667M Standard Drawings. The spreadsheet was written in SI units, although the English unit equivalents are also provided, such that either units can be used. Warning and Error messages are provided where possible. An Error message indicates an input value is incorrect and should be changed, a Warning message flags an input value that is suspect, and the user should verify the value, or in some cases, obtain the approval c
Different sheets (tabs), labeled along the bottom of the window, perform different tasks within the spreadsheet. The first tab in the spreadsheet summarizes the input values by providing a simple list which can be printed and filled in by hand, or used to insert the input values. The current tab is the Main tab where most of the analysis takes place. The Scour tab is available for cases where an additional scour check of the piles is required. The COM624P Input tab is used to generate an template for the COM624P computer program. The load factors for each load case are listed on the Load Factor tab. The Cap Reinforcement tab calculates the area of reinforcement needed for the pile cap. The Pile Data tab lists the properties of available H-pile sections, calculates the properties of concrete filled pipe piles, and lists the current pile properties for insertion into the Main tab.

[ ] - denotes input cells

BRIDGE DATA

Input all the geometric and material data for the proposed bridge. This information should be available from a superstructure design already performed independently, as well as a Type, Size, and Location (TS&L) Report, if available.

The girder material is required to determine the coefficient of thermal expansion of the bridge and the uniform temperature change.

Girder material (S - Steel, C - Concrete) [C]

There are three types of girders which can be used with integral abutments: Steel I-girders, concrete I-girders, or concrete spread box girders.

Girder type (I - I-girder, B - Box girder) [I]

Steel bridge lengths in excess of 120000 mm and concrete bridge lengths in excess of 180000 mm require the written approval of the Chief Bridge Engineer for use with integral abutments. In addition, bridges in excess of these limits require consideration of secondary forces such as those caused by creep, shrinkage, thermal gradient, or differential settlements. The methods of applying secondary forces also require the approval of the Chief Bridge Engineer. — DM-4 Ap.G.1.2.1; DM-4 Ap.G.1.2.7.5

Total bridge length - centerline end bearing to centerline end bearing
[18897.6] mm 62.00 ft

The length of the span adjacent to the abutment is required to calculate the pedestrian loads and wind loads on the abutment. It is also used to assess whether the bridge is simply supported or continuous, and in the simplified procedure to determine axial forces induced in the piles in continuous bridges due to thermal movements. Input the total span length for single span bridges.

Length of span adjacent to abutment - centerline bearing to centerline bearing
[18897.6] mm 62.00 ft — DM-4 Ap.G.1.2.1

Skews are limited to 70 degrees or more for continuous spans and single spans longer than 40000 mm. Skews of up to 60 degrees are allowed for single spans in excess of 27000 mm but not longer than 40000 mm. For single spans 27000 mm and less, skews up to 45 degrees are permitted. Only positive skew values >45 or <90 degrees can be used in the spreadsheet. — DM-4 Ap.G.1.2.2

Skew [90] degrees 1.57 radians

Title: Bridge 222 - 18.9 m Single Span Concrete Prestressed I-girder
90° skew, 3.594 m girder spacing

By: KP
Checked:
Date: 3/10/2006
Date:

The curb-to-curb roadway width, the sum of clear sidewalk widths, and the out-to-out superstructure widths are required input. Warnings will be supplied if these values plus conservative estimates of parapet widths are not consistent. It is the users responsibility to make sure these values are correct, however. The roadway and sidewalk widths are used in calculating live load reactions. The out-to-out superstructure width is used to determine both loadings and the length of the integral abutment.

Curb-to-curb (roadway) width	12192	mm	40.00 ft
Sum of clear widths of sidewalks on bridge	0	mm	0.00 ft
Out-to-out superstructure width	13072	mm	42.89 ft

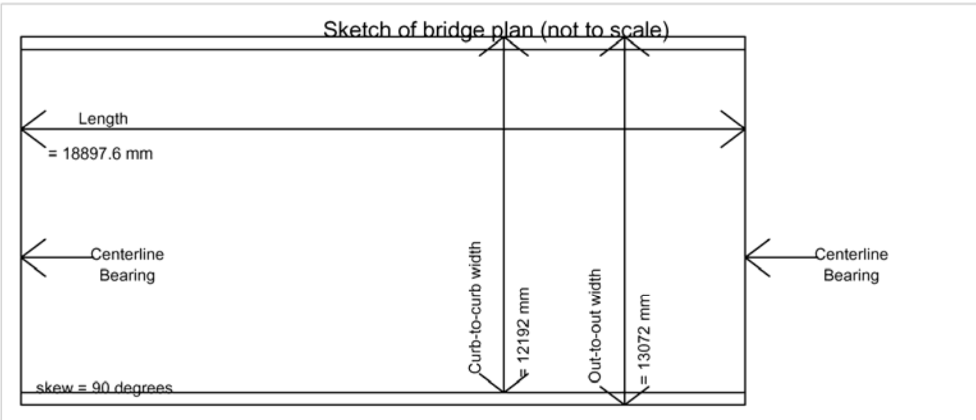

The maximum number of lanes with sidewalks is determined by dividing the width of available roadway (out-to-out of curbs) by the specified lane width (3600 mm) and rounding down to the nearest integer. Widths between 6000 and 7200 mm are assumed to carry two lanes, however. Similarly, the maximum number of lanes without sidewalks is determined by taking the out-to-out width of the structure minus two assumed 440 mm parapets, dividing by the specified lane width, and rounding down to the nearest integer. Again, widths between 6000 and 7200 mm are assumed to carry two lanes.

A3.6.1.1.1

Curb-to-curb width of roadway divided by lane width = 12192/3600 = 3.39
Maximum number of lanes with sidewalks 3

Total bridge clear width divided by lane width = (13072 - 880)/3600 = 3.39
Maximum number of lanes without sidewalks 3

The number of girders and the girder spacing is needed to determine the maximum girder reaction for pile cap design. Other dimensions are used to determine various things such as end diaphragm height and lateral wind area of the span, which are utilized in calculating dead and wind loads.

Number of girders in the cross-section	4			
Girder spacing normal to longitudinal axis	3594.1	mm	11.79 ft	
Girder width (maximum of top or bottom flange width at the abutment)	609.6	mm	2.00 ft	
Girder depth	1219.2	mm	4.00 ft	DM-4 Ap.G.1.2.8
Bearing pad thickness	20	mm	0.79 in	DM-4 Ap.G.1.7
Deck + haunch thickness	274.32	mm	10.80 in	
Parapet height	1143	mm	3.75 ft	

Title: Bridge 222 - 18.9 m Single Span Concrete Prestressed I-girder
90^{o} skew, 3.594 m girder spacing
By: KP
Date: 3/10/2006
Checked:
Date:

Total superstructure depth for wind analysis - top of parapet to bottom of girder
1219.2 + 274.32 + 1143 = 2636.52 mm 8.65 ft

The moment of inertia of the girders about the longitudinal axis of the bridge is calculated as illustrated in the figure below (five I-girders shown for illustrative purposes, the actual number of girders is used in the calculations). This value is used later to determine girder reactions due to transverse and overturning loadings.

Given a group of n girders, the second moment of inertia is calculated by summing the squares of the distances of the girders from the center of gravity of the girder group, or $I = \Sigma d_i^2$. For a single line of n equally spaced girders, the equation $I = n(n^2 - 1) L^2 / 12$ gives the same result, where n is the number of girders, and L is the girder spacing.

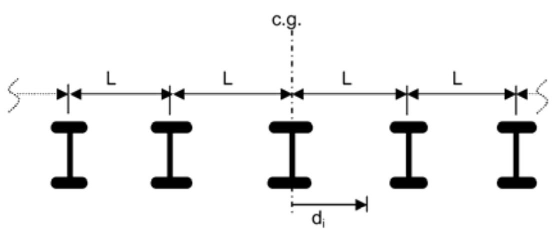

Moment of inertia of 4 I-girders about the longitudinal axis of the bridge:
4(4^2 - 1)(3594.1^2)/12 = 64587774.05 mm^2 100111 in^2

INTEGRAL ABUTMENT DATA

Given the geometry of the superstructure, the location of the proposed abutment, and the topography of the site, the geomety of the integral abutment can be calculated, and the wingwall lengths can be determined. Many of the dimensions are set in the PennDOT standards (see BD-667M Standard Drawing).

The abutment length is measured along the line of bearing. Note that specifying detached wingwalls later in the spreadsheet results in a slightly longer abutment (see BD-667M for detached wingwall details).

Abutment length	(13072+700)/sin(90) =	13772 mm	45.18 ft	

The abutment width is set at 1200 mm so that for any potential skew angle the pile cap reinforcement can fit around the piles.

Abutment width	1200 mm	3.94 ft	DM-4 Ap.G.1.4.1

The minimum pile cap height is 1000 mm. The flexural design of the pile cap is based on the supplied minimum dimension. There are a number of factors which can affect the maximum pile cap height. These include, but are not limited to, bridge width and cross-slopes, superelevation, skew, etc. DM-4 Ap.G.1.4.1

Although PennDOT permits the opposite ends of integral abutments to vary up to 450 mm in height due to superelevation (300 mm for skews less than 80^{o}), sloping the bottom of the pile cap such that the ends are equal is recommended to simplify reinforcement details. DM-4 Ap.G.1.4.1

Left end pile cap height, d_{pc1}	3371.088 mm	11.06 ft
Pile cap height at the crown of the roadway, or at the bridge midwidth for a superelevated roadway, $d_{pc,cl}$	2965.704 mm	9.73 ft
Right end pile cap height, d_{pc2}	2560.32 mm	8.40 ft

Difference between the height of the cap at the ends, $|d_{pc1} - d_{pc2}|$ = | 3371 - 2560 | =
810.768 mm 2.66 ft

Error - difference between ends of pile cap are limited to 450 mm for skews of 80 degrees or greater - bottom of cap must be sloped

The previous three values are used to calculate an average pile cap height and assume a constantly sloping top of cap with a crown at the center, as illustrated in the figure below. Only the minimum value is used to design the pile cap, the average value is used for selfweight calculations. Note that if the cap does not have either a constant cross-slope or crown at the midwidth, the average pile cap height will not be precisely correct. If a more exact selfweight is required, the maximum height at midwidth can be adjusted until the desired average pile cap height is attained.

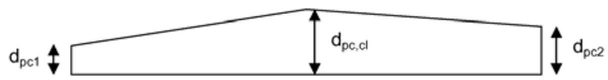

Average pile cap height
(3371.088+2560.32)/4 + 2965.704/2 = 2965.704 mm 9.73 ft

The end diaphragm height is equal to the deck and haunch thickness + girder depth + bearing pad depth.
End diaphragm height 274.32 + 1219.2 + 20 = 1513.52 mm 4.97 ft

The total average abutment height is equal to the end diaphragm height plus the average pile cap height.
Total average abutment height 1514 + 2966 = 4479.224 mm 14.70 ft

WINGWALLS

Attached wingwalls up to 2400 mm long (measured from the back face of the abutment) may be rectangular, extending the full depth of the abutment. Attached wingwalls over 2400 mm up to 4560 mm must be tapered. Wingwalls longer than 4560 mm will be detached. The standard location of the joint for a detached wingwall is 900 mm from the back face of the abutment, as shown in the figure below. The detached portion of the wingwall is to be designed independently. A 300 mm chamfer is provided in the interior corner of the wingwall/abutment connection (see figure). DM-4 Ap.G.1.4.4

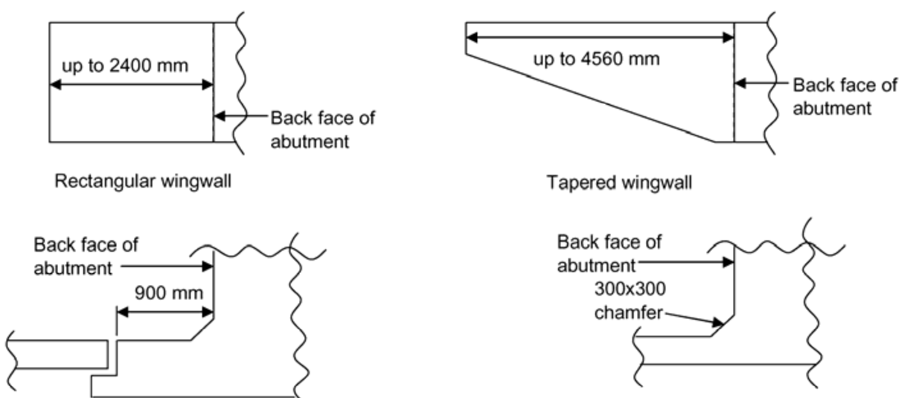

Rectangular wingwall

Tapered wingwall

Detached wingwall

Abutment/wingwall corner chamfer

Type of wingwall (R - Rectangular, T - Tapered, D - Detached) D
Wingwall length (including 300mm chamfer) 900 mm 3.0 ft

The wingwall dimensions are required for dead load calculations.
The average wingwall height at the abutment back face is conservatively assumed to be equal to the average height of the abutment.
Wingwall height at back face of abutment 4479.224 mm 14.70 ft

The height at the end is assumed to be either equal to the height at the abutment for rectangular (R) or detached (D) wingwalls, or 600 mm for tapered (T) wingwalls DM-4 Ap.G.1.4.4
Wingwall height at end 4479.224 mm 14.70 ft

The attached wingwall thickness is assumed to be the same width as the typical concrete parapet. An effective average thickness is assumed for the abutment extension for detached wingwalls. To obtain the effective width, the 250x300 mm overlap section (see BD-667M Standard Drawing) is smeared over the length of the stub.
Wingwall width 440+350+[(250)(300)/900] = 873 mm 2.87 ft

Title: Bridge 222 - 18.9 m Single Span Concrete Prestressed I-girder
90° skew, 3.594 m girder spacing

By: KP Date: 3/10/2006
Checked: Date:

LOAD DATA

LRFD design philosophy employs the equation $\Sigma\eta_i\gamma_i Q_i \le \varphi R_n = R_r$. In this equation, γ_i is a load factor, Q_i is a load effect, φ is a resistance factor, R_n is a nominal resistance, and R_r is a factored resistance. This leaves the η_i (eta) factor, which is a load modifier used to account for ductility, redundancy, and operational importance. $\eta_{i,max}$ is used when maximizing loads. $\eta_{i,min}$ is used when minimizing loads. Penndot currently limits η_i to values greater than or equal to 1.00 and less than or equal to 1.16. A1.3.2.1 D1.3.2

η_i factor 1.00

$\eta_{i,max} = \eta_i \ge 1.00$	1.00	D1.3.2
$\eta_{i,min} = 1/\eta_i \le 1.00$	1.00	A1.3.2.1

The unfactored girder design loads are available from the superstructure design performed using PennDOT's prestressed concrete girder design program. Both the interior and exterior noncomposite girder design dead loads are required input, although if only the controlling value is known, it can be conservatively used for both. The remaining composite dead loads should be the same whether they come from an interior or exterior girder design. The maximum and minimum unfactored live loads, with impact and shear distribution factors included, are also required input. The shear distribution factor is required as well, so that it can be divided out of the given loads to get the reaction per traffic lane. These values are available directly from the PennDOT beam design programs. Either the exterior or interior girder design can be used for the live load values, as long as all the values (reactions and distribution factors) come from the same girder design. Additional loads are calculated later. DM-4 Ap.G.1.2.7

Dead Loads - Unfactored:

Non-composite DC1 loads - include girder, deck, haunch, interior diaphragms		
Interior girder, DC1	328.1 kN	73.76 k
Exterior girder, DC1	290.3 kN	65.26 k
Composite DC2 loads - include parapets,		
Interior girder, DC2	35.7 kN	8.03 k
Exterior girder, DC2	35.7 kN	8.03 k
Composite DW loads - include future wearing surface,		
Interior girder, DW	41.4 kN	9.31 k
Exterior girder, DW	41.4 kN	9.31 k

Live load shear distribution factor 1.069

Live Loads - Unfactored from girder design program (distribution factor included):

PHL-93	max	481.2 kN	108.2 k
	min	0.0 kN	0.0 k
P-82	max	809.5 kN	182.0 k
	min	0.0 kN	0.0 k

Live Loads - Unfactored - distribution factor removed - reaction due to live load on one traffic lane:

PHL-93	max	(481.2)/(1.069) =	450.1 kN	101.2 k
	min	(0)/(1.069) =	0.0 kN	0.0 k
P-82	max	(809.5)/(1.069) =	757.2 kN	170.2 k
	min	(0)/(1.069) =	0.0 kN	0.0 k

The total pedestrian load reaction at the abutment is calculated assuming the approach slab and the first span are simply supported. The first span portion is calculated here, the approach slab portion is added in with the approach slab loads. The pedestrian load per unit area is as specified in the AASHTO LRFD Bridge specification, and the total width of sidewalk input earlier is used. This reaction is then distributed equally to all girders and piles. DM-4 Ap.G.1.2.7.2 A3.6.1.6 D3.6.1.6

Pedestrian	max	(0.0036)(0)(18898)/2000 =			
			0.0 kN	0.0 k	A3.6.1.6
	min		0.0 kN	0.0 k	

Choose the load factors to be used for the DW loads. For new construction or analysis of existing construction, where no future wearing surface is present, the DW load factors are taken as 1.50 max and 0.00 min. For bridges where a future wearing surface is present, the DW load factors are taken as 1.50 max and 0.65 min. Typically, the future wearing surface will not be currently present - N.

Future wearing surface currently present (Y or N)? N

DW load factors Maximum = 1.50 Minimum = 0.00

The extreme girder reactions, interior or exterior, are (conservatively) required for the design of the abutment pile cap. The total reaction with all lanes loaded, or the average pile reaction, is required for the pile design, which also requires both interior and exterior girder reactions. Note: The η_i factor is included here.

Factored Dead + Live reaction for interior girder:

Strength I	max	1.00[1.25(328.1+35.7) + 1.50(41.4) + 1.75(450.14)(3)/4] =	1107.7 kN	249.0 k
	min	1.00[0.90(328.1+35.7) + 0.00(41.4)] + 1.00[1.75(0.00)(3)/4] =	327.4 kN	73.6 k
Strength IP	max	1.00[1.25(328.1+35.7) + 1.50(41.4) + 1.75(0)/4 + 1.35(450.14)(3)/4] =	972.6 kN	218.7 k
	min	1.00[0.90(328.1+35.7) + 0.00(41.4) + 1.75(0.00)/4] + 1.00[1.35(0.00)(3)/4] =	327.4 kN	73.6 k
Strength II	max	1.00[1.25(328.1+35.7) + 1.50(41.4) + 1.35[757.25+450.14(3-1)]/4] =	1076.3 kN	242.0 k
	min	1.00[0.90(328.1+35.7) + 0.00(41.4)] + 1.35[(1.00)(0.00)+(1.00)(0.00)(3-1)]/4 =	327.4 kN	73.6 k
Strength III	max	1.00[1.25(328.1+35.7) + 1.50(41.4)] =	516.9 kN	116.2 k
	min	1.00[0.90(328.1+35.7) + 0.00(41.4)] =	327.4 kN	73.6 k
Strength V	max	1.00[1.25(328.1+35.7) + 1.50(41.4) + 1.35(450.14)(3)/4] =	972.6 kN	218.7 k
	min	1.00[0.90(328.1+35.7) + 0.00(41.4)] + 1.00[1.35(0.00)(3)/4] =	327.4 kN	73.6 k

Factored Dead + Live reaction for exterior girder:

Strength I	max	1.00[1.25(290.3+35.7) + 1.50(41.4) + 1.75(450.14)(3)/4] =	1060.4 kN	238.4 k
	min	1.00[0.90(290.3+35.7) + 0.00(41.4)] + 1.00[1.75(0.00)(3)/4] =	293.4 kN	66.0 k
Strength IP	max	1.00[1.25(290.3+35.7) + 1.50(41.4) + 1.75(0)/4 + 1.35(450.14)(3)/4] =	925.4 kN	208.0 k
	min	1.00[0.90(290.3+35.7) + 0.00(41.4) + 1.75(0.00)/4] + 1.00[1.35(0.00)(3)/4] =	293.4 kN	66.0 k
Strength II	max	1.00[1.25(290.3+35.7) + 1.50(41.4) + 1.35[757.25+450.14(3-1)]/4] =	1029.0 kN	231.3 k
	min	1.00[0.90(290.3+35.7) +0.00(41.4)] + 1.35[(1.00)(0.00)+(1.00)(0.00)(3-1)]/4 =	293.4 kN	66.0 k
Strength III	max	1.00[1.25(290.3+35.7) + 1.50(41.4)] =	469.6 kN	105.6 k
	min	1.00[0.90(290.3+35.7) + 0.00(41.4)] =	293.4 kN	66.0 k
Strength V	max	1.00[1.25(290.3+35.7) + 1.50(41.4) + 1.35(450.14)(3)/4] =	925.4 kN	208.0 k
	min	1.00[0.90(290.3+35.7) + 0.00(41.4)] + 1.00[1.35(0.00)(3)/4] =	293.4 kN	66.0 k

When designing integral abutments, only the girder rotations that are transferred to the piles are needed. Most dead load rotations occur prior to pouring the end diaphragm, and therefore will not be transferred to the piles. The exception to this is any composite dead loads such as future wearing surface or parapets. The extreme live load and composite dead load girder rotations are conservatively used as the design rotations for the piles. The unfactored live load and composite dead load rotations are available from the girder design.

Unfactored Live Load rotations per girder (including distribution factor):

PHL-93	max	0.097 degrees	0.0017	radians
	min	0.000 degrees	0.0000	radians
P-82	max	0.148 degrees	0.0026	radians
	min	0.000 degrees	0.0000	radians

The rotations above are the single girder unfactored rotations. To get the average girder rotations required for the design of integral abutments, the maximum number of traffic lanes on the bridge are loaded and the loads are assumed equally distributed to all girders. To accomplish this using the above results from the girder design program, the distribution factor is divided out to get the rotation of the full traffic lane applied to one girder. Then, the result is multiplied by the number of lanes and divided by the number of girders in the bridge.

Average Live Load rotations per girder:

PHL-93	max	(0.0017/1.069)(3/4) =	
		0.068 degrees	0.0012 radians
	min	(0.0000/1.069)(3/4) =	
		0.000 degrees	0.0000 radians
P-82	max	(0.0026/1.069)(3/4) =	
		0.104 degrees	0.0018 radians
	min	(0.0000/1.069)(3/4) =	
		0.000 degrees	0.0000 radians

The total rotation of any composite dead load rotations (unfactored), e.g. future wearing surface and parapets, can be input here. This value will be factored using the maximum DW load factor, 1.50.

0.018 degrees $\boxed{0.0003}$ radians

Maximum factored rotations are calculated here. The DM-4 allows the P-82 permit load to be placed in only one lane, with PHL-93 load in the remaining lanes. If the P-82 rotation controls the girder design the abutment design rotations are adjusted accordingly to account for P-82 on one lane and PHL-93 on all other lanes. The maximum load factor is used for both the maximum (positive) and minimum (negative) values.

Average factored live load + future dead load rotations (including eta factor):

	Controlling load		
max	PHL-93 all lanes	(1.00)[(1.75)(0.0012) + (1.50)(0.0003)] =	
		0.146 degrees	0.0025 radians
min		(1.00)[(1.75)(0.0000) + (1.50)(0.0000)] =	
		0.000 degrees	0.0000 radians

Additional Loads

Additional loads due to wind and centrifugal force are calculated here. The approach slab dead and live loads, and wingwall and abutment dead loads are calculated in the next section.

Wind Loads — DM-4 Ap.G.1.2.7.3

The appropriate wind pressure on the structure is input here. — A3.8

Wind on structure pressure = $\boxed{0.0024}$ MPa 0.000348 ksi — A3.8.1.2

The wind forces on the abutment are calculated assuming only the bridge span adjacent to the abutment contributes to the load, and that the span is simply supported laterally (half of the wind force on the end span is resisted by the abutment).

lateral force = (0.0024)(18897.6)(2636.52)/2000 = 59.79 kN 13.44 k

Uplift pressure is defined as a constant 0.00096 MPa. The force from this pressure is assumed to act as a line load at a distance of 1/4 of the out-to-out width of the bridge from the edge of the bridge. — A3.8.2

Uplift force (acts @ 1/4 point) pressure = 0.00096 MPa 0.000139 ksi

uplift = (-0.00096)(18897.6)(13072)/2000 = -118.57 kN -26.66 k

moment about the longitudinal axis of the bridge = -(-118.57)(13072)/4000 =

387.50 kN-m 285.81 k-ft

Wind on live load is taken as 1.46 kN/m acting at 1800 mm above the deck — A3.8.1.3

Wind on live load distributed force = 1.46 kN/m 0.10 k/ft

lateral force = (1.46)(18897.6)/2000 = 13.80 kN 3.10 k

Centrifugal force — DM-4 Ap.G.1.2.3

Integral abutments are permitted for curved bridges as long as the girders are straight and parallel within each span, and approval is obtained from the Chief Bridge Engineer. Despite the limited curvature this allows, centrifugal forces can be generated. The centrifugal force and any other lateral forces other than wind forces contributing to overturning moments can be input here. This force will be assumed to act perpendicular to the longitudinal axis of the bridge at a distance 1800 mm above the roadway surface. — A3.6.3

Centrifugal force $\boxed{233.3}$ kN 52.45 k

Girder and Pile Reactions

Girder and pile reactions are calculated assuming overturning moments are resisted by vertical forces only.

Girder reactions due to wind and centrifugal forces:

The top of deck to the top of the pile cap is equal to the end diaphragm height.

Top of deck to the top of the pile cap = 1513.52 mm 4.97 ft

The moment due to the wind on the superstructure is equal to the wind force times half the depth of the structure plus the bearing pad depth.

Wind on structure

moment = (59.79)[(2636.52/2)+20]/1000 = 80.01 kN-m 59.01 k-ft

The moment of the wind on the live load is equal to the force times the moment arm which is equal to the distance from the top of the pile cap to the top of the deck plus 1800 mm.

Wind on live load

moment = (13.80)(1513.52+1800)/1000 = 45.71 kN-m 33.71 k-ft

The moment of the centrifugal force is equal to the centrifugal force times the moment arm which is also equal to the distance from the top of the pile cap to the top of the deck plus 1800 mm.

Centrifugal

moment = (233.30)(1514+1800)/1000 = 773.04 kN-m 570.17 k-ft

The unfactored extreme reactions per girder for wind loads are calculated assuming the vertical wind forces are distributed equally to all girders, and the moments are resisted by vertical reactions of the girders (see figure below - note that five I-girders are used for illustrative purposes only - actual number of girders used in calculations). Forces due to the moments are calculated assuming the superstructure acts as a rigid member transversely, and the vertical force is proportional to the distance from the center of gravity of the girder group. The force at any girder is equal to the moment times the distance from the midwidth of the bridge divided by the second moment of inertia. The extreme overturning reactions are therefore at the exterior girders.

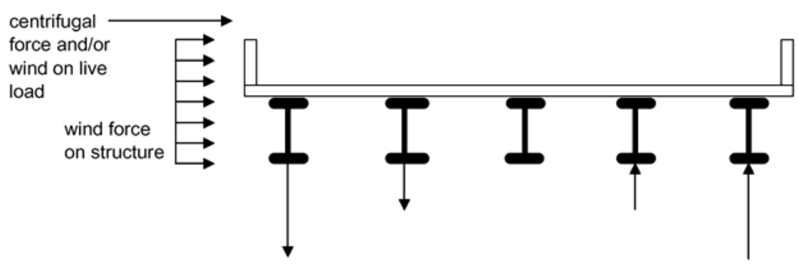

Extreme girder reactions due to wind on the structure

WS	max	(80.01)(1000)(4-1)(3594.1)/(2*64587774.05) =		
			6.68 kN/girder	1.50 k/girder
	min	-(80.01)(1000)(4-1)(3594.1)/(2*64587774.05) =		
			-6.68 kN/girder	-1.50 k/girder

Extreme forces due to uplift

Uplift	max	-118.57/4 + (387.50)(1000)(4-1)(3594.1)/(2*64587774.05) =		
			2.70 kN/girder	0.61 k/girder
	min	-118.57/4 - (387.50)(1000)(4-1)(3594.1)/(2*64587774.05) =		
			-61.99 kN/girder	-13.94 k/girder

Extreme forces due to wind on live load

WL	max	(45.71)(1000)(4-1)(3594.1)/(2*64587774.05) =		
			3.82 kN/girder	0.86 k/girder
	min	-(45.71)(1000)(4-1)(3594.1)/(2*64587774.05) =		
			-3.82 kN/girder	-0.86 k/girder

Extreme forces due to centrifugal forces

CE	max	(773.04)(1000)(4-1)(3594.1)/(2*64587774.05) =		
			64.53 kN/girder	14.51 k/girder
	min	-(773.04)(1000)(4-1)(3594.1)/(2*64587774.05) =		
			-64.53 kN/girder	-14.51 k/girder

Choose a trial pile section at this point. The pile dimensions are needed for the pile location check. The pile

moment of inertia is used to calculate the thermally induced forces in the piles. The pile properties are also required to run the COM624P computer program. Two types of piles are permitted for integral abutments, steel H-piles or concrete filled pipe piles.

Type of piles H - HP shape, P - pipe | H

For H-piles, the yield stress of the steel and the metric designation of the pile is required input. A list of available H-pile sections is provided. The user may then input the additional section properties manually, or press the button to the right, and the properties will be automatically retrieved.

Import Pile Properties

Pile Properties					
Pile designation	HP310x110		(HP12x74)		HP Shapes
Yield stress of pile steel, F_y	245	MPa	36	ksi	HP360x174
Pile section depth, d	308	mm	12.1	in	HP360x152
Flange width, bf	310	mm	12.2	in	HP360x132
Flange thickness, tf	15.50	mm	0.610	in	HP360x108
Pile Area, Ap	14100	mm^2	21.9	in^2	HP310x125
Moment of inertia, $I_{y\text{-}y}$	77.1E+6	mm^4	185	in^4	HP310x110
Elastic section modulus, $S_{y\text{-}y}$	49.7E+4	mm^3	30.3	in^3	HP310x94
Radius of gyration, $r_{y\text{-}y}$	73.9	mm	2.91	in	HP310x79
Plastic section modulus, $Z_{y\text{-}y}$	76.3E+4	mm^3	46.6	in^3	HP250x85
					HP250x62
					HP200x54

PILE DATA

Choose a pile layout. If a geotechnical report is available with a calculated pile capacity, a preliminary number of piles can be found by dividing the total factored dead + live girder reactions by the given pile capacity and rounding up to the next highest integer. If no pile load capacity is available, use an estimate of the load capacity based on the soil conditions. The maximum pile spacing is 3000 mm. The minimum pile spacing is the larger of 900 mm, or 2.5 times the diameter of round piles, or 2 times the diagonal dimension of H-piles (The 2x criteria only controls for HP360 piles). Note that the approximate range of allowed pile spacing calculated below assumes 900 mm is the minimum pile spacing, and may suggest a range which is not permitted based on pile dimensions. The pile location check made below should flag any erroneous spacings attempted, however.

DM-4 Ap.G.1.4.2
D10.7.1.5

Maximum total factored dead + live girder reactions
(1060.41)(2) + (1107.66)(2) = 4336.14 kN 974.80 k

Number of piles | 9

Approximate range of allowed pile spacing for 9 piles is about 1540 to 1600 mm

Chosen pile spacing along abutment	1600	mm	5.25	ft
Total pile length, L_{tot} =	4572	mm	15.00	ft

The minimum and maximum edge distance for the end piles is intended to keep the piles close to the end of the integral abutment in order to provide support for the attached wingwalls, without getting too close to the end of the abutment.

Minimum edge distance to centerline of piles	450	mm	17.72	in	D10.7.1.5
Maximum edge distance to centerline of piles	750	mm	29.53	in	DM-4 Ap.G.1.4.2.1

Pile location check OK

Pile spacing normal to the longitudinal axis of span
1600sin(90) = 1600 mm 5.25 ft

The moment of inertia of the pile group is calculated similarly to the girders above and is used to determine the axial forces in the piles due to overturning moments.

Moment of inertia of pile group about the longitudinal axis of the bridge
9(9^2 - 1)(1600^2)/12 = 153600000 mm^2 238080 in^2

Title: Bridge 222 - 18.9 m Single Span Concrete Prestressed I-girder
90° skew, 3.594 m girder spacing

By: KP
Date: 3/10/2006
Checked:
Date:

Pile loads due to wind and centrifugal forces

At this point, an iterative procedure is initiated to determine the loads on the piles. Initially, a depth to fixity of the piles is assumed. Later, the actual depth to fixity is calculated using the computer program COM624P, and this value is adjusted as necessary. The procedure is repeated until the estimated value is within 10% of the value obtained from the COM624P computer program. An initial choice of 5000-6000 mm to the point of fixity is reasonable.

Assume depth to pile fixity of 3505.2 mm 11.50 ft

The overturning moment resisted by the piles is calculated similarly to the overturning moments resisted by the girders, except the moment arm extends to the point of assumed pile fixity (see figure below - note that five I-girders and six H-piles are used for illustration purposes only). Wind uplift forces result in the same overturning moments on the piles as calculated earlier for the girders.

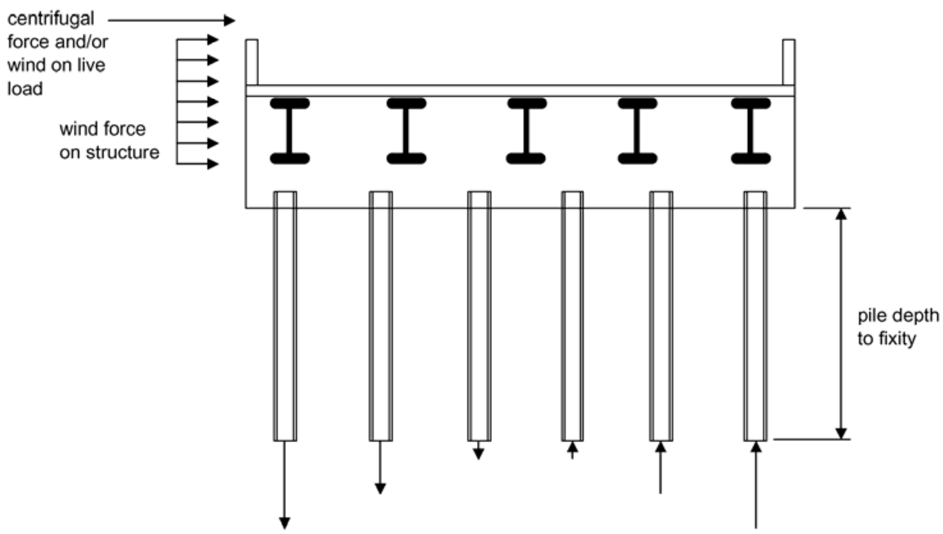

Wind on structure	moment = (59.79)(3505+2965.704+20+2636.52/2)/1000 =		
		466.90 kN-m	344.37 k-ft
Wind on live load	moment = (13.80)(1800+3505+2965.704+1513.52)/1000 =		
		134.98 kN-m	99.56 k-ft
Centrifugal forces	moment = (233.30)(1800+3505+2965.704+1513.52)/1000 =		
		2282.71 kN-m	1683.64 k-ft

The unfactored extreme loads per pile for wind cases are calculated similar to the girder reactions

Extreme forces due to wind on the structure

WS	max	(466.90)(1000)(9-1)(1600)/(2*153600000) =		
			19.45 kN/pile	4.37 k/pile
	min	-(466.90)(1000)(9-1)(1600)/(2*153600000) =		
			-19.45 kN/pile	-4.37 k/pile

Extreme forces due to uplift

Uplift	max	-118.57/9 + (387.50)(1000)(9-1)(1600)/(2*153600000) =		
			2.97 kN/pile	0.67 k/pile
	min	-118.57/9 - (387.50)(1000)(9-1)(1600)/(2*153600000) =		
			-29.32 kN/pile	-6.59 k/pile

Extreme forces due to wind on live load

WL	max	(134.98)(1000)(9-1)(1600)/(2*153600000) =		
			5.62 kN/pile	1.26 k/pile
	min	-(134.98)(1000)(9-1)(1600)/(2*153600000) =		
			-5.62 kN/pile	-1.26 k/pile

Extreme forces due to centrifugal force

CE	max	(2282.71)(1000)(9-1)(1600)/(2*153600000) =		
			95.11 kN/pile	21.38 k/pile
	min	-(2282.71)(1000)(9-1)(1600)/(2*153600000) =		
			-95.11 kN/pile	-21.38 k/pile

Additional Dead + Live Loads (Approach Slab, Wingwalls, and Abutment)

The approach slab live load is calculated assuming the slab is simply supported at the ends, the lane load only is present in all lanes, and the total reaction is distributed equally to all piles. The truck load is not included here because it was already included in the bridge loads. As previously, the multiple presence factor is not used. Dead loads from the approach slab are also distributed equally to all piles.

Approach slab dimensions

Approach slab thickness =	450 mm	18 in	DM-4 App. G 1.5
Approach slab length =	7500 mm	25 ft	

Approach slab loads

Approach Slab Load = (2.4)(9.81)(12192)(7500)(0.45)/2000000 =			
	484.39 kN	108.90 k	
Approach Slab Future Wearing Surface = (0.15)(9.81)(12192)(7500)/2000000 =			D3.5.1
	67.28 kN	15.12 k	
Approach Slab Lane Load (1 lane) = (9.3)(7500)/2000 =			A3.6.1.2.4
	34.88 kN	7.84 k	
Approach Slab Pedestrian Live Load (total reaction) = (0.0036)(0)(7500)/2000 =			
	0.00 kN	0.00 k	
Abutment self-weight Dead Load = (2.4)(9.81)(13772)(1200)(4479)/1000000000 =			
	1742.86 kN	391.81 k	

Wingwalls and parapet load

The parapet weight/length can be input for wingwall dead load calculations. A typical 440 mm wide concrete parapet weighs about 7.60 N/mm. Any other miscellaneous loads can also be included in this number, but note that the value will be multiplied by the length of the wingwall plus abutment (900 + 1200/SIN(90) = 2100 mm) times two since parapets are assumed to be on both sides of the bridge.

Parapet weight/length 7.60 N/mm 0.521 k/ft

Weight of two wingwalls = (2)(2.4)(9.81){(4479.224)(300)(873+300sin(90)/2)+[(900-300)(873)(4479.224+4479.224)/2)]/100000000

Weight of two parapets = (2)(7.60)(900+1200/sin(90))/1000

Total weight of wingwalls and parapets = 207.19 kN 46.58 k

Thermal Expansion

The thermal expansion of the bridge is calculated assuming the entire superstructure length, L, is unrestrained, and undergoes a uniform thermal expansion. This ignores the pier stiffnesses (if any) and passive soil pressure against the backwalls. For design purposes, a percentage of this thermal expansion can be assigned to take place at the abutment under consideration. It is the responsibility of the designer to determine the percentage of expansion. In some cases, such as single spans with identical abutments, simply assigning 50% of the movement to each end may be appropriate. In other cases, such as for continuous structures with unsymmetrical piers, a more in-depth thermal analysis taking pier and abutment stiffnesses into account is required. See DM-4 Ap.G.1.2.7.4 for thermal movement requirements.

The coefficient of thermal expansion and temperature range are assigned based on the girder material, concrete or steel.

Coefficient of thermal expansion, α	10.8E-6 $/^{o}C$	(concrete girders)	D5.4.2.2
Temperature range, Δ_T ($\pm$)	44 ^{o}C		DM-4 Ap.G.1.2.7.4
Load factor, ϕ_T	1.0		DM-4 Ap.G.1.2.7.6

Total $\pm$change in length of the bridge, $\phi_T \alpha \Delta_T L$ = (1.0)(0.0000108)(44)(18897.6) =

9.0 mm 0.35 in

The percentage of thermal expansion that occurs at the abutment being designed is input here. The value should be between 0 and 100%. For symmetrical structures, 50% of the expansion occurs at each abutment. For unsymmetrical structures, use the procedure described in DM-4 Ap.G1.2.7.4 to determine the percentage of movement at each end.

Percentage of expansion at abutment being designed 50 %

Maximum movement (expansion or contraction) at abutment (±), Δ

(0.50)(9.0) = 4.5 mm 0.18 in

The thermal expansion of continuous bridges induces an axial force in the piles, P_T, which is estimated using the simplified elastic procedure illustrated below (see figure on following page). This procedure assumes that the full passive pressure of the soil is acting on the abutment. Note that the additional pile axial force is zero in a simple span with passive pressure acting at the same height on both abutments.

The coefficient of passive earth pressure has been found to vary from about 3.0 for loose sand to about 6 for dense sand. PennDOT requires that the region immediately adjacent to the abutment be only nominally compacted, so 3.0 is an acceptable value. DM-4 Ap.G.1.2.7.4

Coefficient of passive earth pressure, k_p = 3.0

The density of loose sand given in the AASHTO-LRFD Bridge Design Specification is 1600 kg/m³. Multiplying by 9.81 m/s² converts this value to weight. A3.5.1

Soil unit weight, γ = (1600)(9.81) = 15.70 kN/m³ 100 lb/ft³

Using the coefficient of passive earth pressure, the soil density, and the depth of the abutment, the force per unit length on the abutment can be calculated.

Force from soil on abutment, $F=1/2\ k_p\gamma H^2$ = (1/2)(3.0)(15.70)(4479.224/1000)^2 =
472.4 kN/m 32.4 k/ft

The total longitudinal force on the abutment can be found by multiplying by the projected length of the abutment on a line perpendicular to the longitudinal axis of the bridge, which is equal to the out-to-out width of the bridge.

Total passive earth pressure force on abutment, F = (472.4)(13072)/1000 =
6174.9 kN 1388.2 k

The previously assumed depth to pile fixity, L_p = 3505.2 mm 11.50 ft

Using simple equilibrium by taking the moment about point A, the axial reaction per pile due to the force, F, and the displacement, Δ, can be calculated as:

F_p = 2FH / 3L / number of piles = (2)(6174.9)(4479.224)/[(3)(18897.6)]/9 =
108.4 kN/pile 24.4 k/pile

The moment induced in the piles by the thermal movement can be determined using the following equation. The top of the pile is assumed to be fixed.

The moment, $M_T = 6E_pI_p\Delta/L_p^2$ = (6)(200)(77100000)(4.5)/(3505.2^2)/1000 =
33.8 kN-m/pile 24.94 k-ft/pile

Check to make sure the moment, M_T, does not exceed the plastic moment, M_p. Even though the maximum flexural resistance of the pile may be lower, the plastic moment is conservatively used here as an upper bound.

Plastic moment, $M_p = F_yZ_{y\text{-}y}$ = (245)(763000)/1000000 = 186.9 kN-m 137.88 k-ft
since 33.8 < 186.9 - use M_T = 33.8 kN-m 24.94 k-ft

The horizontal force induced in the pile by the thermal deformation can be determined using the following equation. The top of the pile is assumed to be fixed.

The horizontal force, $H_T = 2M_T/L_p$ = (2)(33.8)(1000)/3505.2 =
19.3 kN/pile 4.3 k/pile

The total axial force induced in the pile due to these three components is equal to:

$2FH/3L+H_TH/L+M_T/L$ = 108.4 + (19.3)(4479.224)/18897.6 + 33.8/(18897.6/1000) = 114.8 kN (25.8 k) /pile

Axial force induced in piles, P_T = 0.0 kN/pile 0.0 k/pile

(Note: = 0 is used for single spans because the lateral loads on the two abutments will balance each other and no net vertical load on the piles will exist)

L

Title: Bridge 222 - 18.9 m Single Span Concrete Prestressed I-girder
90^{o} skew, 3.594 m girder spacing

By: KP Date: 3/10/2006
Checked: ________ Date: ________

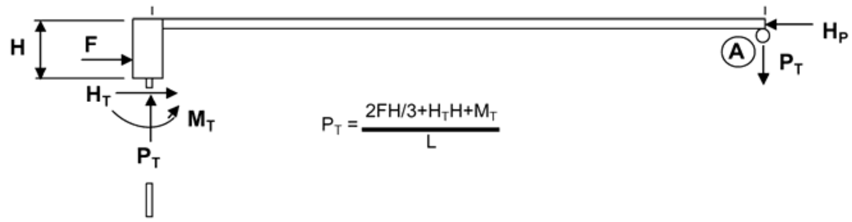

$$P_T = \frac{2FH/3+H_TH+M_T}{L}$$

Calculate the maximum factored load on the most heavily loaded pile (see Load Factors tab for load factors for each load combination). Since the factored dead and live loads from the interior and exterior girders have already been calculated, the sum of the girder loads is calculated assuming two exterior girders and the remaining ones interior. These loads, as well as any additional vertical loads, are distributed equally to all piles. The factored extreme overturning loads, which occur on the exterior piles are added. The η_i modifier is also included.

Extreme Factored Dead + Live Loads per pile

Strength I max [(1107.7)(2)+(1060.4)(2)]/9 + 1.00{[1.25(484.4+1742.9+207.2)+1.50(67.3)+1.75(3)(34.9)]/9 +
1.75(95.1) + 1.00(0.0)} = 1017.91 kN/pile 228.84 k/pile
min [(327.4)(2)+(293.4)(2)]/9 + 1.00{[0.90(484.4+1742.9+207.2)+0.00(67.3)+1.75(3)(0.0)]/9} +
1.00[1.75(-95.1) + 1.00(0.0)] = 214.96 kN/pile 48.32 k/pile

Strength IP max [(972.6)(2)+(925.4)(2)]/9 + 1.00{[1.25(484.4+1742.9+207.2)+1.50(67.3)+1.35(3)(34.9)+1.75(0.0)]/9 +
1.35(95.1) + 1.00(0.0)} = 915.20 kN/pile 205.75 k/pile
min [(327.4)(2)+(293.4)(2)]/9 + 1.00{[0.90(484.4+1742.9+207.2)+0.00(67.3)+1.35(3)(0.0)+1.75(0.0)]/9} +
1.00[1.35(-95.1) + 1.00(0.0)] = 253.00 kN/pile 56.88 k/pile

Strength II max [(1076.3)(2)+(1029.0)(2)]/9 + 1.00{[1.25(484.4+1742.9+207.2)+1.5(67.3)+1.35(3-1)(34.9)]/9 +
1.35(95.1) + 1.0(0.0)} = 956.04 kN/pile 214.93 k/pile
min [(327.4)(2)+(293.4)(2)]/9 + 1.00{[0.9(484.4+1742.9+207.2)+0(67.3)+1.35(2)(0.0)]/9} +
1.00[1.35(-95.1) + 1.0(0.0)] = 253.00 kN/pile 56.88 k/pile

Strength III max [(516.9)(2)+(469.6)(2)]/9 + 1.00{[1.25(484.4+1742.9+207.2)+1.50(67.3)]/9 + 1.40(19.5) +
+ 1.00(0.0)} + 1.00(1.40)(3.0) = 599.94 kN/pile 134.87 k/pile
min [(327.4)(2)+(293.4)(2)]/9 + 1.00{[0.90(484.4+1742.9+207.2)+0.00(67.3)]/9} + 1.00[1.40(-19.5) +
1.00(0.0) + 1.40(-29.3)] = 313.12 kN/pile 70.39 k/pile

Strength V max [(972.6)(2)+(925.4)(2)]/9 + 1.00{[1.25(484.4+1742.9+207.2)+1.50(67.3)+1.35(3)(34.9)]/9 + 0.40(19.5) +
1.00(5.6) + 1.35(95.1) + 1.00(0.0)} = 928.61 kN/pile 208.76 k/pile
min [(327.4)(2)+(293.4)(2)]/9 + 1.00{[0.90(484.4+1742.9+207.2)+0.00(67.3)+1.35(3)(0.0)]/9} + 1.00{0.40(-19.5) +
1.00(-5.6) + 1.35(-95.1) + 1.00(0.0)} = 239.60 kN/pile 53.86 k/pile

Controlling Loads	max STR I	1017.91 kN/pile	228.84 k/pile
	min STR I	214.96 kN/pile	48.32 k/pile

Lateral Pile Analysis

Knowing the soil properties at the abutment (taken from the geotechnical report), and the properties of the piles, and using the calculated design values for maximum factored axial load, live load rotation, and thermal expansion, the computer program COM624P can be used to determine the depth to pile fixity, the depth to the first inflection point of the pile, the unbraced length of the pile, the depth at which the lateral pile deflection is equal to 2% of the pile diameter (needed for friction piles only), and the maximum moment in the pile below the first point of inflection. Since a pre-augered hole, 3000 mm minimum depth, filled with loose sand, is present at the top of the piles, the COM624P analysis should use the properties of the weaker of either the loose sand or the actual soil for the depth of the pre-augered hole. The procedure for running COM624P is as follows:

Run COM624P using the top of pile boundary condition which permits a specified lateral deflection along with an applied moment. Apply the maximum pile vertical axial load to the pile simultaneously with the abutment maximum thermal movement. The axial load and deflection should be input as positive values. Apply the negative plastic moment at the head of the pile and run the analysis.
1 - If the calculated pile head rotation (positive value) is less than the end rotation of the pile due to live loads and composite dead loads, the analysis is complete.
2 - If the calculated pile head rotation is greater than the end rotation of the pile due to live loads and composite dead loads, iteratively reduce the moment at the head of the pile until the rotations are equal (within tolerance).

Title: Bridge 222 - 18.9 m Single Span Concrete Prestressed I-girder
90° skew, 3.594 m girder spacing
By: KP
Date: 3/10/2006
Checked:
Date:

Design values for COM624P:

Pile Section	HP310x110	HP12x74
Pile width or diameter	0.308 m	12.1 in
Pile moment of inertia	0.0000771 m^4	185 in^4
Pile area	0.0141 m^2	21.9 in^2
Vertical axial load	1017.9 kN	228.8 k
Design rotation	0.0025 radians	0.146 degrees
Design thermal movement	0.0045 m	0.18 in
Plastic moment (if required)	-186.9 kN-m	-137.9 k-ft

At this point COM624P should be run. COM624P is run using a text file as input. There are two ways to develop this text input file. The first is to use the input file editor program supplied with COM624P. The second method is to use any text editor to develop the input file using the COM624P users manual as a guide. If this second method is chosen, a template file for COM624P can be created from the COM624P Input tab. Once the template is created, it can be edited using any text editor.

Results from COM624P (See figures below for illustrations of the data required from the program).

The depth to fixity is defined as the shallowest depth at which the pile deflection is equal to zero.

Depth to fixity, L_p = 3487.4 mm 137.30 in

The depth to the uppermost point of inflection is the depth measured from the bottom of the abutment to the first point of zero moment on the pile moment diagram.

Depth to first point of inflection, L_{i1} = 1686.6 mm 66.40 in

The depth to the second point of inflection is the depth measured from the bottom of the abutment to the second point of zero moment on the pile moment diagram. For a short pile with only one point of inflection, input the total pile length

Depth to second point of inflection, L_{i2} = 3937 mm 155.00 in

The depth above which friction is ineffective is input here. For a laterally deflected pile, this depth is defined as the point where the deflection is 2% of the pile diameter. For the present pile (see section properties above), this deflection value is (0.02)(308) = 6.16 mm (0.24 in). The length of pile above this point is considered ineffective in the design of friction piles. If the pile is driven through an embankment fill which is to be neglected in calculating pile friction resistance, input the depth of fill. This value is not required for end bearing piles. DM-4 Ap.G.1.4.2.2

Depth to 2% deflection, L_n = 3246.1 mm 127.80 in

The maximum bending moment in the pile is the maximum moment below the uppermost point of inflection and neglects the moment at the pile-pile cap interface.

Maximum bending moment in pile, M_u = 32.8 kN-m 24.19 k-ft

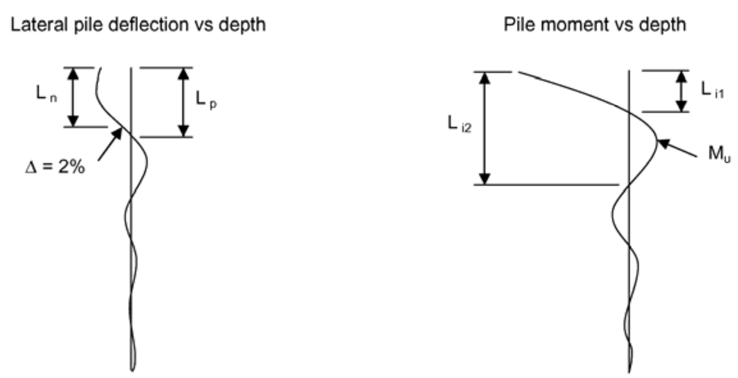

Typical COM624P results (exaggerated)

Title: Bridge 222 - 18.9 m Single Span Concrete Prestressed I-girder
90° skew, 3.594 m girder spacing
By: KP
Date: 3/10/2006
Checked:
Date:

Pile Capacity Analysis

Check the geotechnical resistance of the pile
The geotechnical resistance can be supplied by skin friction, end bearing, or both. The easiest way to eliminate one or the other from contributing to the resistance is to simply put zero in for the unit resistance of the one to be neglected. The resistance factors for bearing capacity and skin friction should be chosen according to the provisions of DM-4.

Shaft and tip resistance factors

Tip (bearing) resistance factor, ϕ_{qp}	0.50	D10.5.4-2
Shaft (skin friction) resistance factor, ϕ_{qs}	0.55	D10.5.4-2

Tip resistance

Unit tip resistance, q_p 398.2 MPa 58 ksi
Nominal pile tip resistance, $Q_p = q_pA_p$ = (398.2)(14100)/1000 =
5614.62 kN 1262.2 k

The effective shaft length is the total shaft length minus a length at the top of the pile which is ineffective due to the lateral movement which occurs. Using a displacement of 2% of the pile diameter as the boundary above which skin friction becomes ineffective has been found to be reasonable. The depth, L_n, at which the displacement reaches this critical value was determined previously using the computer program COM624P.

Shaft resistance (skin friction)

Depth to 2% deflection, L_n = 3246.10 mm 10.65 ft
Effective shaft length, $L_e = L_{tot} - L_n$ = 4572 - 3246.1 =
1325.9 mm 4.35 ft

The unit shaft resistance (skin friction) is required for friction piles. For layered soils, a weighted average unit shaft resistance should be used.

Unit shaft resistance, q_s 0.027 MPa 3.92 psi
Nominal pile shaft resistance, $Q_s = q_sA_s$ = (0.027)(1825)(1325.9)/1000 =
65.34 kN 14.7 k

Total factored resistance per pile, $Q_R = \phi_{qp}Q_p + \phi_{qs}Q_s$
(0.50)(5614.62) + (0.55)(65.34) = 2843.25 kN 639.2 k
2843.2 kN (639.2 k) > 1017.9 kN (228.8 k) - OK

Check the capacity of the pile as a structural member

The pile resistance factors in DM-4 are to be applied assuming only axial forces are present at the tip of the pile, where any driving damage is likely to occur. At the top of the pile, where axial forces and bending are present, the piles are generally undamaged. For these reasons a lower load factor is used when the axial force only is considered. The combined flexure and axial force resistance factors are higher. The calculated nominal axial resistances are also different, as the pile is assumed fully supported at the tip, but an unbraced length is assumed between the top two points of inflection.

Pile resistance factors

Axial compression only, ϕ_c	0.45		D6.5.4.2
Axial compression, ϕ_c plus	0.60	(used together)	D6.5.4.2
Flexure, ϕ_f	0.85		

Compressive resistance (lower portion of pile - axial loads only)

Nominal axial resistance, P_n = FyAs = (245)(14100)/1000 =
3454.5 kN 776.6 k

For the check of axial capacity, the entire axial load is considered for end bearing piles. For friction piles, the load at the pile tip is assumed to be the total pile load minus 50% of the factored friction resistance of the pile.

Check axial capacity

Axial load at tip of pile, P_u = (≥ 0.0)

1017.91 kN 228.8 k

Factored axial resistance, $P_r = \phi P_n$ = (0.45)(3454.50) =

1554.53 kN 349.5 k

1554.53 kN (349.5 k) > 1017.91 kN (228.8 k) - OK

The unbraced length is defined as the distance between the top two points of inflection (zero moment) on the pile moment diagram.

(3937) - (1687) = 2250.4 mm 88.60 in

As a structural member, the pile length between the top two inflection points is assumed to be a pinned-pinned member. The effective length factor, K, of a pinned-pinned member = 1.0.

Compressive resistance (upper portion of pile - under combined axial load and moment)

For steel H-piles

F_e = Fy = 245 MPa

E_e = Est = 200000 MPa

$\lambda = (KL_b/r_s\pi)^2\ (F_e/E_e)$ = [(1.0*2250.4)/(74*3.142)]^2 (245/200000) = 0.115 A6.9.4.1

if $\lambda \le 2.25$, $P_n = 0.66^{\lambda} F_e A_s$, if $\lambda > 2.25$, $P_n = 0.88 F_e A_s / \lambda$

Nominal axial resistance, P_n = 0.66^0.115 (245)(14100)/1000 =

3293.2 kN 740.3 k

Factored axial resistance, $P_r = \phi P_n$ = (0.6)(3293.2) =

1975.9 kN 444.2 k

Flexural resistance of steel H-piles

Plastic Moment, $M_p = F_y Z_y$ = (245)(763000)/1000000 =

186.9 kN-m 137.9 k-ft

Yield Moment, $M_y = F_y S_y$ = (245)(497000)/1000000 =

121.8 kN-m 89.8 k-ft

For H-piles, if the width-to-thickness ratio of the flanges is not sufficient to consider the section compact, an interaction formula from AISC is used to interpolate between the plastic moment resistance and the yield moment resistance.

$M_n = M_p - (M_p - M_y)(\lambda - \lambda_p)/(\lambda_r - \lambda_p) \le M_p$ AISC-LRFD, Ap.F F1., 1994

For pipe piles, if the diameter-to-thickness ratio of the pipe is not sufficient to consider the section compact, then the section is considered non-compact. A6.12.2.3.2

Width-to-thickness ratio of projecting flange element

λ = bf / 2tf = 310/(2*15.5) = 10.00

Width-to-thickness criteria for flange element to reach plastic moment

$\lambda_p = 0.38 * (E / F_y)^{1/2}$ = 0.382*(200000/245)^0.5 = 10.91 A6.10.5.2.3c

Width-to-thickness criteria for flange element to reach yield stress

$\lambda_r = 0.56 * (E / F_y)^{1/2}$ = 0.56*(200000/245)^0.5 = 16.00 A6.9.4.2

Nominal flexural resistance, M_n = Mp

Use M_n = 186.94 kN-m 137.88 k-ft

Pile factored flexural resistance, $M_r = \phi M_n$ = (0.85)(186.9) =

158.9 kN-m 117.19 k-ft

Check moment-axial interaction

P_u / P_r = 1017.9/1975.9 = 0.52 A6.9.2.2

if $P_u / P_r < 0.2$ then $P_u / 2.0P_r + M_u / M_r \le 1.0$

if $P_u / P_r \ge 0.2$ then $P_u / P_r + (8.0 / 9.0)\ M_u / M_r \le 1.0$

Moment - axial interaction = 1017.9/1975.9 + (8.0/9.0)(32.8/158.9) = 0.70 ≤ 1.00 OK

Title: Bridge 222 - 18.9 m Single Span Concrete Prestressed I-girder
90^{o} skew, 3.594 m girder spacing
By: KP
Checked:
Date: 3/10/2006
Date:

Pile Ductility Requirement

Since the top of the pile will often have to undergo inelastic rotations, a check is performed based on a method contained in Greimann et. al. (1987) for determining whether the pile has enough ductility to undergo the required calculated deflections. DM-4 Ap.G.1.4.2.5

Ductility Criterion, $\Delta \leq \Delta_i$, where
Δ = design displacement
Δ_i = allowable displacement

The design displacement is the total displacement due to the full range of thermal expansion / contraction at the abutment being designed. Most of the data for thermal displacements was listed previously, and the percentage of the total displacement of the bridge is denoted by k.

Temperature range, Δ_T = 50 ^{o}C Concrete girders D3.12.2.1

Design displacement, $\Delta = k\phi_T\alpha\Delta_T L$ = (0.50)(1.0)(0.0000108)(50)(18897.6) =
5.1 mm 0.20 in

The design rotation is the total factored rotation at the support due to live load and composite dead loads which is equal to the sum of the absolute values of the maximum and minimum factored rotations.

Total design rotation, $\theta_w = \theta_{min} + \theta_{max}$ = 0.0025 + 0.0000 =
0.0025 radians 0.146 degrees

Pile yield stress, F_y 245 MPa 36 ksi

The plastic rotation is the rotation required to form a plastic hinge in the pile.

Plastic rotation, $\theta_p = F_y Z L_i / 3EI$ = (245)(763000)(1686.6)/(3*200000*77100000) =
0.0068 radians 0.390 degrees

Inelastic rotation capacity reduction factor, C_i ($0 \leq C_i \leq 1.0$)

C_i = 3.17 - 5.68 $\cdot$ $(F_y / E)^{1/2}$ (bf / 2tf) = 3.17 - 5.68 * (245/200000)^0.5 [310/(2*15.5)] = 1.18
Use C_i = 1.00

Inelastic rotation capacity, $\theta_{inel} = (K^*C_iM_pL_i)/EI$ For H-piles, K = 1.500
[(1.500)(1.00)(186.94)(1000)(1686.6)]/[(200)(77100000)] =
0.0307 radians 1.757 degrees

Allowable displacement, $\Delta_i = 4^*L_i^*[(\theta_{inel} - \theta_w)/2 + \theta_p]$ = (4)(1686.6)[(0.0307 - 0.0025)/2 + 0.0068] =
140.9 mm 5.55 in

5.1 mm (0.20 in) < 140.9 mm (5.55 in) - OK

Pile Cap Reinforcing Design

Extreme Factored Dead + Live Loads per girder.

The extreme interior and exterior vertical girder reactions are listed below. When combined with the extreme wind and centrifugal reactions for an exterior girder, the result is a conservative maximum girder reaction for pile cap design.

Strength I	maximum of 1107.66 and 1060.41 =	1107.66 kN	249.01 k
	minimum of 327.42 and 293.40 =	293.40 kN	65.96 k
Strength IP	maximum of 972.62 and 925.37 =	972.62 kN	218.65 k
	minimum of 327.42 and 293.40 =	293.40 kN	65.96 k
Strength II	maximum of 1076.27 and 1029.02 =	1076.27 kN	241.95 k
	minimum of 327.42 and 293.40 =	293.40 kN	65.96 k
Strength III	maximum of 516.85 and 469.60 =	516.85 kN	116.19 k
	minimum of 327.42 and 293.40 =	293.40 kN	65.96 k
Strength V	maximum of 972.62 and 925.37 =	972.62 kN	218.65 k
	minimum of 327.42 and 293.40 =	293.40 kN	65.96 k

Title: Bridge 222 - 18.9 m Single Span Concrete Prestressed I-girder
90^{o} skew, 3.594 m girder spacing

By: KP
Date: 3/10/2006
Checked: ________
Date: ________

The following reactions are the extreme factored dead and live load girder reaction calculated previously, plus the extreme reactions on the exterior girder due to wind, centifugal, and thermal forces. It is recognized that the extreme reactions due to lateral forces occur on the exterior girders, while the extreme gravity reaction may occur on the interior girders, but combining the two should not be overly conservative. The η_i modifier is included here as well.

Strength I	max	1107.66 + 1.00[1.75(64.53) + 1.00(0.00)(9/4)] =		
			1220.58 kN/girder	274.40 k/girder
	min	293.40 + 1.00[1.75(-64.53) + 1.00(0.00)(9/4)] =		
			126.95 kN/girder	28.54 k/girder
Strength IP	max	972.62 + 1.00[1.35(64.53) + 1.00(0.00)(9/4)] =		
			1059.73 kN/girder	238.24 k/girder
	min	293.40 + 1.00[1.35(-64.53) + 1.00(0.00)(9/4)] =		
			206.29 kN/girder	46.38 k/girder
Strength II	max	1076.27 + 1.00[1.35(64.53) + 1.00(0.00)(9/4)] =		
			1163.38 kN/girder	261.54 k/girder
	min	293.40 + 1.00[1.35(-64.53) + 1.00(0.00)(9/4)] =		
			206.29 kN/girder	46.38 k/girder
Strength III	max	516.85 + 1.00[1.40(2.70)] + 1.00[1.40(6.68) + 1.00(0.00)(9/4)] =		
			529.98 kN/girder	119.14 k/girder
	min	293.40 + 1.00[1.40(-61.99+ -6.68) + 1.00(0.00)(9/4)] =		
			197.27 kN/girder	44.35 k/girder
Strength V	max	972.62 + 1.00[0.40(6.68) + 1.00(3.82) + 1.35(64.53) + 1.00(0.00)(9/4)] =		
			1066.21 kN/girder	239.69 k/girder
	min	293.40 + 1.00[0.40(-6.68) + 1.00(-3.82) + 1.35(-64.53) + 1.00(0.00)(9/4)] =		
			158.51 kN/girder	35.63 k/girder

Controlling Loads	max STR I	1220.58 kN/girder	274.40 k/girder
	min STR I	126.95 kN/girder	28.54 k/girder

Pile Cap Reinforcing

Knowing the maximum girder reaction, the pile spacing, the dimensions of the cap and diaphragm, and the material properties, the pile cap reinforcing can be calculated. The loads used for design are the maximum simply supported beam moments reduced by 20% to account for the continuity over the piles. Calculations for reinforcement are performed on the Cap Reinforcement tab.

Concrete compressive strength, f'_c	20.7 MPa	3.0 ksi
Reinforcing steel yield strength, F_y	413.7 MPa	60 ksi
Maximum factored girder reaction, R_u	1220.6 kN	274.4 k
Pile Spacing	1600 mm	5.25 ft

Pile cap reinforcement - use 4 # 25 bars top and bottom of cap beam

Title: Bridge 222 - 18.9 m Single Span Concrete Prestressed I-girder
90° skew, 3.594 m girder spacing

By: KP
Checked: ________
Date: 3/10/2006
Date: ________

ANALYSIS SUMMARY PAGE

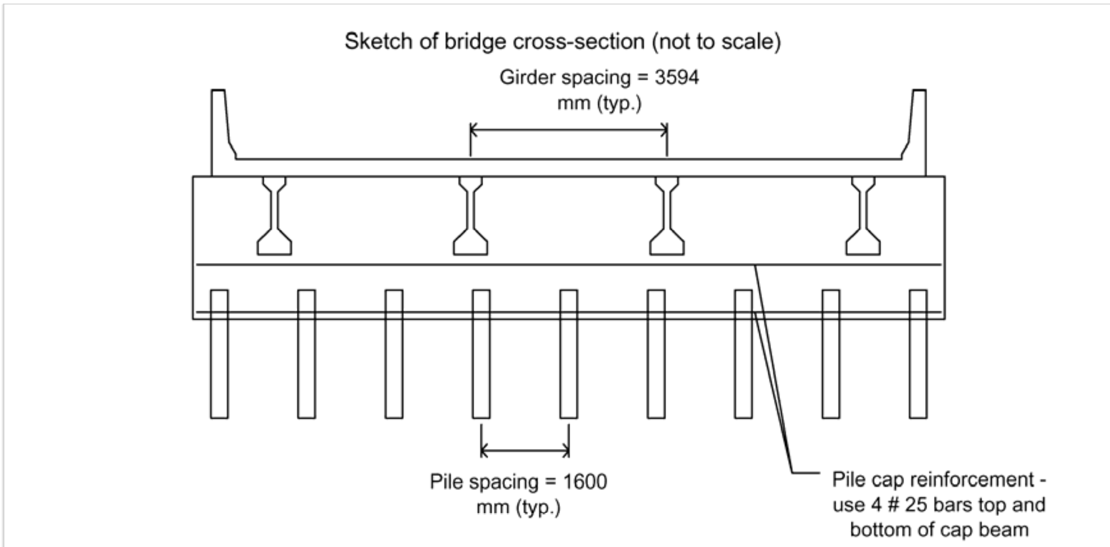

Bridge Description
Bridge length: 18897.6 mm (62.00 ft) simple span.
Skew: 90 degrees.
Maximum number of traffic lanes: 3.
Curb-to-curb roadway width: 12192 mm (40.00 ft).
Total width of sidewalk(s): 0 mm (0.00 ft).
Out-to-out superstructure width: 13072 mm (42.89 ft).
Maximum number of traffic lanes with no sidewalks: 3.
Number of girders: 4 prestressed concrete I-girders
Girder spacing: 3594.1 mm (11.79 ft).
Moment of inertia of the girders about the longitudinal axis of the bridge: 64587774 mm^2 (100111 in^2).
Girders depth: 1219.2 mm (11.79 ft).
Girder width: 609.6 mm (2.00 ft).
Bearing pad thickness 20 mm (0.8 in).
Average deck + haunch thickness: 274.32 mm (10.80 in).
Parapet height: 1143 mm (3.75 ft).

Integral Abutment Description
Abutment width: 1200 mm (3.94 ft).
Abutment length: 13772 mm (45.18 ft).
Pile cap depth: 3371.088 mm (11.06 ft) at the left end.
2965.704 mm (9.73 ft) at the center.
2560.32 mm (8.40 ft) at the right end.
Average pile cap depth: 2965.704 mm (9.73 ft).
Pile cap reinforcement: 4 # 25 bars top and bottom.
End diaphragm height (equal to the deck + haunch + girder + bearing pad depth): 1513.52 mm (4.97 ft).
Total average abutment height: 4479.224 mm (14.70 ft).
Wingwall length: 900 mm (2.95 ft) long stubs for detached wingwalls at each end of the abutment.

Pile Description
Number of piles: 9 - HP310x110 (HP12x74) piles.
Pile spacing: 1600 mm (5.25 ft) in a single row along the centerline of bearing of the abutment.
Moment of inertia of the piles about the longitudinal axis of the bridge: 153600000 mm^2 (238080 in^2).
Design pile length: 4572 mm (15.00 ft).
Depth to fixity: 3487.4 mm (137.30 in).
Unbraced length: 2250.4 mm (88.60 in).
Depth to the first point of inflection: 3937 mm (155.00 in).
Depth to the point where the lateral deflection is 2% of the pile width (friction engaged): 3246.1 mm (127.80 in).
Pile yield moment, My: 121.8 kN-m (89.8 k-ft).
Pile plastic moment, Mp: 186.9 kN-m (137.9 k-ft).

Title: Bridge 222 - 18.9 m Single Span Concrete Prestressed I-girder
90° skew, 3.594 m girder spacing

By: KP Date: 3/10/2006
Checked: ________ Date: ________

Total factored geotechnical capacity of the pile: 2843.2 kN (639.2 k).
Factored axial resistance of the pile at the tip: 1554.5 kN (349.5 k).
Factored axial resistance of upper portion of pile for use in interaction equation: 1975.9 kN (444.20 k).
Factored flexural resistance of upper portion of pile for use in interaction equation: 158.9 kN-m (117.2 k-ft).

Loads and Deformations
Maximum girder reaction: 1220.6 kN (274.4 k) due to the STR I load case
Maximum axial force in the pile: 1017.9 kN (228.8 k) due to the STR I load case.
Maximum bending moment in the pile (other than at the pile-abutment connection): 32.8 kN-m (24.2 k-ft).
Total maximum design movement for the abutment: 10.2 mm (0.40 in).
Maximum movement in one direction: 4.5 mm (0.18 in).
Maximum design rotation: 0.0025 radians (0.146 degrees).
Axial load-moment interaction equation result for the pile (maximum allowable is 1.00): 0.70.

Warnings and Errors
The spreadsheet generated 0 warning(s) and 1 error(s).

The 1 error(s) must be addressed to satisfy design requirements.

An evaluation of the above-presented PennDOT IA program output was performed through comparisons with field data and bridge 222 original design. The five program design sections were evaluated individually and are summarized in Table 7.3.

Table 7.3. Bridge 222: Program Evaluation

Design Part	Discussion	Suggested Improvements
1) Bridge Data (pp. 1-3)	Input data sequence and explanations are clearly presented.	-
2) Integral Abutment Data (pp. 3-4)	An error regarding a difference in abutment end heights greater than 18 inches due to the requirement of 8 percent transverse slope is reported.	-
3) Load Data (pp. 5-8)		
• Dead and live load girder reactions (p. 6)	Calculation in the program strictly follows DM-4 Ap.G 1.2.7.2, which is based on the assumption of equally distributed loads to all piles and removal of the multiple presence provision. However, this assumption was not applied to the original design calculation.	More study is required to ensure that this assumption does not produce either over- or underestimated results for both narrow and wide bridges.
• Girder end rotation due to composite dead and live loads (pp. 6-7)	The original design calculation assumed integral abutment rigid-body movement and did not consider effects of girder-end rotations on the pile head rotations. Discussion of this issue is continued in section 4.	See design section 4 under *iterative procedure interacting with COM624P*.
4) Pile Data (pp. 9-18)		

• Pile properties (p. 9)	The geotechnical report recommends that a 1/16-inch loss in pile thickness (all around) due to corrosion be incorporated. This corrosion effect has been considered in the original design calculation. The pile properties used in the PennDOT IA program above did not consider this effect - only short-term results are shown.	Input of the anticipated pile thickness loss as well as an option to automatically compute deteriorated pile properties are suggested.
• Temperature range (p. 11)	The structural continuity of bridge 211 was established during mid Jul. 2003 with an average ambient temperature of 70 ºF. Measured extreme maximum and minimum ambient temperatures were 95 ºF and -8 ºF, respectively, over the 43-month period, below the design value of ±80 ºF.	Modification of the design temperature range as specified in DM-4 Ap.G 1.2.7.4 for U.S. customary units (111 ºF) is required to eliminate inconsistent conversion between Fahrenheit and Celsius.
• Maximum abutment movement (p. 12)	Maximum measured abutment thermal displacements are 0.11 inch and 0.13 inch for expansion and contraction movements, respectively. This is compared to the PennDOT IA program design value of 0.18 inch.	IA program abutment displacement was overestimated due to the extremely large design temperature range and large thermal mass of the bridge. A modification of the temperature range is possible to allow more accurate predictions of displacements.
• Coefficient of passive earth pressure (p. 12)	The maximum measured earth pressure was 16 psi. The calculated effective vertical stress at this pressure cell location was 5.4 psi, indicating a maximum equivalent coefficient of earth pressure of 2.96, which is very close to the design value of 3.0.	-
• Axial load per pile (p. 13)	The maximum measured pile axial dead load was 120 k/pile, as	-

	compared to the total predicted unfactored axial dead load of 95.3 k/pile, a difference of -20.6%.	
• Iterative procedure interacting with COM624P (p. 14)	Measured girder and abutment rotations, pile strains, and abutment displacements all indicate that the abutment-to-backwall connection is not rigid and the abutment rotates away from the backfill. Assumption of a rigid connection by the PennDOT IA program leads to excessively conservative results. Measured pile moments are 25 ft-kip as compared to predicted 116.2 ft-kip, nearly 5 times larger.	The PennDOT IA program poorly predicts the behavior of the abutment and backwall movement and program assumptions are not valid. A behavior model that incorporates rotational flexibility of the structure needs to be incorporated.
• Axial load-moment interaction (p. 16)	Neither original design nor PennDOT IA program design accounts for x-axis pile bending under wind loads and thermally induced abutment movements in the transverse direction.	Corrections of structure flexibility as described above and the inclusion of wind and transverse thermal behavior are required to more accurately predict behavior.
• Abutment/pile cap reinforcement (p. 18)	The PennDOT IA program is limited to design of longitudinal reinforcement for abutment/pile cap.	The design of vertical reinforcement for abutment/pile cap member is suggested.
5) Analysis Summary (pp. 19-20)	Analysis summary is concisely and clearly presented.	-

In addition to the issues discussed in Table 7.3, creep and shrinkage of prestressed concrete members were identified as producing a significant and adverse effect on the long-term behavior of IA bridges, including longitudinal abutment movement and pile stresses. As can be observed from extensometer and pile strain gage data (see Chapter 3), the abutment longitudinal displacement in the 2^{nd} year is about 1.7 times greater than the initial displacement and, similarly, the pile moment at the depth near the abutment of the 2^{nd} year is about 2.8 times greater than the initial moment. This behavior is largely due to the effects of concrete creep and shrinkage, which should also be considered in IA bridge design.

7.5 BRIDGE 109 EVAUATION

Unlike bridges 203, 211, and 222, the bridge 109 design was based on the PennDOT IA program. The design philosophy used in the design of bridge 109 is, therefore, based on load resistance factor design. Because the PennDOT IA program was used and field data were not available, neither comparison nor evaluation is provided for this bridge.

The PennDOT program results, complete with input data, are presented below. Four sources were used to obtain bridge material and geometric information: (1) design drawings, (2) design calculations, (3) the geotechnical report, and (4) actual pile driving records. The design drawings, design calculations, and geotechnical report were obtained from KCI technologies Inc., of Harrisburg (the design consultant of this bridge). The average as-built pile length was used in the PennDOT IA program, as presented below.

Title: Birdge 109 - 128 m 4-Span Concrete Prestressed I-girder
90^{o} skew, 3.505 m girder spacing

By: WS
Date: 3/10/2003
Checked: __________
Date: __________

SPREADSHEET PROGRAM DESCRIPTION

This spreadsheet is intended to be used as an aid in designing and analyzing integral abutments. No users manual is provided, but explanations of input values are given throughout the spreadsheet. The spreadsheet is intended to be used in conjunction with the computer program COM624P, which analyzes the lateral behavior of piles, and with PennDOT's steel or prestressed concrete girder design programs. Design Specifications for integral abutments are available in PennDOT Design Manual Part 4 (DM-4), Appendix G. References to applicable provisions in the DM-4, as well as to the AASHTO LRFD Bridge Design Specifiction, 1994, are made near the right hand margin. Many dimensions for integral abutments are set forth in PennDOT's BD-667M Standard Drawings. The spreadsheet was written in SI units, although the English unit equivalents are also provided, such that either units can be used. Warning and Error messages are provided where possible. An Error message indicates an input value is incorrect and should be changed, a Warning message flags an input value that is suspect, and the user should verify the value, or in some cases, obtain the approval c
Different sheets (tabs), labeled along the bottom of the window, perform different tasks within the spreadsheet. The first tab in the spreadsheet summarizes the input values by providing a simple list which can be printed and filled in by hand, or used to insert the input values. The current tab is the Main tab where most of the analysis takes place. The Scour tab is available for cases where an additional scour check of the piles is required. The COM624P Input tab is used to generate an template for the COM624P computer program. The load factors for each load case are listed on the Load Factor tab. The Cap Reinforcement tab calculates the area of reinforcement needed for the pile cap. The Pile Data tab lists the properties of available H-pile sections, calculates the properties of concrete filled pipe piles, and lists the current pile properties for insertion into the Main tab.

[ ] - denotes input cells

BRIDGE DATA

Input all the geometric and material data for the proposed bridge. This information should be available from a superstructure design already performed independently, as well as a Type, Size, and Location (TS&L) Report, if available.

The girder material is required to determine the coefficient of thermal expansion of the bridge and the uniform temperature change.

Girder material (S - Steel, C - Concrete) [C]

There are three types of girders which can be used with integral abutments: Steel I-girders, concrete I-girders, or concrete spread box girders.

Girder type (I - I-girder, B - Box girder) [I]

Steel bridge lengths in excess of 120000 mm and concrete bridge lengths in excess of 180000 mm require the written approval of the Chief Bridge Engineer for use with integral abutments. In addition, bridges in excess of these limits require consideration of secondary forces such as those caused by creep, shrinkage, thermal gradient, or differential settlements. The methods of applying secondary forces also require the approval of the Chief Bridge Engineer. DM-4 Ap.G.1.2.1 DM-4 Ap.G.1.2.7.5

Total bridge length - centerline end bearing to centerline end bearing
[128016] mm 420.00 ft

The length of the span adjacent to the abutment is required to calculate the pedestrian loads and wind loads on the abutment. It is also used to assess whether the bridge is simply supported or continuous, and in the simplified procedure to determine axial forces induced in the piles in continuous bridges due to thermal movements. Input the total span length for single span bridges.

Length of span adjacent to abutment - centerline bearing to centerline bearing
[26517.6] mm 87.00 ft DM-4 Ap.G.1.2.1

Skews are limited to 70 degrees or more for continuous spans and single spans longer than 40000 mm. Skews of up to 60 degrees are allowed for single spans in excess of 27000 mm but not longer than 40000 mm. For single spans 27000 mm and less, skews up to 45 degrees are permitted. Only positive skew values >45 or <90 degrees can be used in the spreadsheet. DM-4 Ap.G.1.2.2

Skew [90] degrees 1.57 radians

Title: Birdge 109 - 128 m 4-Span Concrete Prestressed I-girder
90° skew, 3.505 m girder spacing

By: WS
Checked:
Date: 3/10/2003
Date:

The curb-to-curb roadway width, the sum of clear sidewalk widths, and the out-to-out superstructure widths are required input. Warnings will be supplied if these values plus conservative estimates of parapet widths are not consistent. It is the users responsibility to make sure these values are correct, however. The roadway and sidewalk widths are used in calculating live load reactions. The out-to-out superstructure width is used to determine both loadings and the length of the integral abutment.

Curb-to-curb (roadway) width	12192	mm	40.00 ft
Sum of clear widths of sidewalks on bridge	0	mm	0.00 ft
Out-to-out superstructure width	13072	mm	42.89 ft

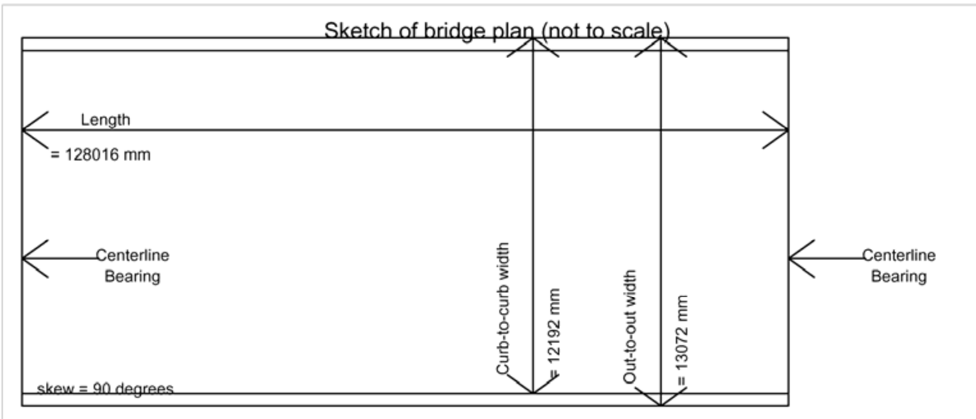

The maximum number of lanes with sidewalks is determined by dividing the width of available roadway (out-to-out of curbs) by the specified lane width (3600 mm) and rounding down to the nearest integer. Widths between 6000 and 7200 mm are assumed to carry two lanes, however. Similarly, the maximum number of lanes without sidewalks is determined by taking the out-to-out width of the structure minus two assumed 440 mm parapets, dividing by the specified lane width, and rounding down to the nearest integer. Again, widths between 6000 and 7200 mm are assumed to carry two lanes. A3.6.1.1.1

Curb-to-curb width of roadway divided by lane width = 12192/3600 = 3.39
Maximum number of lanes with sidewalks 3

Total bridge clear width divided by lane width = (13072 - 880)/3600 = 3.39
Maximum number of lanes without sidewalks 3

The number of girders and the girder spacing is needed to determine the maximum girder reaction for pile cap design. Other dimensions are used to determine various things such as end diaphragm height and lateral wind area of the span, which are utilized in calculating dead and wind loads.

Number of girders in the cross-section	4			
Girder spacing normal to longitudinal axis	3505.2	mm	11.50 ft	
Girder width (maximum of top or bottom flange width at the abutment)	1066.8	mm	3.50 ft	
Girder depth	1981.2	mm	6.50 ft	DM-4 Ap.G.1.2.8

Warning - girders deeper than 1825 mm (6.0 ft.) require the written approval of the Chief Bridge Engineer as per DM-4 Ap. G1.2.8

Bearing pad thickness	20	mm	0.79 in	DM-4 Ap.G.1.7
Deck + haunch thickness	273.5	mm	10.77 in	
Parapet height	1070	mm	3.51 ft	

Title: Birdge 109 - 128 m 4-Span Concrete Prestressed I-girder
90^o skew, 3.505 m girder spacing

By: WS
Checked:
Date: 3/10/2003
Date:

Total superstructure depth for wind analysis - top of parapet to bottom of girder

1981.2 + 273.5 + 1070 = 3324.7 mm 10.91 ft

The moment of inertia of the girders about the longitudinal axis of the bridge is calculated as illustrated in the figure below (five I-girders shown for illustrative purposes, the actual number of girders is used in the calculations). This value is used later to determine girder reactions due to transverse and overturning loadings.

Given a group of n girders, the second moment of inertia is calculated by summing the squares of the distances of the girders from the center of gravity of the girder group, or $I = \Sigma d_i^2$. For a single line of n equally spaced girders, the equation $I = n (n^2 - 1) L^2 / 12$ gives the same result, where n is the number of girders, and L is the girder spacing.

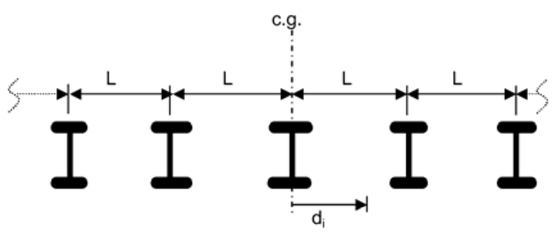

Moment of inertia of 4 I-girders about the longitudinal axis of the bridge:

4(4^2 - 1)(3505.2^2)/12 = 61432135.2 mm^2 95220 in^2

INTEGRAL ABUTMENT DATA

Given the geometry of the superstructure, the location of the proposed abutment, and the topography of the site, the geomety of the integral abutment can be calculated, and the wingwall lengths can be determined. Many of the dimensions are set in the PennDOT standards (see BD-667M Standard Drawing).

The abutment length is measured along the line of bearing. Note that specifying detached wingwalls later in the spreadsheet results in a slightly longer abutment (see BD-667M for detached wingwall details).

Abutment length	(13072)/sin(90) =	13072 mm	42.89 ft	

The abutment width is set at 1200 mm so that for any potential skew angle the pile cap reinforcement can fit around the piles.

Abutment width	1200 mm	3.94 ft	DM-4 Ap.G.1.4.1

The minimum pile cap height is 1000 mm. The flexural design of the pile cap is based on the supplied minimum dimension. There are a number of factors which can affect the maximum pile cap height. These include, but are not limited to, bridge width and cross-slopes, superelevation, skew, etc. DM-4 Ap.G.1.4.1

Although PennDOT permits the opposite ends of integral abutments to vary up to 450 mm in height due to superelevation (300 mm for skews less than 80^o), sloping the bottom of the pile cap such that the ends are equal is recommended to simplify reinforcement details. DM-4 Ap.G.1.4.1

Left end pile cap height, d_{pc1}	1213.1	mm	3.98 ft
Pile cap height at the crown of the roadway, or at the bridge midwidth for a superelevated roadway, $d_{pc,cl}$	1118.6	mm	3.67 ft
Right end pile cap height, d_{pc2}	1024.13	mm	3.36 ft

Difference between the height of the cap at the ends, $|d_{pc1} - d_{pc2}|$ = | 1213 - 1024 | =

188.97 mm 0.62 ft

The previous three values are used to calculate an average pile cap height and assume a constantly sloping top of cap with a crown at the center, as illustrated in the figure below. Only the minimum value is used to design the pile cap, the average value is used for selfweight calculations. Note that if the cap does not have either a constant cross-slope or crown at the midwidth, the average pile cap height will not be precisely correct. If a more exact selfweight is required, the maximum height at midwidth can be adjusted until the desired average pile cap height is attained.

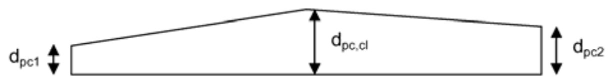

Average pile cap height
(1213.1+1024.13)/4 + 1118.6/2 = 1118.6075 mm 3.67 ft
The end diaphragm height is equal to the deck and haunch thickness + girder depth + bearing pad depth.
End diaphragm height 273.5 + 1981.2 + 20 = 2274.7 mm 7.46 ft
The total average abutment height is equal to the end diaphragm height plus the average pile cap height.
Total average abutment height 2275 + 1119 = 3393.3075 mm 11.13 ft

WINGWALLS

Attached wingwalls up to 2400 mm long (measured from the back face of the abutment) may be rectangular, extending the full depth of the abutment. Attached wingwalls over 2400 mm up to 4560 mm must be tapered. Wingwalls longer than 4560 mm will be detached. The standard location of the joint for a detached wingwall is 900 mm from the back face of the abutment, as shown in the figure below. The detached portion of the wingwall is to be designed independently. A 300 mm chamfer is provided in the interior corner of the wingwall/abutment connection (see figure). DM-4 Ap.G.1.4.4

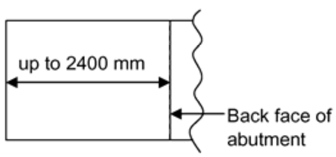

Rectangular wingwall

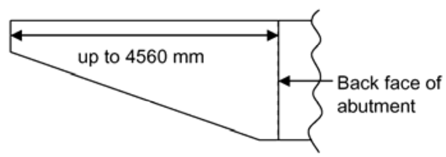

Tapered wingwall

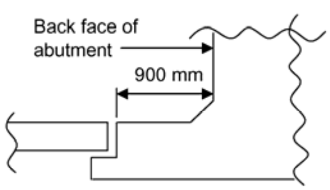

Detached wingwall

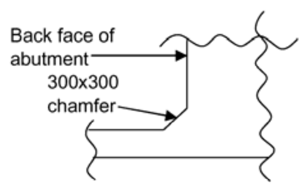

Abutment/wingwall corner chamfer

Type of wingwall (R - Rectangular, T - Tapered, D - Detached) T
Wingwall length (including 300mm chamfer) 3657.6 mm 12.0 ft

The wingwall dimensions are required for dead load calculations.
The average wingwall height at the abutment back face is conservatively assumed to be equal to the average height of the abutment.
Wingwall height at back face of abutment 3393.3075 mm 11.13 ft
The height at the end is assumed to be either equal to the height at the abutment for rectangular (R) or detached (D) wingwalls, or 600 mm for tapered (T) wingwalls DM-4 Ap.G.1.4.4
Wingwall height at end 600 mm 1.97 ft
The attached wingwall thickness is assumed to be the same width as the typical concrete parapet. An effective average thickness is assumed for the abutment extension for detached wingwalls. To obtain the effective width, the 250x300 mm overlap section (see BD-667M Standard Drawing) is smeared over the length of the stub.
Wingwall width 440 mm 1.44 ft

Title: Birdge 109 - 128 m 4-Span Concrete Prestressed I-girder
90^{o} skew, 3.505 m girder spacing

By: WS
Checked:
Date: 3/10/2003
Date:

LOAD DATA

LRFD design philosophy employs the equation $\Sigma\eta_i\gamma_iQ_i \leq \varphi R_n = R_r$. In this equation, γ_i is a load factor, Q_i is a load effect, φ is a resistance factor, R_n is a nominal resistance, and R_r is a factored resistance. This leaves the η_i (eta) factor, which is a load modifier used to account for ductility, redundancy, and operational importance. $\eta_{i,max}$ is used when maximizing loads. $\eta_{i,min}$ is used when minimizing loads. Penndot currently limits η_i to values greater than or equal to 1.00 and less than or equal to 1.16. — A1.3.2.1, D1.3.2

η_i factor	1.00	
$\eta_{i,max} = \eta_i \geq 1.00$	1.00	D1.3.2
$\eta_{i,min} = 1/\eta_i \leq 1.00$	1.00	A1.3.2.1

The unfactored girder design loads are available from the superstructure design performed using PennDOT's prestressed concrete girder design program. Both the interior and exterior noncomposite girder design dead loads are required input, although if only the controlling value is known, it can be conservatively used for both. The remaining composite dead loads should be the same whether they come from an interior or exterior girder design. The maximum and minimum unfactored live loads, with impact and shear distribution factors included, are also required input. The shear distribution factor is required as well, so that it can be divided out of the given loads to get the reaction per traffic lane. These values are available directly from the PennDOT beam design programs. Either the exterior or interior girder design can be used for the live load values, as long as all the values (reactions and distribution factors) come from the same girder design. Additional loads are calculated later. — DM-4 Ap.G.1.2.7

Dead Loads - Unfactored:

Non-composite DC1 loads - include girder, deck, haunch, interior diaphragms		
Interior girder, DC1	528.4 kN	118.79 k
Exterior girder, DC1	482.8 kN	108.54 k
Composite DC2 loads - include parapets,		
Interior girder, DC2	50.3 kN	11.31 k
Exterior girder, DC2	50.3 kN	11.31 k
Composite DW loads - include future wearing surface,		
Interior girder, DW	58.1 kN	13.06 k
Exterior girder, DW	58.1 kN	13.06 k

Live load shear distribution factor: 1.05

Live Loads - Unfactored from girder design program (distribution factor included):

PHL-93	max	529.5 kN	119.0 k
	min	-85.8 kN	-19.3 k
P-82	max	931.1 kN	209.3 k
	min	-143.0 kN	-32.1 k

Live Loads - Unfactored - distribution factor removed - reaction due to live load on one traffic lane:

PHL-93	max	(529.5)/(1.05) =	504.3 kN	113.4 k
	min	(-85.8)/(1.05) =	-81.7 kN	-18.4 k
P-82	max	(931.1)/(1.05) =	886.8 kN	199.4 k
	min	(-143)/(1.05) =	-136.2 kN	-30.6 k

The total pedestrian load reaction at the abutment is calculated assuming the approach slab and the first span are simply supported. The first span portion is calculated here, the approach slab portion is added in with the approach slab loads. The pedestrian load per unit area is as specified in the AASHTO LRFD Bridge specification, and the total width of sidewalk input earlier is used. This reaction is then distributed equally to all girders and piles. — DM-4 Ap.G.1.2.7.2, A3.6.1.6, D3.6.1.6

Pedestrian	max	(0.0036)(0)(26518)/2000 =			
			0.0 kN	0.0 k	A3.6.1.6
	min		0.0 kN	0.0 k	

Choose the load factors to be used for the DW loads. For new construction or analysis of existing construction, where no future wearing surface is present, the DW load factors are taken as 1.50 max and 0.00 min. For bridges where a future wearing surface is present, the DW load factors are taken as 1.50 max and 0.65 min. Typically, the future wearing surface will not be currently present - N.

Future wearing surface currently present (Y or N)? N

DW load factors Maximum = 1.50 Minimum = 0.00

Title: Birdge 109 - 128 m 4-Span Concrete Prestressed I-girder
90° skew, 3.505 m girder spacing

By: WS
Checked:
Date: 3/10/2003
Date:

The extreme girder reactions, interior or exterior, are (conservatively) required for the design of the abutment pile cap. The total reaction with all lanes loaded, or the average pile reaction, is required for the pile design, which also requires both interior and exterior girder reactions. Note: The η_i factor is included here.

Factored Dead + Live reaction for interior girder:

Strength I	max	1.00[1.25(528.4+50.3) + 1.50(58.1) + 1.75(504.29)(3)/4] =		
			1472.4 kN	331.0 k
	min	1.00[0.90(528.4+50.3) + 0.00(58.1)] + 1.00[1.75(-81.71)(3)/4] =		
			413.6 kN	93.0 k
Strength IP	max	1.00[1.25(528.4+50.3) + 1.50(58.1) + 1.75(0)/4 + 1.35(504.29)(3)/4] =		
			1321.1 kN	297.0 k
	min	1.00[0.90(528.4+50.3) + 0.00(58.1) + 1.75(0.00)/4] + 1.00[1.35(-81.71)(3)/4] =		
			438.1 kN	98.5 k
Strength II	max	1.00[1.25(528.4+50.3) + 1.50(58.1) + 1.35[886.76+504.29(3-1)]/4] =		
			1450.2 kN	326.0 k
	min	1.00[0.90(528.4+50.3) + 0.00(58.1)] + 1.35[(1.00)(-136.19)+(1.00)(-81.71)(3-1)]/4 =		
			419.7 kN	94.4 k
Strength III	max	1.00[1.25(528.4+50.3) + 1.50(58.1)] =		
			810.5 kN	182.2 k
	min	1.00[0.90(528.4+50.3) + 0.00(58.1)] =		
			520.8 kN	117.1 k
Strength V	max	1.00[1.25(528.4+50.3) + 1.50(58.1) + 1.35(504.29)(3)/4] =		
			1321.1 kN	297.0 k
	min	1.00[0.90(528.4+50.3) + 0.00(58.1)] + 1.00[1.35(-81.71)(3)/4] =		
			438.1 kN	98.5 k

Factored Dead + Live reaction for exterior girder:

Strength I	max	1.00[1.25(482.8+50.3) + 1.50(58.1) + 1.75(504.29)(3)/4] =		
			1415.4 kN	318.2 k
	min	1.00[0.90(482.8+50.3) + 0.00(58.1)] + 1.00[1.75(-81.71)(3)/4] =		
			372.5 kN	83.8 k
Strength IP	max	1.00[1.25(482.8+50.3) + 1.50(58.1) + 1.75(0)/4 + 1.35(504.29)(3)/4] =		
			1264.1 kN	284.2 k
	min	1.00[0.90(482.8+50.3) + 0.00(58.1) + 1.75(0.00)/4] + 1.00[1.35(-81.71)(3)/4] =		
			397.1 kN	89.3 k
Strength II	max	1.00[1.25(482.8+50.3) + 1.50(58.1) + 1.35[886.76+504.29(3-1)]/4] =		
			1393.2 kN	313.2 k
	min	1.00[0.90(482.8+50.3) +0.00(58.1)] + 1.35[(1.00)(-136.19)+(1.00)(-81.71)(3-1)]/4 =		
			378.7 kN	85.1 k
Strength III	max	1.00[1.25(482.8+50.3) + 1.50(58.1)] =		
			753.5 kN	169.4 k
	min	1.00[0.90(482.8+50.3) + 0.00(58.1)] =		
			479.8 kN	107.9 k
Strength V	max	1.00[1.25(482.8+50.3) + 1.50(58.1) + 1.35(504.29)(3)/4] =		
			1264.1 kN	284.2 k
	min	1.00[0.90(482.8+50.3) + 0.00(58.1)] + 1.00[1.35(-81.71)(3)/4] =		
			397.1 kN	89.3 k

When designing integral abutments, only the girder rotations that are transferred to the piles are needed. Most dead load rotations occur prior to pouring the end diaphragm, and therefore will not be transferred to the piles. The exception to this is any composite dead loads such as future wearing surface or parapets. The extreme live load and composite dead load girder rotations are conservatively used as the design rotations for the piles. The unfactored live load and composite dead load rotations are available from the girder design.

Unfactored Live Load rotations per girder (including distribution factor):

PHL-93	max	0.028 degrees	0.0005	radians
	min	-0.062 degrees	-0.0011	radians
P-82	max	0.047 degrees	0.0008	radians
	min	-0.100 degrees	-0.0018	radians

Title: Birdge 109 - 128 m 4-Span Concrete Prestressed I-girder
90° skew, 3.505 m girder spacing
By: WS
Checked:
Date: 3/10/2003
Date:

The rotations above are the single girder unfactored rotations. To get the average girder rotations required for the design of integral abutments, the maximum number of traffic lanes on the bridge are loaded and the loads are assumed equally distributed to all girders. To accomplish this using the above results from the girder design program, the distribution factor is divided out to get the rotation of the full traffic lane applied to one girder. Then, the result is multiplied by the number of lanes and divided by the number of girders in the bridge.

Average Live Load rotations per girder:

PHL-93	max	(0.0005/1.05)(3/4) =		
		0.020 degrees	0.0003 radians	
	min	(-0.0011/1.05)(3/4) =		
		-0.044 degrees	-0.0008 radians	
P-82	max	(0.0008/1.05)(3/4) =		
		0.034 degrees	0.0006 radians	
	min	(-0.0018/1.05)(3/4) =		
		-0.072 degrees	-0.0013 radians	

The total rotation of any composite dead load rotations (unfactored), e.g. future wearing surface and parapets, can be input here. This value will be factored using the maximum DW load factor, 1.50.

0.008 degrees $\boxed{0.0001}$ radians

Maximum factored rotations are calculated here. The DM-4 allows the P-82 permit load to be placed in only one lane, with PHL-93 load in the remaining lanes. If the P-82 rotation controls the girder design the abutment design rotations are adjusted accordingly to account for P-82 on one lane and PHL-93 on all other lanes. The maximum load factor is used for both the maximum (positive) and minimum (negative) values.

Average factored live load + future dead load rotations (including eta factor):

	Controlling load		
max	PHL-93 all lanes	(1.00)[(1.75)(0.0003) + (1.50)(0.0001)] =	
		0.047 degrees	0.0008 radians
min	PHL-93 all lanes	(1.00)[(1.75)(-0.0008) + (1.50)(0.0000)] =	
		-0.078 degrees	-0.0014 radians

Additional Loads

Additional loads due to wind and centrifugal force are calculated here. The approach slab dead and live loads, and wingwall and abutment dead loads are calculated in the next section.

Wind Loads — DM-4 Ap.G.1.2.7.3
The appropriate wind pressure on the structure is input here. — A3.8
Wind on structure pressure = $\boxed{0.0024}$ MPa 0.000348 ksi — A3.8.1.2

The wind forces on the abutment are calculated assuming only the bridge span adjacent to the abutment contributes to the load, and that the span is simply supported laterally (half of the wind force on the end span is resisted by the abutment).

lateral force = (0.0024)(26517.6)(3324.7)/2000 = 105.80 kN 23.78 k

Uplift pressure is defined as a constant 0.00096 MPa. The force from this pressure is assumed to act as a line load at a distance of 1/4 of the out-to-out width of the bridge from the edge of the bridge. — A3.8.2

Uplift force (acts @ 1/4 point) pressure = 0.00096 MPa 0.000139 ksi
uplift = (-0.00096)(26517.6)(13072)/2000 = -166.39 kN -37.41 k
moment about the longitudinal axis of the bridge = -(-166.39)(13072)/4000 =
543.75 kN-m 401.05 k-ft

Wind on live load is taken as 1.46 kN/m acting at 1800 mm above the deck — A3.8.1.3

Wind on live load distributed force = 1.46 kN/m 0.10 k/ft
lateral force = (1.46)(26517.6)/2000 = 19.36 kN 4.35 k

Centrifugal force — DM-4 Ap.G.1.2.3, A3.6.3

Integral abutments are permitted for curved bridges as long as the girders are straight and parallel within each span, and approval is obtained from the Chief Bridge Engineer. Despite the limited curvature this allows, centrifugal forces can be generated. The centrifugal force and any other lateral forces other than wind forces contributing to overturning moments can be input here. This force will be assumed to act perpendicular to the longitudinal axis of the bridge at a distance 1800 mm above the roadway surface.

Centrifugal force $\boxed{0}$ kN 0.00 k

Girder and Pile Reactions

Girder and pile reactions are calculated assuming overturning moments are resisted by vertical forces only.

Girder reactions due to wind and centrifugal forces:

The top of deck to the top of the pile cap is equal to the end diaphragm height.

Top of deck to the top of the pile cap = 2274.7 mm 7.46 ft

The moment due to the wind on the superstructure is equal to the wind force times half the depth of the structure plus the bearing pad depth.

Wind on structure

moment = (105.80)[(3324.7/2)+20]/1000 = 177.99 kN-m 131.28 k-ft

The moment of the wind on the live load is equal to the force times the moment arm which is equal to the distance from the top of the pile cap to the top of the deck plus 1800 mm.

Wind on live load

moment = (19.36)(2274.7+1800)/1000 = 78.88 kN-m 58.18 k-ft

The moment of the centrifugal force is equal to the centrifugal force times the moment arm which is also equal to the distance from the top of the pile cap to the top of the deck plus 1800 mm.

Centrifugal

moment = (0.00)(2275+1800)/1000 = 0.00 kN-m 0.00 k-ft

The unfactored extreme reactions per girder for wind loads are calculated assuming the vertical wind forces are distributed equally to all girders, and the moments are resisted by vertical reactions of the girders (see figure below - note that five I-girders are used for illustrative purposes only - actual number of girders used in calculations). Forces due to the moments are calculated assuming the superstructure acts as a rigid member transversely, and the vertical force is proportional to the distance from the center of gravity of the girder group. The force at any girder is equal to the moment times the distance from the midwidth of the bridge divided by the second moment of inertia. The extreme overturning reactions are therefore at the exterior girders.

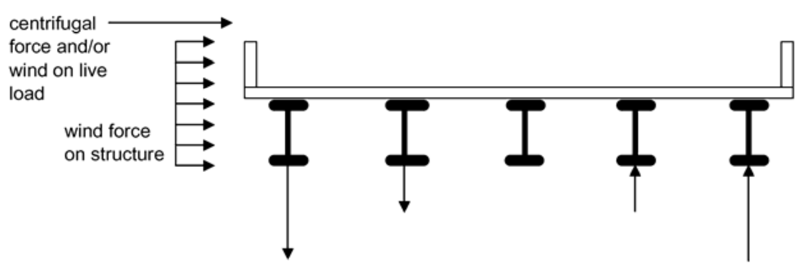

Extreme girder reactions due to wind on the structure

WS	max	(177.99)(1000)(4-1)(3505.2)/(2*61432135.2) =		
			15.23 kN/girder	3.42 k/girder
	min	-(177.99)(1000)(4-1)(3505.2)/(2*61432135.2) =		
			-15.23 kN/girder	-3.42 k/girder

Extreme forces due to uplift

Uplift	max	-166.39/4 + (543.75)(1000)(4-1)(3505.2)/(2*61432135.2) =		
			4.94 kN/girder	1.11 k/girder
	min	-166.39/4 - (543.75)(1000)(4-1)(3505.2)/(2*61432135.2) =		
			-88.13 kN/girder	-19.81 k/girder

Extreme forces due to wind on live load

WL	max	(78.88)(1000)(4-1)(3505.2)/(2*61432135.2) =		
			6.75 kN/girder	1.52 k/girder
	min	-(78.88)(1000)(4-1)(3505.2)/(2*61432135.2) =		
			-6.75 kN/girder	-1.52 k/girder

Extreme forces due to centrifugal forces

CE	max	(0.00)(1000)(4-1)(3505.2)/(2*61432135.2) =		
			0.00 kN/girder	0.00 k/girder
	min	-(0.00)(1000)(4-1)(3505.2)/(2*61432135.2) =		
			0.00 kN/girder	0.00 k/girder

Choose a trial pile section at this point. The pile dimensions are needed for the pile location check. The pile

moment of inertia is used to calculate the thermally induced forces in the piles. The pile properties are also required to run the COM624P computer program. Two types of piles are permitted for integral abutments, steel H-piles or concrete filled pipe piles.

Type of piles H - HP shape, P - pipe | H

For H-piles, the yield stress of the steel and the metric designation of the pile is required input. A list of available H-pile sections is provided. The user may then input the additional section properties manually, or press the button to the right, and the properties will be automatically retrieved.

Import Pile Properties

Pile Properties					HP Shapes
Pile designation	HP310x110		(HP12x74)		HP360x174
Yield stress of pile steel, F_y	245	MPa	36	ksi	HP360x152
Pile section depth, d	308	mm	12.1	in	HP360x132
Flange width, bf	310	mm	12.2	in	HP360x108
Flange thickness, tf	15.50	mm	0.610	in	HP310x125
Pile Area, Ap	14100	mm^2	21.9	in^2	HP310x110
Moment of inertia, $I_{y\text{-}y}$	77.1E+6	mm^4	185	in^4	HP310x94
Elastic section modulus, $S_{y\text{-}y}$	49.7E+4	mm^3	30.3	in^3	HP310x79
Radius of gyration, $r_{y\text{-}y}$	73.9	mm	2.91	in	HP250x85
Plastic section modulus, $Z_{y\text{-}y}$	76.3E+4	mm^3	46.6	in^3	HP250x62
					HP200x54

PILE DATA

Choose a pile layout. If a geotechnical report is available with a calculated pile capacity, a preliminary number of piles can be found by dividing the total factored dead + live girder reactions by the given pile capacity and rounding up to the next highest integer. If no pile load capacity is available, use an estimate of the load capacity based on the soil conditions. The maximum pile spacing is 3000 mm. The minimum pile spacing is the larger of 900 mm, or 2.5 times the diameter of round piles, or 2 times the diagonal dimension of H-piles (The 2x criteria only controls for HP360 piles). Note that the approximate range of allowed pile spacing calculated below assumes 900 mm is the minimum pile spacing, and may suggest a range which is not permitted based on pile dimensions. The pile location check made below should flag any erroneous spacings attempted, however.

DM-4 Ap.G.1.4.2
D10.7.1.5

Maximum total factored dead + live girder reactions
(1415.40)(2) + (1472.40)(2) = 5775.60 kN 1298.41 k

Number of piles 12

Approximate range of allowed pile spacing for 12 piles is about 1060 to 1100 mm

Chosen pile spacing along abutment	1104.9	mm	3.63	ft
Total pile length, L_{tot} =	27660.87	mm	90.75	ft

The minimum and maximum edge distance for the end piles is intended to keep the piles close to the end of the integral abutment in order to provide support for the attached wingwalls, without getting too close to the end of the abutment.

Minimum edge distance to centerline of piles	450	mm	17.72	in	D10.7.1.5
Maximum edge distance to centerline of piles	750	mm	29.53	in	DM-4 Ap.G.1.4.2.1

Pile location check OK

Pile spacing normal to the longitudinal axis of span
1104.9sin(90) = 1105 mm 3.63 ft

The moment of inertia of the pile group is calculated similarly to the girders above and is used to determine the axial forces in the piles due to overturning moments.

Moment of inertia of pile group about the longitudinal axis of the bridge
12(12^2 - 1)(1105^2)/12 = 174574973 mm^2 270592 in^2

Title: Birdge 109 - 128 m 4-Span Concrete Prestressed I-girder
90° skew, 3.505 m girder spacing

By: WS
Date: 3/10/2003
Checked:
Date:

Pile loads due to wind and centrifugal forces

At this point, an iterative procedure is initiated to determine the loads on the piles. Initially, a depth to fixity of the piles is assumed. Later, the actual depth to fixity is calculated using the computer program COM624P, and this value is adjusted as necessary. The procedure is repeated until the estimated value is within 10% of the value obtained from the COM624P computer program. An initial choice of 5000-6000 mm to the point of fixity is reasonable.

Assume depth to pile fixity of 3521.96 mm 11.55 ft

The overturning moment resisted by the piles is calculated similarly to the overturning moments resisted by the girders, except the moment arm extends to the point of assumed pile fixity (see figure below - note that five I-girders and six H-piles are used for illustration purposes only). Wind uplift forces result in the same overturning moments on the piles as calculated earlier for the girders.

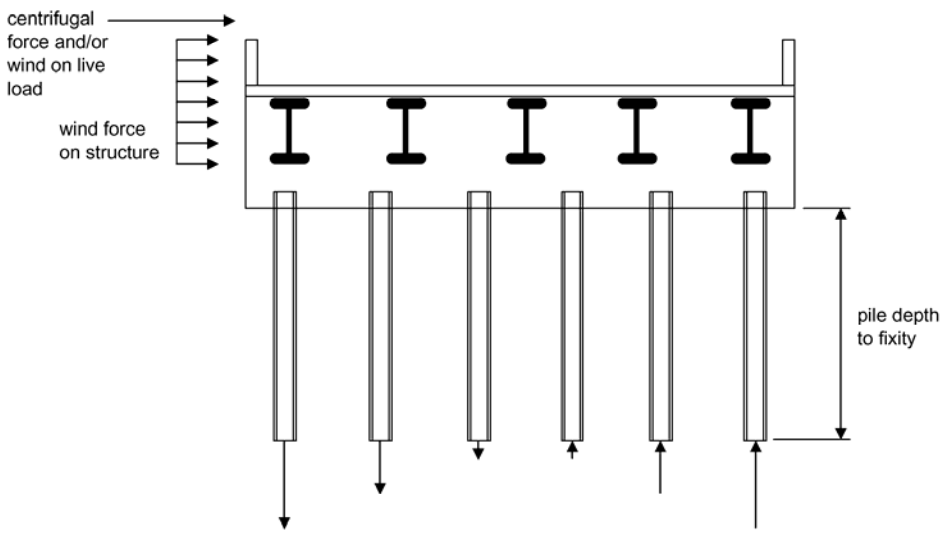

Wind on structure	moment = (105.80)(3522+1118.6+20+3324.7/2)/1000 =		
		668.94 kN-m	493.38 k-ft
Wind on live load	moment = (19.36)(1800+3522+1118.6+2274.7)/1000 =		
		168.71 kN-m	124.43 k-ft
Centrifugal forces	moment = (0.00)(1800+3522+1118.6+2274.7)/1000 =		
		0.00 kN-m	0.00 k-ft

The unfactored extreme loads per pile for wind cases are calculated similar to the girder reactions

Extreme forces due to wind on the structure

WS	max	(668.94)(1000)(12-1)(1105)/(2*174574973) =		
			23.29 kN/pile	5.23 k/pile
	min	-(668.94)(1000)(12-1)(1105)/(2*174574973) =		
			-23.29 kN/pile	-5.23 k/pile

Extreme forces due to uplift

Uplift	max	-166.39/12 + (543.75)(1000)(12-1)(1105)/(2*174574973) =		
			5.06 kN/pile	1.14 k/pile
	min	-166.39/12 - (543.75)(1000)(12-1)(1105)/(2*174574973) =		
			-32.79 kN/pile	-7.37 k/pile

Title: Birdge 109 - 128 m 4-Span Concrete Prestressed I-girder
90^o skew, 3.505 m girder spacing

By: WS
Checked:
Date: 3/10/2003
Date:

Extreme forces due to wind on live load

WL	max	(168.71)(1000)(12-1)(1105)/(2*174574973) =		
		5.87 kN/pile	1.32 k/pile	
	min	-(168.71)(1000)(12-1)(1105)/(2*174574973) =		
		-5.87 kN/pile	-1.32 k/pile	

Extreme forces due to centrifugal force

CE	max	(0.00)(1000)(12-1)(1105)/(2*174574973) =		
		0.00 kN/pile	0.00 k/pile	
	min	-(0.00)(1000)(12-1)(1105)/(2*174574973) =		
		0.00 kN/pile	0.00 k/pile	

Additional Dead + Live Loads (Approach Slab, Wingwalls, and Abutment)

The approach slab live load is calculated assuming the slab is simply supported at the ends, the lane load only is present in all lanes, and the total reaction is distributed equally to all piles. The truck load is not included here because it was already included in the bridge loads. As previously, the multiple presence factor is not used. Dead loads from the approach slab are also distributed equally to all piles.

Approach slab dimensions

Approach slab thickness =	450 mm	18 in	DM-4 App. G 1.5
Approach slab length =	7500 mm	25 ft	

Approach slab loads

Approach Slab Load = (2.4)(9.81)(12192)(7500)(0.45)/2000000 =
484.39 kN 108.90 k

Approach Slab Future Wearing Surface = (0.15)(9.81)(12192)(7500)/2000000 = D3.5.1
67.28 kN 15.12 k

Approach Slab Lane Load (1 lane) = (9.3)(7500)/2000 = A3.6.1.2.4
34.88 kN 7.84 k

Approach Slab Pedestrian Live Load (total reaction) = (0.0036)(0)(7500)/2000 =
0.00 kN 0.00 k

Abutment self-weight Dead Load = (2.4)(9.81)(13072)(1200)(3393)/1000000000 =
1253.22 kN 281.73 k

Wingwalls and parapet load

The parapet weight/length can be input for wingwall dead load calculations. A typical 440 mm wide concrete parapet weighs about 7.60 N/mm. Any other miscellaneous loads can also be included in this number, but note that the value will be multiplied by the length of the wingwall plus abutment (3657.6 + 1200/SIN(90) = 4858 mm) times two since parapets are assumed to be on both sides of the bridge.

Parapet weight/length $\boxed{7.60}$ N/mm 0.521 k/ft

Weight of two wingwalls = (2)(2.4)(9.81){(3393.3075)(300)(440+300sin(90)/2)+[(3658-300)(440)(3393.3075+600)/2)]/1000000000}

Weight of two parapets = (2)(7.60)(3657.6+1200/sin(90))/1000

Total weight of wingwalls and parapets = 241.01 kN 54.18 k

Thermal Expansion

The thermal expansion of the bridge is calculated assuming the entire superstructure length, L, is unrestrained, and undergoes a uniform thermal expansion. This ignores the pier stiffnesses (if any) and passive soil pressure against the backwalls. For design purposes, a percentage of this thermal expansion can be assigned to take place at the abutment under consideration. It is the responsibility of the designer to determine the percentage of expansion. In some cases, such as single spans with identical abutments, simply assigning 50% of the movement to each end may be appropriate. In other cases, such as for continuous structures with unsymmetrical piers, a more in-depth thermal analysis taking pier and abutment stiffnesses into account is required. See DM-4 Ap.G.1.2.7.4 for thermal movement requirements.

The coefficient of thermal expansion and temperature range are assigned based on the girder material, concrete or steel.

Coefficient of thermal expansion, α	10.8E-6 /^{o}C	(concrete girders)	D5.4.2.2
Temperature range, Δ_T ($\pm$)	44 ^{o}C		DM-4 Ap.G.1.2.7.4
Load factor, ϕ_T	1.0		DM-4 Ap.G.1.2.7.6

Total $\pm$change in length of the bridge, $\phi_T \alpha \Delta_T L$ = (1.0)(0.0000108)(44)(128016) =
60.8 mm 2.40 in

Title: Birdge 109 - 128 m 4-Span Concrete Prestressed I-girder
90° skew, 3.505 m girder spacing

By: WS
Checked:
Date: 3/10/2003
Date:

The percentage of thermal expansion that occurs at the abutment being designed is input here. The value should be between 0 and 100%. For symmetrical structures, 50% of the expansion occurs at each abutment. For unsymmetrical structures, use the procedure described in DM-4 Ap.G1.2.7.4 to determine the percentage of movement at each end.

Percentage of expansion at abutment being designed 50 %

Maximum movement (expansion or contraction) at abutment (±), Δ

(0.50)(60.8) = 30.4 mm 1.20 in

The thermal expansion of continuous bridges induces an axial force in the piles, P_T, which is estimated using the simplified elastic procedure illustrated below (see figure on following page). This procedure assumes that the full passive pressure of the soil is acting on the abutment. Note that the additional pile axial force is zero in a simple span with passive pressure acting at the same height on both abutments.

The coefficient of passive earth pressure has been found to vary from about 3.0 for loose sand to about 6 for dense sand. PennDOT requires that the region immediately adjacent to the abutment be only nominally compacted, so 3.0 is an acceptable value. DM-4 Ap.G.1.2.7.4

Coefficient of passive earth pressure, k_p = 3.0

The density of loose sand given in the AASHTO-LRFD Bridge Design Specification is 1600 kg/m^3. Multiplying by 9.81 m/s^2 converts this value to weight. A3.5.1

Soil unit weight, γ = (1600)(9.81) = 15.70 kN/m^3 100 lb/ft^3

Using the coefficient of passive earth pressure, the soil density, and the depth of the abutment, the force per unit length on the abutment can be calculated.

Force from soil on abutment, $F=1/2\ k_p\gamma H^2$ = (1/2)(3.0)(15.70)(3393.3075/1000)^2 =
271.1 kN/m 18.6 k/ft

The total longitudinal force on the abutment can be found by multiplying by the projected length of the abutment on a line perpendicular to the longitudinal axis of the bridge, which is equal to the out-to-out width of the bridge.

Total passive earth pressure force on abutment, F = (271.1)(13072)/1000 =
3543.8 kN 796.7 k

The previously assumed depth to pile fixity, L_p = 3521.96 mm 11.55 ft

Using simple equilibrium by taking the moment about point A, the axial reaction per pile due to the force, F, and the displacement, Δ, can be calculated as:

F_p = 2FH / 3L / number of piles = (2)(3543.8)(3393.3075)/[(3)(26517.6)]/12 =
25.2 kN/pile 5.7 k/pile

The moment induced in the piles by the thermal movement can be determined using the following equation. The top of the pile is assumed to be fixed.

The moment, $M_T = 6E_pI_p\Delta/L_p^2$ = (6)(200)(77100000)(30.4)/(3521.96^2)/1000 =
226.9 kN-m/pile 167.33 k-ft/pile

Check to make sure the moment, M_T, does not exceed the plastic moment, M_p. Even though the maximum flexural resistance of the pile may be lower, the plastic moment is conservatively used here as an upper bound.

Plastic moment, $M_p = F_yZ_{y\text{-}y}$ = (245)(763000)/1000000 = 186.9 kN-m 137.88 k-ft

since 186.9 < 226.9 - use M_T = 186.9 kN-m 137.88 k-ft

The horizontal force induced in the pile by the thermal deformation can be determined using the following equation. The top of the pile is assumed to be fixed.

The horizontal force, $H_T = 2M_T/L_p$ = (2)(186.9)(1000)/3521.96 =
106.2 kN/pile 23.9 k/pile

The total axial force induced in the pile due to these three components is equal to:

$2FH/3L+H_TH/L+M_T/L$ = 25.2 + (106.2)(3393.3075)/26517.6 + 226.9/(26517.6/1000) = 47.3 kN (10.6 k) /pile

Axial force induced in piles, P_T = 47.3 kN/pile 10.6 k/pile

L

Title: Birdge 109 - 128 m 4-Span Concrete Prestressed I-girder
90° skew, 3.505 m girder spacing
By: WS
Checked:
Date: 3/10/2003
Date:

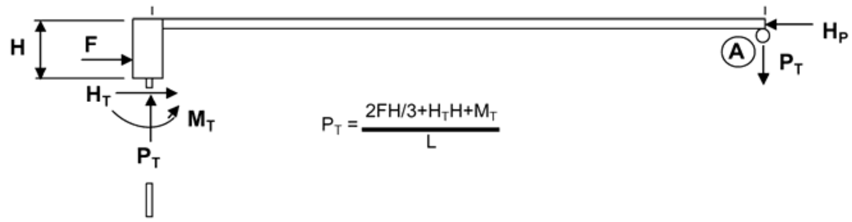

Calculate the maximum factored load on the most heavily loaded pile (see Load Factors tab for load factors for each load combination). Since the factored dead and live loads from the interior and exterior girders have already been calculated, the sum of the girder loads is calculated assuming two exterior girders and the remaining ones interior. These loads, as well as any additional vertical loads, are distributed equally to all piles. The factored extreme overturning loads, which occur on the exterior piles are added. The η_i modifier is also included.

Extreme Factored Dead + Live Loads per pile

Strength I	max	[(1472.4)(2)+(1415.4)(2)]/12 + 1.00{[1.25(484.4+1253.2+241.0)+1.50(67.3)+1.75(3)(34.9)]/12 + 1.75(0.0) + 1.00(47.3)} =	758.41 kN/pile	170.50 k/pile
	min	[(413.6)(2)+(372.5)(2)]/12 + 1.00{[0.90(484.4+1253.2+241.0)+0.00(67.3)+1.75(3)(0.0)]/12} + 1.00[1.75(0.0) + 1.00(0.0)] =	279.42 kN/pile	62.82 k/pile
Strength IP	max	[(1321.1)(2)+(1264.1)(2)]/12 + 1.00{[1.25(484.4+1253.2+241.0)+1.50(67.3)+1.35(3)(34.9)+1.75(0.0)]/12 + 1.35(0.0) + 1.00(47.3)} =	704.49 kN/pile	158.38 k/pile
	min	[(438.1)(2)+(397.1)(2)]/12 + 1.00{[0.90(484.4+1253.2+241.0)+0.00(67.3)+1.35(3)(0.0)+1.75(0.0)]/12} + 1.00[1.35(0.0) + 1.00(0.0)] =	287.59 kN/pile	64.65 k/pile
Strength II	max	[(1450.2)(2)+(1393.2)(2)]/12 + 1.00{[1.25(484.4+1253.2+241.0)+1.5(67.3)+1.35(3-1)(34.9)]/12 + 1.35(0.0) + 1.0(47.3)} =	743.60 kN/pile	167.17 k/pile
	min	[(419.7)(2)+(378.7)(2)]/12 + 1.00{[0.9(484.4+1253.2+241.0)+0(67.3)+1.35(2)(0.0)]/12} + 1.00[1.35(0.0) + 1.0(0.0)] =	281.46 kN/pile	63.27 k/pile
Strength III	max	[(810.5)(2)+(753.5)(2)]/12 + 1.00{[1.25(484.4+1253.2+241.0)+1.50(67.3)]/12 + 1.40(23.3) + + 1.00(47.3)} + 1.00(1.40)(5.1) =	562.21 kN/pile	126.39 k/pile
	min	[(520.8)(2)+(479.8)(2)]/12 + 1.00{[0.90(484.4+1253.2+241.0)+0.00(67.3)]/12} + 1.00[1.40(-23.3) + 1.00(0.0) + 1.40(-32.8)] =	236.66 kN/pile	53.20 k/pile
Strength V	max	[(1321.1)(2)+(1264.1)(2)]/12 + 1.00{[1.25(484.4+1253.2+241.0)+1.50(67.3)+1.35(3)(34.9)]/12 + 0.40(23.3) + 1.00(5.9) + 1.35(0.0) + 1.00(47.3)} =	719.68 kN/pile	161.79 k/pile
	min	[(438.1)(2)+(397.1)(2)]/12 + 1.00{[0.90(484.4+1253.2+241.0)+0.00(67.3)+1.35(3)(0.0)]/12} + 1.00{0.40(-23.3) + 1.00(-5.9) + 1.35(0.0) + 1.00(0.0)} =	272.40 kN/pile	61.24 k/pile

Controlling Loads	max STR I	758.41 kN/pile	170.50 k/pile
	min STR III	236.66 kN/pile	53.20 k/pile

Lateral Pile Analysis

Knowing the soil properties at the abutment (taken from the geotechnical report), and the properties of the piles, and using the calculated design values for maximum factored axial load, live load rotation, and thermal expansion, the computer program COM624P can be used to determine the depth to pile fixity, the depth to the first inflection point of the pile, the unbraced length of the pile, the depth at which the lateral pile deflection is equal to 2% of the pile diameter (needed for friction piles only), and the maximum moment in the pile below the first point of inflection. Since a pre-augered hole, 3000 mm minimum depth, filled with loose sand, is present at the top of the piles, the COM624P analysis should use the properties of the weaker of either the loose sand or the actual soil for the depth of the pre-augered hole. The procedure for running COM624P is as follows:

Run COM624P using the top of pile boundary condition which permits a specified lateral deflection along with an applied moment. Apply the maximum pile vertical axial load to the pile simultaneously with the abutment maximum thermal movement. The axial load and deflection should be input as positive values. Apply the negative plastic moment at the head of the pile and run the analysis.
1 - If the calculated pile head rotation (positive value) is less than the end rotation of the pile due to live loads and composite dead loads, the analysis is complete.
2 - If the calculated pile head rotation is greater than the end rotation of the pile due to live loads and composite dead loads, iteratively reduce the moment at the head of the pile until the rotations are equal (within tolerance).

Title: Birdge 109 - 128 m 4-Span Concrete Prestressed I-girder
90^{o} skew, 3.505 m girder spacing

By: WS
Date: 3/10/2003
Checked: __________
Date: __________

Design values for COM624P:

Pile Section	HP310x110	HP12x74
Pile width or diameter	0.308 m	12.1 in
Pile moment of inertia	0.0000771 m^4	185 in^4
Pile area	0.0141 m^2	21.9 in^2
Vertical axial load	758.4 kN	170.5 k
Design rotation	0.0014 radians	0.078 degrees
Design thermal movement	0.0304 m	1.20 in
Plastic moment (if required)	-186.9 kN-m	-137.9 k-ft

At this point COM624P should be run. COM624P is run using a text file as input. There are two ways to develop this text input file. The first is to use the input file editor program supplied with COM624P. The second method is to use any text editor to develop the input file using the COM624P users manual as a guide. If this second method is chosen, a template file for COM624P can be created from the COM624P Input tab. Once the template is created, it can be edited using any text editor.

Results from COM624P (See figures below for illustrations of the data required from the program).

The depth to fixity is defined as the shallowest depth at which the pile deflection is equal to zero.

Depth to fixity, L_p = 3521.96 mm 138.66 in

The depth to the uppermost point of inflection is the depth measured from the bottom of the abutment to the first point of zero moment on the pile moment diagram.

Depth to first point of inflection, L_{i1} = 1192.28 mm 46.94 in

The depth to the second point of inflection is the depth measured from the bottom of the abutment to the second point of zero moment on the pile moment diagram. For a short pile with only one point of inflection, input the total pile length

Depth to second point of inflection, L_{i2} = 4607.05 mm 181.38 in

The depth above which friction is ineffective is input here. For a laterally deflected pile, this depth is defined as the point where the deflection is 2% of the pile diameter. For the present pile (see section properties above), this deflection value is (0.02)(308) = 6.16 mm (0.24 in). The length of pile above this point is considered ineffective in the design of friction piles. If the pile is driven through an embankment fill which is to be neglected in calculating pile friction resistance, input the depth of fill. This value is not required for end bearing piles.

DM-4 Ap.G.1.4.2.2

Depth to 2% deflection, L_n = 2253.23 mm 88.71 in

The maximum bending moment in the pile is the maximum moment below the uppermost point of inflection and neglects the moment at the pile-pile cap interface.

Maximum bending moment in pile, M_u = 100.12 kN-m 73.84 k-ft

Lateral pile deflection vs depth

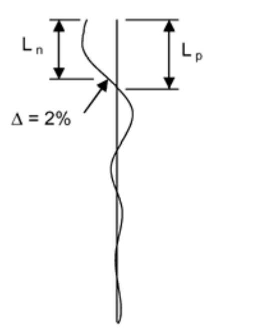

Pile moment vs depth

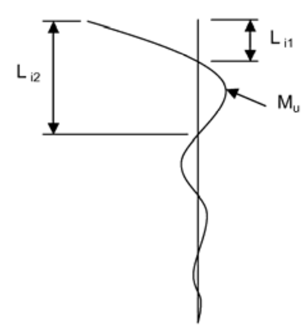

Typical COM624P results (exaggerated)

Title: Birdge 109 - 128 m 4-Span Concrete Prestressed I-girder
90° skew, 3.505 m girder spacing

By: WS
Checked:
Date: 3/10/2003
Date:

Pile Capacity Analysis

Check the geotechnical resistance of the pile
The geotechnical resistance can be supplied by skin friction, end bearing, or both. The easiest way to eliminate one or the other from contributing to the resistance is to simply put zero in for the unit resistance of the one to be neglected. The resistance factors for bearing capacity and skin friction should be chosen according to the provisions of DM-4.

Shaft and tip resistance factors

Tip (bearing) resistance factor, ϕ_{qp}	0.25		D10.5.4-2
Shaft (skin friction) resistance factor, ϕ_{qs}	0.40		D10.5.4-2

Tip resistance

Unit tip resistance, q_p	248.22 MPa	36 ksi	
Nominal pile tip resistance, $Q_p = q_pA_p$ =	(248.22)(14100)/1000 =		
	3499.90 kN	786.8 k	

The effective shaft length is the total shaft length minus a length at the top of the pile which is ineffective due to the lateral movement which occurs. Using a displacement of 2% of the pile diameter as the boundary above which skin friction becomes ineffective has been found to be reasonable. The depth, L_n, at which the displacement reaches this critical value was determined previously using the computer program COM624P.

Shaft resistance (skin friction)

Depth to 2% deflection, L_n =	2253.23 mm	7.39 ft
Effective shaft length, $L_e = L_{tot} - L_n$ =	27660.87 - 2253.23 =	
	25407.64 mm	83.36 ft

The unit shaft resistance (skin friction) is required for friction piles. For layered soils, a weighted average unit shaft resistance should be used.

Unit shaft resistance, q_s	0.004 MPa	0.58 psi
Nominal pile shaft resistance, $Q_s = q_sA_s$	= (0.004)(1825)(25407.64)/1000 =	
	185.50 kN	41.7 k

Total factored resistance per pile, $Q_R = \phi_{qp}Q_p + \phi_{qs}Q_s$

(0.25)(3499.90) + (0.40)(185.50) = 949.17 kN 213.4 k

949.2 kN (213.4 k) > 758.4 kN (170.5 k) - OK

Check the capacity of the pile as a structural member

The pile resistance factors in DM-4 are to be applied assuming only axial forces are present at the tip of the pile, where any driving damage is likely to occur. At the top of the pile, where axial forces and bending are present, the piles are generally undamaged. For these reasons a lower load factor is used when the axial force only is considered. The combined flexure and axial force resistance factors are higher. The calculated nominal axial resistances are also different, as the pile is assumed fully supported at the tip, but an unbraced length is assumed between the top two points of inflection.

Pile resistance factors

Axial compression only, ϕ_c	0.45		D6.5.4.2
Axial compression, ϕ_c plus	0.60	(used together)	D6.5.4.2
Flexure, ϕ_f	0.85		

Compressive resistance (lower portion of pile - axial loads only)

Nominal axial resistance, P_n = FyAs = (245)(14100)/1000 =

3454.5 kN 776.6 k

For the check of axial capacity, the entire axial load is considered for end bearing piles. For friction piles, the load at the pile tip is assumed to be the total pile load minus 50% of the factored friction resistance of the pile.

Check axial capacity

Axial load at tip of pile, P_u = (≥ 0.0)

758.41 kN   170.5 k

Factored axial resistance, $P_r = \phi P_n$ = (0.45)(3454.50) =

1554.53 kN   349.5 k

1554.53 kN (349.5 k) > 758.41 kN (170.5 k) - OK

The unbraced length is defined as the distance between the top two points of inflection (zero moment) on the pile moment diagram.

(4607) - (1192) = 3414.77 mm   134.44 in

As a structural member, the pile length between the top two inflection points is assumed to be a pinned-pinned member. The effective length factor, K, of a pinned-pinned member = 1.0.

Compressive resistance (upper portion of pile - under combined axial load and moment)

For steel H-piles

F_e = Fy = 245 MPa

E_e = Est = 200000 MPa

$\lambda = (KL_b/r_s\pi)^2 (F_e/E_e)$ = [(1.0*3414.77)/(74*3.142)]^2 (245/200000) = 0.265   A6.9.4.1

if $\lambda \leq 2.25$, $P_n = 0.66^{\lambda} F_e A_s$, if $\lambda > 2.25$, $P_n = 0.88 F_e A_s / \lambda$

Nominal axial resistance, P_n = 0.66^0.265 (245)(14100)/1000 =

3094.3 kN   695.6 k

Factored axial resistance, $P_r = \phi P_n$ = (0.6)(3094.3) =

1856.6 kN   417.4 k

Flexural resistance of steel H-piles

Plastic Moment, $M_p = F_y Z_y$ = (245)(763000)/1000000 =

186.9 kN-m   137.9 k-ft

Yield Moment, $M_y = F_y S_y$ = (245)(497000)/1000000 =

121.8 kN-m   89.8 k-ft

For H-piles, if the width-to-thickness ratio of the flanges is not sufficient to consider the section compact, an interaction formula from AISC is used to interpolate between the plastic moment resistance and the yield moment resistance.

$M_n = M_p - (M_p - M_y)(\lambda - \lambda_p)/(\lambda_r - \lambda_p) \leq M_p$ AISC-LRFD, Ap.F F1., 1994

For pipe piles, if the diameter-to-thickness ratio of the pipe is not sufficient to consider the section compact, then the section is considered non-compact.   A6.12.2.3.2

Width-to-thickness ratio of projecting flange element

λ = bf / 2tf = 310/(2*15.5) = 10.00

Width-to-thickness criteria for flange element to reach plastic moment

$\lambda_p = 0.38 * (E / F_y)^{1/2}$ = 0.382*(200000/245)^0.5 = 10.91   A6.10.5.2.3c

Width-to-thickness criteria for flange element to reach yield stress

$\lambda_r = 0.56 * (E / F_y)^{1/2}$ = 0.56*(200000/245)^0.5 = 16.00   A6.9.4.2

Nominal flexural resistance, M_n = Mp

Use M_n = 186.94 kN-m   137.88 k-ft

Pile factored flexural resistance, $M_r = \phi M_n$ = (0.85)(186.9) =

158.9 kN-m   117.19 k-ft

Check moment-axial interaction

P_u / P_r = 758.4/1856.6 = 0.41   A6.9.2.2

if $P_u / P_r < 0.2$ then $P_u / 2.0P_r + M_u / M_r \leq 1.0$

if $P_u / P_r \geq 0.2$ then $P_u / P_r + (8.0 / 9.0)\, M_u / M_r \leq 1.0$

Moment - axial interaction = 758.4/1856.6 + (8.0/9.0)(100.12/158.9) = 0.97 ≤ 1.00 OK

Title: Birdge 109 - 128 m 4-Span Concrete Prestressed I-girder
90^o skew, 3.505 m girder spacing
By: WS
Checked:
Date: 3/10/2003
Date:

Pile Ductility Requirement

Since the top of the pile will often have to undergo inelastic rotations, a check is performed based on a method contained in Greimann et. al. (1987) for determining whether the pile has enough ductility to undergo the required calculated deflections. DM-4 Ap.G.1.4.2.5

Ductility Criterion, $\Delta \leq \Delta_i$, where
Δ = design displacement
Δ_i = allowable displacement

The design displacement is the total displacement due to the full range of thermal expansion / contraction at the abutment being designed. Most of the data for thermal displacements was listed previously, and the percentage of the total displacement of the bridge is denoted by k.

Temperature range, Δ_T = 50 ^oC Concrete girders D3.12.2.1

Design displacement, $\Delta = k\phi_T\alpha\Delta_T L$ = (0.50)(1.0)(0.0000108)(50)(128016) =
34.6 mm 1.36 in

The design rotation is the total factored rotation at the support due to live load and composite dead loads which is equal to the sum of the absolute values of the maximum and minimum factored rotations.

Total design rotation, $\theta_w = \theta_{min} + \theta_{max}$ = 0.0008 + 0.0014 =
0.0022 radians 0.125 degrees

Pile yield stress, F_y 245 MPa 36 ksi

The plastic rotation is the rotation required to form a plastic hinge in the pile.

Plastic rotation, $\theta_p = F_y Z L_i / 3EI$ = (245)(763000)(1192.28)/(3*200000*77100000) =
0.0048 radians 0.276 degrees

Inelastic rotation capacity reduction factor, C_i ($0 \leq C_i \leq 1.0$)

$C_i = 3.17 - 5.68 \cdot (F_y / E)^{1/2}$ (bf / 2tf) = 3.17 - 5.68 * (245/200000)^0.5 [310/(2*15.5)] = 1.18
Use C_i = 1.00

Inelastic rotation capacity, $\theta_{inel} = (K^*C_i M_p L_i)/EI$ For H-piles, K = 1.500
[(1.500)(1.00)(186.94)(1000)(1192.28)]/[(200)(77100000)] =
0.0217 radians 1.242 degrees

Allowable displacement, $\Delta_i = 4^*L_i^*[(\theta_{inel} - \theta_w)/2 + \theta_p]$ = (4)(1192.28)[(0.0217 - 0.0022)/2 + 0.0048] =
69.5 mm 2.74 in

34.6 mm (1.36 in) < 69.5 mm (2.74 in) - OK

Pile Cap Reinforcing Design

Extreme Factored Dead + Live Loads per girder.

The extreme interior and exterior vertical girder reactions are listed below. When combined with the extreme wind and centrifugal reactions for an exterior girder, the result is a conservative maximum girder reaction for pile cap design.

Strength I	maximum of 1472.40 and 1415.40 =	1472.40 kN	331.01 k
	minimum of 413.58 and 372.54 =	372.54 kN	83.75 k
Strength IP	maximum of 1321.11 and 1264.11 =	1321.11 kN	297.00 k
	minimum of 438.09 and 397.05 =	397.05 kN	89.26 k
Strength II	maximum of 1450.20 and 1393.20 =	1450.20 kN	326.02 k
	minimum of 419.71 and 378.67 =	378.67 kN	85.13 k
Strength III	maximum of 810.53 and 753.53 =	810.53 kN	182.21 k
	minimum of 520.83 and 479.79 =	479.79 kN	107.86 k
Strength V	maximum of 1321.11 and 1264.11 =	1321.11 kN	297.00 k
	minimum of 438.09 and 397.05 =	397.05 kN	89.26 k

Title: Birdge 109 - 128 m 4-Span Concrete Prestressed I-girder
90^{o} skew, 3.505 m girder spacing

By: WS
Checked:
Date: 3/10/2003
Date:

The following reactions are the extreme factored dead and live load girder reaction calculated previously, plus the extreme reactions on the exterior girder due to wind, centifugal, and thermal forces. It is recognized that the extreme reactions due to lateral forces occur on the exterior girders, while the extreme gravity reaction may occur on the interior girders, but combining the two should not be overly conservative. The η_i modifier is included here as well.

Strength I	max	1472.40 + 1.00[1.75(0.00) + 1.00(47.33)(12/4)] =		
			1614.40 kN/girder	362.93 k/girder
	min	372.54 + 1.00[1.75(0.00) + 1.00(0.00)(12/4)] =		
			372.54 kN/girder	83.75 k/girder
Strength IP	max	1321.11 + 1.00[1.35(0.00) + 1.00(47.33)(12/4)] =		
			1463.11 kN/girder	328.92 k/girder
	min	397.05 + 1.00[1.35(0.00) + 1.00(0.00)(12/4)] =		
			397.05 kN/girder	89.26 k/girder
Strength II	max	1450.20 + 1.00[1.35(0.00) + 1.00(47.33)(12/4)] =		
			1592.20 kN/girder	357.94 k/girder
	min	378.67 + 1.00[1.35(0.00) + 1.00(0.00)(12/4)] =		
			378.67 kN/girder	85.13 k/girder
Strength III	max	810.53 + 1.00[1.40(4.94)] + 1.00[1.40(15.23) + 1.00(47.33)(12/4)] =		
			980.77 kN/girder	220.49 k/girder
	min	479.79 + 1.00[1.40(-88.13+ -15.23) + 1.00(0.00)(12/4)] =		
			335.08 kN/girder	75.33 k/girder
Strength V	max	1321.11 + 1.00[0.40(15.23) + 1.00(6.75) + 1.35(0.00) + 1.00(47.33)(12/4)] =		
			1475.96 kN/girder	331.81 k/girder
	min	397.05 + 1.00[0.40(-15.23) + 1.00(-6.75) + 1.35(0.00) + 1.00(0.00)(12/4)] =		
			384.21 kN/girder	86.37 k/girder

Controlling Loads	max STR I	1614.40 kN/girder	362.93 k/girder
	min STR III	335.08 kN/girder	75.33 k/girder

Pile Cap Reinforcing

Knowing the maximum girder reaction, the pile spacing, the dimensions of the cap and diaphragm, and the material properties, the pile cap reinforcing can be calculated. The loads used for design are the maximum simply supported beam moments reduced by 20% to account for the continuity over the piles. Calculations for reinforcement are performed on the Cap Reinforcement tab.

Concrete compressive strength, f'_c	20.7	MPa	3.0	ksi
Reinforcing steel yield strength, F_y	413.7	MPa	60	ksi
Maximum factored girder reaction, R_u	1614.4	kN	362.9	k
Pile Spacing	1105	mm	3.63	ft

Pile cap reinforcement - use 4 # 25 bars top and bottom of cap beam

Title: Birdge 109 - 128 m 4-Span Concrete Prestressed I-girder
90° skew, 3.505 m girder spacing

By: WS
Checked:
Date: 3/10/2003
Date:

ANALYSIS SUMMARY PAGE

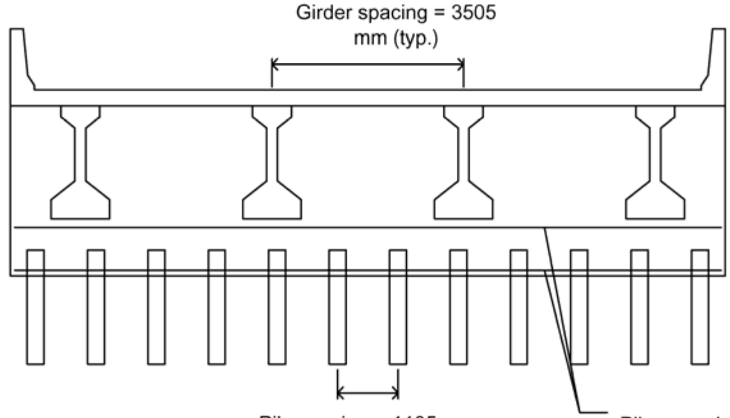

Bridge Description
Bridge length: 128016 mm (420.00 ft) continuous span.
Skew: 90 degrees.
Maximum number of traffic lanes: 3.
Curb-to-curb roadway width: 12192 mm (40.00 ft).
Total width of sidewalk(s): 0 mm (0.00 ft).
Out-to-out superstructure width: 13072 mm (42.89 ft).
Maximum number of traffic lanes with no sidewalks: 3.
Number of girders: 4 prestressed concrete I-girders
Girder spacing: 3505.2 mm (11.50 ft).
Moment of inertia of the girders about the longitudinal axis of the bridge: 61432135 mm^2 (95220 in^2).
Girders depth: 1981.2 mm (11.50 ft).
Girder width: 1066.8 mm (3.50 ft).
Bearing pad thickness 20 mm (0.8 in).
Average deck + haunch thickness: 273.5 mm (10.77 in).
Parapet height: 1070 mm (3.51 ft).

Integral Abutment Description
Abutment width: 1200 mm (3.94 ft).
Abutment length: 13072 mm (42.89 ft).
Pile cap depth: 1213.1 mm (3.98 ft) at the left end.
1118.6 mm (3.67 ft) at the center.
1024.13 mm (3.36 ft) at the right end.
Average pile cap depth: 1118.6075 mm (3.67 ft).
Pile cap reinforcement: 4 # 25 bars top and bottom.
End diaphragm height (equal to the deck + haunch + girder + bearing pad depth): 2274.7 mm (7.46 ft).
Total average abutment height: 3393.3075 mm (11.13 ft).
Wingwall length: 3657.6 mm (12.00 ft) long tapered wingwalls at each end of the abutment.

Pile Description
Number of piles: 12 - HP310x110 (HP12x74) piles.
Pile spacing: 1104.9 mm (3.63 ft) in a single row along the centerline of bearing of the abutment.
Moment of inertia of the piles about the longitudinal axis of the bridge: 174574973 mm^2 (270592 in^2).
Design pile length: 27660.87 mm (90.75 ft).
Depth to fixity: 3521.96 mm (138.66 in).
Unbraced length: 3414.77 mm (134.44 in).
Depth to the first point of inflection: 4607.05 mm (181.38 in).
Depth to the point where the lateral deflection is 2% of the pile width (friction engaged): 2253.23 mm (88.71 in).
Pile yield moment, My: 121.8 kN-m (89.8 k-ft).
Pile plastic moment, Mp: 186.9 kN-m (137.9 k-ft).

Title: Birdge 109 - 128 m 4-Span Concrete Prestressed I-girder
90^{o} skew, 3.505 m girder spacing

By: WS
Date: 3/10/2003
Checked: ________
Date: ________

Total factored geotechnical capacity of the pile: 949.2 kN (213.4 k).
Factored axial resistance of the pile at the tip: 1554.5 kN (349.5 k).
Factored axial resistance of upper portion of pile for use in interaction equation: 1856.6 kN (417.38 k).
Factored flexural resistance of upper portion of pile for use in interaction equation: 158.9 kN-m (117.2 k-ft).

Loads and Deformations
Maximum girder reaction: 1614.4 kN (362.9 k) due to the STR I load case
Maximum axial force in the pile: 758.4 kN (170.5 k) due to the STR I load case.
Maximum bending moment in the pile (other than at the pile-abutment connection): 100.1 kN-m (73.8 k-ft).
Total maximum design movement for the abutment: 69.1 mm (2.72 in).
Maximum movement in one direction: 30.4 mm (1.20 in).
Maximum design rotation: 0.0014 radians (0.078 degrees).
Axial load-moment interaction equation result for the pile (maximum allowable is 1.00): 0.97.

Warnings and Errors
The spreadsheet generated 1 warning(s) and 0 error(s).
The 1 warning(s) should should be checked to make sure requirements are satisfied.

7.6 CONCLUDING REMARKS

Rigidly connected construction joints between abutment and backwall are a conservative assumption. This assumption allows rotational compatibility between end girder and pile head rotations to be incorporated into the PennDOT IA program. However, the measured behavior indicates the occurrence of relative rotations between abutment and girders and does not agree with this assumption. Although this assumption bears on a safe side, the safety margin of the assumption tends to be uncertain due to other unforeseen bridge behavior. The unforeseen behavior is twofold: beneficial behavior and adverse behavior.

The beneficial behavior of IA bridges, as observed from field data, includes: (1) slow concrete responses to daily temperature changes and (2) passive earth pressures occurring only at the center and top portion of abutments. Slow concrete responses to daily temperature changes were observed from a small variation in displacement data due to large thermal bridge mass. However, a relatively large design temperature range is utilized in the PennDOT IA program. Passive earth pressures measured from pressure cells were distributed locally at the center and top portion of abutments. Smaller earth pressures were observed at other locations. However, passive earth pressures distributed equally on the entire abutment surface area are utilized in the PennDOT IA program.

The adverse behavior of IA bridges observed from field data includes: (1) creep and shrinkage effects, (2) strong axis bending moment of piles, (3) secondary moment of continuous IA bridges due to thermal effects on substructures, and (4) additional pile head movements due to earth pressures. Creep and shrinkage of prestressed concrete members are identified as producing a significant effect on the total IA bridge movements. Magnitudes of additional pile stresses due to strong axis bending can become a significant effect, particularly for a short bridge where longitudinal and transverse dimensions are similar (bridge 222 for instance). Thermally induced loads on abutment and pier for continuous IA bridges can also result in significant magnitudes of redistributed secondary moments, particularly for tall piers and stub abutments. Due to flexibility of abutment-backwall connections, significant pile head movements can be generated when subjected to earth pressures, particularly for a tall abutment. The worst combination of these four sources can overcome a safety margin given by the rigid-connection assumption and the aforementioned beneficial behavior.

Finally, it is concluded that the rigid connection assumption utilized in the PennDOT IA program does not represent the actual IA bridge behavior. Although the rigid connection assumption is an overly conservative approach, an uncertain degree of safety margin still exists where the combination of all unforeseen adverse behavior is significant and the combination of all unforeseen beneficial behavior is insignificant. Therefore, an analysis and design approach based on a partially rigid connection with inclusion of both beneficial and adverse behaviors is more appropriate for future design of IA bridges.

CHAPTER 8

SUMMARY

The project described in this report involved the instrumentation of bridge 109 on the new I-99 extension in central Pennsylvania and continued monitoring and collection of engineering bridge response data at the three previously instrumented bridges and the weather station. The development of a bridge 109 numerical model and evaluation of the PennDOT IA Design spreadsheet was completed. Detailed instrument descriptions and installation of each bridge 109 instrument are provided in this report. Bridge response data are presented for bridges 203, 211, and 222, composed of longitudinal abutment displacements, abutment earth pressures, abutment and girder rotations, H-pile bending moments about the weak axis and axial forces, girder strains, and approach slab strains. Four 3-dimensional numerical models were developed to predict IA bridge response for bridges 203, 211, 222, and 109. Comparison between observed bridge response and predicted bridge response is presented and discussed. Finally, evaluation of the PennDOT IA Design Spreadsheet was performed to provide suggested program improvements for all four instrumented bridges. Comparison of predicted bridge response based on the PennDOT IA program and the original design to observed bridge response was also presented and discussed.

REFERENCES

AASHTO LRFD Bridge Design Specification (2004), American Association of State Highway and Transportation Officials.

ACI Committee 209 (2004), "Prediction of Creep, Shrinkage, and Temperature Effects in Concrete Structures," *ACI Manual of Concrete Practice Part 1*, American Concrete Institute.

ANSYS Release 10.0, ANSYS University Advanced, ANSYS, Inc.

Arockiasamy, M., Butrieng, N. and Sivakumar, M. (2004), "State-of-the-Art of Integral Abutment Bridges: Design and Practice," *Journal of Bridge Engineering*, ASCE, Vol. 9, No. 5.

Arockiasamy, M. and Sivakumar, M. (2005), "Time-Dependent Behavior of Continuous Composite Integral Abutment Bridges," *Practice Periodical on Structural Design and Construction*, ASCE, Vol. 10, No. 3.

Arsoy, S., Barker, R. M., Duncan, J. M. and Via, C. E. (1999), *Behavior of Integral Abutment Bridges*, Final Report, FHWA/VTRC-00/CR3, Virginia Transportation Research Council, Charlottesville.

Ashour, M. and Norris, G. (2000), "Modeling Lateral Soil-Pile Response Based on Soil-Pile Interaction," *Journal of Geotechnical and Geoenvironmental Engineering*, ASCE, Vol. 126, No. 5.

BD-667M (2005), "Standard Integral Abutment Drawings," Bureau of Design, Commonwealth of Pennsylvania, Department of Transportation.

Barr, P. J., Stanton, J. F. and Eberhard, M. O. (2005), "Effects of Temperature Variation on Precast, Prestressed Concrete Bridge Girders," *Journal of Bridge Engineering*, ASCE, Vol. 10, No. 2.

Boulanger, R. W., Curras, C. J., Kutter, B. L., Wilson, D. W. and Abghari, A. (1999), "Seismic Soil-Pile-Structure Interaction Experiments and Analyses," *Journal of Geotechnical and Geoenvironmental Engineering*, V. 125, No. 9, pp. 750-759.

Darley, P., Carder, D. R. and Alderman, G. H. (1996), *Seasonal Thermal Effects on the Shallow Abutment of an Integral Bridge in Glasgow*, TRL Report 178, E465A/BG,Transport Research Laboratory, ISSN 0968-4107.

Das, B. M. (1999), *Principles of Foundation Engineering*, PWS Publishing, 4th Edition.

DeJong, J. T., Howey, D. S., Civjan, S. A., Brena, S. F., Butler, D. S., Crovo, D. S., Hourani, N. and Connors, P. (2004), "Influence of Daily and Annual Thermal Variations on Integral Abutment Bridge Performance," *Proceedings, GeoTrans 2004*, ASCE.

Delattre, L. (2001), *A Century of Design Methods for Retaining Walls – The French Point of View: I. Calculation – Based Approaches – Conventional and Subgrade Reaction Methods*, BLPC-2001/234, Laboratoire Central des Ponts et Chaussées.

Dicleli, M. (2000), "Simplified Model for Computer-Aided Analysis of Integral Bridges," *Journal of Bridge Engineering*, Vol. 5, No. 3, pp. 240-248.

Dicleli, M. and Albhaisi, S. M. (2003), "Estimation of Length Limits for Integral Bridges Built on Clay," *Journal of Bridge Engineering*, ASCE, Vol. 9, No. 6.

Dicleli, M. and Albhaisi, S. M. (2004), "Effect of Cyclic Thermal Loading on the Performance of Steel H-Piles in Integral Bridges with Stub-Abutments," *Journal of Construction Steel Research*, 60, pp. 161-182.

Dicleli, M. (2005), "Integral Abutment-Backfill Behavior on Sand Soil—Pushover Analysis Approach," *Journal of Bridge Engineering*, ASCE, Vol. 10, No. 3.

Duncan, J. M. (2000), "Factors of Safety and Reliability in Geotechnical Engineering," *Journal of Geotechnical and Geoenvironmental Engineering*, ASCE, Vol. 126, No. 4.

Duncan, J. M. and Mokwa, R. L. (2001), "Passive Earth Pressure: Theories and Tests," *Journal of Geotechnical and Geoenvironmental Engineering*, ASCE, Vol. 127, No. 3.

Elbadry, M. M. and Ghali, A. (2001), "Analysis of Time-Dependent Effects in Concrete Structures Using Conventional Linear Computer Programs," *Canadian Journal of Civil Engineering*, CNRC Canada, Vol. 28, pp.190-200.

EM 1110-2-2504 (1994), "Design of Sheet Pile Walls," *Engineering Manual*, U.S. Army Corps of Engineers, Department of the Army, Washington, D.C.

Faraji, S., Ting, J. M., Crovo, D. S. and Ernst, H. (2001), "Nonlinear Analysis of Integral Bridges: Finite-Element Model", *Journal of Geotechnical and Geoenvironmental Engineering*, ASCE, Vol. 127, No. 5.

Fennema, J. L. (2003), "Prediction and Measured Response of Integral Abutment Bridges," M.S. Thesis, The Pennsylvania State University, University Park, PA.

Fennema, J. L., Laman, J. A. and Linzell, D. G. (2005), "Predicted and Measured Response of an Integral Abutment Bridge," *Journal of Bridge Engineering*, V. 10, No. 6, pp. 666-677.

Fu, K. and Lu, F. (2003), "Nonlinear Finite-Element Analysis for Highway Bridge Superstructures," *Journal of Bridge Engineering*, ASCE, Vol. 8, No. 3.

Ghali, A., Favre, R. and Elbadry, M. (2002), *Concrete Structures: Stresses and Deformation*, Spon Press, London, 3rd Edition.

Girton, D. D., Hawkinson, T. R. and Greimann, L. F. (1991), "Validation of Design Recommendations for Integral-Abutment Piles," *Journal of Structural Engineering*, ASCE, Vol. 117, No. 7, pp. 2117-2134.

Horvath, J. S. (2004), "Integral-Abutment Bridges: A Complex Soil-Structure Interaction Challenge," *Proceedings, GeoTrans 2004*, ASCE.

Jirásek, M. and Bažant, Z. P. (2001), *Inelastic Analysis of Structures*, John Wiley & Sons, New York.

Koskinen, M., *Soil-Structure-Interaction of Jointless Bridges on Piles*. Geotechnical Laboratory, Tampere University of Technology, Finland, pp. 1091-1096.

Kunin, J. and Alampalli, S. (2000), "Integral Abutment Bridges: Current Practice in United States and Canada," *Journal of Performance of Constructed Facilities*, ASCE, Vol. 14, No. 3, pp. 104-111.

Laman, J. A., Linzell, D. G., Leighty, C. A. and Fennema, J. L. (2003), *Methodology to Predict Movement and Stresses in Integral Abutment Bridges*, Report No. FHWA-PA-2002-039-97-04(80), Pennsylvania Transportation Research Council.

Lin, S. and Liao, J. (1999), "Permanent Strains of Piles in Sand Due to Cyclic Lateral Loads," *Journal of Geotechnical and Geoenvironmental Engineering*, V. 125, No. 9, pp. 798-802.

Mourad, S. and Tabsh, S. W. (1999), "Deck Slab Stresses in Integral Abutment Bridges," *Journal of Bridge Engineering*, ASCE, Vol. 4, No. 2, pp. 125-130.

Ndon, U. J. and Bergeson, K. L. (1995), "Thermal Expansion of Concretes: Case Study in Iowa," *Journal of Materials in Civil Engineering*, ASCE, Vol. 7, No. 4, pp. 246-251.

NEHRP Recommended Provisions for Seismic Regulations for New Buildings and Other Structures and Commentary: FEMA 368 and FEMA 369 (2000), Chapter 13: Commentary – Seismically Isolated Structures Design Requirements.

Neville, A. M., Dilger, W. H. and Brooks, J. J. (1983), *Creep of Plain and Structural Concrete*, Construction Press, London and New York.

Noorzaei, J., Viladkar, M. N. and Godbole, P. N. (1995), "Elasto-Plastic Analysis for Soil-Structure Interaction in Framed Structures," *Computers & Structures*, Vol. 55, No. 5, pp. 797-807.

Paul, M. D. (2003), "Thermally Induced Superstructure Stress in Prestressed Girder Integral Abutment Bridges," M.S. Thesis, The Pennsylvania State University, University Park, PA.

Paul, M. D., Laman, J. A. and Linzell, D. G. (2005), "Thermally Induced Superstructure Stresses in Prestressed Girder Integral Abutment Bridges," *Transportation Research Record: Journal of the Transportation Research Board*, Transportation Research Board of the National Academies, Washington D.C., pp. 287-297.

PennDOT Design Manual Part 4 (2000), "Structures: Procedures-Design-Plans Presentation," Commonwealth of Pennsylvania, Department of Transportation, V. 1.

Reese, L. C. (1984), *Handbook on Design of Piles and Drilled Shafts Under Lateral Load*, Report No. FHWA-IP-84-11, U.S. Department of Transportation.

Taciroglu, E., Rha, C., Stewart, J. P. and Wallace, J. W. (2003), "Robust Numerical Models for Cyclic Response of Columns Embedded in Soil," The 16th ASCE Engineering Mechanics Conference, University of Washington, Seattle, July 16-18.

Thomson, T. A., Jr. and Lutenegger, A. J. (1998), "Passive Earth Pressure Tests on an Integral Bridge Abutment," *Proceedings: Fourth International Conference on Case Histories in Geotechnical Engineering*, St. Louis, Missouri.

Thippeswamy, H. K., GangaRao, H. V. S. and Franco, J. M. (2002), "Performance Evaluation of Jointless Bridges," *Journal of Bridge Engineering*, ASCE, Vol. 7, No. 5.

Thomas, M. E. (1999), "Field Study of Integral Abutment Bridges," M.S. Thesis, Iowa State University, Ames, Iowa.

Wang, S. and Reese, L. C. (1993), *COM624P – Laterally Loaded Pile Analysis Program for the Microcomputer*, Report No. FHWA-SA-91-048, U.S. Department of Transportation, Washington, D.C.

Yazdani, N., Eddy, S. and Cai, C. S. (2000), "Effect of Bearing Pads on Precast Prestressed Concrete Bridges", *Journal of Bridge Engineering*, ASCE, Vol. 5, No. 3.